ROLES FOR TELOMERE-LED CHROMOSOME MOTION AND CROSSOVER RESOLUTION DURING MEIOSIS IN *SACCHAROMYCES CEREVISIAE*

A Dissertation

Presented to the Faculty of the Graduate School

of Cornell University

in Partial Fulfillment of the Requirements for the Degree of

Doctor of Philosophy

by

Megan Sonntag Brown

January 2013

ROLES FOR TELOMERE-LED CHROMOSOME MOTION AND CROSSOVER RESOLUTION DURING MEIOSIS IN *SACCHAROMYCES CEREVISIAE*

Megan Sonntag Brown, Ph. D.

Cornell University 2013

During meiosis, multiple mechanisms act to promote accurate segregation of chromosomes, ensuring that all progeny receive exactly one copy of each chromosome. To achieve this during meiosis, chromosomes need to pair, recombine, and correctly attach to the meiotic spindle. The focus of my thesis is to understand early events in meiosis that promote chromosome segregation, including telomere-led chromosome movements and crossover placement and regulation.

Telomere-led chromosome movements are a conserved feature of Meiosis I. Various roles have been proposed for such chromosome motions, including promoting homolog pairing and removing inappropriate chromosomal interactions. Using a "one-dot/two-dot tetR-GFP" assay in budding yeast, I found that *csm4Δ* strains, which are defective in telomere-led chromosome movements and proper Meiosis I disjunction, are also defective in homolog pairing. I then performed a systematic mutational analysis of *CSM4*. This screen yielded one allele, *csm4-3*, that conferred a null-like meiotic delay but had near wild-type levels of spore viability. Interestingly, compared to wild-type, *csm4-3* conferred an intermediate phenotype in homolog pairing, but reduced average chromosome velocity. Furthermore, I found that the meiotic delay was essential for spore viability and Meiosis I disjunction in *csm4-3*. Based on these observations, I propose that occasional and rapid chromosome movements over an extended

period of time are sufficient to promote wild-type levels of recombination and high spore viability; however, sustained and rapid chromosome movements are required to promote efficient meiotic progression.

Crossover regulation is also important in promoting disjunction of homologs in Meiosis I, and is regulated through an interference-dependent mechanism involving Msh4-Msh5 and Mlh1-Mlh3. Crossover interference helps ensure that each homolog pair receives an obligate crossover, facilitating proper disjunction in the first meiotic division. Previously, the Alani laboratory detected a crossover threshold in *msh4/5* mutants where meiotic crossover levels could be decreased up to two-fold without lowering spore viability. I show that a set of *mlh3* ATPase mutants do not confer a crossover threshold pattern; instead, a linear relationship was observed between spore viability and meiotic crossing over. These data are consistent with Mlh1-Mlh3 acting after obligate crossover decisions have been made.

BIOGRAPHICAL SKETCH

Megan Elizabeth Sonntag was born on May 14th, 1985 in Minnesota. From an early age, she spent most of her time playing sports, playing with her dog Murphy, or reading fiction books, mostly science fiction and fantasy. Megan breezed through her early years in school, where she won first place in a math competition of all 6th graders in Minnesota. Her one setback was getting upset in second grade during free time that there wasn't enough work to do. Megan continued doing sports in high school, at one point juggling volleyball, basketball, track (hurdles), and soccer all at the same time. Despite difficult family problems, Megan ended up graduating with above a 12.0 GPA on a scale weighted for AP classes. Always interested in science and stars, Megan entered her undergraduate studies at University of Wisconsin, Madison intending to major in astrophysics. After the first year, however, she realized that physics is really boring, and she was already 1/3 of the way to a major in mathematics. She decided to major in mathematics just for fun, but also continued to pursue her interests in science, getting a double major in math and molecular biology. Having started some research in Dr. Audrey Gasch's lab in Madison, Megan realized she really loved the hands-on approach to science, and decided to continue her career in science in the Biochemistry, Molecular, and Cellular Biology department at Cornell University. She joined the lab of Dr. Eric Alani where she began to study meiosis and convinced Dr. Alani to buy her a microscope to look at fluorescent foci all day long, which visually was fairly similar to her initial goal of looking at stars all day (or night) long. After almost seven years of dating, she decided it was about time to marry her college boyfriend, Nicholas Brown, and she changed her name to Megan Sonntag Brown. Megan still loves the same activities, reading science fiction and fantasy novels and playing with her dog Lior, but now she mostly just watches sports (Badger basketball and football, Vikings, and Timberwolves) as she's too lazy to play them herself. Megan will be continuing her career in science and

meiosis at the Stowers Institute for Medical Research in Kansas City in Scott Hawley's lab, where she is looking forward to many more years of "seeing stars" in microscopes.

I would like to dedicate this work to my husband, Nicholas Brown, and all my dogs, past, present, and future. You have each loved, supported me, and kept me sane.

ACKNOWLEDGEMENTS

I would like to thank the entire Alani Lab for advice and support during my time in the lab. I would like to give a special thanks to SaraH Zanders, for getting me excited about meiosis in the first place and providing invaluable guidance throughout my early years in the lab. SaraH was an excellent role model in terms of work ethic, enthusiasm, and occasionally, in standing up to Eric. I am very grateful for her continual help scientifically and otherwise after she left the lab.

Dr. Eric Alani's enthusiasm and support throughout my time in my lab has been indispensable for my success. He has always pushed me to think for myself and come up with new ideas. He was very encouraging in helping me to pursue microscopy, which wasn't previously a strength for the lab. I am grateful for all his advice, wisdom, and support in helping me become an independent scientist.

My committee, Dr. Mariana Wolfner and Dr. John Schimenti, have also been excellent help throughout my project. I would like to thank them for taking the time to learn about my project and all the suggestions they have given. Dr. Anthony Bretscher was also a big help when I thought about pursuing a project in actin. He took the time to learn about meiosis and my project, for which I am very grateful.

I would also like to thank my friends and family for all of the mental and emotional support they have given me through the years. I would particularly like to thank my husband, Nick Brown, for listening to me complain about things that he didn't understand, and for making a legitimate attempt at trying to understand the basics of what I do. I truly appreciate his patience, love, and understanding.

TABLE OF CONTENTS

LIST OF FIGURES

LIST OF TABLES

LIST OF ABBREVIATIONS

DNA- Deoxyribonucleic acid

MI-Meiosis I

MII- Meiosis II

DSBs- Double-strand breaks

SC- synaptonemal complex

S. cerevisiae- Saccharomyces cerevisiae

C. elegans- Caenorhabditis elegans

S. pombe- Schizzosaccharomyces pombe

FISH- Fluorescent In situ hybridization

Drosophila- Drosophila melanogaster

APC/C-anaphase promoting complex/cyclosome

DAPI- 4',6-diamidino-2-phenylindole

GFP-green fluorescent protein

SPM- sporulation media

NE-nuclear envelope

Δ-deletion

μm- micrometers

S- seconds

sec- seconds

Mbp-Mega base pairs

Kb-kilobases

SC- synthetic complete

C-celsius

YPD- yeast, peptone, dextrose

bp-base pair

PCR-polymerase chain reaction

tRNA-transfer ribonucleotide amino acids

GAL-galactose

LACZ- beta-galactosidase encoding gene

ATP- Adenosine triphosphate

MMR-Mismatch repair

MSH-MutS homolog

nt-nucleotide

MLH-MutL homolog

SEI-single end invasion

dHJs-double holliday junctions

HJs-holliday junctions

JMs-joint molucules

cM- centimorgan

SV- spore viability

n- number

PD- parental ditype

TT- tetratype

NPD- nonparental ditype

WT- wild type

μM- micromolar

mL-milliliter

YPA- yeast, peptone, potassium acetate

μl- microliter

KAc- Potassium Acetate

msec- millisecond

tetO- *tet* operator

tetR- *tet* repressor

t- time

SD- standard deviation

HA- Hemagglutinin

CO- crossover

hr- hour

cfu- colony forming units

GST- glutathione *S*-transferase

as- analog sensitive

Chapter 1

Introduction to chromosome segregation mechanisms in meiosis

Introduction

Meiosis is an important aspect of sexual reproduction that preserves genetic material from one generation to the next. Meiosis involves one round of DNA replication, but two rounds of division: a reductional division (MI), where homologs segregate from each other, and an equational division (MII), where sister chromatids segregate (Figure 1.1A). Mistakes in either of these divisions, though particularly in MI where recombination between homologous chromosomes occurs, can lead to aneuploidy. Levels of aneuploidy differ drastically between organisms. In budding yeast, for example, an individual chromosome has about a 1 in 10,000 chance of segregating incorrectly (Sears *et al.* 1992), while in humans, it has been estimated that 10-30% of fertilized eggs are aneuploid (Jamieson *et al.* 1994; Delhanty 1997; Hassold 1998; Jacobs 1992; Marquez *et al.* 1998; Volarcik *et al.* 1998; reviewed in Hassold and Hunt, 2001).

In humans, most cases of aneuploidy are fatal; in fact, few cases can survive past the earliest stages of development (Bugge, 1998; Hassold *et al.* 1995; Lamb *et al.* 1996; Robinson *et al.* 1993; MacDonald *et al.* 1994; Zaragoza *et al*. 1994 and 1998). The causes of aneuploidy are varied, and cannot only differ between organisms, but between chromosomes within an organism. Most aneuploidy in humans is thought to occur during oogenesis, possibly due to oogenesis occurring over an extended period of time, with MI beginning in the fetus and not completing for 10-50 years (Hassold *et al.* 2007). For example, Trisomy 21, which causes Down syndrome, is most likely due to maternal MI nondisjunction, while Trisomy 18 usually involves

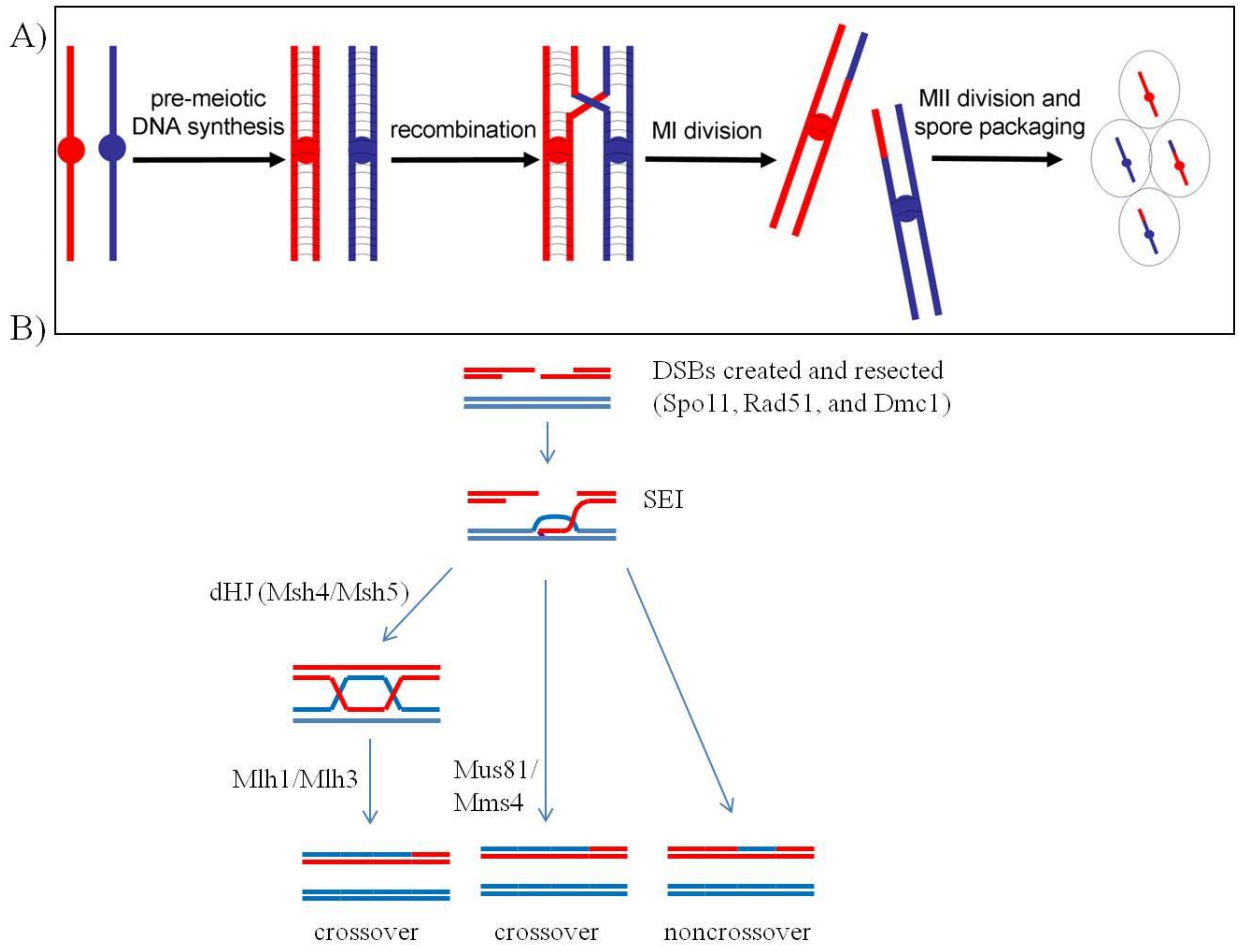

Figure 1.1. Overview of meiosis. A) During meiosis I, chiasmata are important for promoting segregation of the homologs. In the second meiotic division, sister chromatids segregate from each other, resulting in haploid gametes. B) The meiotic recombination pathway is shown. Double strand breaks are initiated by the Spo11 complex, and the ends are resected. In the crossover pathway, single end invasion occurs, leading to a Holliday junction intermediate. Holliday junction intermediates are resolved by a variety of endonucleases, including Mlh1/Mlh3, resulting in crossovers. Mus81/Mms4 can also create crossovers in an interference-independent manner. Noncrossovers are thought to occur through a distinct pathway, most likely dependent on synthesis-dependent strand annealing.

maternal MII nondisjunction. However, some conditions, such as Klinefelter's syndrome (47, XXY) are thought to occur equally from maternal or paternal nondisjunction (Hassold and Hunt, 2001).

While parental origin of the aneuploidy can usually be distinguished based on molecular markers, the underlying causes of the nondisjunction are much more complicated. During the first meiotic division, crossover regulation is considered the major regulator of disjunction in most organisms (Zickler, 2006). However other mechanisms are in place that either help crossover regulation, or provide proper disjunction of homologs when crossover placement is misregulated. These mechanisms include telomere-led chromosome motion, centromere pairing, sister cohesion, the spindle checkpoint, and distributive disjunction. These mechanisms of ensuring chromosome segregation, along with newly emerging evidence of a role of heterochromatin threads in proper disjunction of chromosomes in Drosophila, are discussed.

Crossover formation and placement

Crossover formation is the major method for promoting proper disjunction of homologs in almost all organisms studied (male Drosophila is the most noted exception; Vazquez *et al.* 2002). In budding yeast, approximately 200 double strand breaks (DSBs) are created by a Spo11 complex, eventually resulting in ~90 crossovers per meiotic cell (Cao *et al.* 1990; Gilbertson and Stahl, 1996; Keeney, 1997; Buhler *et al.* 2006; Chen *et al.* 2008; Robine *et al.* 2007). The majority of these crossovers are either created through the Msh4/5-Mlh1/3 interference-dependent pathway, or through an Mms4/Mus81 pathway (Figure 1.1B). The rest of the DSBs are converted into noncrossover products, which are not thought to contribute directly to chromosome segregation, but may promote more stable DNA-DNA interactions (Smithies and

Powers, 1986; Carpenter, 1986; Carpenter, 1987; Allers and Lichten, 2001; Bishop and Zickler, 2004).

Crossover levels and placement are regulated in a variety of ways. First, crossover placement is regulated by DSB placement. DSBs are enriched at certain regions called hotspots, which tend to correlate with nuclease-hypersensitive regions and active chromatin (Petes, 2001; Borde *et al.* 2009). DSBs tend to correspond to intergenic regions, and are not present near telomeres (Blitzblau *et al.* 2007). Second, there are multiple mechanisms in place to control crossover placements and levels. At least one crossover, called the obligate crossover, is thought to be necessary to promote proper disjunction of homologs. Indeed, in mutants with decreased levels of crossing over, a higher level of nondisjunction is observed (Hawley, 1988; Ross-Macdonald and Roeder, 1994; Sym and Roeder, 1994). Crossovers are so important in ensuring disjunction that crossover levels are maintained at the expense of noncrossovers, a process called crossover homeostasis (Martini *et al.* 2006). However, since many organisms generate more than one crossover per homolog pair, crossover placement must be regulated to ensure proper disjunction, since too many crossovers close together can also cause nondisjunction (Page and Hawley, 2003; Martinez-Perez and Colaiacovo, 2009). Crossover interference, where the presence of one crossover decreases the likelihood of a second crossover nearby, is a major mechanism to distribute crossovers evenly across the genome in many organisms (Jones and Franklin, 2006; Figure 1.2). One explanation that has received recent attention is the stress relief model, where a crossover physically changes the structure of chromosomes, releasing mechanical stress and inhibiting the need for nearby crossovers to relieve the stress (Kleckner *et al*. 2004; Storlazzi *et al.* 2008; Martinez-Perez *et al.* 2008).

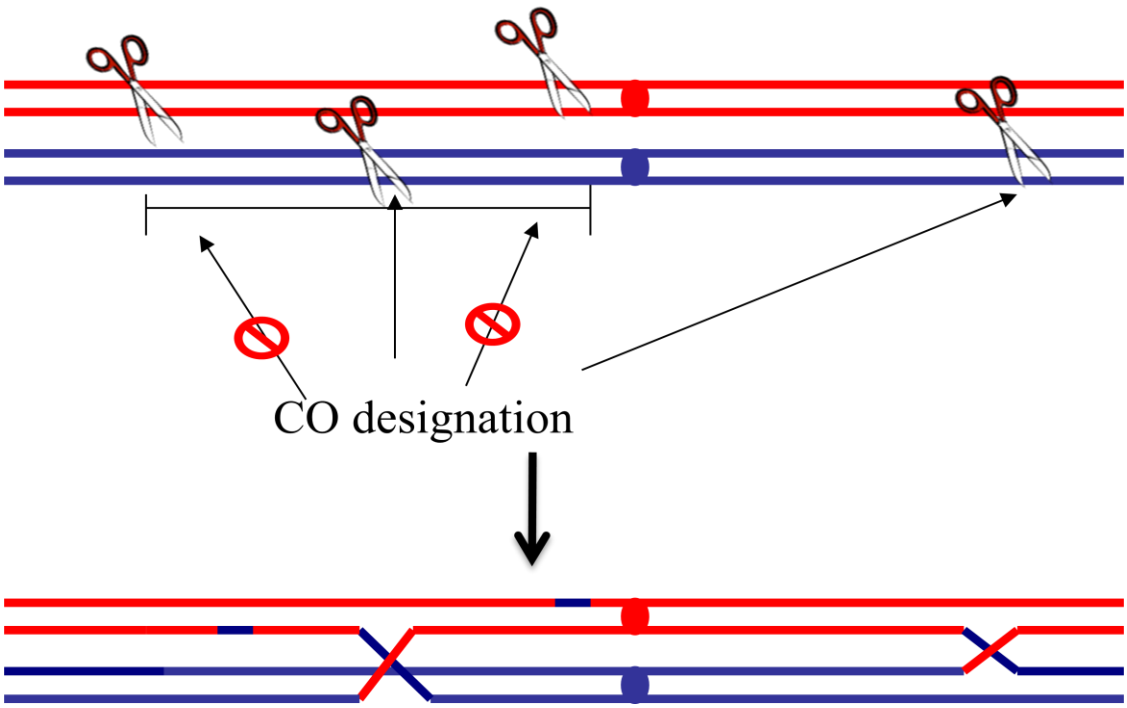

Figure 1.2. Crossover Interference. A diagram illustrating crossover interference is shown. Scissors represent the action of Spo11, which creates DSBs. Arrows point to all potential crossover sites. The presence of one crossover represses the chances of a second crossover from occurring nearby. Therefore, two potential crossover sites are crossed out and repaired as noncrossovers, since one potential site nearby was designated as a crossover. The second figure shows the outcome of this hypothetical situation, where the Holliday junctions will be resolved as crossovers, and the remaining two DSB sites were repaired as noncrossovers. Figure adapted from SaraH Zanders.

As mentioned above, interference-dependent crossovers are mediated by the Msh4/5-Mlh1/3 complex in a variety of organisms. In *C. elegans*, this complex is the only way crossovers form; this results in crossover interference so complete that each chromosome pair only receives a single crossover (Meneely *et al.* 2002; Zalevsky *et al.* 1999). Conversely, fission yeast only use the interference-independent, Mus81/Mms4 pathway, and do not show evidence of crossover interference (Boddy *et al.* 2001). Finally, evenly spaced crossovers are not enough to promote disjunction. Crossovers too near the telomere or too near the centromere can prevent proper chromosome segregation (Mancera *et al.* 2008; Chen *et al.* 2008; Rockmill *et al.* 2006). For example, the Roeder lab found that spore clones containing two copies of chromosome III were more likely to contain a crossover near the centromere (Rockmill *et al.* 2006).

Crossovers are thought to be important for chromosome disjunction because they provide a physical interaction between homologs, which allows proper tension on the meiotic spindles (Ostergren, 1951). In addition to this role, evidence from fission yeast suggest that crossovers that form chiasmata could help promote monopolar attachment of sister chromatids during meiosis I (Yokobayashi and Watanabe, 2005; Kitajima *et al.* 2003) or generate a bias towards poleward movement of chromosomes (Hirose *et al.* 2011). For more information on crossover formation and placement, see Chapters 2, 3, and 4.

Pairing methods: Synaptonemal complex, Telomere led chromosome motion, and Bouquet formation

Synaptonemal Complex: In order for chromosomes to recombine and segregate, homologous chromosomes need to find each other and pair. Multiple mechanisms have been proposed that contribute to meiotic pairing. The synaptonemal complex (SC) is a conserved

proteinaceous structure composed of axial elements, Red1 and Hop1 in budding yeast, and a transverse or central element, Zip1 (Rockmill and Roeder, 1990; Smith and Roeder, 1997; Hollingsworth *et al.* 1990; Sym *et al.* 1993; Sym and Roeder, 1995). Some organisms (*C. elegans* and *Drosophila melanogaster*) depend on the SC in order to pair homologs (Dernburg *et al.* 1998; McKim *et al.* 2002), while in other organisms (budding yeast, mouse, corn), the SC may form after recombination events have been initiated (Mahadevaiah *et al.* 2001; Peoples *et al.* 2002; Storlazzi *et al.* 2003; Pawlowski *et al.* 2004). However, there is some evidence in budding yeast that SC components, in particular Zip1, 2, and 3, are important for stabilizing initial pairing (Peoples-Holst and Burgess, 2005). It is currently unclear to what extent the synaptonemal complex may play in pairing homologs, but it is likely to be organism-specific. However, the SC does play a role in crossover function. The last place the SC dissolves is at chiasmata in some organisms. In mutants that disrupt SC, crossing over is usually reduced, and the crossovers that do occur do not promote proper segregation (von Wettstein *et al.* 1984; Engebrecht *et al.* 1990; Rockmill and Roeder, 1990; Rockmill and Roeder, 1991). However, chromosome pairing can occur in the absence of recombination, although it tends to be nonhomologous, such as in some *spo11* mutants in budding yeast (Cha *et al.* 2000; Tsubouchi and Roeder, 2005; Zickler, 2006). Whether formation of the SC plays a role in initial pairing events is unclear, however it is very important for recombination and stabilizing chromosome interactions.

Bouquet formation: Telomeres congregate opposite the spindle pole bodies during early meiosis, in what is called bouquet formation (Gelei, 1921; Hiraoka, 1952). Because of the close organization of chromosomes at this stage, it has been suggested that this conformation may be important for homolog pairing (Chikashige *et al.* 1994; Scherthan *et al.* 1996; Bass *et al.* 1997; Trelles-Sticken *et al.* 1999). In support of this, mutants in many organisms (i.e. *ndj1*, *csm4*, and

mps3 in budding yeast, *pam1* in maize, and *bqt2* in fission yeast) that are defective in bouquet formation also show defects in pairing (Peoples-Holst and Burgess, 2005; Sonntag Brown *et al.* 2011; Conrad *et al.* 2008; Kosaka *et al.* 2008; Golubovskaya *et al.* 2002; Davis and Smith, 2006). Furthermore, studies in oats and humans have found correlations between the timing of homolog pairing, as determined cytologically, and the initiation of telomere clustering (Bass *et al.* 2000; Scherthan *et al.* 1998)

Despite the general correlation in timing and phenotypes, it is still unclear whether bouquet formation promotes homolog pairing. For example, initial alignment of homologs in *Sordaria* and synaptic initiation in female mice and cattle occurs before the bouquet forms (Storlazzi *et al.* 2003; Joseph and Lustig, 2007; Tankimanova *et al.* 2004; Pfeifer *et al.* 2003). Recent evidence from budding yeast suggests that formation of a bouquet does not correlate with pairing (Lee *et al.* 2012). Furthermore, *ndj1* mutants, which are deficient for bouquet formation, do show decreases in homolog alignment, but this may be due to defects in recombination, (Peoples-Holst and Burgess, 2005). Finally, *Drosophila* and *C. elegans* do not have a canonical telomere bouquet, but still have homologous pairing (Bass, 2003; Harper *et al.* 2004).

What might the highly conserved bouquet be doing if it is not important for homolog pairing? The bouquet does not appear to be important for promoting recombination; in *S. pombe* the bouquet is independent of both recombination and synapsis (Joseph and Lustig, 2007). Furthermore, in *rec12* mutants (a Spo11 homolog) in *S. pombe*, a bouquet forms normally, but no recombination occurs (Tomita and Cooper, 2007). It is likely, however, that recombination is needed for resolution of the bouquet conformation, which is necessary for metaphase alignment of chromosomes (Trelles-Sticken *et al.* 1999). The bouquet may be important in restricting ectopic recombination, nonhomologous synapsis, or preventing chromosome entanglements

(interlocks), however much work needs to be done to separate out the role of the bouquet from secondary phenotypes (Niwa *et al.* 2000; Davis and Smith, 2006; de La Roche, 2007; Golubovskaya *et al.* 2002).

Chromosome motion: Telomere-led chromosome motions during zygotene and pachytene are highly conserved, and involve many of the same proteins necessary for bouquet formation (Parvinen and Soderstrom, 1976; Chikashige *et al.* 2007; Bhalla and Dernberg, 2008; Chikashige *et al.* 1994; Scherthan, 2007; Conrad *et al.* 2008). The force for these movements appears to be generated through the cytoskeleton, although the exact mechanisms (actin vs. microtubules) is organism-specific (Koszul *et al.* 2008; Chickashige *et al.* 2007; Trelles-Sticken *et al.* 2005; Scherthan 2007; Wynee *et al.* 2012; Harper *et al.* 2004).

It initially was thought that these rapid chromosome movements began at zygotene, after recombination and presumably pairing has occurred. However, more recent evidence has suggested that these movements are occurring through the same mechanism, just to a lesser extent, during the time that pairing takes place (Hunter and Kleckner, 2001; Scherthan, 2007; Koszul *et al.* 2008; Conrad *et al.* 2008; Lee *et al.* 2012). Indeed, chromosome movements have been shown to promote homolog pairing in a variety of organisms (Sonntag Brown *et al.* 2011; Lee *et al.* 2012; Conrad *et al.* 2007; Wynee *et al.* 2012). Furthermore, the Alani and Dresser labs have shown through various mutants defective in chromosome motion that the extent of defect in motion correlates with the defect in homolog pairing (Sonntag Brown *et al.* 2011; Lee *et al.* 2012).

It is still unclear how telomere-led chromosome motion may promote homolog pairing. Chromosome motion may promote pairing directly by a stirring force mechanism, increasing the

chance of homologs finding each other (Zickler and Kleckner, 1998). However, more recent evidence has suggested that chromosome motion may play an indirect role in pairing by removing inappropriate interactions between chromosomes (reviewed in Koszul and Kleckner, 2009). This could be by resolving interlocks that are seen in several organisms (von Wettstein *et al.* 1984; Golubovskaya *et al.* 2002), possibly occurring through synaptonemal complex entanglements. Better microscopy techniques may help to resolve whether increased interlocks form in the absence of motion in the future. This motion could also help prevent ectopic recombination, since mutants defective in chromosome motion have a slight increase in ectopic recombination (Harper *et al.* 2004; Conrad *et al.* 2008; Wanat *et al.* 2008; Goldman and Lichten, 2000; Schlecht *et al.* 2004). For more information on the mechanisms and roles of chromosome motion during meiosis, see Chapters 2 and 3.

Centromere Pairing

During early meiosis, centromeres of nonhomologous chromosomes pair, followed by a reorganization where homologous centromere pairing occurs (Stewart and Dawson, 2008). The number of foci marking centromeres will remain stable throughout prophase in budding yeast, while the level of homologous interactions increases. This suggests that dissociation of nonhomologous interactions and reassociation of homologous chromosomes is a very quick process. In wheat, a hexaploid plant, this switch progresses through four steps: initial clustering of centromeres, nonhomologous pairing, homeologous clustering (through slightly diverged sequences), and finally homologous centromere pairing (Stewart and Dawson, 2008). Interestingly, the central element of the synaptonemal complex, Zip1, appears to play a major role in centromere pairing during meiosis in budding yeast. Zip1 foci in a *spo11Δ* background, where DSBs do not occur, were found to localize at or near centromeres. Furthermore, when

looking at a centromeric marker, wild type cells in prophase of MI will have 16 foci: one for each homolog. However, in a *zip1Δ* background, 32 foci are observed, suggesting a total absence of centromere pairing (Tsubouchi and Roeder, 2005). Similarly, when a kinetochore marker is observed, 16 foci are observed in meiotic wild type cells, and this number increases to 23 in *zip1* (Gladstone *et al.* 2009). Zip1-dependent pairing is both homologous and nonhomologous: In a *spo11Δ* haploid, 8 centromeric foci are seen, suggesting centromere pairing of nonhomologous chromosomes. However, in a *zip1* background, 16 foci are observed (Tsubouchi and Roeder, 2005). Cohesins, which will be discussed further below, also play a role in promoting nonhomologous centromere pairing. Deletion of Rec8, a meiosis-specific member of the cohesin complex, confers a similar phenotype to *zip1* mutants, showing a lack of centromere coupling (Klein *et al.* 1999; Bardhan *et al.* 2010). Interestingly, Zip1 and Rec8 appear to act in the same pathway to promote centromere pairing, as the double mutant looks similar to either single mutant alone. Furthermore, Rec8 may play a role in recruiting Zip1 to centromeres, as Rec8 binds at centromeres during meiotic S phase, before Zip1, and binding of Zip1 to centromeres is reduced in the absence of Rec8 (Bardhan *et al.* 2010).

What role might centromere pairing play? Zip1-dependent centromere pairing is not directly needed for homolog pairing, since homolog pairing still occurs in *zip1* mutants (Tsubouchi and Roeder, 2005). Furthermore, FISH studies have shown that telomeric regions pair earlier than centromere pairing, and the homologous centromere associations are most likely driven by these initial pairings at other regions of the chromosomes (Corredor *et al.* 2007; Clarke and Carbon, 1983). Finally, swapping out centromeric regions has no effect on chromosome pairing or segregation (Clarke and Carbon, 1983). However, there is evidence that centromere pairing might help correctly orient chromosomes on the meiotic spindle. In the absence of a

spindle checkpoint, chromosome disjunction rates increase from 10% to ~50% in *zip1* (Gladstone *et al.* 2009). This suggests that a major role of centromere pairing is to increase the chances of a bipolar spindle orientation on the first attempt, particularly in achiasmate chromosomes (see distributive disjunction). Additionally, early nonhomologous centromere pairing could play a role in suppressing crossovers near centromeres, which is detrimental to chromosome segregation, because it could sequester centromeric regions away from their recombination partners (Rockmill *et al.* 2006; Stewart and Dawson, 2008).

In *C. elegans*, which do not have canonical centromeres (reviewed in Dernberg, 2001), specific pairing centers have evolved for each chromosome that may provide similar roles to centromere pairing. Pairing centers were first identified through observations of recombination and pairing between chromosomes with translocations or duplications and deletions near one end of the chromosome (Rosenbluth and Baille, 1981; McKim *et al.* 1988; Herman and Kari, 1989; McKim *et al.* 1993; Villeneuve, 1994; MacQueen *et al.* 2005). Later work has identified specific zinc-finger proteins that bind to pairing centers, namely ZIM-1, ZIM-2, ZIM-3, and HIM-8. Mutations in these genes can confer defects in homolog pairing, recombination, and segregation (Phillips *et al.* 2005; Phillips and Dernburg, 2006). Specific target sequences have also been identified as binding sites for each of these proteins (Phillips *et al.* 2009). It is thought that these pairing centers and their associated proteins help stabilize chromosome pairing in a synapasis-independent manner (MacQueen *et al.* 2002; MacQueen *et al.* 2005).

Cohesins

Cohesion between sister chromatids during meiosis plays an essential role in preventing sisters from disjoining during meiosis I (reviewed in Lee and Orr-Weaver, 2001), and in

maintaining associations between chiasmate chromosomes (Figure 1.1; Buonomo *et al.* 2000; Bickel *et al.* 2002; Hodges *et al.* 2005). The cohesion complex is composed of four subunits in meiosis: structural maintenance of chromosome proteins Smc1 and Smc3, a kleisin subunit (Rec8 in budding yeast and mammals, reviewed in Barbero, 2009), and a stromalin subunit Scc3 (Figure 1.3A; Michaelis *et al.* 1997; Klein *et al.* 1999; Parisi *et al.* 1999; Watanabe and Nurse, 1999; Pasierbek *et al*. 2001; Eijpe *et al.* 2003; reviewed in Barbero, 2009). Interestingly, Rec8 function in cohesion is independent of its function in centromere pairing (see above) (Toth *et al.* 2000; Brar *et al.* 2008). Cohesins are loaded onto chromosomes at an organism-specific time: G1-S phase in budding yeast, and telophase in most other organisms (reviewed in Nasmyth, 2001). Loading of cohesins is dependent on the adherin complex, Scc2/Scc4 (Ciosk *et al.* 2000; Watrin *et al.* 2006). Based on electronic microscopy images, it is thought that the SMC subunits form a ring around the chromatids, either with one ring enclosing both chromatids or with two connected rings each encircling a single chromatid (Gruber *et al.* 2003; Zhang *et al.* 2008; Figure 1.3A).

Control of removal of cohesin is critical to allow proper segregation of homologs during the first meiotic division, and segregation of sister chromatids during the second meiotic division (Figure 1.1). During the metaphase/anaphase transition of meiosis I, cohesion is lost along chromosome arms, allowing homologs to separate (Buonomo *et al.* 2000). Cohesion near centromeres is retained until anaphase II, ensuring that sister chromatids do not separate during the first meiotic division (Figure 1.3B; Page *et al.* 2006; Revenkova and Jessberger, 2006; Marston and Amon, 2004). Control of cohesin removal is regulated by the shugoshin family of proteins (Sgo1 in budding and fission yeast, MEI-S332 in Drosophila; reviewed in Clift and Marston, 2011), which protects Rec8 from cleavage by separase, which opens the ring structure

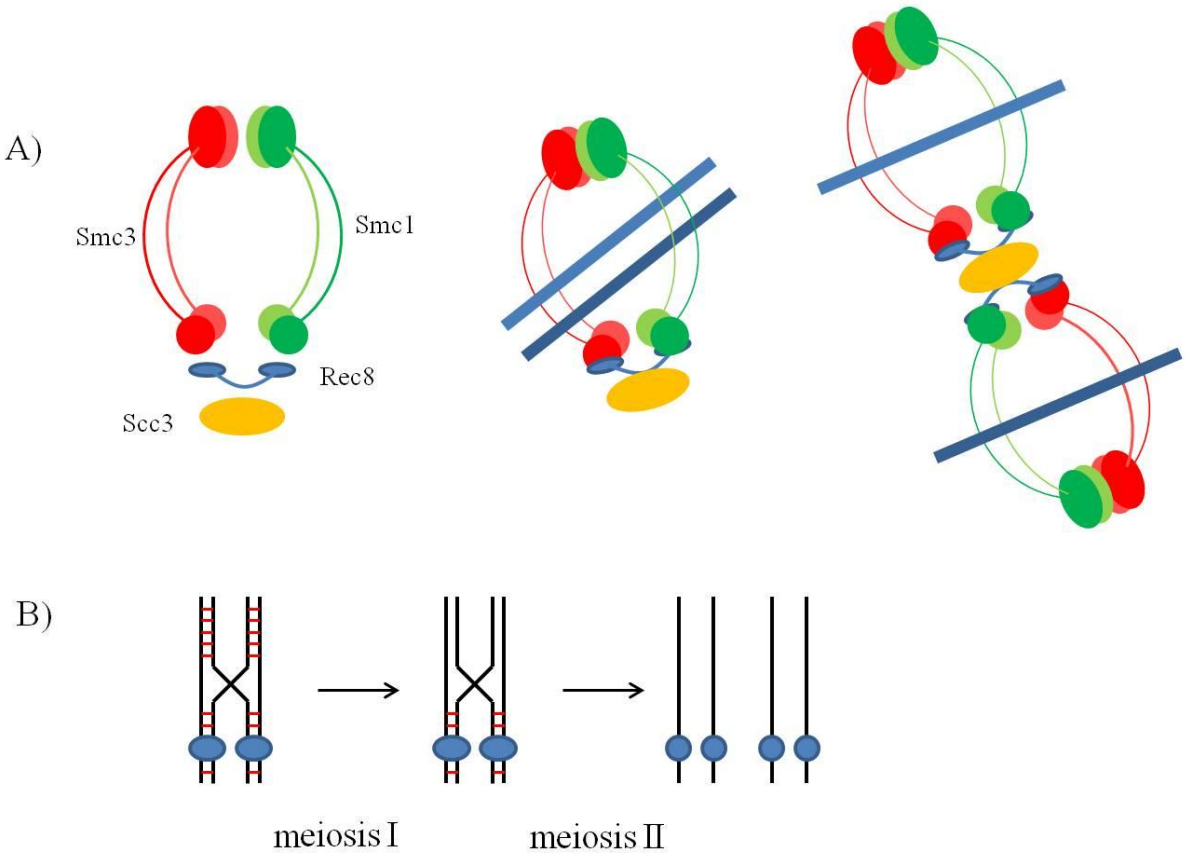

Figure 1.3. Meiotic Cohesion. A) The cohesin ring complex is shown with subunits labeled (left) and interacting in two different forms. Center, one cohesin ring surrounds both chromatids. Right, two connected cohesin rings each surround a single chromatid. Figure modified from Barbero, 2011. B) Cohesin removal during meiosis. Blue circles represent centromeres, red lines represent cohesin. Cohesin is initially removed from chromosome arms during meiosis I, but retained at the centromeres. During meiosis II, cohesin is removed from centromeres, allowing sister chromatids to segregate.

of the cohesin complex, releasing chromatid associations. Sgo1 was first identified in a screen in fission yeast, looking for genes that when overexpressed, allowed Rec8 to persist on chromosomes, resulting in failure to separate chromosomes (Kitajima *et al.* 2004). *sgo1* mutants in both budding and fission yeast do not retain cohesion of sisters during meiosis I, resulting in random chromosome segregation during meiosis II (Katis *et al.* 2004; Kitajima *et al.* 2004; Marston *et al.* 2004; Rabitsch *et al.* 2004). Sgo1 is able to protect cohesin cleavage by recruiting a protein phosphatase 2A subunit, PP2A-B', to centromeres. In fact, artificially tethering PP2A-B' to centromeres in the absence of Sgo1 is sufficient to protect Rec8 from separase cleavage (Kitajima *et al.* 2006; Riedel *et al.* 2006). Furthermore, in an *sgo1* mutant unable to contact PP2A-B', called *sgo1-3A*, PP2A-B' is unable to localize to centromeres, and Rec8 is cleaved, despite the presence of *sgo1-3A* at the centromeres (Xu *et al.* 2009). PP2A-B' is able to prevent Rec8 from being phosphorylated, which is necessary for separase cleavage (Riedel *et al.* 2006; Brar *et al.* 2006; Katis *et al.* 2010). In addition, it is thought that the shugoshin-PP2A-B' complex acts directly to dephosphorylate Rec8 (Ishiguro *et al.* 2010).

Multiple kinases have been shown to be important for phosphorylation of Rec8, promoting its cleavage by separase. A polo-like kinase, called Cdc5, casein kinase CK1, and Db4f-dependent Cdc7 kinase (DDK) have all been shown to phosphorylate Rec8 in meiosis I (Clyne *et al.* 2003; Lee and Amon, 2003; Katis *et al.* 2010; Ishiguro *et al.* 2010). CK1 and DDK are thought to be the main kinases responsible for phosphorylation, as the double mutant reduces phosphorylation of Rec8 to similar levels as a non-phosphorylatable Rec8 mutant (Katis *et al.* 2010). Furthermore, Rec8 cleavage is still able to occur in *cdc5* mutant cells (Brar *et al.* 2006).

The spindle checkpoint protein Bub1 is important for localizing Sgo1 on centromeres (Bernard *et al.* 2001; Riedel *et al.* 2006; Kitajima *et al.* 2004; Kiburz *et al.* 2005). Bub1

phosphorylates histone H2A, which is necessary for Sgo1 localization to centromeres (Kawashima *et al.* 2010). This role is independent of its checkpoint function, as mutating the kinase domain of Bub1 delocalizes Sgo1 without affecting the spindle checkpoint (Fernius and Hardwick, 2007; Kawashima *et al.* 2010; Perera and Taylor, 2010). Additional proteins, such as Aurora B, the chromosomal passenger complex, and the heterochromatin protein HP1 are also known to recruit shugoshin to centromeres in an organism-dependent manner (Resnick *et al.* 2006; Huang *et al.* 2007; Tsukahara *et al.* 2010; Monje-Casas *et al.* 2007; Yu and Koshland, 2007; Yamagishi *et al.* 2008). It is unclear how these factors interact to promote shugoshin localization and function.

Shugoshin protection of Rec8 must eventually be eliminated in order for sister chromatids to segregate during MII (Figure 1.3B). In fission yeast, the anaphase-promoting complex/cyclosome (APC/C) is responsible for degrading Sgo1, leaving Rec8 unprotected from phosphorylation (Kitajima *et al.* 2004). However, simple degradation of shugoshin is unlikely to be how shugoshin is inactivated. Ectopic expression of Sgo1 in fission yeast during meiosis II and preventing shugoshin dissociation from centromeres in *Drosophila* or non-degradable Sgo1 in human cells still allows sister chromatid separation (Rabitsch *et al.* 2004; Gregan *et al.* 2008; Karamysheva *et al.* 2009). Instead, two labs proposed that tension provided by proper spindle orientation at MII might inactivate shugoshin (Gomez *et al.* 2007; Lee *et al.* 2008). In addition, fission yeast mutants that allow bi-orientation of sister chromatids during meiosis I lose centromere cohesion prematurally (Vaur *et al.* 2005).

Cohesins have been shown to be necessary to prevent telomere separation prior to anaphase in mitosis. In budding yeast mutants defective for cohesins, telomeres have been shown to separate more frequently, and to a larger degree, than centromeres (Antoniacci and

Skibbens, 2006). Furthermore, yeast lacking Rec8 and mice lacking SMC1β have defects in telomere clustering (Trelles-Sticken *et al.* 2005; Revenkova *et al.* 2004; Scherthan, 2007).

Cohesion between chromatids decreases with the age of the organism, which could lead to increases in chromosome missegregation (Jeffreys *et al.* 2003; Subramanian and Bickel, 2008; Hassold and Hunt, 2001). In support of this, mutations in *Drosophila* cohesion genes, *ORD* and *SMC1*, have been shown to be associated with increased levels of nondisjunction during MI in aged oocytes. The increase in nondisjunction events is independent of crossovers, and appears to be due to pairing defects in centromere-proximal regions (Subramanian and Bickel, 2009; Subramanian and Bickel, 2008). Furthermore, cohesion levels were shown to gradually decline during prophase arrest in mouse oocytes. This loss was made worse in cohesin mutants in mouse, correlating with increases in chromosome nondisjunction (Lister *et al.* 2010).

Besides supporting chromatid interactions during meiosis, cohesins also play additional roles in the cell. Shugoshins have been shown to play a role in the tension-sensing mechanism (Gomez *et al.* 2007; Huang *et al.* 2007; Lee *et al.* 2008). Cohesins also play roles in DNA damage repair (Watrin and Peters, 2006), heterochromatin formation (Gullerova and Proudfoot, 2008), neuronal development (Takagi *et al.* 1997; Seitan *et al.* 2006), and gene expression (Donze *et al.* 1999; Lara-Pezzi *et al.* 2004; Wendt *et al.* 2008). Additionally, it has been proposed that holding together sister chromatids at the centromeres throughout meiosis may provide a barrier to sister-sister chromatid recombination, which is downregulated in meiosis (Smith and Roeder, 1997; Schwacha and Kleckner, 1997).

The Spindle checkpoint

While a lot of different mechanisms are in place to ensure that chromosomes pair and are able to segregate properly at the correct time, all this is in vain if the homologs are not able to correctly attach to the spindle poles. Nicklas (1974) proposed that homologs, forming a bivalent, have a large chance of correctly orientating on the spindles initially, due to the nature of the bivalent. Because of the cross-shape created by two homologs during meiosis, if one kinetochore faces towards one pole, the other kinetochore will face the opposite pole. The pole each kinetochore faces is most likely the one to which it will be attached (Figure 1.4; Nicklas, 1974; Ostergren, 1951). Micromanipulations of grasshopper chromosomes confirmed this proposal. In addition, manipulating chromosomes such that both kinetochores face the same direction led both kinetochores to become attached to the same spindle (Nicklas, 1967 and 1974).

In an ideal situation, each kinetochore would be attached to a different pole, so that during anaphase, each homolog would be pulled to opposite sides of the cell, contributing to proper disjunction. However, occasionally, chromosomes fail to attach to the spindle pole, or both homologs attach to the same spindle pole. In order to prevent nondisjunction from occurring in these cases, a spindle checkpoint occurs, which halts meiosis until proper chromosome configuration is achieved (Figure 1.5).

There are two main ideas of what the spindle checkpoint senses. The first is that the spindle checkpoint senses tension between the kinetochores (Nicklas, 1967 and 1974). This tension would be propogated through the meiotic spindles, with crossovers playing a key role in creating a physical connection to produce tension between homologs. The second model is that the spindle checkpoint senses unattached microtubules. Experiments that have destroyed an unattached kinetochore, when all others are connected to chromosomes, do not elicit a checkpoint in somatic cells. This leaves an "unpaired" kinetochore, which would not be under

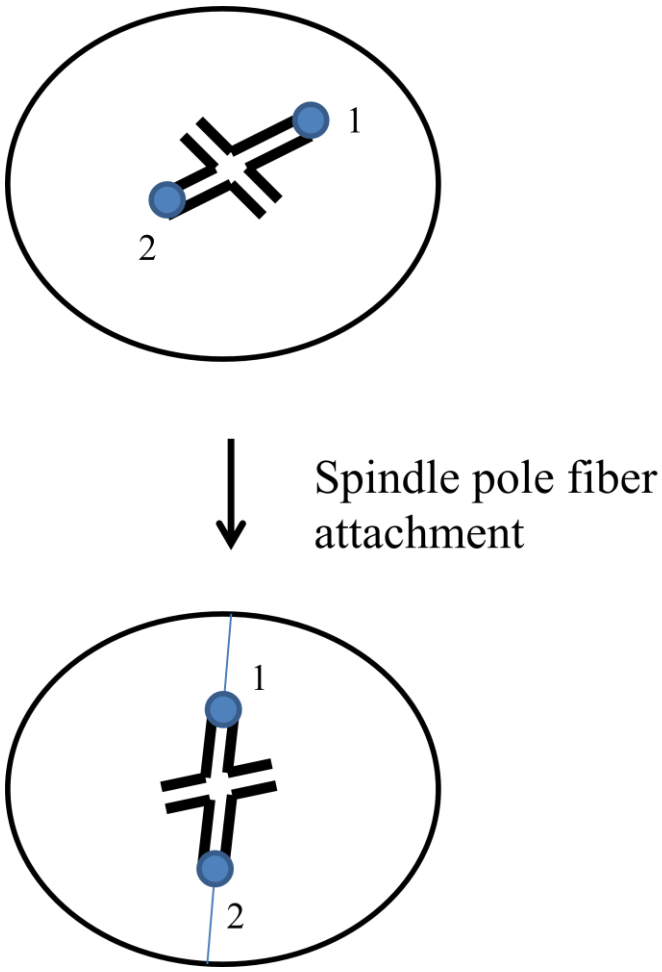

Figure 1.4. Kinetochore orientation. Due to the nature of bivalents during meiosis, one kinetochore is most likely to be facing a particular pole, while the other kinetochore will face the opposite pole. This allows spindle assembly to more easily "catch" the kinetochore facing the spindle pole, allowing for correct assembly of the meiotic spindles. Kinetochores are shown as blue circles. Chromosomes are labeled "1" and "2" in order to track spindle fiber attachment. Figure modified from Nicklas, 1974.

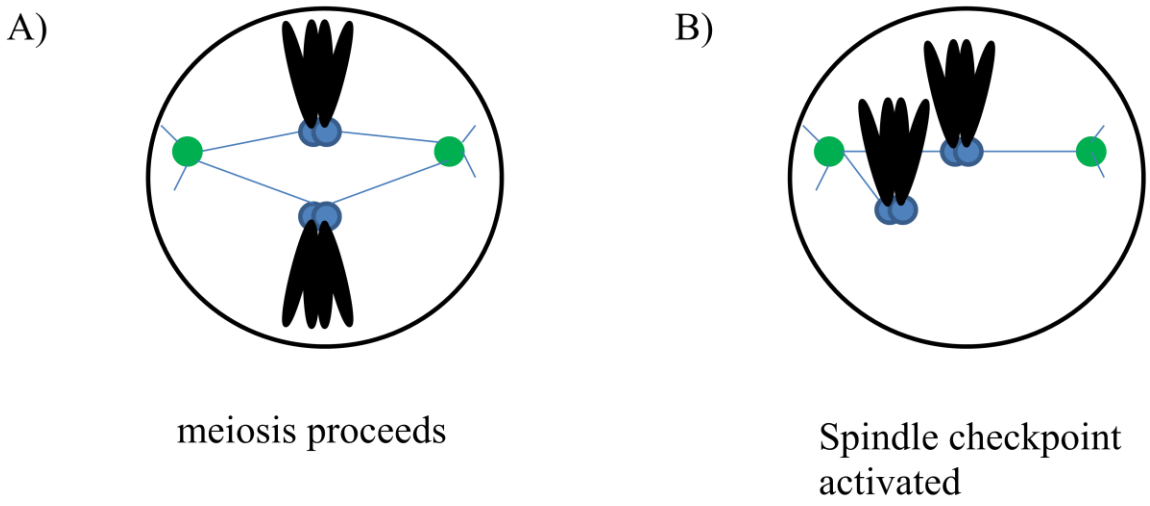

Figure 1.5. The spindle checkpoint. A) Two chromosome pairs are shown. Chromosomes are correctly orientated on the meiotic spindle, with each kinetochore of each homolog pair attached to a distinct spindle, resulting in proper tension. B) One homolog pair is correctly attached as seen in A). However, the second homolog pair is only attached to one spindle. This leads to activation of the spindle checkpoint. Centromeres are shown in blue and spindle pole bodies in green. Figure modified from Taylor *et al.* 2004.

tension (Rieder *et al.* 1995). In support of this, Mad2 in grasshopper and maize, a spindle checkpoint protein, localizes to unattached kinetochores (Yu *et al.* 1999). However, this localization may not hold across all species, since Mad2 remains at kinetochores throughout meiosis I in mice (Kallio *et al.* 2000).

A variety of proteins have been identified that are important for the spindle checkpoint. Most of these proteins are located at the kinetochores, making them ideal components to sense kinetochore/microtubule interactions (reviewed in Sun and Kim, 2011). Mad1, Mad2, Bub1, and Bub3 are known components of the spindle checkpoint in a variety of organisms. In yeast and mice, these mutants have chromosome segregation defects and complete anaphase I more quickly than WT, presumably due to their role in inhibiting APC/C activation and preventing cyclin B and securin degredation (Cheslock *et al.* 2005; Shonn *et al.* 2000; Homer *et al.* 2005; Sun and Kim, 2011).

While most of these proteins localize to the kinetochore under normal conditions, localization to the kinetochore is neither necessary nor sufficient for the spindle checkpoint to occur. A dominant negative *mad1* mutant allows anaphase to continue, even while Mad2 is still bound to the kinetochore (Canman *et al.* 2002; Ditchfield *et al.* 2003). Likewise, mutations can be found that delocalize spindle checkpoint proteins from the kinetochore, and the arrest still takes place (Martin-Lluesma *et al.* 2002).

The kinetochore components most likely halt anaphase by inhibiting cyclin activity. Indeed, Mad2 has been found to interact with Cdc20, an activator of APC/C (Hwang *et al.* 1998; Kim *et al.* 1998; reviewed in Taylor *et al.* 2004). By binding to and sequestering Cdc20, Mad2 may prevent APC/C activation, preventing anaphase. Depletion of Bub1 induces cyclin B degredation, leaving to early anaphase (Yin *et al.* 2006; McGuinness *et al.* 2009). Bub1 is also

important for holding together sister kinetochores during meiosis I, probably through its role in localizing Sgo1 and Sgo2 (see above discussion on cohesins; Bernard *et al.* 2001; McGuiness *et al.* 2009; Kitajima *et al.* 2004; Kiburz *et al.* 2005).

The spindle checkpoint may be particularly important when meiotic crossovers do not occur near the centromere. Lacefield and Murray found that in *mad2Δ* cells in yeast, chromosomes that segregated properly had more crossovers near the centromeres than in WT. Additionally, an artificial tether placed near centromeres between homologous chromosomes was able to partially rescue a nondisjunction phenotype in these cells (Lacefield and Murray, 2007). This suggests that in the absence of the spindle checkpoint, crossovers near the centromere are critical for chromosome segregation.

Besides the checkpoint proteins, additional proteins help regulate the attachment of the microtubules to the kinetochores, ensuring proper chromosome disjunction. The Ndc80 complex in yeast is important for recruiting some of the spindle checkpoint proteins to the kinetochore (Ciferri *et al.* 2007; Tanaka and Desai, 2008). Ndc80 may also be important for the formation of the spindles (Diaz-Rodriguez *et al.* 2008; Sun *et al.* 2011). The chromosomal passenger complex, consisting of Aurora B, INCENP, survivin and borealin has been shown to provide a scaffold that can recruit the spindle checkpoint proteins in male mice (Parra *et al.* 2009). Aurora B, in particular, is important for regulation of the spindle checkpoint proteins (George *et al.* 2006; Swain *et al.* 2008; Vogt *et al.* 2009; Lane *et al.* 2010). This role may be due to its involvement in cohesion (Yu and Koshland, 2007). Finally, the monopolin complex in yeast is important for proper spindle attachments during meiosis. Without this complex, sister kinetochores in meiosis I will attach to opposite spindle poles, similar to mitosis. These sister

chromosomes are unable to segregate, since they are still being held together by cohesins, leading to meiotic catastrophe (Rabitsch *et al.* 2003; Toth *et al.* 2000).

As described above, a lot of proteins are important for regulating the meiotic spindle checkpoint. The exact relationships and interactions between these proteins are still unclear. Localization of these proteins appears to be species specific, and investigating whether this results in different roles for the proteins in each organism will be an interesting area of investigation. Furthermore, there appears to be a strong connection between cohesins and the spindle checkpoint machinery. Identifying the role and involvement of cohesins to the checkpoint will be important in future work.

Distributive Disjunction

While the recombination-based mechanisms discussed above are the major players in chromosome segregation during meiosis in most organisms, achiasmatic mechanisms, such as distributive disjunction, play a backup role in most organisms. In fact, distributive disjunction is the major mechanism of homolog disjunction in meiosis in male *Drosophila* and for segregating the fourth chromosome in female *Drosophila* (Grell, 1962 and 1976; McKee, 1996).

Chiasmata are thought to play an important role in maintaining chromosomes at the metaphase plate by providing tension for the opposing forces acting on the kinetochores of each homolog (Nickas, 1975). Studies in Drosophila meiotic mutants in which all homologs are achiasmate have shown that these chromosomes move towards the spindle poles, away from the metaphase plate (Jang *et al.* 1995; McKim *et al.* 1993). This has been shown in wild-type by cytology, where the obligate achiasmate chromosome 4 is displaced from the main chromosomal mass. This would allow the homologs to pair independently of the main chromosome mass, and

help to ensure their disjunction (Puro and Nokkala, 1977; Theurkauf and Hawley, 1992). However, more recent data has shown by coordinating dorsal appendage length, which is a good indicator of oocyte age (King, 1970), that this outlying position of achiasmate chromosomes is an intermediate phenotype, and these chromosomes do aggregate at the metaphase plate at later stages in meiosis (Gilliland *et al.* 2009). It is still likely that this temporary segregation from the main mass of chromosomes helps in disjunction. It is unclear how these chromosomes eventually do stabilize at the metaphase plate without chiasmata, however the kinesin-like protein Nod likely plays a role in Drosophila (Matthies *et al.* 2001; Theurkauf and Hawley, 1992; Levesque and Compton, 2001).

Unlike in *Drosophila* males, distributive disjunction does not appear to play the primary role in other organisms. However, it does appear to serve as an important backup to chromosome segregation. Such a backup system has been analyzed in *Saccharomyces cerevisiae* monosomic strains. When strains doubly monosomic for both chromosomes I and III were analyzed for spore viability patterns, 89% of the asci resulted in 0 viable: 4 inviable spores. This pattern should only result if each monosome segregates away from the other monosomic chromosome, leaving each spore void of a particular chromosome, causing lethality (Figure 1.6). Similar results were obtained for a bisected chromosome and a *CEN* plasmid, suggesting that distributive disjunction is not reliant on chromosome size, unlike in *Drosophila* (Guacci and Kaback, 1991; Carpenter, 1991).

The mechanism of distributive disjunction in budding yeast has been analyzed cytologically. While in wild type cells, 16 SCs are observed during pachytene, in strains monosomic for both chromosomes I and III, only 14 full length SCs are formed (Loidl *et al.* 1994). In these strains, an additional structure is observed, which could be the two monosomic

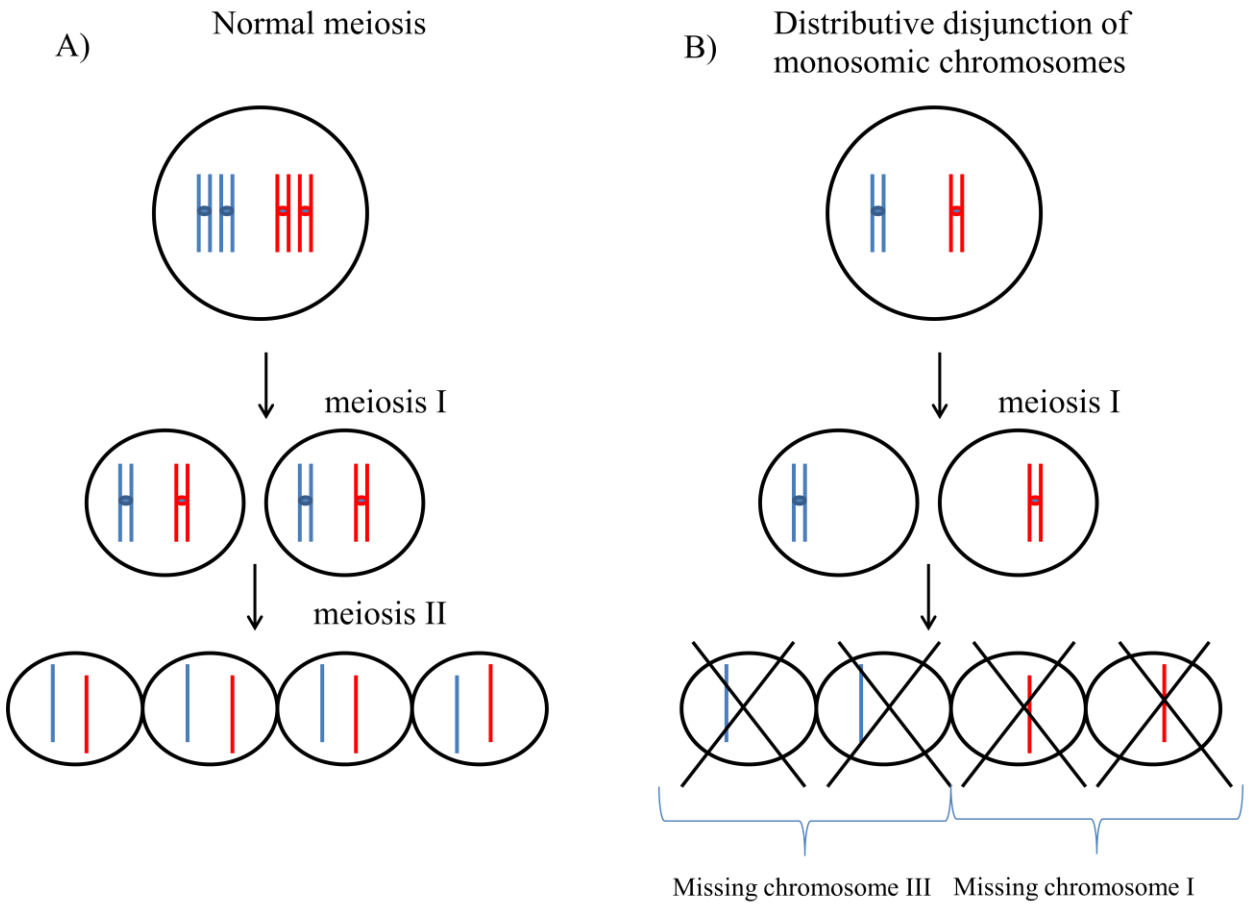

Figure 1.6. Distributive Disjunction. A) Chromosome segregation in a normal meiosis is shown, similar to Figure 1.1A, but with two homolog pairs (chromosome I in blue, chromosome III in red). Homologs disjoin at meiosis I and sister chromatids segregate at meiosis II, leading to haploid gametes with one of each chromosome. B) Chromosome segregation of monosomic chromosomes (chromosome I in blue, chromosome III in red) is shown. During the first meiotic division, each homolog segregates away from the other, resulting in each meiosis I product missing a particular homolog. At the second meiotic division, sister chromatids segregate normally. However, due to errors in meiosis I, each gamete is missing a particular chromosome, resulting in cell death.

chromosomes interacting. In support of this, FISH experiments showed that in most cases (69%), the probes for chromosomes I and III overlapped, suggesting a physical interaction between the two chromosomes (Loidl *et al.* 1994). These results agree closely with the genetic data above. If chromosomes distributively disjoin due to physical interactions 69% of the time, and the other 31% segregate randomly, approximately 85% (69% + 15% (1/2 of 31%)) would appear to be distributively disjoining by genetic analysis (Loidl *et al.* 1994; Guacci and Kaback, 1991).

Distributive disjunction only applies to monosomic strains in budding yeast. Specifically, studies in budding yeast strains trisomic for chromosomes I and VI exhibit random segregation (Guacci 1990). During meiosis, homologous trisomes can create trivalent pairing structures, which may interfere with the two "extra" chromosomes from interacting and disjoining distributively (Shafer *et al.* 1971; Culbertson and Hentry, 1973; Guacci and Kaback, 1991). In *Drosophila*, three achiasmate elements can distributively disjoin, but they do so in a size-dependent manner (Carpenter, 1991).

While details about how the nonhomologous chromosomes may physically interact are still unknown, mechanisms for distributive disjunction involving spindle motors and kinetochore components have been proposed. In crickets, there is a microtubule bridge that connects the X kinetochore to an autosomal kinetochore, helping the chromosomes "communicate" along the spindles through unknown protein interactions (Kubai and Wise, 1981). While it is not known whether these same interactions occur between achiasmate chromosomes in *Drosophila*, the same type of communication takes place. This would provide a bond, similar to a chiasma, to equalize forces from the microtubules. Once a physical connection has been made, either through microtubule bridges or unknown proteins, the polar ejection forces could push these

outlying chromosomes (see above) away from the spindle poles, back towards the metaphase plate (reviewed in Carpenter 1991; Rieder and Salmon, 1994). Two members of the kinesin heavy chain family have been implicated in chromosome segregation in *Drosophila* (Zhang *et al.* 1990; Endow *et al.* 1990; McDonald and Goldstein, 1990). These proteins could be helpful in stabilizing microtubule interactions with achiasmate chromosomes, helping to ensure proper disjunction. Currently, the mechanism for distributive disjunction is unknown, and determining how these chromosomes interact with each other and the spindle poles in order to ensure proper segregation is an important area of study.

Centromere pairing, discussed above, is also thought to play a major role in distributive disjunction. Achiasmate chromosomes were shown to associate at their centromeres in budding yeast. Disruption of these associations led to increases in nondisjunction, suggesting these interactions are important for proper segregation (Kemp *et al.* 2004). The synaptonemal complex proteins Zip1, 2, and 3 are important for chromosome disjunction of achiasmatic chromosomes, as well. Using two homeologous chromosome Vs, (from *S. carlsbergensis* and *S. cerevisiae)* and GFP tags near centromeres, *zip1*, *zip2*, and *zip3* mutants were shown to nondisjoin achiasmatic chromosomes 45% of the time, compared with 25% for wild type (Gladstone *et al.* 2009). Furthermore, in wild type, 56% of homeologous centromeres pair; however, in *zip1*, this level is reduced 5-fold, suggesting a direct role of Zip1 in centromere pairing (Newnham *et al.* 2010). Centromere pairing of achiasmatic chromosomes in budding yeast begins to dissociate in early metaphase, however centromere pairing in *Drosophila* is maintained longer. This could be a reason why distributive disjunction is more efficient in *Drosophila* (~99%) than in budding yeast (~90%) (Kemp *et al.* 2004; Gilliland *et al.* 2007; Hawley and Theurkaul, 1993).

Heterochromatin threads

Chromosomes can also be held together by thin DNA bridges, which have been observed in both mitosis and meiosis. In mitosis, these DNA threads connect sister kinetochores, and may originate from either incompletely replicated DNA or from fully replicated DNA that is still intertwined (Chan *et al.* 2007). The threads are sensitive to treatment with DNaseI, but not RNase A in human cells, suggesting they are composed of DNA; however, the threads are so thin that they are often not visible by DAPI staining (Chan *et al.* 2007). Interestingly, helicases are known to localize to these threads during anaphase in human cell lines. PICH (Plk1-interacting checkpoint helicase), BLM (a member of the RecQ helicase family), and Incenp (a centromere protein) all localize to these bridges and may play a role in dissolving the threads (Baumman *et al.* 2007; Chan *et al.* 2007; Wang *et al.* 2008). In BLM^- human cells, DNA bridges accumulate, which could lead to genomic instability (Hoffelder *et al.* 2004; Chan *et al.* 2007).

The existence of DNA tethers in meiosis was proposed by Forer in 1966. Forer found that by irradiating kinetochore fibers in crane-fly spermatocytes, chromosome segregation was disrupted (Forer, 1966; Forer and Koch, 1973). More recent studies in crane-fly spermatocytes show that chromosome arms during anaphase of meiosis I appear tethered to their partners, with trailing arms stretching backwards. By perfoming laser microsurgery to detach these stretched arms, the authors showed an immediate and rapid movement of the detached chromosome fragment towards the opposite spindle pole (LaFountain *et al.* 2002). Unlike the centromere-mediated DNA bridges observed in mitosis, these chromosome attachments appear to be mediated by a telomere-proximal element. Cutting a chromosome arm twice, once to detach from the main chromosome, and then recutting that fragment again, showed that only the telomere-proximal fragment continued poleward movement, while the intermediate fragment

halted when the second cut was made. Furthermore, direct laser ablation of the telomere halted motion, while cutting the kinetochore had mixed results, with only some chromosome fragments exhibiting backward motions (LaFountain *et al.* 2002). The motion towards the opposite homolog of these chromosome fragments when released from the main chromosome body suggests an elastic tether that holds homologs together during meiosis.

Previous studies of achiasmate homologs in *Drosophila* have shown that heterochromatin homology between homologs is important for proper segregation; in fact, heterochromatic sequences play a role in the physical interaction between homologs (Hawley *et al.* 1993; Dernberg *et al.* 1996). Threads have been observed between the X and Y chromosomes (Cooper, 1964), the 4th chromosomes, (Hartl *et al.* 2008; Hughes *et al.* 2009), between two X chromosomes, and between an X and 4th chromosome (Hughes *et al.* 2009). Using FISH probes, it was shown that these threads are comprised at least in part of heterochromatin (Hughes *et al.* 2009). While this last interaction between the X and 4th chromosome could be an artifact, there is a correlation in nondisjunction rates between these two chromosomes, and an extra portion of either chromosome can increase nondisjunction rates of the other chromosome (Baker and Hall, 1976; Zitron and Hawley, 1989; Sekelsky *et al.* 1999; Sandler and Novitski, 1956; Grell, 1976). Genetic interactions between chromosomes suggest that the physical linkage may be real. Similar to the DNA threads observed in mitosis, Incenp was found to localize to heterochromatin threads in Drosophila female meiosis, suggesting a common function (Hughes *et al.* 2009).

What role in chromosome segregation could these tethers be playing? The tethers could be serving to provide communication between homologs, likely through protein interactions (Ilagen *et al.* 1997), or the tension that the tethers create could be necessary for stabilizing kinetochore attachments. Maintenance of tension has been shown to be important for silencing

of the spindle assembly checkpoint (Hui-Ching Wang *et al.* 2008), and DNA tethers present in anaphase could help maintain this tension (Nicklas, 1997; LaFountain *et al.* 2002; Gorbsky and Ricketts, 1993; Waters *et al.* 1998; Clute and Pines, 1999; Hui-ChingWang *et al.* 2008; Hughes *et al.* 2009). Additionally, chromosome tethers present at centromeres could assist centromere cohesion in ensuring sister chromatid pairing (Diaz-Martinez *et al.* 2007; Hui-Ching Wang *et al.* 2008).

Evidence from DNA threads in mitosis suggest that topoisomerases (topo IIα and topo IIIα;) are involved in resolving the DNA threads (Baumman *et al.* 2007; Hui-Ching Wang *et al.* 2008; Chan *et al.* 2007). However, it is also possible that the threads are cut by a nuclease, the DNA is brought back in towards the main chromosomal mass by motor proteins, or that the forces exerted on segregating chromosomes is enough to break the thin strands directly (Hui-Ching Wang *et al.* 2008).

While initial observations of threads between chromosomes were made long ago (Cooper, 1964), it has only been recently that the functions of these threads have been investigated. While initial evidence suggests that the mitotic and meiotic threads are formed by a similar mechanism for a similar purpose (Hughes *et al.* 2009; Wang *et al.* 2008), most of the details still need to be worked out. Exactly how these threads are made and resolved, what they are composed of, and what purpose they serve are all important areas of investigation. Furthermore, it is unclear whether these threads exist in all species, or whether they exist in all cells within a particular species.

Conclusions

While crossing over is thought to be the major mechanism in ensuring disjunction of homologs during MI, there are a lot of backup mechanisms in place to ensure that homologs pair and segregate properly. Interestingly, many of the mechanisms have overlapping components. Determining how each component works by itself and in conjunction with the other mechanisms will be an important area of study in order to understand how chromosomes nondisjoin, leading to aneuploidy and human disease.

I investigated two mechanisms to ensure chromosome disjunction during meiosis in budding yeast. First, I show that defects in telomere-led chromosome motion correlate with defects in homolog pairing, suggesting that telomere-led chromosome motion may promote homolog pairing, either directly or indirectly, by removing interlocks. I suggest that small amounts of motion over an extended period of time are sufficient to promote homolog pairing (Chapters 2 and 3). Second, I analyzed crossover regulation with a set of ATPase mutants of *mlh3* (Chapter 4). I found that decisions to maintain the obligate crossover have already been made by the time Mlh1/Mlh3 acts, resulting in a linear relationship between crossing over and spore viability. This is in contrast to previously published work from the Alani lab, where *msh4/5* mutants were able to maintain spore viability for up to a two-fold reduction in crossing over, suggesting that the obligate crossover is still being formed at this step (Nishant *et al*. 2010). As discussed above and in the following chapters, both telomere-led chromosome motion and crossover regulation are important mechanisms in ensuring proper segregation of chromosomes.

REFERENCES

Allers, T., M. Lichten, 2001 Intermediates of yeast meiotic recombination contain heteroduplex DNA. Mol. Cell 8: 225-231.

Antoniacci, L. M., R. V. Skibbens, 2006 Sister-chromatid telomere cohesion is non-redundant and resists both spindle forces and telomere motility. Curr Biol 16: 902-906.

Baker, B. S., J. C. Hall, 1976 Meiotic mutants; genetic control of meiotic recombination and chromosome segregation. Genetics and Mol Biology of Drosophila, Vol 1a pp 351-434.

Barbero, J. L., 2009 Cohesins: chromatin architects in chromosome segregation, control of gene expression and much more. Cell Mol Life Sci 66: 2025-2035.

Bardhan, A., 2010 Many functions of the meiotic cohesin. Chomosome Res 18: 909-924.

Bass, H. W., W. F. Marshall, J. W. Sedat, D. A. Agard, and W. Z. Cande, 1997 Telomers cluster de novo before the initiation of synapsis: a three-dimensional spatial analysis of telomere positions before and during meiotic prophase. J Cell Biol 137: 5-18.

Bass, H. W., O. Riera-Lizarazu, E. V. Ananiev, S. J. Bordoli, H. W. Rines, *et al*., 2000 Evidence for the coincident initiation of homolog pairing and synapsis during the telomere-clustering (bouquet) stage of meiotic prophase. J Cel Sci 113: 1033-1042.

Bass, H. W., 2003. Telomere dynamics unique to meiotic prophase: formation and significance of the bouquet. Cell Mol Life Sci 60: 2319-2324.

Baumman, C., R. Korner, K. Hofmann, E.A. Nigg, 2007 PICH, a centromere-associated SNF2 family ATPase, is regulated by Plk1 and required for the spindle checkpoint. Cell 128: 101-114.

Bernard, P., J. F. Maure, F. Partridge, S. Genier, J. P. Javerzat, *et al.*, 2001 Requirement of heterochromatin for cohesion at centromeres. Science 294: 2539-2542.

Bhalla, N. A. F. Dernberg, 2008 Prelude to a division. Annu Rev Cell Dev Biol 24: 397-424.

Bickel, S. E., T. Orr-Weaver, E. M. Balicky, 2002 The sister chromatid cohesion protein ORD is required for chiasma maintenance in Drosophila oocytes. Curr Biol 12: 925-929.

Bishop, D. K., D. Zickler, 2004 Early decision: meiotic crossover interference prior to stable strand exchange and synapsis. Cell 177: 9-15.

Blitzblau, H. G., G. W. Bell, J. Rodriguez, S. P. Bell, A. Hochwagen, 2007 Mapping of meiotic single-stranded DNA reveals double-stranded-break hotspots near centromeres and telomeres. Curr Biol 17: 2003-2012.

Boddy, M. N., P. H. Gaillard, W. H. McDonald, P. Shanahan, J. R. Yates, *et al.*, 2001 Mus81-Eme1 are essential components of a Holliday junction resolvase. Cell 107: 537-548.

Borde, V., N. Robine, W. Lin, S. Bonfils, V. Geli, *et al.*, 2009 Histone H3 lysince 4 trimethylation makrs meiotic recombination initiation sites. EMBO J 28: 99-111.

Brar, A., B. M. Kiburz, Y. Zhang, J. E. Kim, F. White, *et al.*, 2006 Rec8 phosphorylation and recombination promote the step-wise loss of cohesins in meiosis. Nature, 441:532-536.

Brar, G. A., A. Amon, 2008 Emerging roles for centromeres in meiosis I chromosome segregation. Nat. Rev. Genet 12: 899-910.

Bugge, M., A. Collins, M. B. Petersen, J. Fisher, C. Brandt, *et al.*, 1998 Non-disjunction of chromosome 18. Hum Mol Genet 7: 661-669.

Buhler, C., R. Schroff, M. Lichten, 2006 Genome-wide mapping of meiotic DNA double-strand breaks in *Saccharomyces cerevisiae.* Methods Mol Biol 557: 143-64.

Buonomo, S. B., R. K. Clyne, J. Fuchs, J. Loidl, F. Uhlmann, *et al.*, 2000 Disjunction of homologous chromosomes in meiosis I depends on proteolytic cleavage of the meiotic cohesin Rec8 by separin. Cell 103: 387-398.

Canman, J. C., N. Sharma, A. Straight, K.B. Shannon, G. Fang, *et al.*, 2002 Anaphase onset does not require the microtubule-dependent depletion of kinetochore and centromere-binding proteins. J Cell Sci 115: 3787-3795.

Cao, L., E. Alani, N. Kleckner, 1990 A pathway for generation and processing of double strand breaks during meiotic recombination in *S. cerevisiae.* Genetics 185: 459-467.

Carpenter, A. T., 1987 Gene conversion, recombination nodules, and the initiation of meiotic synapsis. Bioessays 6:232-236.

Carpenter, A.T., 1991 Distributive Segregation: Motors in the Polar Wind? Cell 64: 885-890

Cha, R. S., B. M. Weiner, S. Keeney, J. Dekker, N. Kleckner, 2000 Progression of meiotic DNA replication is modulated by interchromosomal interaction proteins, negatively by Spo11p and positively by Rec8p. Genes Dev. 14: 493-503.

Chan, K. L., P. S. North, I. D. Hickson, 2007 BLM is required for faithful chromosome segregation and its localization defines a class of ultrafine anaphase bridges. EMBO J 26: 3397-3409.

Chen, S. Y., T. Tsubouchi, B. Rockmill, J. S. Sandler, D. R. Richards, *et al.*, 2008 Global analysis of the meiotic crossover landscape. Dev Cell 15: 401-415.

Cheslock, P. S., B. J. Kemp, R. M. Boumil, D. S. Dawson, 2005 The roles of MAD1, MAD2, and MAD3 in meiotic progression and the segregation of nonexchange chromosomes. Nat Genet 37: 756-760.

Chikashige, Y., D. Q. Ding, H. Funabiki, T. Haraguchi, S. Mashiko, *et al.*, 1994 Telomere-led premeiotic chromosome movement in fission yeast. Science 264: 270-273.

Chikashige, Y., T. Haraguchi, Y. Hiraoka, 2007 Another way to move chromosomes. Chromosoma, 116: 497-505.

Ciferri, C., A. Musacchio, A. Petrovic, 2007 The Ndc80 complex: hub of kinetochore activity. FEBS Leff 581: 2862-2869.

Ciosk, R., M. Shirayama, A. Shevchenko, T. Tanaka, A. Toth, *et al.*, 2000 Cohesin's binding to chromosomes depends on a separate complex consisting of Scc2 and Scc4 proteins. Mol Cell 2: 243-254.

Clarke, L., J. Carbon, 1983 Genomic substitutions of centromeres in *Saccharomyces cerevisiae.* Nature 305: 23-28.

Clift, D., A. L. Marston, 2011 The role of shugoshin in meiotic chromosome segregation. Cytogenet Genome Res 133: 234-242.

Clute, P., J. Pines, 1999 Temporal and spatial control of cyclin B1 destruction in metaphase. Nat Cell Biol 1: 82-87.

Clyne, R. K., V. L. Katis, L. Jessop, K. R. Benjamin, I. Herskowitz, *et al.*, 2003 Polo-like kinase Cdc5 promotes chiasmate formation and cosegregation of sister centromeres at meiosis I. Nat. Cell Biol. 5: 480-485.

Conrad, M. N., C. Y. Lee, J. L. Wilkerson, M.E. Dresser, 2007 MPS3 mediates meiotic bouquet formation in *Saccharomyces cerevisiae*. PNAS, 104: 8863-8.

Conrad, M. N., C. Y. Lee, G. Chao, M. Shinohara, H. Kosaka, *et al*., 2008 Rapid telomere movement in meiotic prophase is promoted by NDJ1, MPS3, and CSM4 and is modulated by recombination. Cell **133**: 1175-1187.

Cooper, K. W., 1964 Meiotic conjunctive elements not involving chiasmate. PNAS USA 52: 1248-1255.

Corredor, E., A. J. Lukaszewski, P. Pachon, D. C. Allen, T. Naranjo, 2007 Terminal regions of wheat chromosomes select their pairing partners in meiosis. Genetics 177: 699-706.

Culbertson, M.R., S. A. Henry, 1973 Genetic analysis of hybrid strains trisomic for the chromosome containing a fatty acid synthetase gene complex (fas1) in yeast. Genetics 75: 441-458.

Davis, L., G. R. Smith, 2006 The meiotic bouquet promotes homolog interactions and restricts ectopic recombination in *Schizosaccharomyces pombe*. Genetics **174**: 167-177.

de La Roche Saint-Andre, 2007. Alternative ends: Telomeres and meiosis. Biochimie, 90: 181-189.

Delhanty, J. D., 1997 Chromosome analysis by FISH in human preimplantation genetics. Hum Reprod 12: 153-155.

Dernburg, A.F., 2001 Here, there, and everywhere: kinetochore function on holocentric chromosomes. J Cell Biol 153: 33-38.

Dernburg, A. F., J. W. Sedat, R. S. Hawley, 1996 Direct evidence of a role for heterochromatin in meiotic chromosome segregation. Cell 86: 135-146.

Dernburg, A.F., K. McDonald, G. Moulder, R. Barstead, M. Dresser, *et al.*, 1998 Meiotic recombination in C. elegans initiates by a conserved mechanism and is dispensable for homologous chromosome synapsis. Cell 94: 387-398.

Diaz-Martinez, L. A., J. F. Gimenez-Abian, D. J. Clarke, 2007 Regulation of centromeric cohesion by sororin independently of the APC/C. Cell Cycle 6: 714-724.

Diaz-Rodriguez, E., R. Sotillo, J. M. Schvartzman, R. Benezra, 2008. Hec1 overexpression hyperactivates the mitotic checkpoint and induces tumor formation *in vivo.* PNAS USA 105:16719-16724.

Ditchfield, C., V. L. Johnson, A. Tighe, R. Ellston, C. Haworth, *et al.*, 2003 Aurora B couples chromosome alignment with anaphase by targeting BubR1, Mad2, and Cenp-E to kinetochores. J Cell Biol 161: 267-280.

Donze, D., C. R. Adams, J. Rine, R. T. Kamakaka, 1999 The boundaries of the silenced HMR domain in *Saccharomyces cerevisiae.* Genes Dev 13: 698-708.

Eijpe, M., H. Offenberg, R. Jessberger, E. Revenkova, C. Heyting, 2003 Meiotic cohesin REC8 marks the axial elements of rat synaptonemal complexes before cohesins SMC1beta and SMC3. J Cell Biol 160: 657-670.

Endow, S. A., S. Henikoff, L. Soler-Niedziela, 1990 Mediation of meiotic and early mitotic chromosome segregation in Drosophila by a protein related to kinesin. Nature 345: 81-83.

Engebrecht J., J. Hirsch, G. S. Roeder, 1990 Meiotic gene conversion and crossing over: their relationship to each other and to chromosome synapsis and segregation. Cell 62: 927-937.

Fernius, J., K. G. Hardwick, 2007 Bub1 kinase targets Sgo1 to ensure efficient chromosome biorientation in budding yeast mitosis. PLoS genet 3: e213.

Forer, A., C. Kock, 1973 Influence of autosome movements and of sex-chromosome movements on sex-chromosome segregation in crane-fly spermatocytes. Chromosoma 40: 417-442.

Forer, A., 1966 Characterization of the mitotic traction system and evidence that birefringent spindle fibers neither produce nor transmit force for chromosome movement. Chromosoma 19: 44-98.

Gelei, J., 1921 Weitere Studien uber die Oogenese des *Dendrocoelum lacteum.* II. Die Langskonjugation der Chromosomen. *Archiv fur Zellforschung* 16: 88-169.

George, O., M. A. Johnston, C. B. Shuster, 2006 Aurora B kinase maintains chromatin organization during the MI to MII transition in surf clam oocytes. Cell Cycle 5: 2648-2656.

Gilbertson, L. A., F. W. Stahl, 1996 A test of the double-strand break repair model for meiotic recombination in Saccharomyces cerevisiae. Genetics 144: 27-41

Gilliland, W. D., S. E. Hughes, J. L. Cotitta , S. Takeo, Y. Xiang, *et al.*, 2007 The multiple roles of mps1 in *Drosophila* female meiosis. PLoS Genet 3: 113

Gilliland, W. D., S. E. Hughes, D. R. Vietti, R. S. Hawley, 2009 Congression of achiasmate chromosomes to the metaphase plate in *Drosophila melanogaster* oocytes. Dev Biol 325: 122-128.

Gladstone, M. N., D. Obeso, H. Chuong, D. S. Dawson, 2009 The synaptonemal complex protein Zip1 promotes bi-orientation of centromeres at meiosis I. PLoS Genet. 5: e1000771.

Goldman, A.S., M. Lichten, 2000 Restriction of ectopic recombination by interhomolog interactions during *Saccharomyces cerevisiae* meiosis. PNAS, 97: 9537-9542.

Golubovskaya, I. N., L. C. Harper, W. P. Pawlowski, D. Schichnes, W. Z. Cande, 2002 The pam1 gene is required for meiotic bouquet formation and efficient homologous synapsis in maize (Zea mays L). Genetics, 162: 179-193.

Gomez, R., A. Valdeolmillos, M. T. Parra, A. Viera, C. Carrerior, *et al.*, 2007 Mammalian SGO2 appears at the inner centromere domain and redistributes depending on tension across centromeres during meiosis II and mitosis. EMBO Rep 8: 173-180.

Gorbsky, G. J., W. A. Ricketts, 1993 Differential expression of a phosphoepitope at the kinetochores of moving chromosomes. J Cell Biol 122: 1311-1321.

Gregan, J., C. Rumpf, Z. Li, L. Cipak, 2008 What makes centromeric cohesion resistant to separase cleavage during meiosis I but not during meiosis II? Cell Cycle 7: 151-153.

Grell, R.F., 1962 A new hypothesis on the nature and sequence of meiotic eents in the female of *Drosophila melanogaster.* Proc. Natl. Acad. Sci. USA 48: 165-172.

Grell, R.F., 1976 Distributive pairing. Genetics and Biology of *Drosophila* Volume 1, pages 425-486.

Gruber, S., C. H. Haering, K. Nasmyth, 2003 Chromosomal cohesin forms a ring. Cell 112:765-777.

Guacci, V., 1990 Meiotic chromosome disjunction in yeast. PhD thesis, University of Medicine and Dentistry of New Jersey, Newark.

Guacci, V., D. B. Kaback, 1991 Distributive Disjunction of Authentic Chromosomes in *Saccharomyces cerevisiae.* Genetics 127: 475-488.

Gullerova, M., N. J. Proudfoot, 2008 Cohesin complex promotes transcriptional termination between convergent genes in S. pombe. Cell 132: 983-985.

Harper, L., I. Golubovskaya, W. Z. Cande, 2004 A bouquet of chromosomes. Journal of Cell Science, 117: 4025-4032.

Hartl, T. A., S. J. Sweeney, P. J. Knepler, G. Bosco G, 2008 Condensin II resolves chromosomal associations to enable anaphase I segregation in Drosophila male meiosis. PLoS Genet 4: e1000228.

Hassold, T., M. Merrill, K. Adkins, S. Freeman, S. Sherman, 1995 Recombination and maternal age-dependent nondisjunction: molecular studies of trisomy 16. Am J Hum Genet 57: 867-874.

Hassold, T., 1998 Nondisjunction in the human male. Curr Top Dev Biol 37:383-406.

Hassold, T., P. Hunt, 2001 To err (meiotically) is human: the genesis of human aneuploidy. Nat. Rev. Genet. **2**: 280-291.

Hassold, T., H. Hall, P. Hunt, 2007 The origin of human aneuploidy: where we have been, where we are going. Hum Mol Genet 16 Spec No 2: R203-R208.

Hawley, R. S. W. E. Theurkaul, 1993 Requiem for distributive segregation: achiasmate segregation in Drosophila females. Trends Genet 9: 310-317.

Hawley, R. S., H. Irick, A. E. Zitron, D. A. Haddox , A. Lohe, *et al*., 2003 There are two mechanisms of achiasmate segregation in *Drosophila*, one of which requires heterochromatin homology. Dev Genet 13: 440-467.

Hawley, R. S., 1988 Exchange and chromosomal segregation in eukaryotes. Genetic Recombination pp 497-527

Herman, R. K., C. K. Kari, 1989 Recombination between small X chromosome duplications and the X chromosome in *Caenorhabditis elegans*. Genetics 121: 723-737.

Hiraoka, T., 1952 Observational and experimental studies of meiosis with special reference to the bouquet stage. XIV. Some considerations on a probably mechanism of the bouquet formation. Cytologia 17: 292-299.

Hirose, Y., R. Suzuki, T. Ohba, Y. Hinohara, H. Matsuhara, et *al.*, 2011 Chiasmata promote monopolar attachment of sister chromatids and their co-segregation toward the proper pole during meiosis I. PLoS Genet 7: e1001329.

Hodges, C. A., E. Revenkova, R. Jessberger, T. J. Hassold, P. A. Hunt, 2005 SMC1beta-deficient female mice provide evidence that cohesins are a missing link in age-related nondisjunction. Nat Genet 37: 1351-1355.

Hoffelder, D. R., L. Luo, N. A. Burke, S. C. Watkins, S. M. Gollin, *et al.*, 2004 Resolution of anaphase bridges in cancer cells. Chromosoma 112: 389-397.

Hollingsworth, N. M., L. Goetsch, B. Byers, 1990 The HOP1 gene encodes a meiosis-specific component of yeast chromosomes. Cell 61: 73-84.

Homer, H. A., A. McDougall, M. Levassuer, K. Yallop, A. P. Murdoch, *et al.*, 2005 Mad2 prevents aneuploidy and premature proteolysis of cyclin B and securing during meiosis I in mouse oocytes. Genes Dev 19: 202-207.

Huang, H., J. Feng, J. Famulsi, J. B. Rattner, S. T. Liu, *et al.*, 2007 Tripin/hSgo2 recruits MCAK to the inner centromere to correct defective kinetochore attachments. J Cell Biol 177: 24-413.

Hughes, S. E., W. D. Gilliland, J. L. Cotitta, S. Takeo, K. A. Collins, *et al.*, 2009 Heterochromatic threads connect oscillating chromosomes during prometaphase I in Drosophila oocytes. PLoS Genet 5: e1000348.

Hunter, N., N. Kleckner, 2001 The single-end invasion: an asymmetric intermediate at the double-strand break to double-holliday junction transition of meiotic recombination. Cell **106**: 59-70.

Hwang, L. H., L. F. Lau, D. L. Smith, C. A. Mistrot, K. G. Hardwick, *et al.*, 1998 Budding yeast Cdc20: a target of the spindle checkpoint. Science 279: 1041-1044.

Ilagen, A. B., A. Forer, T. Spurck, 1997 Backward chromosome movement in anaphase, after irradiation of kinetochores and kinetochore fibers. Protoplasma 198: 20-26.

Ishiguro, T., K. Tanaka, T. Sakuno, Y. Watanabe, 2010 Shugoshin-PP2A counteracts casein-kinase-1-dependent cleavage of Rec8 by separase. Nat Cell Biol 12: 500-506.

Jacobs, P. A., 1992 The chromosome complement of human gametes. Oxf Rev Reprod Biol 14: 47-72.

Jamieson, M. E., J. R. Coutts, J. M. Connor, 1994 The chromosome constitution of human preimplanation embryos fertilized *in vitro*. Hum Reprod 9: 709-715.

Jang, J. K., L. Messina, M. B. Erdman, T. Arbel, R. S. Hawley, 1995 Induction of metaphase arrest in *Drosophila* oocytes by chiasma-based kinetochore tension. Science 268: 1917-1919.

Jeffreys, C. A., P. S. Burrage, S. E. Bickel, 2003 A model system for increased meiotic nondisjunction in older oocytes. Cur Biol 13: 498-503.

Jones, G. H., F. C. Franklin, 2006 Meiotic crossing-over: obligation and interference. Cell 126: 246-248.

Joseph, I., A. J. Lustig, 2007 Telomeres in meiotic recombination: the yeast side story. Cell Mol. Life Sci. **64**: 125-130.

Kallio, M., J. E. Eriksson, G. J. Gorbsky, 2000 Differences in spindle association of the mitotic checkpoint protein Mad2 in mammalian spermatogenesis and oogenesis. Dev Biol 225: 112-123.

Karamysheva, Z., L. A. Diaz-Martinez, S. E. Crow, B. Li, H. Yu, 2009 Multiple anaphase-promoting complex/cyclosome degrons mediate the degradation of human Sgo1. J Biol Chem 284: 1772-1780.

Katis, V. L., M. Galova, K. P. Rabitsch, J. Gregan, K. Nasmyth, 2004 Maintenance of cohesin at centromeres after meiosis I in budding yeast requires a kinetochore-associated protein related to MEI-S332. Curr Biol 14: 560-572.

Katis, V. L., J. J. Lipp, R. Imre, A. Bogdanova, E. Okaz, *et al.*, 2010 Rec8 phosphorylation by casein kinase I and Cdc7-Dbf4 kinase regulated cohesin cleavage by separase during meiosis. Dev Cell 18: 397-409.

Kawashima, S. A., Y. Yamagishi, T. Honda, K. Ishiguro, Y. Watanabe, 2010 Phosphorylation of H2A by Bub1 prevents chromosomal instability through localizing shugoshin. Science 327: 172-177.

Keeney, S., C. N. Giroux, N. Kleckner, 1997 Meiosis-specific DNA double-strand breaks are catalyzed by Spo11, a member of a widely conserved protein family. Cell 88: 375-384.

Kemp, B., R. M. Boumil, M. N. Stewart, D. S. Dawon, 2004 A role for centromere pairing in meiotic chromosome segregation. Genes Dev. 18: 1946-1951.

Kiburz, B. M., D. B. Reynolds, P. C. Megee, A. L. Marston, B. H. Lee, *et al.*, 2005 The core centromere and Sgo1 establish a 50-kb cohesin-protected domain around centromeres during meiosis I. Genes Dev 19: 3017-3030.

Kim, S. H., D. P. Lin, S. Matsumoto, A. Kitazono, T. Matsumoto, 1998 Fission yeast Slp1: an effector of the Mad2-dependent spindle checkpoint. Science 279: 1045-1047.

King, R. C., 1970 Ovarian development in *Drosophila melanogaster*. Academic Press Inc. New York.

Kitajima, T. S., S. Yokobayashi, M. Yamamoto, Y. Watanabe, 2003 Distinct cohesin complexes organize meiotic chromosome domains. Science 300: 1152-1155.

Kitajima, T. S., S. A. Kawashima, Y. Watanabe, 2004 The conserved kinetochore protein shugoshin protects centromeric cohesion during meiosis. Nature 427: 510-517.

Kitajima, T. S., T. Sakuno, K. Ishiguro, S. Iemura, T. Natsume, *et al.*, 2006 Shugoshin collaborates with protein phosphatase S1 to protect cohesin. Nature 441: 46-52.

Kleckner, N., D. Zickler, G. H. Jones, J. Dekker, R. Padmore, *et al.*, 2004 A mechanical basis for chromosome function. Proc Natl Acad Sci 101: 12592-7.

Klein, F., P. Mahr, M. Galova, S. B. Buonomo, C. Michaelis *et al.*, 1999 A central role for cohesins in sister chromatid cohesin, formation of axial elements and recombination during yeast meiosis. J Cell Biol 117: 935-948.

Kosaka, H., M. Shinohara, A. Shinohara A, 2008 Csm4-dependent telomere movement on nuclear envelope promotes meiotic recombination. PLoS Genet. **4**: e1000196.

Koszul, R., N. Kleckner, 2009 Dynamic chromosome movements during meiosis: a way to eliminate unwanted connections? Trends in Cell Biol 19: 716-724.

Koszul, R., K. Kim, M. Prentiss, N. Kleckner, S. Kameoka, 2008 Meiotic chromosomes move by linkage to dynamic actin cables with transduction of force through the nuclear envelope. Cell **133**: 1188-1201.

Kubai, D. F., D. Wise, 1981 Nonrandom chromosome segregation in *neocurtilla (Gryllotalpa) hexadactyla;* an ultrastructural study. J Cell Biol 88: 281-293.

Lacefield, S., A. W. Murray, 2007 The spindle checkpoint rescues the meiotic segregation of chromosomes whose crossovers are far from the centromere. Nat. Genet. **39**: 1273-1277.

LaFountain, J. R. Jr., R. W. Cole, C. L. Rieder, 2002 Partner telomeres during anaphase in crane-fly spermatocytes are connected by an elastic tether that exerts a backward force and resists poleward motion. J Cell Sci 115: 1541-1549.

Lamb, N. E., S. B.Freeman, A. Savage-Austin, D. Pettay, L. Taft, *et al.*,, 1996 Susceptible chiasmate configurations of chromosome 21 predispose to non-disjunction in both maternal meiosis I and meiosis II. Nat Genet 14: 400-405.

Lane, S. I., H. Y. Chang, P. C. Jennings, K. T. Jones, 2010 The Aurora kinase inhibitor ZM447439 accelerates first meiosis in mouse oocytes by overriding the spindle assembly checkpoint. Reproduction 140: 521-530.

Lara-Pezzi, E., N. Pezzi, I. Prieto, I. Barthelemy, C. Carrerior, *et al.*, 2004 Evidence of a transcriptional co-activator function of cohesin STAG/SA/Scc3. J Biol Chem 279: 6553-6559.

Lee, B. H., A. Amon, 2003 Role of Polo-like kinase CDC5 in programming meiosis I chromosome segregation. Science 300: 482-486.

Lee, J. Y., T. L. Orr-Weaver, 2001 The molecular basis of sister-chromatid cohesion. Annu Rev Cell Dev Biol 17: 753-777.

Lee, J., T. S. Kitajima, Y. Tanno, K. Yoshida, T. Morita, *et al.*, 2008 Unified mode of centromeric protection by shugoshin in mammalian oocytes and somatic cells. Nat Cell Biol 10: 42-52.

Lee, C., M. N. Conrad, M. E. Dresser, 2012 Meiotic chromosome pairing is promoted by telomere-led chromosome movements independent of bouquet formation. PLoS Genet 8: e1002730.

Levesque, A. A., D. A. Compton, 2001 The chromokinesin Kid is necessary for chromosome arm orientation and oscillation, but not congression, on mitotic spindles. J Cell Biol 154: 1135-1146.

Lister, L. M., A. Kouznetsova, L. A. Hyslop, D. Kalleas, S. I. Pace, *et al.*, 2010 Age related meiotic segregation errors in mammalian oocytes are preceded by depletion of cohesin and Sgo2. Current Biol 20: 1-11

Loidl, J., F. Klein, H. Scherthan, 1994 Homologous pairing is reduced but not abolished in asynaptic mutants of yeast. J. Cell Biol. 125: 1191-1200.

MacDonald, M., T. Hassold, J. Harvey, L. H. Wang, N. E. Morton, *et al.*, 1994 The origin of 47,XXY and 47, XXX aneuploidy: heterogeneous mechanisms and role of aberrant recombination. Hum Mol Genet 3: 1365-1371.

MacQueen, A. J., M. P. Colaiacovo, K. McDonald, A. M. Villeneuve, 2002 Synapsis-dependent and –independent mechanisms stabilize homolog pairing during meiotic prophase in *C. elegans*. Genes Dev 16: 2428-2442.

MacQueen, A. J., C. M. Phillips, N. Bhalla, P. Weiser, A. M. Villeneuve, *et al.*, 2005 Chromosome sites play dual roles to establish homologous synapsis during meiosis in *C. elegans*. Cell 123: 1037-1050.

Mahadevaiah, S. K., J. M. Turner, F. Baudat, E. P. Rogakou, P. de Boer, *et al.*, 2001 Recombinational DNA double-strand breaks in mice precede synapsis. Nat Genet 27: 271-276.

Mancera, E., R. Bourgon, A. Brozzi, W. Huber, L. M. Steinmetz, 2008 High-resolution mapping of meiotic crossovers and non-crossovers in yeast. Nature 454: 479-485.

Marquez, C., J. Cohen, S. Munne, 1998 Chromosome identification in human oocytes and polar bodies by spectral karyotyping. Cytogenet Cell Genet 81: 254-258.

Marston, A. L., A. Amon, 2004 Meiosis: cell cycle controls shuffle and deal. Nat Rev Mol Cell Biol 5: 983-997.

Martson, A. L., W. H. Tham, H. Shah, A. Amon, 2004 A genome-wide screen identifies genes required for centromeric cohesion. Science **303**: 367-370.

Martinez-Perez, E., M. P. Colaiacovo, 2009 Distribution of meiotic recombination events: talking to your neighbors. Curr. Opin. Genet. Dev. **19**: 105-112.

Martinez-Perez, E., M. Schvarzstein, C. Barroso, J. Lightfoot, A. F. Dernburg, *et al.*, 2008 Crossovers trigger a remodeling of meiotic chromosome axis composition that is linked to two-step los of sister chromatid cohesion. Genes Dev 22: 2886-2901.

Martini, E., R. L. Diaz, N. Hunter, S. Keeney, 2006 Crossover homeostasis in yeast meiosis. Cell **126**: 285-295.

Martin-Lluesma, S., V. M. Stucke, E. A. Nigg, 2002 Role of Hec1 in spindle checkpoint signaling and kinetochore recruitment of Mad1/Mad2. Science 297: 2267-2270.

Matthies, H. J., R. J. Baskin, R. S. Hawley, 2001 Orphan kinesin NOD lacks motile properties but does possess a microtubule-stimulated ATPase activity. Mol Biol Cell 12: 4000-4012.

McDonald, H. B., L. S. Goldstein, 1990 Identification and characterization of a gene encoding a kinesin-like protein in Drosophila. Cell 61: 991-1000.

McGuinness, B. E., M. Anger, A. Kouznetsova, A. M. GilBernabe, W. Helmhart, *et al.,* 2009 Regulation of APC/C activity in oocytes by a Bub-dependent spindle assembly checkpoint. Curr Biol 19: 369-380.

McKee, B. D., 1996 The license to pair: identification of meiotic pairing sites in Drosophila. Chromosoma 105: 135-141.

McKim, K. S., A. M. Howell, A. M. Rose, 1988 The effects of translocations on recombination frequency in Caenorhabditis elegans. Genetics 120: 987-1001.

Mckim, K. S., J. K. Jang, W. E. Theurkaff, R. S. Hawley, 1993 Mechanical basis of meiotic metaphase arrest. Nature 362: 364-366.

Meneely, P. M., A. F. Farago, T. M. Kauffman, 2002 Crossover distribution and high interference for both the X chromosome and an autosome during oogenesis and spermatogenesis in *Caenorhabditis elegans*. Genetics 162: 1169-1177.

Michaelis, C., R. Ciosk, K. Nasmyth, 1997 Cohesins: chromosomal proteins that prevent premature separation of sister chromatids. Cell 91: 35-45.

Monje-Casas, F., V. R. Prabhu, B. H. Lee, M. Boselli, A. Amon, 2007 Kinetochore orientation during meiosis is controlled by Aurora B and the monopolin complex. Cell 128: 477-490.

Nasmyth, K., 2001 Disseminating the genome: joining, resolving, and separating sister chromatids during mitosis and meiosis. Annu Rev Genet 35: 673-745.

Newnham, L., P. Jordan, B. Rockmill, G. S. Roeder, E. Hoffmann, 2010 The synaptonemal complex protein, Zip1, promotes the segregation of nonexchange chromosomes at meiosis I. Proc Natl Acad Sci USA 107: 781-5.

Nicklas, R. B., 1967 Chromosome micromanipulation II. Induced reorientation and the experimental control of segregation in meiosis. Chromosoma 21: 17-50.

Nicklas, R. B., 1974 Chromosome segregation mechanisms. Genetics 78: 205-213.

Nicklas, R. B., 1975 Chromosome movement: current models and experiments on living cells. Soc Gen Physiol Ser 30: 97-117.

Nicklas, R. B., 1997 How cells get the right chromosomes. Science 275: 632-637.

Nishant, K. T., C. Chen, M. Shinohara, A. Shinohara, E. Alani, 2010 Genetic analysis of baker's yeast Msh4-Msh5 reveals a threshold crossover level for meiotic viability. PLoS Genet. 6: e1001083.

Niwa, O., M. Shimanuki, F. Miki, 2000 Telomere-led bouquet formation facilitates homologous chromosome pairing and restricts ectopic interaction in fission yeast meiosis. EMBO J. **19**: 3831-3840.

Ostergren, G., 1951 The mechanism of co-orientation in bivalents and multivalent. Hereditas 37: 85-156.

Page ,S. L., R. S. Hawley, 2003 Chromosome choreography: the meiotic ballet. Science 301: 785-789.

Page, J., R. de la Fuente, R. Gomez, A. Calvente, A. Vierar, *et al.*, 2006 Sex chromosomes, synapsis, and cohesins: a complex affair. Chromosoma 115: 250-259.

Parisi, S., M. J. McKay, M. Molnar, M. A. Thompson, P. J. van der Spek, *et al.*, 1999 Rec8p, a meiotic recombination and sister chromatid cohesion phosphoprotein of the Rad21p family conserved from fission yeast to humans. Mol Cell Biol 19: 3515-3528.

Parra, M. T., R. Gómez, A. Viera, E. Llano, A. M. Pendás, *et al.*, 2009 Sequential assembly of centromeric proteins in male mouse meiosis. PLoS Genet 5: e1000417.

Parvinem, M., K. O. Soderstrom, 1976 Chromosome rotation and formation of synapsis. Nature **260:** 534-5.

Pasierbek, P., M. Jantsch, M. Melcher, A. Schleiffer, D. Schweizer, *et al.*, 2001 A *Caenorhabditis elegans* cohesion protein with functions in meiotic chromosome pairing and disjunction. Genes Dev 15: 1349-1360.

Pawlowski, W. P., I. N. Golubovskaya, L. Timofejeva, R. B. Meeley,W. F. Sheridan, *et al.*, 2004 Coordination of meiotic recombination, pairing, and synapsis by PHS1. Science 303: 89-92.

Peoples, T. L., E. Dean, O. Gonzalez, L. Lambourne, S. M. Burgess, 2002 Close, stable homolog juxtaposition during meiosis in budding yeast is dependent on meiotic recombination, occurs independently of synapsis, and is distinct from DSB-independent pairing contacts. Genes Dev. **16**: 1682-1695.

Peoples-Holst, T. L., S. M. Burgess, 2005 Multiple branches of the meiotic recombination pathway contribute independently to homolog pairing and stable juxtaposition during meiosis in budding yeast. Genes Dev 19: 863-874.

Perera, D., S. S. Taylor, 2010 Sgo1 establishes the centromeric cohesion protection mechanism in G2 before subsequent Bub1-dependent recruitment in mitosis. J Cell Sci 123: 653-659.

Petes, T. D., 2001 Meiotic recombination hot spots and cold spots. Nat Rev Genet 2: 360-369.

Pfeifer, C., H. Scherthan, P.D. Thomsen, 2003 Sex-specific telomere redistribution and synapsis initation in cattle oogenesis. Dev Biol 225: 206-215.

Phillips, C. M., A. F. Dernberg, 2006 A family of zinc-finger proteins is required for chromosome-specific pairing and synapsis during meiosis in *C. elegans.* Dev Cel 11: 817-829.

Phillips, C. M., C. Wong, N. Bhalla, P. M. Carlton, P. Weiser, *et al.*, 2005 HIM-8 binds to the X chromosome pairing center and mediates chromosome-specific meiotic synapsis. Cell 123: 1051-1063.

Phillips, C. M., X. Megn, L. Zhang, J. H. Chretien, F. D. Urnov, *et al.*, 2009 Identification of chromosome sequence motifs that mediate meiotic pairing and synapsis in *C. elegans.* Nat Cell Biol 11: 934-942.

Puro, J., S. Nokkala, 1977 Meiotic segregation of chromosomes in *Drosophila melanogaster* oocytes. Chromosoma 63: 273-286.

Rabitsch, K. P., M. Petronczki, J. P. Javerzat, S. Genier, B. Chwalla, *et al*., 2003 Kinetochore recruitment of two nucleolar proteins is required for homolog segregation in meiosis I. Dev Cell 4: 535-548.

Rabitsch, K. P., J. Gregan, A. Schleiffer, J. P. Javerzat, F. Eisenhaber, *et al.*, 2004 Two fission yeast homologs of *Drosophila* Mei-S332 are required for chromosome segregation during meiosis I and II. Curr Biol 14: 287-301.

Resnick, T. D., D. L. Satinover, F. MacIsaac, P. T. Stukenberg, W. C. Earnshaw, *et al*., 2006 INCENP and Auroar B promote meiotic sister chromatid cohesion through localization of the Shugoshin MEI-S332 in Drosophila. Dev Cell 11: 57-68.

Revenkova, E., R. Jessberger, 2006 Shaping meiotic prophase chromosomes: cohesins and synaptonemal complex proteins. Chromosoma 115: 235-240.

Revenkova, E., M. Eijpe, C. Heyting, C. A. Hodges, P. A. Hunt *et al.*, 2004 Cohesin SMC1beta is required for meiotic chromosome dynamics, sister chromatid cohesion and DNA recombination. Nat Cell Biol 6: 555-562.

Riedel, C. G., V. L. Katis, Y. Katou, S. Mori, T. Itoh, *et al.*, 2006 Protein phosphatase 2A protects centromeric sister chromatid cohesion during meiosis I. Nature 441: 53-61.

Rieder, C. L., E. D. Salmon, 1994 Motile kinetochore and polar ejection forces dictate chromosome position on the vertebrate mitotic spindle. J Cell Biol. 124: 223-33.

Rieder, C. L., R. W. Cole, A. Khojakov, G. Sluder, 1995 The checkpoint delaying anaphase in response to chromosome monoorientation is mediated by an inhibitory signal produced by unattached kinetochores. J Cell Biol 162: 991-1001.

Robine, N., N. Uematsu, F. Amiot, X. Gidrol, E. Barillot, *et al.*, 2007 Genome-wide redistribution of meiotic double-strand breaks in *Saccharomyces cerevisiae.* Mol Cell Biol. 27: 1868-80.

Robinson, W.P., F. Bernasconi, A. Mutirangura, D. H. Ledbetter, S. Langlois, *et al.*, 1993 Nondisjunction of chromosome 15:origin and recombination. Am J Hum Genet 53: 740-751.

Rockmill, B., G. S. Roeder, 1990 Meiosis in asynaptic yeast. Genetics 126:563-574.

Rockmill, B., G. S. Roeder, 1991 A meiosis-specific protein kinase homolog required for chromosome synapsis and recombination. Genes Dev 5: 2392-2404.

Rockmill, B., K. Voelkel-Meiman, G. S. Roeder, 2006 Centromere-proximal crossovers are associated with precocious separation of sister chromatids during meiosis in *Saccharomyces cerevisiae.* Genetics **174**: 1745-1754.

Rosenbluth, R. E., D. L. Baille, 1981 The genetic analysis of a reciprocal translocation. Annu Rev Biochem 77: 229-257.

Ross-Macdonald, P., G. S. Roeder, 1994 Mutation of a meiosis-specific MutS homolog decreases crossing over but not mismatch correction. Cell 79: 1069-1706.

Sandler, L., E. Novitski, 1956 Evidence for genetic homology between chromosomes I and IV in Drosophila melanogaster, with a proposed explanation for the crowding effect in triploids. Genetics 41: 189-193.

Scherthan, H., S. Weich, H. Schwegler, C. Heyting, M. Harle, *et al*., 1996 Centromere and telomere movements during early meiotic prophase of mouse and man are associated with the onset of chromosome pairing. J. Cell Biol. **134**: 1109-1125.

Scherthan, H., R. Eils, E. Trelles-Sticken, S. Dietzel, T. Cremer, *et al.*, 1998 Aspects of three-dimensional chromosome reorganization during the onset of human male meiotic prophase. J Cell Sci 111: 2337-2351.

Scherthan, H., 2007 Telomere attachment and clustering during meiosis. Cell Mol Life Sci 64: 117-124.

Schlecht, H. B., M. Lichten, A. S. Goldman, 2004 Compartmentalization of the yeast meiotic nucleus revealed by analysis of ectopic recombination. Genetics 168: 1189-1203.

Schwacha, A., N. Kleckner, 1995 Identification of double Holliday junctions as intermediates in meiotic recombination. Cell **83**: 783-791.

Sears, D. D., J. H. Hegemann, P. Hieter, 1992 Meiotic recombination and segregation of human-derived artificial chromosomes in *Saccharomyces cerevisiae.* Proc Natl Acad Sci USA 89: 5296-5300.

Seitan, V. C., P. Banks, S. Laval, N. A. Majid, D. Dorsett, *et al.*, 2006 Metazoan Scc4 homologs link sister chromatid cohesion to cell and axon migration guidance. PLoS Biol 4: 1411-1425.

Sekelsky, J. J., K. S. McKim, L. Messina, R. L. French, W. D. Hurle, *et al.*, 1999 Identification of novel Drosophila meiotic genes recovered in a P-element screen. Genetics 152: 529-542.

Shaffer, B., I. Brearley, R. Littlewood, G. R. Fink, 1971 A stable aneuploidy of *Saccharomyces cerevisiae.* Genetics 67: 483-495.

Shonn, M. A., R. McCarroll, A. W. Murray, 2000 Requirement of the spindle checkpoint for proper chromosome segregation in budding yeast meiosis. Science 289: 300-303.

Smith, A. V., G. S. Roeder, 1997 The yeast Red1 protein localizes to the cores of meiotic chromosomes. J Cell Biol 136: 957-967.

Smithies, O., P. A. Powers, 1986 Gene conversions and their relation to homologous chromosome pairing. Phil Trans R Soc London Ser B 312: 291-302.

Sonntag Brown, M., S. Zanders, E. Alani, 2011 Sustained and rapid chromosome movements are critical for chromosome pairing and meiotic progression in budding yeast. Genetics 188: 21-32.

Stewart, M. N., D. S. Dawson, 2008 Changing partners: moving from non-homologous to homologous centromere pairing in meiosis. Trends Genet 24: 564-573.

Storlazzi, A., S. Tessé, S. Gargano, F. James, N. Kleckner, *et al.*, 2003 Meiotic double-strand breaks at the interface of chromosome movement, chromosome remodeling, and reductional division. Genes Dev, 17: 2675-87.

Storlazzi, A., S. Tesse, G. Ruprich-Robert, S. Gargano, S. Poggeler, *et al.*, 2008 Coupling meiotic chromosome axis integrity to recombination. Genes Dev 22: 796-809.

Subramanian, V. V., S. E. Bickel, 2008 Aging predisposes oocytes to nondisjunction when the cohesin subunit SMC1 is reduced. PLoS Genet 4: e1000263.

Subramanian, V. V., S. E. Bickel, 2009 Heterochromatin mediated association of achiasmate homologs declines with age when cohesin is compromised. Genetics 181: 1207-1218.

Sun, S. C., N. H. Kim, 2012 Spindle assembly checkpoint and its regulators in meiosis. Hum Reprod Upd 18: 60-72.

Sun, S. C., D. X. Zhang, S. E. Lee, Y. N. Xu, N. H. Kim, 2011 Ndc80 regulates meiotic spindle organization, chromosome alignment, and cell cycle progression in mouse oocytes. Microsc Mincroanal 17: 431-439.

Swain, J. E., J. Ding, J. Wu, G. D. Smith, 2008 Regulation of spindle and chromatin dynamics during early and late stages of oocyte maturation by aurora kinases. Mol Hum Reprod 14: 291-299.

Sym, M., G. S. Roeder, 1994 Crossover interference is abolished in the absence of a synaptonemal complex protein. Cell 79: 283-292.

Sym, M., G. S. Roeder, 1995 Zip1-induced changes in synaptonemal complex structure and polycomplex assembly. J Cell Biol 128: 455-466.

Sym, M., J. A. Engebrecht, G. S. Roeder, 1993 ZIP1 is a synaptonemal complex protein required for meiotic chromosome synapsis. Cell 72: 365-378.

Takagi, S., C. Benard, J. Pak, D. Livingstone, S. Hekimi, 1997 Cellular and axonal migrations are misguided along both body axes in the maternal-effect mau-2 mutants of *Caenorhabditis elegans.* Development 124: 5115-5126.

Tanaka, T. U., A. Desai, 2008 Kinetochore microtubule interactions: the means to the end. Curr Opin Cell Biol 20: 53-63.

Tankimanova, M., M. A. Hulten, C. Tease, 2004 The initiation of homologous chromosome synapsis in mouse fetal oocytes is not directly driven by centromere and telomere clustering in the bouquet. Cytogenet Genome Res 105: 172-181.

Taylor, S. S., M. I. Scott, A. J. Holland, 2004 The spindle checkpoint: a quality control mechanism which ensures accurate chromosome segregation. Chromosome Res 12: 599-616.

Theurkauf, W. E., R. S. Hawley, 1992 Meiotic spindle assembly in Drosophila females: behavior of nonexchange chromosomes and the effects of mutations in the *nod* kinesin-like protein. J Cell Biol 116: 1167-1180.

Tomita, K., J. P. Cooper, 2007 The telomere bouquet controls the meiotic spindle. Cell, 130: 113-126.

Toth, A., K. P. Rabitsch, M. Galova, A. Schleiffer, S. B. Buonomo, *et al*., 2000 Functional genomics identifies monopolin: a kinetochore protein required for segregation of homologs during meiosis I. Cell **103**: 1155-1168.

Trelles-Sticken, E., J. Loidl, H. Scherthan, 1999 Bouquet formation in budding yeast: initiation of recombination is not required for meiotic telomere clustering. J. Cell Sci. **112**: 651-658.

Trelles-Sticken, E., C. Adelfalk, J. Loidl, H. Scherthan, 2005 Meiotic telomere clustering requires actin for its formation and cohesin for its resolution. J. Cell Biol. 170: 213-223.

Tsubouchi, T., G. S. Roeder, 2005 A synaptonemal complex protein promotes homology-independent centromere coupling. Science 308: 870-3.

Tsukahara, T., Y. Tanno, Y. Watanabe, 2010 Phosphorylation of the CPC by Cdk1 promotes chromosome bi-orientation. Nature 467: 719-723.

Vazquez, J., A. S. Belmont, J. W. Sedat, 2002 The dynamics of homologous chromosome pairing during male *Drosophila* meiosis. Curr Biol 12: 1473-83.

Vaur, S., F. Cubizolles, G. Plane, S. Genier, K. P. Rabitsch, *et al*., 2005 Control of shugoshin function during fission-yeast meiosis. Curr Biol 15: 2263-2270.

Villeneuve, A. M., 1994 A cis-acting locus that promotes crossing over between X chromosomes in *Caenorhabditis elegans*. Genetics 136: 887-902.

Vogt, E., A. Kipp, U. Eichenlabu-Ritter, 2009 Aurora kinase B, epigenetic state of centromeric heterochromatin and chiasma resolution in oocytes. Reprod Biomed Online 19: 352-368.

Volarcik, K., L. Sheean, J. Goldfarb, L. Woods, F. W. Abdul-Karim, *et al.*, 1998 The meiotic competence of in-vivo matured oocytes is influenced by donor age: evidence that folliculogenesis is compromised in the reproductively aged ovary. Hum Reprod 13: 154-160.

Von Wettstein, D., S. V. Rasmusen, P. B. Holm, 1984 The synaptonemal complex in genetic segregation. Annu Rev Genet 18: 331-314.

Wanat, J. J., K. P. Kim, R. Koszul, S. Zanders, B. Weiner, *et al.*, 2008 Csm4, in collaboration with Ndj1, mediates telomere-led chromosome dynamics and recombination during yeast meiosis. PLoS Genet. 4: e1000188.

Wang, L. H., T. Schwarzbraun, M. R. Speicher, E. A. Nigg, 2008 Persistence of DNA threads in human anaphase cells suggests late completion of sister chromatid decatenation. Chromosoma 117: 123-135.

Watanabe, Y., P. Nurse, 1999 Cohesin Rec8 is required for reductional chromosome segregation at meiosis. Nature 400: 461-464.

Waters, J. C., R. H. Chen, A. W. Murray, E. D. Salmon, 1998 Localization of Mad2 to kinetochores depends on microtubule attachment, not tension. J Cell Biol 141: 1181-1191.

Watrin, E., J. M. Peters, 2006 Cohesin and DNA damage repair. Exp Cell Res 312: 2687-2693.

Watrin, E., A. Schleiffer, K. Tanaka, F. Eisenhaber, K. Nasmyth, *et al.*, 2006 Human Scc4 is required for cohesin binding to chromatin, sister-chromatid cohesion, and mitotic progression. Curr Biol 16: 863-874.

Wendt, K. S., K. Yoshida, T. Itoh, M. Bando, B. Koch, *et al.*, 2008 Cohesin mediates transcriptional insulation by CCCTC-binding factors. Nature 451: 796-801.

Wynee, D. J., O. Rog, P. M. Carlton, A. F. Dernburg, 2012 Dynein-dependent processive chromosome motions promote homologous pairing in C. elegans meiosis. JCB 196: 47-64.

Xu, Z., B. Cetin, M. Anger, U. S. Cho, W. Helmhart, *et al.*, 2009 Structure and function of the PP2A-shugoshin interaction. Mol Cell 35: 426-441.

Yamagishi, Y., T. Sakuno, M. Shimura, Y. Watanabe, 2008 Heterochromatin links to centromeric protection by recruiting shugoshin. Nature 455: 251-255.

Yin, S., Q. Wang, J. H. Liu, J. S. Ai, C. G. Liang, *et al.*, 2006 Bub1 prevents chromosome misalignment and precocious anaphase during mouse oocyte meiosis. Cell Cycle 5: 2130-2137.

Yokobayashi, S., Y. Watanabe, 2005 The kinetochore protein Moa1 enables cohesion-mediated monopolar attachment at meiosis I. Cell 123: 803-817.

Yu, H. G., D. Koshland, 2007 The Aurora kinase Ipl1 maintains the centromeric localization of PP2A to protect cohesin during meiosis. J Cell Biol 176: 911-918.

Yu, H. G., M. G. Muszynski, R. Kelly Dawe, 1999 The maize homologue of the cell cycle checkpoint protein MAD2 reveals kinetochore substructure and contrasting mitotic and meiotic localization patterns. J Cell Boil 145: 425-435.

Zalevsky, J., A. J. MacQueen, J. B. Duffy, K. J. Kemphues, A. M. Villeneuve, 1999 Crossing over during *Caenorhabditis elegans* meiosis requires a conserved MutS-based pathway that is partially dispensable in budding yeast. Genetics 153: 1271-1283.

Zaragoza, M. V., P. A. Jacobs, R. S. James, P. Rogan, S Sherman, et *al.*, 1994 Nondisjunction of human acrocentric chromosomes: studies of 432 trisomic fetuses and liveborns. Hum Genet 94: 411-417.

Zaragoza, M. V., E. Millie, R. W. Redline, T. J. Hassold, 1998 Studies of non-disjunction in trisomies 2, 7, 15, and 22: does the parental origin of trisomy influence placental morphology? J Med Genet 35: 924-931.

Zhang, P., B. A. Knowles, L. S. Goldstein, R. S. Hawley, 1990 A kinesin-like protein required for distributive chromosome segregation in Drosophila. Cell 62: 1053-1062.

Zhang, N., S. G. Kuznetsov, S. K. Sharan, K. Li, P. H. Rao, *et al.*, 2008 A handcuff model for the cohesin complex. J Cell Biol 183: 1019-1031.

Zicker, D., 2006 From early homologue recognition to synaptonemal complex formation. Chromosoma **115**: 158-174.

Zickler, D., N. Kleckner, 1998 The leptotene-zygotene transition of meiosis. Annu Rev Genet 32: 619-697.

Zitron, A. E., R. S. Hawley, 1989 The genetic analysis of distributive disjunction segregation in *Drosophila melanogaster*. I. Isolation and characterization of Aberrant X segregation (Axs), a mutation defective in chromosome partner choice. Genetics 122: 801-821

Chapter 2

Sustained and rapid chromosome movements are critical for chromosome pairing and meiotic progression in budding yeast

Megan Sonntag Brown, Sarah Zanders*, and Eric Alani

Department of Molecular Biology and Genetics, Cornell University, Ithaca, NY

*Present address: Division of Basic Sciences, Fred Hutchinson Cancer Research Center, Mail Stop A2-025, P.O. Box 19024, Seattle, WA 98109-1024

This chapter was originally published in the May 2011 issue of Genetics:

Sonntag Brown, M., S. Zanders, E. Alani, 2011 Sustained and rapid chromosome movements are critical for chromosome pairing and meiotic progression in budding yeast. Genetics 188: 21-32.

Contributions: S.Zanders made some of the initial *csm4* allele strains and initiated the project by doing preliminary tetrad dissections.

ABSTRACT

Telomere-led chromosome movements are a conserved feature of Meiosis I prophase. Several roles have been proposed for such chromosome motion, including promoting homolog pairing and removing inappropriate chromosomal interactions. Here, we provide evidence in budding yeast that rapid chromosome movements affect homolog pairing and recombination. We found that *csm4*Δ strains, which are defective for telomere-led chromosome movements, show defects in homolog pairing as measured in a "one-dot/two-dot tetR-GFP" assay; however, pairing in *csm4*Δ eventually reaches near wild-type (WT) levels. Charged-to-alanine scanning mutagenesis of *CSM4* yielded one allele, *csm4-3*, that confers a *csm4Δ*-like delay in meiotic prophase but promotes high spore viability. The meiotic delay in *csm4-3* strains is essential for spore viability because a null mutation (*rad17Δ*) in the Rad17 checkpoint protein suppresses the delay but confers a severe spore viability defect. *csm4-3* mutants show a general defect in chromosome motion but an intermediate defect in chromosome pairing. Chromosome velocity analysis in live cells showed that while average chromosome velocity was strongly reduced in *csm4-3*, chromosomes in this mutant displayed occasional rapid movements. Lastly, we observed that *spo11* mutants displaying lower levels of meiosis-induced double-strand breaks showed higher spore viability in the presence of the *csm4-3* mutation compared to *csm4Δ*. Based on these observations, we propose that during meiotic prophase the presence of occasional fast moving chromosomes over an extended period of time is sufficient to promote WT levels of recombination and high spore viability; however, sustained and rapid chromosome movements are required to prevent a checkpoint response and promote efficient meiotic progression.

INTRODUCTION

Cells that enter meiosis undergo a single round of DNA replication followed by two divisions to yield haploid gametes, such as sperm and eggs in humans, and spores in baker's yeast. Accurate segregation of chromosomes at the meiosis I (MI) and II (MII) divisions is a critical part of this process. Improper segregation can lead to aneuploidy, which in humans is a leading cause of infertility, miscarriages, and mental retardation (HASSOLD and HUNT 2001). One of the main causes of aneuploidy is nondisjunction of homologous chromosomes during MI. In most organisms, at least one crossover per homolog pair is essential for MI disjunction (ROEDER 1997; ZICKLER and KLECKNER 1999). Chromosome nondisjunction can occur if there are too few or too many crossovers, or if crossovers are not properly placed, such as in close proximity to centromeres and telomeres (HASSOLD and HUNT 2001; LACEFIELD AND MURRAY 2007; ROCKMILL, VOELKEL-MEIMAN and ROEDER 2006). In the latter case, crossing over far from the centromere increases the likelihood of chromosomes segregating to the same spindle pole, resulting in aneuploidy (MARTINEZ-PEREZ and COLAIACOVO 2009; LACEFIELD and MURRAY 2007).

In baker's yeast, crossing over is initiated in meiosis by the formation of Spo11-dependent DNA double strand breaks (DSBs; KEENEY 2001). These breaks can be repaired as either crossovers or non-crossovers, with approximately 60% of the 140-170 DSBs processed as crossovers (BUHLER, BORDE, LICHTEN 2008; MANCERA *et al.* 2008). In the interference-dependent crossover pathway, which leads to more widely-spaced crossovers, DSBs are processed to form single-end invasion intermediates (SEIs) that result from the invasion of a DSB end into an intact homolog. These intermediates undergo second-end capture with the intact homolog to form double Holliday junctions (dHJs) that are ultimately resolved to form

crossovers (BÖRNER *et al*. 2004; SCHWACHA and KLECKNER 1995; ALLERS and LICHTEN 2001; LAO *et al*. 2008).

During meiotic prophase in *S. cerevisiae*, distinct chromosome motions are observed which have been hypothesized to promote chromosome disjunction at MI. At the end of leptotene, telomeres attach to the nuclear envelope and move towards the spindle pole body, forming a bouquet-like structure (TRELLES-STICKEN, LOIDL and SCHERTHAN 1999; TRELLES-STICKEN *et al.* 2005). This bouquet structure is transient, but has been proposed to play a role in meiotic crossing over, since mutants in a variety of organisms that are defective for bouquet formation show defective or altered steps in recombination (CHUA and ROEDER 1997; HARPER, GOLUBOVSKAYA and CANDE 2004; WU and BURGESS 2006; GOLUBOVSKAYA *et al.* 2002; WANAT *et al.* 2008; KOSAKA *et al*. 2008; DAVIS and SMITH 2006; YAMAMOTO *et al*. 1999; NIWA, SHIMANUKI and MIKI 2000; BASS 2003). The synaptonemal complex (SC), a proteinaceous structure that holds homologous chromosomes together and acts as a scaffold for crossing over, begins to form at the same time as bouquet formation (PAGE and HAWLEY 2004; JOSEPH and LUSTIG 2007). After the bouquet stage ends, in early zygotene in baker's yeast, rapid prophase movements led by dispersed telomeres ensue concurrently with extension of the SC and continue into pachytene (SCHERTHAN *et al.* 2007; KOSZUL *et al.* 2008; CONRAD *et al*. 2008). The SC dissolves in diplotene, leaving chiasmata, the physical manifestations of crossovers, intact (HARPER, GOLUBOVSKAYA and CANDE 2004). The chromosomes then proceed through anaphase, and complete the MI division.

Many roles have been proposed for telomere-led movements seen in zygotene and pachytene. Studies have found that mutants defective in these movements have a small increase

in ectopic recombination, suggesting motion may prevent ectopic interactions (GOLDMAN AND LICHTEN 2000; CHUA and ROEDER 1997). Telomere-led movements have been proposed to untangle nonhomologous chromosomes, possibly from interlocks formed during SC formation (RASMUSSEN 1986; SCHERTHAN, BAHLER and KOHLI 1994; WANAT *et al.* 2008; STORLAZZI *et al.* 2010). These movements have also been proposed to promote homolog pairing, SC formation, and sister chromatid cohesion (ROCKMILL and ROEDER 1998; HARPER, GOLUBOVSKAYA and CANDE 2004; SATO *et al.* 2009; SCHERTHAN *et al*. 1996).

In budding yeast, Mps3, Ndj1, and Csm4 are required for bouquet formation and zygotene to pachytene telomere-led movements (TRELLES-STRICKEN, DRESSER and SCHERTHAN 2000; CONRAD *et al.* 2007; WANAT *et al*. 2008). Mps3 interacts with Ndj1, which is a meiosis-specific protein that localizes to telomeres (CONRAD, DOMINGUEZ and DRESSER 1997; CHUA and ROEDER 1997). Both Ndj1 and Mps3, a SUN domain nuclear envelope protein, are required to attach telomeres to the nuclear envelope, one of the key steps in forming a bouquet (CONRAD *et al*. 2007). Csm4, a cytoplasmic tail-anchored protein, interacts with both Ndj1 and Mps3 (RABITSCH *et al.* 2001; CONRAD *et al*. 2008; KOSAKA, SHINOHARA and SHINOHARA 2008). Csm4 is not needed for telomere attachment to the nuclear envelope, but is required for rapid telomere-led movements during meiosis (CONRAD *et al*. 2008; KOSZUL *et al*. 2008; WANAT *et al*. 2008; KOSAKA, SHINOHARA and SHINOHARA 2008). The cytoskeleton is also necessary for chromosome motion, because disruption of microtubules in *S. pombe,* or actin in budding yeast, arrests chromosome motion and prevents bouquet formation (YAMAMOTA *et al.* 1999; CHIKASHAGE, HARAGUCHI and HIRAOKA 2007; KOSZUL *et al.* 2008; TRELLES-STICKEN *et al.* 2005; SCHERTHAN *et*

al. 2007). The attachment of chromosomes through Mps3, Ndj1, and Csm4 to the actin cytoskeleton in budding yeast appears to be passive. Telomeres are thought to associate with dynamic cytoplasmic actin cables that hug the nucleus, with lead chromosome(s) directing the movement of other chromosomes (KOSZUL *et al.* 2008; CONRAD *et al.* 2008). In support of this notion, chromosome motion occurs at a similar speed to actin cable extension (~0.3 μm/sec; YANG and PON 2002).

Previous studies have shown Csm4 is important for MI disjunction of chromosomes (WANAT *et al*. 2008; KOSAKA, SHINOHARA and SHINOHARA 2008). The *csm4Δ* mutation confers a spore viability defect (60-65% compared to ~90-95% for WT) with patterns of spore viability (prevalence of 4, 2, 0 viable spores) and chromosome segregations in two-spore viable tetrads consistent with MI nondisjunction. Crossing over, however, is not decreased, but occurs at higher than WT levels (WANAT *et al.* 2008). Furthermore, analysis of two spore viable tetrads that had undergone MI nondisjunction showed similar crossover levels to WT but differences in crossover placement (WANAT *et al.* 2008). Lastly, all aspects of recombination after the initiation of DSBs are delayed in *csm4Δ*, resulting in an overall four to five hour delay in completion of MI.

In this study, we identified a defect in homolog pairing in *csm4*Δ. We then analyzed a set of charged-to-alanine scanning mutagenesis alleles to tease apart the role of chromosome motion in pairing. We found one allele, *csm4-3*, that conferred high spore viability, but an MI delay similar to the null. We further characterized this allele, showing it confers a defect in chromosome motion and pairing, but each to a lesser degree than the null. Our data are consistent with sustained and rapid chromosome movements being required in meiosis to promote chromosome pairing and efficient meiotic progression.

MATERIALS AND METHODS

Media and yeast strains: Yeast strains were grown at 30˚C on YPD (YP (yeast, peptone) plus dextrose) supplemented with complete amino acid mix (ROSE, WINSTON and HIETER 1990). Sporulation plates and other media have been described previously (WACH *et al.* 1994; WANAT *et al.* 2008). When appropriate, minimal selective media, synthetic complete media supplemented with 5 μM copper sulfate, and YPD supplemented with complete amino acid mix and 3 mg/l cycloheximide were used (ROSE, WINSTON and HIETER 1990). When required, Geneticin (Invitrogen) and hygromycin B (Calbiochem) were included in YPD media as previously described (GOLDSTEIN and MCCUSKER 1999).

Parental strains (Table 2.1) in this work included the isogenic SK1 strain NHY943/NHY942 (DE LOS SANTOS *et al*. 2003), the congenic SK1 strain EAY1108/EAY1112 (ARGUESO *et al.* 2004; TSUBOUCHI and ROEDER 2003), Nup49-GFP and Zip1-GFP SK1 strains (KOSZUL *et al.* 2008), one-dot/two-dot tetR-GFP pairing assay SK1 strains (MARSTON *et al.* 2004; BRAR *et al.* 2009*;* TOTH *et al.* 2000; ALEXANDRU *et al.* 2001) and SK1 *spo11* hypomorph strains (DIAZ *et al*. 2002; HENDERSON and KEENEY 2004; MARTINI *et al.* 2006). The *spo11(Y135F)-HA3His6/spo11-HA* genotype described by Keeney and colleagues (MARTINI *et al*. 2006) is referred to in this study as *spo11-HA/yf.*

Yeast strains were constructed using standard transformation protocols (GIETZ *et al.* 1995) and integration events were confirmed using PCR primers flanking insertion regions. Site-specific mutations in *csm4* were also confirmed by DNA sequencing of *CSM4* DNA PCR amplified from the strain of interest. The *csm4*Δ allele contains a complete deletion of the open reading frame. *csm4-3* contains two mutations, K22A and K24A. Other allele information can be found in Table 2.1.

Table 2.1. Yeast strains used in this study

Strain Names	Genotype
NH943	*MATa, ho::hisG, ade2*Δ*, ura3(*Δ*Sma-Pst), leu2::hisG, CEN3::ADE2, lys5-P, cyh2*^{r}*, his4-B*
SKY665	as NH943 except *MATα, spo11(Y135F)-HA3His6::KANMX4*
EAY3036	as NH943 except *MATα, spo11(Y135F)-HA3His6::KANMX4, csm4*Δ*::HPHMX4*
EAY1483	as NH943 except *csm4*Δ*::KANMX4*
NH942	*MATα, ho::hisG, ade2*Δ*, can1, ura3(*Δ*Sma-Pst), met13-B, trp5-S, CEN8::URA3, thr1-A, cup1*^{s}
SKY633	as NH942 except *MATa, spo11-HA3His6::KANMX4*
EAY3037	as NH942 except *MATa, spo11-HA3His6::KANMX4, csm4*Δ*::HPHMX4*
EAY3038	as NH942 except *MATa, spo11-HA3His6::KANMX4, csm4(K22A;K24A)::KANMX4*
EAY1484	as NH942 except *csm4*Δ*::KANMX4*
EAY3039	as NH942 except *csm4(K22A;K24A)::KANMX4*
EAY1108	*MATa, ho::hisG, lys2, ura3, leu2::hisG, trp1::hisG, URA3-CEN15, iLEU2-chXV, iLYS2-chXV*
EAY1480	as EAY1108, but *csm4*Δ*::HPHMX4*
EAY1977	as EAY1108 but *csm4*Δ*::KANMX4, pch2*Δ*::KANMX4*
EAY3041	as EAY1108 but *csm4(K22A;K24A)::KANMX4, pch2*Δ*::NATMX4*
EAY1981	as EAY1108, but *csm4*Δ*::KANMX4, rad17*Δ*::HPHMX4*
EAY3040	as EAY1108 but *csm4(K22A;K24A)::KANMX4, rad17*Δ*::HPHMX4*
EAY2885	as EAY1108, but *csm4(K22A;K24A)::KANMX4*
EAY2887	as EAY1108, but *csm4(D40A)::KANMX4*
EAY2888	as EAY1108, but *csm4(E80A)::KANMX4*
EAY2890	as EAY1108, but *csm4(K96A)::KANMX4*
EAY2891	as EAY1108, but *csm4(E100A)::KANMX4*
EAY2889	as EAY1108, but *csm4(D123A;E124A)::KANMX4*
EAY2886	as EAY1108, but *csm4(E155A)::KANMX4*
EAY1112	*MATα, ho::hisG, lys2, ura3, leu2::hisG, trp1::hisG, ade2::hisG, his3::hisG, TRP1-CEN15*
EAY1481	as EAY1112, but *csm4*Δ*:: HPHMX4*
EAY1978	as EAY1112, but *csm4*Δ*::KANMX4, pch2*Δ*::KANMX4*

EAY1982	as EAY1112, but *csm4*Δ::*KANMX4, rad17*Δ*::HPHMX4*
EAY3042	*MATa, ho::hisG, leu2::hisG, URA3::NUP49-GFP-URA3*
YKK254/EAY2151	*MATa, ho::hisG, leu2::hisG, URA3::NUP49-GFP-URA3 , csm4*Δ*::HPHMX4*
EAY2225	as EAY3042 except *csm4(D3A)::KANMX4*
EAY3044	as EAY3042 except *csm4(R8A;K9A)::KANMX4*
EAY2223	as EAY3042 except *csm4(K22A;K24A)::KANMX4*
EAY2235	as EAY3042 except *csm4(E31A;R32A;K33A)::KANMX4*
EAY2233	as EAY3042 except *csm4(D40A)::KANMX4*
EAY3045	as EAY3042 except *csm4(D47A)::KANMX4*
EAY2227	as EAY3042 except *csm4(E54A)::KANMX4*
EAY2220	as EAY3042 except *csm4(K57A;K59A;E60A)::KANMX4*
EAY2241	as EAY3042 except *csm4(E66A)::KANMX4*
EAY3046	as EAY3042 except *csm4(E80A)::KANMX4*
EAY2229	as EAY3042 except *csm4(D83A;R84A;E85A)::KANMX4*
EAY2237	as EAY3042 except *csm4(D92A;D93A)::KANMX4*
EAY2239	as EAY3042 except *csm4(K96A)::KANMX4*
EAY2249	as EAY3042 except *csm4(E100A)::KANMX4*
EAY2221	as EAY3042 except *csm4(K109A;R111A)::KANMX4*
EAY2245	as EAY3042 except *csm4(D123A;E124A)::KANMX4*
EAY2217	as EAY3042 except *csm4(H128A;K130A)::KANMX4*
EAY2243	as EAY3042 except *csm4(E135A)::KANMX4*
EAY2231	as EAY3042 except *csm4(E155A)::KANMX4*
EAY3043	*MATα, ho::hisG, leu2::hisG, URA3::NUP49-GFP-URA3*
YKK255	*MATα, ho::hisG, leu2::hisG, URA3::NUP49-GFP-URA3 , csm4*Δ*::HPHMX4*
YKK713	*MATa, ho::hisG, leu2::hisG, ZIP1::ZIP1-GFP(700), ura3, csm4*Δ*::HPHMX4*
EAY3047	*MATa, ho::hisG, leu2::hisG, ZIP1::ZIP1-GFP(700), ura3*
EAY3049	*MATa, ho::hisG, leu2::hisG, ZIP1::ZIP1-GFP(700), ura3, csm4(K22A;K24A)::KANMX4*
YKK720	*MATα, ho::hisG, leu2::hisG, ZIP1::ZIP1-GFP(700), ura3, csm4*Δ*::HPHMX4*
EAY3048	*MATα, ho::hisG, leu2::hisG, ZIP1::ZIP1-GFP(700), ura3*
A9785	*MATa ho::LYS2, ura3, his3::hisG, trp1::hisG, lys2::TetOx240:URA3, leu2::LEU2-tetR-GFP,*

	ndt80Δ::PSTE5:URA3
EAY2995	as EAY2985 except *csm4Δ::HPHMX4*
A9786/EAY2984	*MATα ho::LYS2, ura3, his3::hisG, trp1::hisG, lys2::TetOx240:URA3, leu2::LEU2-tetR-GFP, ndt80Δ::PSTE5:URA3*
EAY2994	as EAY2984 except *csm4Δ::HPHMX4*
EAY3050	as EAY2984 except *csm4(K22A;K24A)::KANMX4*
A16204/EAY2987	*MATa ho::LYS2, lys2, ura3, leu2::hisG, trp1::hisG, promURA3::tetR:: GFP-LEU2, TelV::tetOx224::URA3, ndt80Δ::PSTE5:URA3*
EAY2997	as EAY2987 except *csm4Δ::HPHMX4*
A16203/EAY2988	*MATα ho::LYS2, lys2, ura3, leu2::hisG, trp1::hisG, promURA3::tetR:: GFP-LEU2, TelV::tetOx224::URA3, ndt80Δ::PSTE5:URA3*
EAY2998	as EAY2988 except *csm4Δ::HPHMX4*
EAY3051	as EAY2988 except *csm4(K22A;K24A)::KANMX4*
A16199/EAY2981	*MATa, ho::LYS2, lys2, leu2::hisG, ura3, trp1::hisG, his3::hisG, leu2::pURA3-TetR-GFP::LEU2, CENV::TetOx224::HIS3, ndt80Δ::PSTE5:URA3*
EAY2991	as EAY2981 except *csm4Δ::HPHMX4*
A16201/EAY2986	*MATα, ho::LYS2, lys2, leu2::hisG, ura3, trp1::hisG, his3::hisG, leu2::pURA3-TetR-GFP::LEU2, CENV::TetOx224::HIS3, ndt80Δ::PSTE5:URA3*
EAY2996	as EAY2986 except *csm4Δ::HPHMX4*
EAY3052	as EAY2986 except *csm4(K22A;K24A)::KANMX4*
A5047/EAY2982	*MATa, ho::LYS2, ura3, leu2::hisG, his3::hisG, trp1::hisG, leu2::LEU2::tetR-GFP::TetO-HIS3, ndt80Δ::PSTE5:URA3*
EAY2992	as EAY2982 except *csm4Δ::HPHMX4*
A5049/EAY2983	*MATα, ho::LYS2, ura3, leu2::hisG, his3::hisG, trp1::hisG, leu2::LEU2::tetR-GFP::TetO-HIS3, ndt80Δ::PSTE5:URA3*
EAY2993	as EAY2983 except *csm4Δ::HPHMX4*
EAY3053	as EAY2983 except *csm4(K22A;K24A)::KANMX4*
A6644/EAY2979	*MATa, ho::LYS2, ura3, leu2::hisG, his3::hisG, trp1::hisG, pURA3::tetR::GFP::LEU2, tetOx224::URA3, ndt80Δ::PSTE5:URA3*
EAY2989	as EAY2979 except *csm4Δ::HPHMX4*

Alanine scanning mutagenesis: The *CSM4* one step integrating vector pEAA381 (*CSM4::KANMX, URA3, ARSH4 CEN6*) was modified by Quick Change (Stratagene, La Jolla CA) site-directed mutagenesis to create 19 *csm4* derivatives. The entire *CSM4* open reading frame, including 400 bp upstream, was sequenced in the mutant plasmids to ensure that only the desired amino acid changes were introduced. pEAA381 and mutant derivatives were digested with *Sac*I and *Sph*I to release a DNA fragment containing *CSM4* (or *csm4* alleles), the *KANMX* marker, and DNA sequence downstream of *CSM4*. The *KANMX* marker is located between the CSM4 open reading frame and the downstream *CSM4* sequence. The DNA fragments were then transformed into yeast and integration of *CSM4::KANMX* and *csm4::KANMX* derivatives was confirmed by PCR analysis and DNA sequencing. The DNA sequences of the oligonucleotides used to create the *csm4* alleles and the resulting plasmids are available upon request.

Meiotic time courses: Meiotic time courses were performed as follows: 0.35 ml of a saturated YPD overnight culture of the desired strain were inoculated into 200 ml YPA (YP + 2% potassium acetate) plus complete amino acid mix and grown for 16-17 hours at 30˚C. Cells in the YPA culture were spun down, washed once in 100 ml 1.0 % potassium acetate, resuspended in 100 ml 1.0 % potassium acetate, and then incubated with vigorous shaking at 30˚C. All strains for a single time course were grown in the same batch of media under identical conditions. The *csm4* alleles were initially analyzed in the Nup49-GFP background. Strains bearing *spo11* and *rad17Δ* mutations were analyzed in the NH942/NH943 and EAY1108/EAY1112 strain backgrounds, respectively.

Aliquots of cells at specific time points were DAPI stained to determine the percent of cell that completed at least the first meiotic division (cells in which 2, 3, or 4 nuclei were observed by DAPI staining; MI +/- MII; GALBRAITH *et al.* 1997). Cells were visualized using

Olympus BX60 microscope and at least 150 cells were counted for each time point. For each strain the time required for 40% cells to have completed MI was recorded and mutant phenotypes were presented with respect to the delay (hrs) in completing MI relative to WT.

Tetrad dissection and analysis: Diploids were constructed using the zero growth mating protocol (ARGUESO *et al.* 2003). Haploid parental strains were mated for four to five hours on YPD plates before being spread onto sporulation plates. The plates were incubated at 30˚C for at least two days before dissection. All strains were dissected onto synthetic complete media. Colonies derived from germinated spores were incubated at 30˚C for two to three days before being replica-plated to appropriate selective media. Replica-plates were scored after a one-day incubation at 30˚C. The distributions of each tetrad type and map distances were calculated using RANA software (ARGUESO *et al.* 2004).

Live cell imaging: Cells were observed at room temperature using a Zeiss Imager M2 fluorescent microscope equipped with DAPI, GFP, and TexRed filters, an Axiocam MR camera, and a ZipL Piezo Z device for acquiring z-stacks. Images were acquired using Axiovision software.

Nup49-GFP motion assays were conducted in live WT, *csm4*Δ, and *csm4-3* cells (KOSZUL *et al.* 2008). Time courses were performed as described above. In initial studies, samples obtained from each time point were incubated at 4˚C overnight prior to analyzing Nup49-GFP motion by light microscopy. These assays have since been repeated in the absence of the 4˚C incubation step; no significant differences were seen in Nup49-GFP motion using the two methods. To maximize aeration of cells, at each time point 3 µl aliquots of vortexed cells were placed on an untreated glass slide and then covered with a cover slip. Only cells located near air bubbles were analyzed (KOSZUL, KAMEOKA and WEINER 2009). Images were

taken at one-second intervals with exposure times for Nup49-GFP cells ranging from 600 to 700 msec. Zip1-GFP time courses (KOSZUL *et al.* 2008) were analyzed in the same manner as in the Nup49-GFP experiments, but without including the 4˚C incubation step. The exposure time for Zip1-GFP cells was 600 msec. Chromosome velocities in the Zip1-GFP time courses were calculated using a manual tracking plugin on ImageJ. Clearly isolated chromosomes in a cell were manually marked at the telomere and monitored at each exposure time for at least 15 consecutive frames. This resulted in at least 15 velocity measurements for each chromosome. Average speeds for each chromosome were calculated from the mean of the 15-25 velocity measurements. The maximum velocity seen between frames (~one-second intervals) for each chromosome was determined to be the maximum for that chromosome. 30 chromosomes from 30 independent cells were analyzed for each genotype.

One-dot/two-dot tetR-GFP time courses were performed, similar to BRAR *et al,* 2009, as follows. 0.35 ml of a saturated overnight YPD culture of the desired strain were inoculated into 100 ml YPA and grown for 16-17 hours at 30˚C. The YPA culture was subsequently washed once in 1% KAc, resuspended in 50 ml 1% KAc, and then incubated with vigorous shaking at 30˚C. Cell aliquots were taken at specific time points and examined with the GFP filter in Z-stacks (~20 planes separated by 0.3 μm) with an exposure time of 150 msec. See "Media and Yeast Strains" and Table 2.1 for strain details.

RESULTS

Csm4 acts in chromosome pairing: We used a one-dot/two-dot tetR-GFP assay developed by the Amon laboratory (BRAR *et al.* 2009) to test whether *csm4*Δ mutants display a defect in homolog pairing in meiosis. Diploid strains analyzed in this assay contain an array of

tet operator (*tetO)* sequences in both copies of a particular locus (*LYS2*, *TELV*, and *CENV*). These strains also contain a tet repressor (tetR)-GFP fusion construct present at another location. A visible GFP focus is seen when tetR binds the *tetO* array. Pairing is assayed in unfixed cells by determining whether one (paired) or two (unpaired) clear GFP dots are observed (Figure 2.1). Strains used in the pairing assays contain the *ndt80*Δ mutation (*NDT80* is required for exit from pachytene) so that maximum pairing levels can be assessed (WEINER and KLECKNER 1994; PEOPLES *et al.* 2002). It is important to note that in our study, only strains used for live cell imaging contain the *ndt80* mutation. Cells enter meiosis (T = 0) with a high level of one-dot cells which is thought to be due to residual somatic pairing and/or the Rabl orientation, where centromeres cluster during interphase (LOIDL, KLEIN and SCHERTHAN 1994; WEINER and KLECKNER, 1994; BURGESS, KLECKNER and WEINER 1999). The one-dot phenotype is lost in the first few hours of meiosis, before *SPO11*-dependent pairing is observed (see BRAR *et al.* 2009 and Figure 2.2 for examples). Here, we use the term "pairing" loosely to incorporate a wide range of homolog interactions, ranging from the initial alignment of homologs (400 nM; ZICKLER and KLECKNER 1999) to DNA interactions (e.g. SEI formation) that occur after initial homolog interactions have occurred. Pairing was assayed at three distinct sites in the genome: *LYS2*, located on an arm of chromosome II, and *TELV* and *CENV*, located near a telomere and the centromere of chromosome V, respectively. Pairing was also assessed in strains containing *tetO* arrays at nonhomologous sites (*LEU2* and *CENV; URA3* and *LYS2*). These strains allow us to visualize the loss of one-dot cells through meiotic prophase. They also serve as controls to measure the frequency of GFP dots that co-localize by chance.

We analyzed homolog pairing in WT and *csm4*Δ cells at *LYS2*, *CENV*, and *TELV*, and observed a pairing defect in *csm4*Δ (Figure 2.2). Pairing occurred with dynamics similar to WT

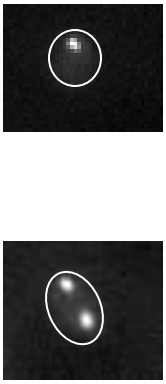

Figure 2.1. Representative images for one-dot/two-dot cells. Cells with one (paired, top) and two (unpaired, bottom) *tetO/tetR-GFP* dots are shown. The approximate borders of the nucleus of each cell are outlined.

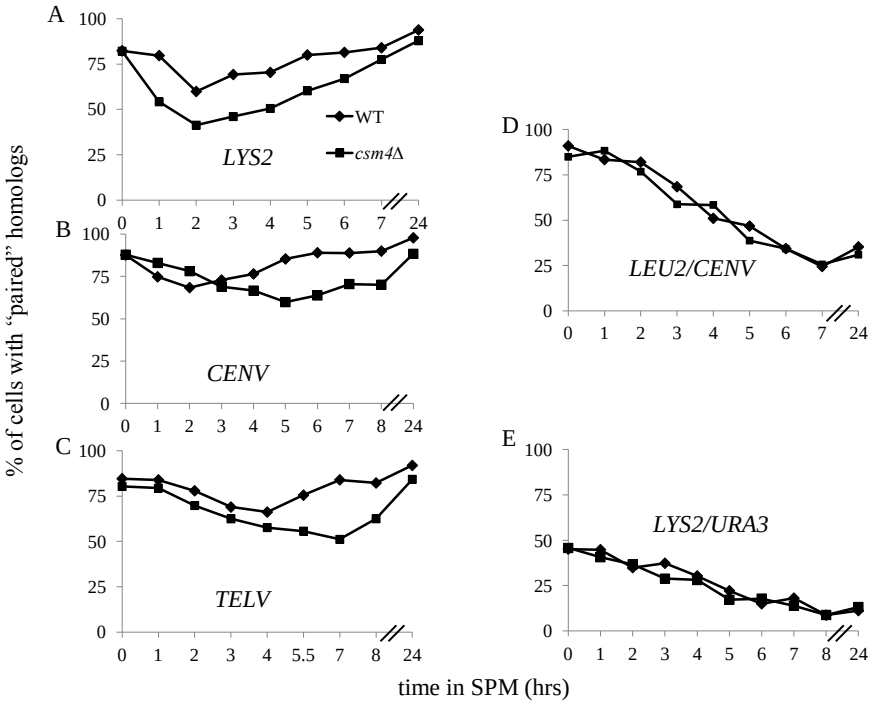

Figure 2.2. Chromosome pairing is defective in *csm4*Δ. Chromosome pairing was assessed in diploid SK1 strains ectopically expressing tetR-GFP and bearing *tet0* arrays at homologous positions (BRAR *et al.* 2009; MATERIALS and METHODS). Homologs were considered paired when only one GFP dot was observed and were considered unpaired when two clear GFP dots were seen (Figure 2.1). Cells were analyzed using z-stacks to visualize the entire cell volume. (A, B, C) Representative time courses (chosen from four to eight independent experiments) with *tetO* arrays at *LYS2* (A), *CENV* (B), and *TELV* (C). Pairing was considered maximum in these *ndt80Δ* strains at T = 24 hrs. (D, E) Representative time courses demonstrating non-homologous pairing, with one *tetO* array at *LEU2* and another at *CENV* (D), and one at *LYS2* and another at *URA3* (E).

for the first few hours after entry into sporulation media; however *csm4Δ* strains consistently reached a lower pairing level at all three loci (Figure 2.2 A, B, C; Figure 2.3). Furthermore, while *csm4*Δ reached near WT levels of pairing by 24 hours, there was a delay in reaching maximal pairing levels at all three loci. This delay could be due solely to the four to five hour meiotic delay in *csm4*Δ*;* however this appears unlikely, because as discussed below, an allele with the same meiotic delay progressed through pairing more rapidly than the null. The slightly lower values of homolog pairing at 24 hours may be due to the slight sporulation defect seen in *csm4Δ* (WANAT *et al*. 2008); one possibility is that a small percentage of *csm4Δ* cells do not proceed to the homolog pairing stage of meiosis. However, *csm4*Δ showed a phenotype identical to WT when looking at nonhomologous loci (Figure 2.2 D and E). It is important to note that the initial high levels of pairing observed in the *LEU2/CENV* strains is likely due to *LEU2* being near a centromere, and thus showing residual vegetative pairing with *CENV* due to the Rabl orientation. Our data suggest that *csm4*Δ does not have a defect in removing the "pairing" seen between nonhomologous chromosomes at early stages in meiosis. The data also suggest that the *csm4*Δ strains do not have an increased likelihood in random overlap of GFP dots.

Analysis of *csm4* alleles: To further investigate whether the rapid chromosome motion that takes place during meiotic prophase is necessary for homolog pairing and spore viability, and to determine whether these phenotypes can be separated, we created a set of nineteen alleles of *CSM4* by charged-to-alanine scanning mutagenesis (Figure 2.4 A). This approach allowed mutagenesis of a large number of residues in Csm4 with the expectation that protein-protein interactions would involve solvent-exposed residues. *csm4*Δ has a low spore viability (~60%) and a long meiotic delay of four to five hours compared with WT. We analyzed meiotic delay

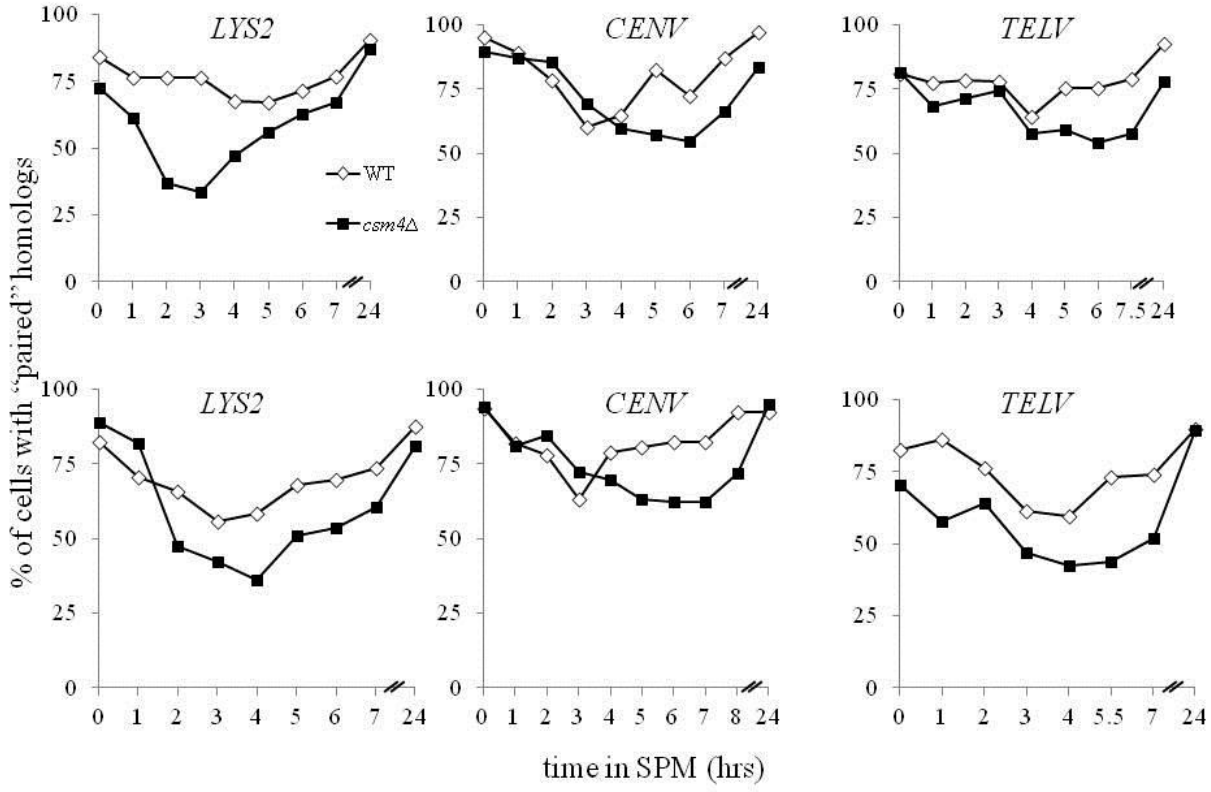

Figure 2.3. Additional time courses for WT and *csm4Δ* with *tetO* arrays at *LYS2, CENV,* and *TELV*. See Figure 2.2 for details.

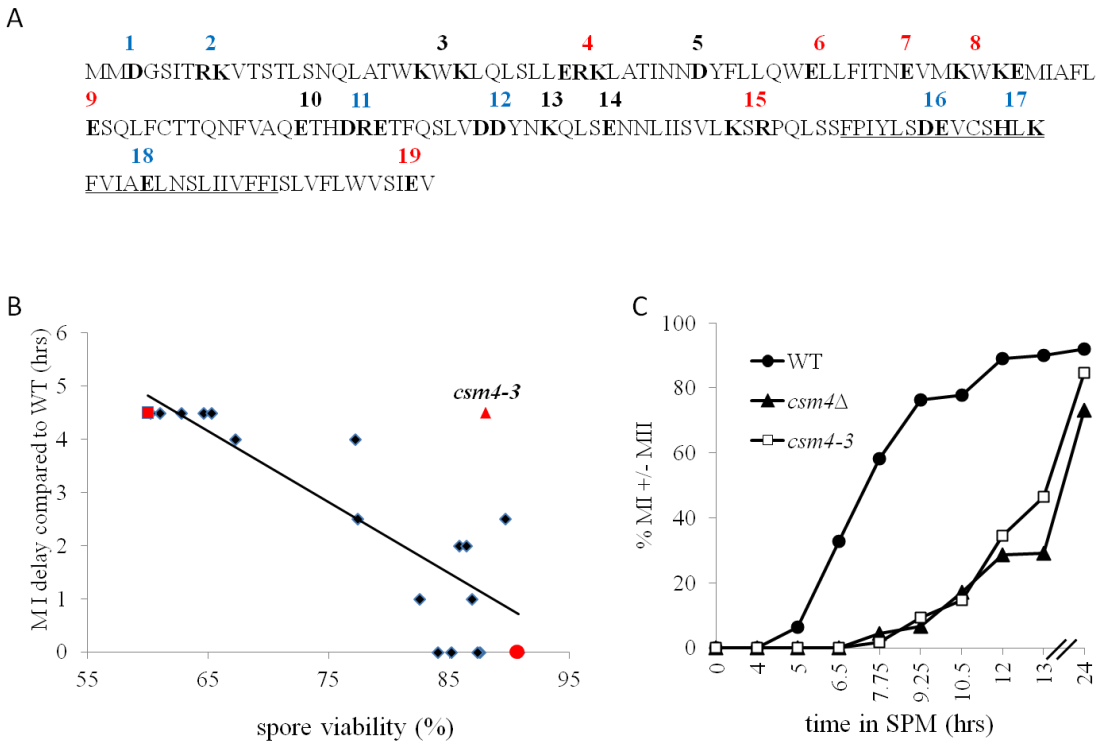

Figure 2.4. *csm4-3* is a separation of function allele. (A) Amino acids in the Csm4 polypeptide were mutated to alanine residues as indicated in bold. The allele designation is shown above each set of amino acid substitutions. The putative transmembrane domain is underlined near the C-terminus. Alleles that conferred a WT phenotype as measured by spore viability and timing of the MI division (MATERIALS and METHODS) are shown in blue; alleles that displayed a null phenotype in these assays are shown in red. Intermediate alleles are shown in black. (B) The phenotypes of *csm4* alleles (Table 2.2) are presented in a graph in which spore viability is plotted vs. MI delay, relative to WT, in completing the MI division. Cells with two, three, or four nuclei were counted as having completed M1 (MI +/-MII). The phenotypes of WT (red circle), and *csm4*Δ (red square) are indicated. *csm4-3*, a separation of function allele, is highlighted (red triangle). (C) Representative time course showing the completion of the MI division (MI +/-MII) in WT, *csm4Δ*, and *csm4-3* strains.

and spore viability for these 19 mutants and found a wide range of spore viabilities, ranging from the null (60%) to WT (90%), as well as a wide range of meiotic delays, from no delay to a null-like five-hour delay (Table 2.2; MATERIALS and METHODS). We found that the null alleles grouped into two regions of the proteins, from amino acids 31 to 66, and 100 to 111. This suggests that these two regions are important for function, and may contain an interaction domain for Ndj1 or Mps3, or a yet-to-be discovered interacting protein. As expected, a negative correlation was seen between meiotic delay and spore viability; as spore viability increased, the meiotic delay decreased (Figure 2.4 B). One strain, *csm4-3*, is an outlier to this pattern, showing high spore viability and sporulation, but a meiotic delay similar to the null (Figure 2.4 C).

Chromosome motion is strongly reduced in *csm4-3:* Telomere-led chromosome motion was studied for a subset of the *csm4* mutants. Strains that showed near WT spore viability and no meiotic delay (*csm4-1, 2, 12, 17,* and *18*) or those that showed null-like spore viability and a long meiotic delay (*csm4-4, 6, 9,* and *15*) were not analyzed further (Table 2.2). Initially we analyzed motion in strains containing Nup49-GFP, a nuclear pore protein that marks the nuclear envelope (BELGAREH and DOYE 1997). When chromosome movement occurs in meiotic prophase, chromosomes are rocketed into the nuclear envelope; this movement is clearly seen in WT strains expressing Nup49-GFP (Figure 2.5 A; KOSZUL *et al.* 2008). The nuclear envelope distortions were seen beginning in zygotene and reached maximum levels during pachytene (four to six hours after induction of meiosis; KOSZUL *et al.* 2008). Cells were assigned as having chromosome motion based on the presence or absence of nuclear envelope distortions (Table 2.2). Mutants with null levels of Nup49-GFP motion (nuclear envelope appears spherical in *csm4-3, 7, 8,* and *14*) all have long meiotic delays (ranging from 2.5-4.5 hours), but their spore viabilities varied greatly, from 63 to 88%. Mutants with intermediate to

Table 2.2. Characterization of *csm4* mutants with respect to spore viability, completion of the meiosis I division, nuclear envelope distortions, and genetic map distances.

Strain	% SV (n)	MI delay (hrs)	NE distortions	map distance in cM (n)
WT	91 (120)	0	+	101 (1068*)
csm4Δ	60 (120)	4.5	-	146(531*)
CSM4/csm4Δ	90 (240)	ND	+	109 (160)
csm4-1	88 (100	0	ND	ND
csm4-2	85 (220)	0	ND	ND
csm4-3	88 (360)	4.5	–	126 (238)
csm4-4	61 (100)	4.5	ND	ND
csm4-5	86 (260)	2.0	+/-	141 (100)
csm4-6	65 (60)	4.5	ND	ND
csm4-7	67 (40)	4.0	-	ND
csm4-8	63 (100)	4.5	-	ND
csm4-9	60 (140)	4.5	ND	ND
csm4-10	82 (240)	1.0	+/-	124 (120)
csm4-11	89 (200)	0	+	ND
csm4-12	87 (60)	0	ND	ND
csm4-13	83 (420)	2.0	+/-	140 (200)
csm4-14	77 (280)	2.5	-	146 (160)
csm4-15	65 (60)	4.5	ND	ND
csm4-16	89 (320)	2.5	+	147 (200)
csm4-17	87 (160)	1.0	ND	ND
csm4-18	91 (100)	0	ND	ND
csm4-19	78 (380)	4.0	+/-	141 (160)

Spore viabilities (SV, with the number (n) of tetrads dissected), delay in hours in completing MI relative to WT, and the nuclear envelope (NE) distortion phenotype in the Nup49-GFP strain (Table 2.1) background are shown. +, +/-, – represent WT, intermediate, and defective Nup49-GFP motion, respectively. Cumulative genetic distance between *URA3* and *HIS3* on chromosome XV in EAY1108/EAY1112 derived strains was determined from tetrad data (n = number dissected). Complete tetrad data are provided in Table 2.3. *Data from WANAT *et al.* (2008). ND, not determined. See MATERIALS and METHODS for details.

Table 2.3. Map distances and distributions of parental and recombinant progeny for the EAY1108/1112 background.

Strain	PD	TT	NPD	Map distance (cM)
URA3- LEU2:				
WT	607	456	5	21.9-23.8
*csm4*Δ	203	319	9	33.3-36.9
*CSM4/csm4*Δ	46	40	2	24.4-34.6
csm4-3	117	107	1	23.1-27.1
csm4-5	30	31	1	24.4-35.2
csm4-10	73	59	1	21.4-27.4
csm4-13	85	72	2	23.3-29.5
csm4-14	26	35	3	33.6-49.2
csm4-16	59	69	3	29.0-37.4
csm4-19	49	72	0	27.6-32.0
*pch2*Δ	563	423	18	25,0-27.8
*csm4-3 pch2*Δ	31	30	1	23.6-34.4
LEU2-LYS2:				
WT	496	569	5	26.6-28.5
*csm4*Δ	216	312	3	29.9-32.7
*CSM4/csm4*Δ	44	44	0	22.3-27.7
csm4-3	84	138	3	32.1-37.3
csm4-5	21	38	3	37.3-53.1
csm4-10	52	81	0	28.4-32.6
csm4-13	59	96	4	33.9-41.5
csm4-14	29	34	1	26.1-36.5
csm4-16	50	80	1	29.9-35.8
csm4-19	54	65	2	27.9-35.7
*pch2*Δ	395	561	39	38.2-41.8
*csm4-3 pch2*Δ	26	33	3	33.0-49.0
LYS2-ADE2:				
WT	803	263	2	12.1-13.7
*csm4*Δ	362	128	1	12.6-14.9
*CSM4/csm4*Δ	29	19	0	7.5-13.3
csm4-3	158	66	1	14.0-18.0
csm4-5	48	14	0	8.6-14.0
csm4-10	88	45	0	14.9-19.0
csm4-13	105	53	1	16.0-21.2
csm4-14	41	23	0	15.0-21.0
csm4-16	91	40	0	13.3-17.3
csm4-19	79	42	0	15.2-19.6
*pch2*Δ	649	344	7	18.2-20.4
*csm4-3 pch2*Δ	34	25	3	26.5-42.9

ADE2-HIS3:				
WT	343	709	16	36.5-38.9
*csm4*Δ	120	378	33	51.3-57.1
*CSM4/csm4*Δ	22	64	2	38.4-48.0
csm4-3	60	153	12	45.8-54.2
csm4-5	14	44	4	46.2-63.4
csm4-10	33	92	8	46.9-58.3
csm4-13	38	109	12	51.1-62.7
csm4-14	18	41	5	46.2-64.8
csm4-16	30	87	14	58.0-72.6
csm4-19	26	84	11	55.0-69.0
*pch2*Δ	243	638	115	63.9-69.5
*csm4-3 pch2*Δ	19	36	7	51.8-74.0

*pch2*Δ data are from ZANDERS and ALANI (2009). WT and *csm4*Δ tetrad data are from WANAT *et al.* (2008). All mutants are isogenic derivatives of EAY1108/EAY1112. Intervals on chromosome XV correspond to the genetic distance calculated from tetrad distribution data +/- one standard error, calculated using the Stahl Laboratory Online Tools website (http://www.molbio.uoregon.edu/~fstahl/).

Figure 2.5. Analysis of *csm4-3* in Nup49-GFP and Zip1-GFP motion assays. (A) Representative time-lapse images of WT, *csm4*Δ, and *csm4-3* cells expressing Nup49-GFP, which marks the nuclear envelope. Images were taken at one-second intervals for 30-45 seconds. Every other frame is shown for WT; every fourth frame for *csm4*Δ and *csm4-3*. Elapsed time is shown in the upper left corner for each frame. (B) Representative time-lapse images of WT, *csm4*Δ, and *csm4-3* strains expressing Zip1-GFP, which localizes to synapsed chromosomes. Images were taken at one-second intervals for 45 seconds. Every other frame for a portion of the time lapse is shown (see MATERIALS and METHODS). Elapsed time is shown in the upper left corner for each frame. Maximum and mean chromosome velocity for all chromosomes analyzed is shown below each genotype in μm/sec based on 30 chromosome measurements from 30 different cells across four time courses.

A

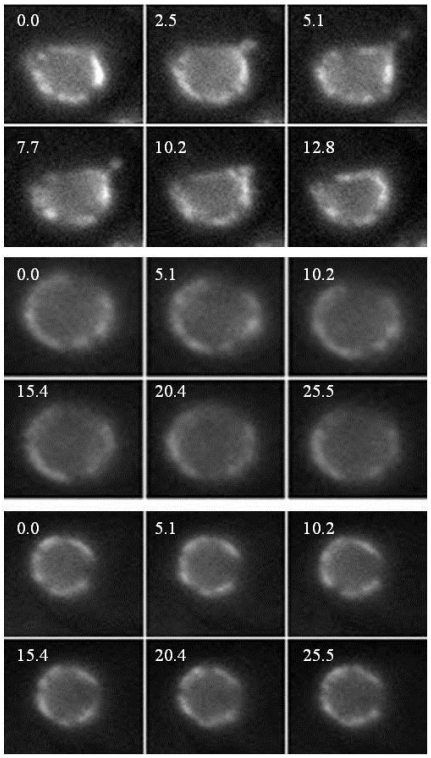

WT
one second intervals

csm4Δ
four second intervals

csm4-3
four second intervals

B

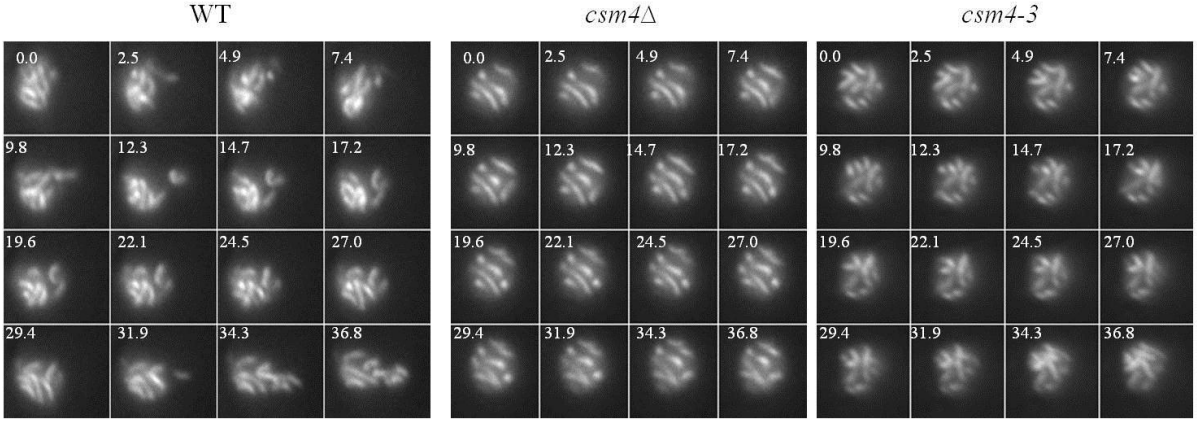

	WT	*csm4Δ*	*csm4-3*
Max. velocity (μm/sec):	1.19	0.39	0.70
Avg. velocity (μm/sec):	0.30	0.12	0.18

WT levels of motion (occasional nuclear envelope distortions in *csm4-5, 10, 11, 13, 16,* and *19*) displayed intermediate to WT levels of spore viability (81-89%), however meiotic delays in these mutants ranged from no delay, to a four-hour delay.

As mentioned above, *csm4-3* strains retain high spore viability but display a null-like MI delay and *csm4Δ*-like defect in the Nup49-GFP chromosome motion assay (Figure 2.5 A). Since nuclear envelope distortions provide only an indirect measure of chromosome motion, we directly examined chromosome motion in strains expressing Zip1-GFP. Zip1 loads onto chromosomes in foci early in meiosis, and then localizes along the central element in fully synapsed chromosomes during zygotene and pachytene (CHUA and ROEDER 1998; BÖRNER, BAROT, and KLECKNER 2008). Such a localization pattern is ideal for measuring chromosome motion (SCHERTHAN *et al.* 2007; KOSZUL *et al.* 2008; CONRAD *et al.* 2008; WANAT *et al*. 2008; KOSAKA, SHINOHARA and SHINOHARA 2008). In WT strains in zygotene and pachytene expressing Zip1-GFP (T = 4 to 6 hrs after meiotic induction), chromosomes rapidly move within the nucleus, at rates up to 1.2 μm/sec, with an average velocity of 0.30 +/- 0.08 (standard deviation, SD) μm/sec (Figure 2.5 B). Similar to previous studies (KOSZUL *et al.* 2008; CONRAD *et al*. 2008), chromosome motion is severely reduced in *csm4*Δ with a maximum velocity of 0.39 μm/sec and an average velocity of 0.12 +/- 0.03 μm/sec. Chromosomes in *csm4*-3 reached a maximum velocity of 0.70 μm/sec and displayed an average velocity of 0.18 +/- 0.04 μm/sec (Figure 2.5 B), which differed significantly from the null ($p < 0.0001$ by one-sided Mann-Whitney test), mostly due to the contribution of a few chromosomes moving rapidly in *csm4-3* (Figures 2.5, 2.6, 2.7). The presence of occasional, fast moving chromosomes in *csm4-3* is clearly seen in an analysis of chromosome velocity in

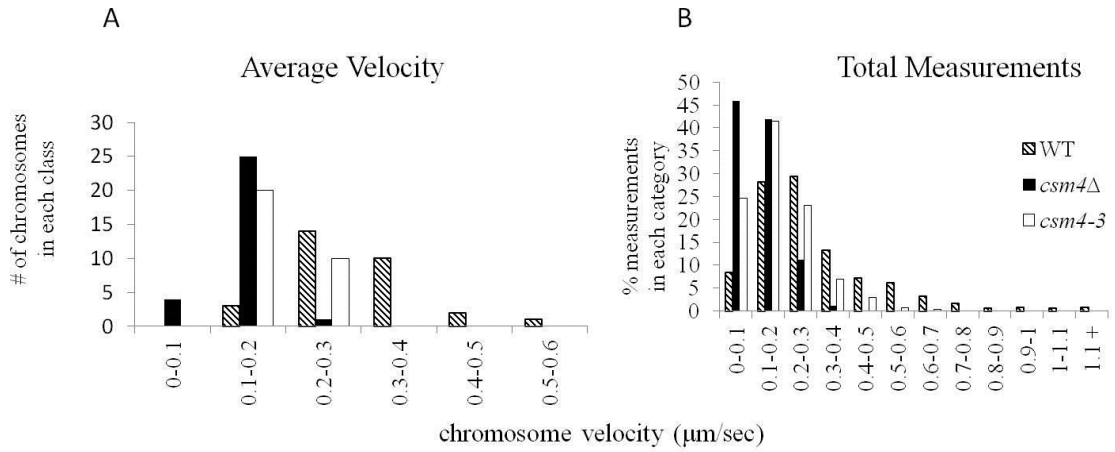

Figure 2.6. *csm4-3* shows a defect in chromosome motion in cells expressing Zip1-GFP. (A) Distributions of average velocities for each chromosome measured (30 each for WT, *csm4Δ*, and *csm4-3).* Average values for each chromosome were obtained from 15-25 velocity measurements determined in one-second intervals. (B) Chromosome velocity measurements in one-second intervals presented as a percentage of the total number recorded (678, 654, and 738 measurements for WT, *csm4Δ* and *csm4-3*, respectively).

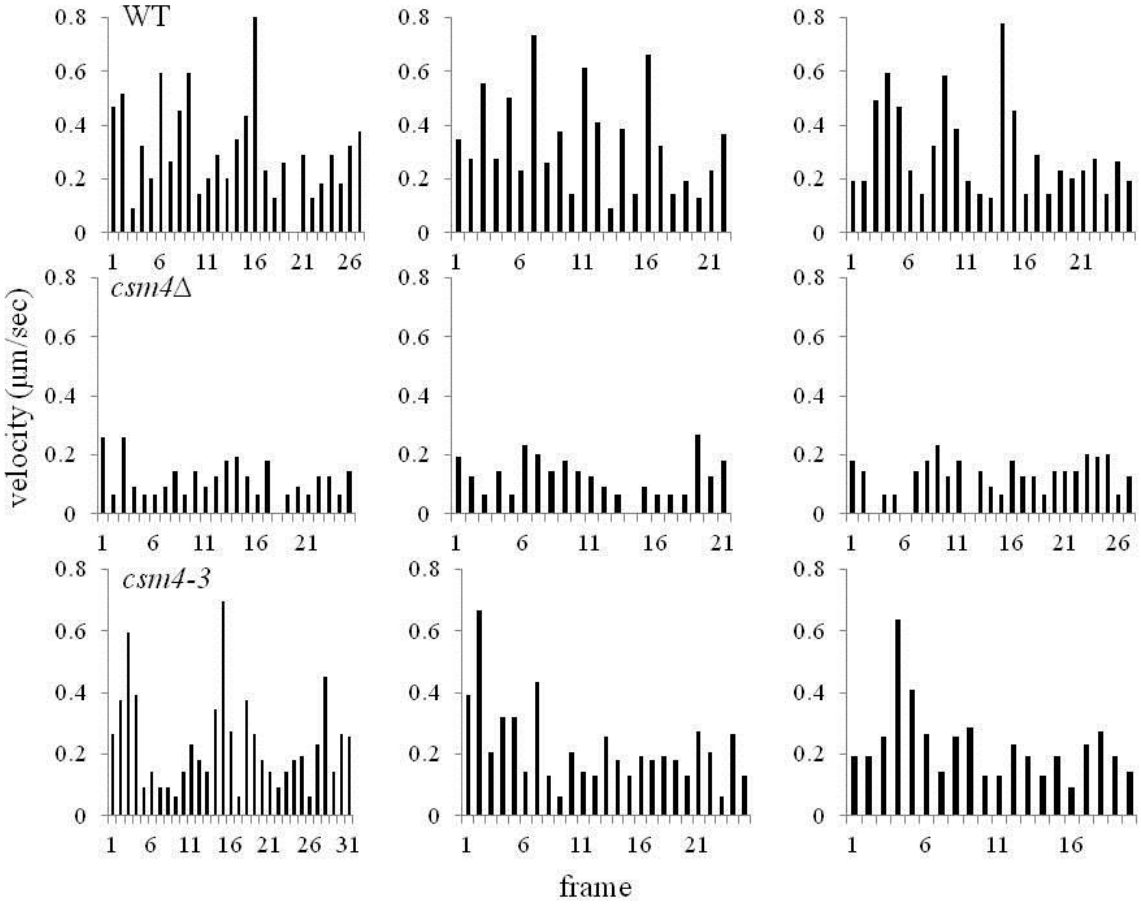

Figure 2.7. *csm4-3* strains display occasional rapid chromosome movements. Chromosome velocity was measured in consecutive one-second intervals for three representative chromosomes in WT, *csm4Δ*, and *csm4-3* strains expressing Zip1-GFP. Each graph shows velocity measurements for a single chromosome over at least a twenty second timeframe. Each bar represents the velocity of that particular chromosome between a one-second interval.

consecutive one-second intervals for three representative chromosomes of each genotype (Figure 2.7). For WT, 26% of chromosome movements were above 0.4 μM/sec; in contrast only 9.2% and 0% were above this value in *csm4-3* and *csm4Δ*, respectively. Together these data suggest that high levels of chromosome motion are not essential to achieve WT levels of spore viability.

Homolog pairing is defective in *csm4-3:* *csm4-3* strains show defects in chromosome motion in the Nup49-GFP and Zip1-GFP assays. If WT levels of chromosome movements are important for homolog pairing in meiosis, we would expect *csm4-3* strains to show pairing defects. We analyzed the *csm4-3* pairing phenotype in the one-dot/two-dot tetR-GFP assay (BRAR *et al.* 2009). As shown in Figure 2.8, *csm4-3* strains displayed similar kinetics for initial loss of chromosome pairing; however, at later time points, pairing in *csm4-3* occurred more rapidly than in *csm4Δ*, but still slower than seen in WT. Similar to WT and the null, *csm4-3* did not show any difference in dynamics or levels of nonhomologous pairing (Figure 2.8 D and E). Together these data suggest that *csm4-3* strains are capable of removing nonhomologous interactions as efficiently as WT. In addition, these observations suggest that the pairing defect in *csm4*Δ is not due solely to meiotic progression delays seen in the null, because *csm4-3* displays a delay in completing MI similar to *csm4Δ*, but is more proficient than the null in chromosome pairing.

Chromosome motion is important for meiotic progression: Based on the above observations, we hypothesize that WT levels of chromosome motion, while not needed to maintain high spore viability, are important for promoting meiotic progression. To test this, we looked at the phenotype of *csm4*Δ and *csm4-3* mutants in the presence of a deletion of the DNA damage checkpoint protein Rad17. As shown above, both *csm4*Δ and *csm4-3* exhibit four to five hour delays in completing MI. Previously WANAT *et al*. (2008) examined physical

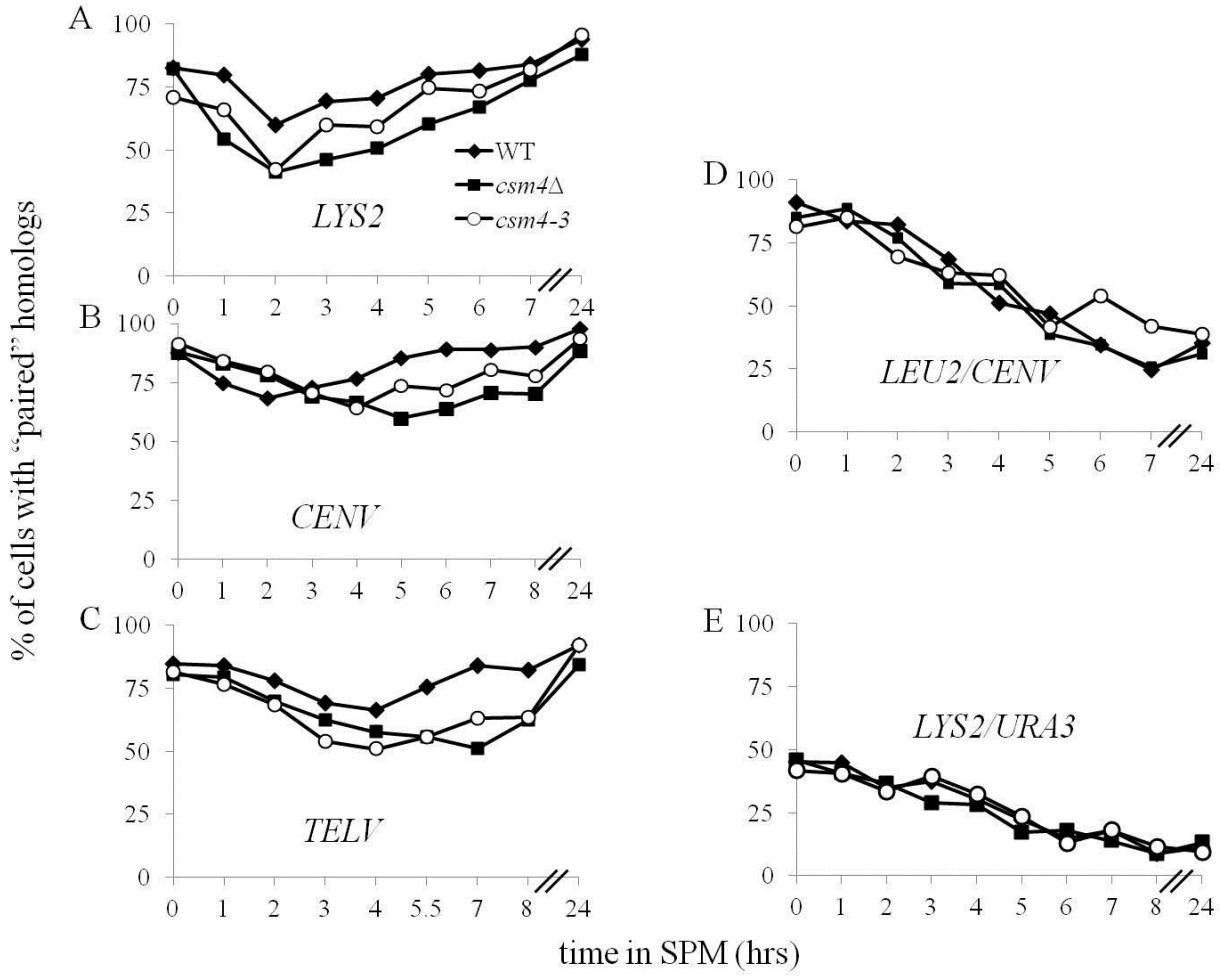

Figure 2.8. Chromosome pairing is defective in *csm4*Δ and to a lesser extent *csm4-3*. Chromosome pairing was assayed as described in Figure 2.1 for *csm4-3* strains. (A, B, C) Representative time courses with *tetO* arrays at *LYS2* (A), *CENV* (B), and *TELV* (C). Pairing was considered maximum in these *ndt80Δ* strains at T = 24 hrs. (D, E) Representative time courses demonstrating non-homologous pairing, with one *tetO* array at *LEU2* and another at *CENV* (D), and one at *LYS2* and another at *URA3* (E). Data from Figure 2.2 for WT and *csm4Δ* are shown for comparison purposes.

recombination intermediates that occur in meiosis (DSB, SEI, dHJ) and found that in *csm4Δ*, recombination steps following DSB formation were delayed. Moreover, each stage was more progressively delayed than the previous step, with the largest delay occurring in the step from DSB to SEI formation. This suggests a major defect occurs in *csm4Δ* strains in an early step in recombination, possibly partner identification or juxtaposition (WANAT *et al.* 2008). The *rad17Δ* mutation was shown previously to eliminate meiotic delays in a variety of mutants, including *dmc1*Δ*, ndj1*Δ*,* and *pch2*Δ (WU and BURGESS, 2006; LYDALL *et al.* 1996; WU, HO and BURGESS 2010; GRUSHCOW *et al.* 1999). We found that *rad17*Δ completely rescued the meiotic delay of both *csm4*Δ and *csm4-3* (Figure 2.9 A and B; WANAT *et al.* 2008); however spore viability was extremely low in both double mutants (1 to 3%) compared to 65% in *csm4*Δ and 88% in *csm4-3* (Table 2.4). These observations suggest that the *csm4-3* mutation elicits a checkpoint response that is required to maintain high spore viability.

One explanation for the poor spore viability phenotype seen in *csm4Δ* is that the mutant is defective in meiotic recombination progression and accumulates a small amount of recombination intermediates that are unrepaired and elicit the Rad17-dependent (recombination) checkpoint (WANAT *et al*. 2008). The *spo11*Δ mutation rescues the MI delay of many meiotic recombination mutants. In most cases this phenotype can be explained by *spo11Δ* eliminating the formation of meiosis-induced DSBs and thus preventing the accumulation of DNA recombination intermediates in mutants that activate the Rad17-dependent checkpoint (e.g. WU and BURGESS, 2006; LYDALL *et al.* 1996; WU, HO and BURGESS 2010). This loss of meiotic DSBs, however, results in spore inviability due to a loss in crossing over. We examined whether lowering the number of DSBs through a *spo11* hypomorph mutation (MARTINI *et al*.

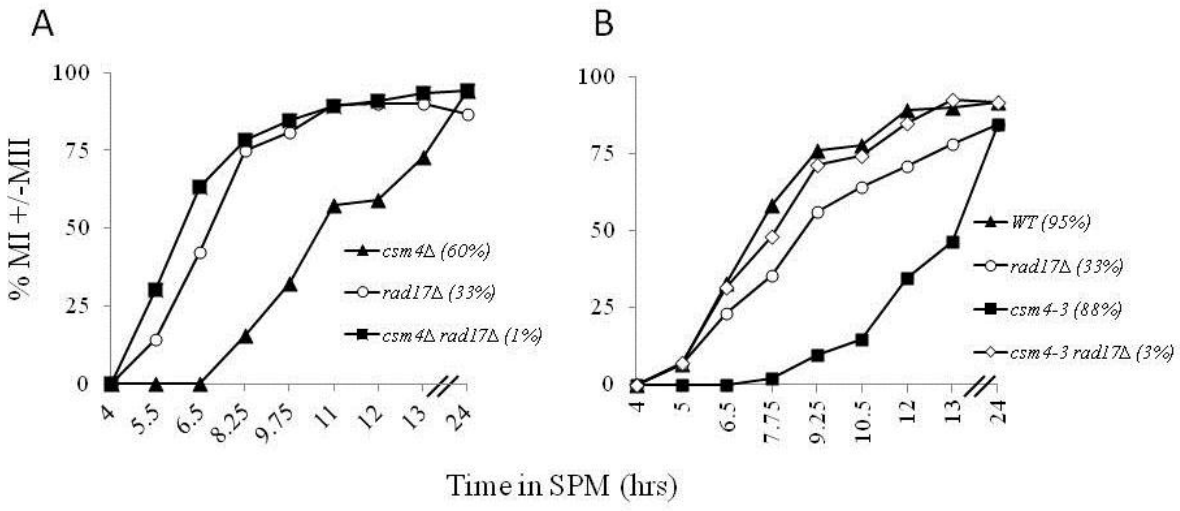

Figure 2.9. The meiotic delays observed in *csm4Δ* and *csm4-3* are fully rescued by the *rad17*Δ mutation. Meiosis I completion (MI +/- MII) time course experiments are shown for the indicated mutant strains. The spore viability of each strain is shown in parentheses following the genotype. (A, B) Representative time courses from at least three independent experiments showing that a null mutation in *RAD17*, a DNA-damage checkpoint protein, rescues the meiotic delay of *csm4-3* (panel A) and *csm4Δ* (panel B). See MATERIALS and METHODS for details.

Table 2.4 Spore viabilities and genetic map distances of *csm4*Δ and *csm4-3* mutants in the presence and absence of *rad17*Δ, *spo11-HA*, *spo11-HA/yf*, and *pch2*Δ mutations.

Strain	% spore viability (n)	cumulative distance for indicated chromosome (cM) XV	III	VII	VIII
EAY1108/EAY1112 derived strains					
WT*	97 (1068)	101			
*csm4Δ**	65 (531)	146			
csm4-3	88 (238)	126			
rad17Δ	33 (100)	ND			
csm4Δ rad17Δ	1 (40)	ND			
csm4-3 rad17Δ	3 (120)	ND			
*pch2Δ***	98 (1015)	152			
csm4Δ pch2Δ	31 (200)	ND			
csm4-3 pch2Δ	56 (300)	167			
NH942/NH943 derived strains					
WT*	90 (491)		41	63	46
*csm4Δ**	60 (559)		43	90	54
csm4-3	77 (180)		51	102	57
*spo11-HA/yf****	76 (60)		29	71	49
csm4Δ spo11-HA/yf	39 (200)		ND	ND	ND
csm4-3 spo11-HA/yf	63 (300)		33	75	52

Spore viabilities and cumulative map distances were determined from tetrad data (Tables 2.3 and 2.5). The number of tetrads dissected (n) to determine map distances is shown. *Map distance and SV data from WANAT *et al.* (2008); **Map distance and spore viability data from ZANDERS and ALANI (2009); ***Map distance data from MARTINI *et al.* (2006).

Table 2.5. Map distances and distributions of parental and recombinant progeny for the NH942/943 background.

Strain	PD	TT	NPD	cM
Chromosome III				
HIS4-LEU2:				
WT	669	213	3	12.2-14.0
*csm4*Δ	413	114	3	11.2-13.8
csm4-3	77	30	0	11.8-16.2
spo11yf	719	197	2	10.6-12.2
csm4-3 spo11yf	42	4	0	2.2-6.4
LEU2-CEN3:				
WT	774	128	1	6.7-8.1
*csm4*Δ	426	99	5	10.7-13.7
csm4-3	82	23	2	12.1-20.7
spo11yf	828	94	0	4.6-5.6
csm4-3 spo11yf	39	6	1	6.2-19.8
CEN3-MATa:				
WT	590	300	10	18.7-21.3
*csm4*Δ	353	173	4	17.1-20.1
csm4-3	68	38	1	17.1-24.1
spo11yf	696	221	2	11.9-13.5
csm4-3 spo11yf	32	14	0	11.8-18.6
Chromosome VII				
LYS2-MET13:				
WT	569	311	1	17.1-18.9
*csm4*Δ	288	229	6	23.6-27.0
csm4-3	54	55	3	27.8-37.4
spo11yf	603	282	3	15.9-17.9
csm4-3 spo11yf	28	18	0	16.0-23.2
MET13-CYH2:				
WT	706	182	0	9.5-10.9
*csm4*Δ	370	152	1	14.0-16.2
csm4-3	70	42	0	16.5-21.1
spo11yf	707	154	2	8.8-10.4
csm4-3 spo11yf	40	6	0	4.0-9.0
CYH2-TRP5:				
WT	364	524	18	33.5-36.5
*csm4*Δ	150	344	29	46.7-52.3
csm4-3	33	72	7	44.5-57.3
spo11yf	271	591	36	43.0-46.8
csm4-3 spo11yf	11	33	2	40.4-57.4
Chromosome VIII				
URA3-THR1:				

WT	532	330	3	19.1-21.1
*csm4*Δ	291	231	5	23.2-26.4
csm4-3	56	50	1	22.7-29.7
spo11yf	569	266	4	16.2-18.4
csm4-3 spo11yf	29	16	1	16.9-30.9
THR1-CUP1:				
WT	439	416	6	25.0-27.4
*csm4*Δ	256	263	8	27.7-31.3
csm4-3	51	54	2	26.5-35.1
spo11yf	373	453	14	30.5-33.5
csm4-3 spo11yf	28	17	1	18.0-32.0

All mutants are derivatives of NH942/NH943. WT and *spoll-HA/yf* data are from MARTINI *et al.* (2006), and *csm4*Δ data are from WANAT *et al.* (2008). Intervals were calculated as in Table 2.3.

2006) could rescue the meiotic delay phenotypes of *csm4*Δ and *csm4-3*. We used a strain heterozygous for the *spo11-HA* and *spo11-yf-HA* alleles (referred to as *spo11-HA/yf)*. This strain makes 30% of WT DSB levels (MARTINI *et al.* 2006; HENDERSON and KEENEY, 2004). We analyzed meiotic progression in *csm4*Δ *spo11-HA/yf* and *csm4-3 spo11-HA/yf* by DAPI staining, and saw in both cases a partial rescue of the meiotic delay (Figure 2.10). Interestingly, *spo11-HA/yf* decreased spore viability by roughly the same amount in WT and *csm4-3* strain backgrounds (17% in WT, 18% in *csm4-3*). However, *spo11-HA/yf* reduced spore viability to a greater extent in *csm4Δ* (35%; Table 2.4). The spore viability in both double mutants showed a pattern indicative of MI nondisjunction (4, 2, 0 > 3, 1 viable spores; Figure 2.11). We also measured genetic map distance on three chromosomes (III, VII, and VIII) in *csm4-3 spo11-HA/yf* and *spo11-HA/yf* (Table 2.4 and Table 2.5). Such an analysis could not be performed in *csm4Δ spo11-HA/yf* due to poor spore viability. Map distances in the two mutants were similar across each chromosome (total for all three chromosomes, 159 cM in *csm4-3 spo11-HA/yf* vs. 150 cM in *spo11-HA/yf*).

The partial rescue of the MI delay in *csm4Δ spo11-HA/yf* suggests that the *csm4Δ* pairing defect could cause poor or inappropriate repair of recombination intermediates. However, the double mutant analysis does not directly address why spore viability is greatly decreased in *csm4Δ* (see below and DISCUSSION). To further understand the role of Csm4 in meiotic recombination, we tested the effect of the *pch2Δ* mutation on the spore viability of *csm4-3* and *csm4Δ* mutants. Pch2 is a meiotic protein proposed to play a role in the crossover/noncrossover decision, as well as in suppressing inappropriate repair of double-strand breaks (ZANDERS and ALANI 2009; JOSHI *et al*. 2009; S. ZANDERS, M. SONNTAG BROWN, C. CHEN, and E.

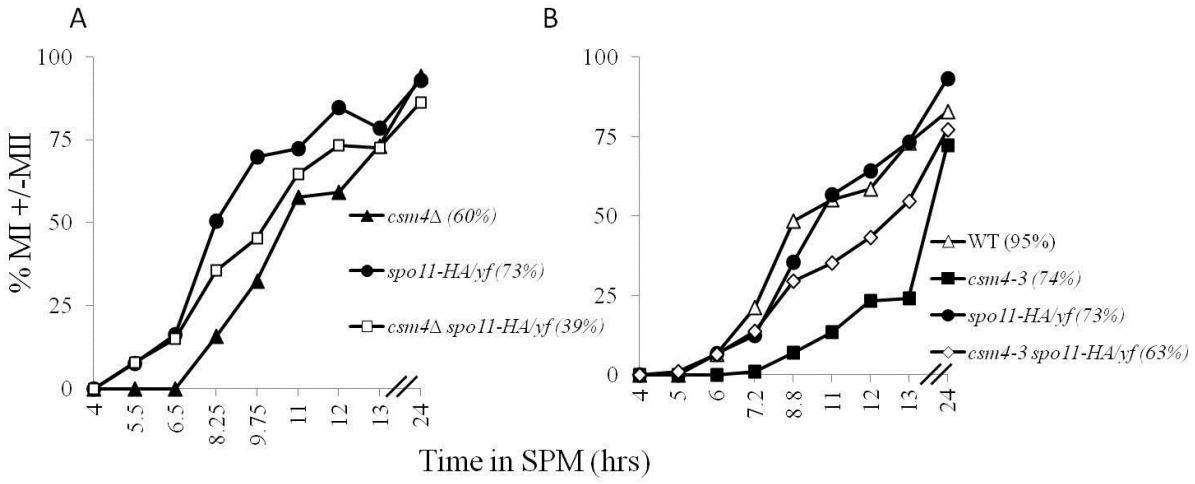

Figure 2.10. The meiotic delays observed in *csm4Δ* and *csm4-3* are partially rescued by a *spo11* hypomorph mutation. (A, B) Representative time courses from at least 5 independent experiments showing that a *spo11* hypomorph, *spo11-HA/yf*, can partially rescue the meiotic delay, as measured by completion of MI (MI +/- MII) of *csm4Δ* (panel A) and *csm4-3* (panel B).

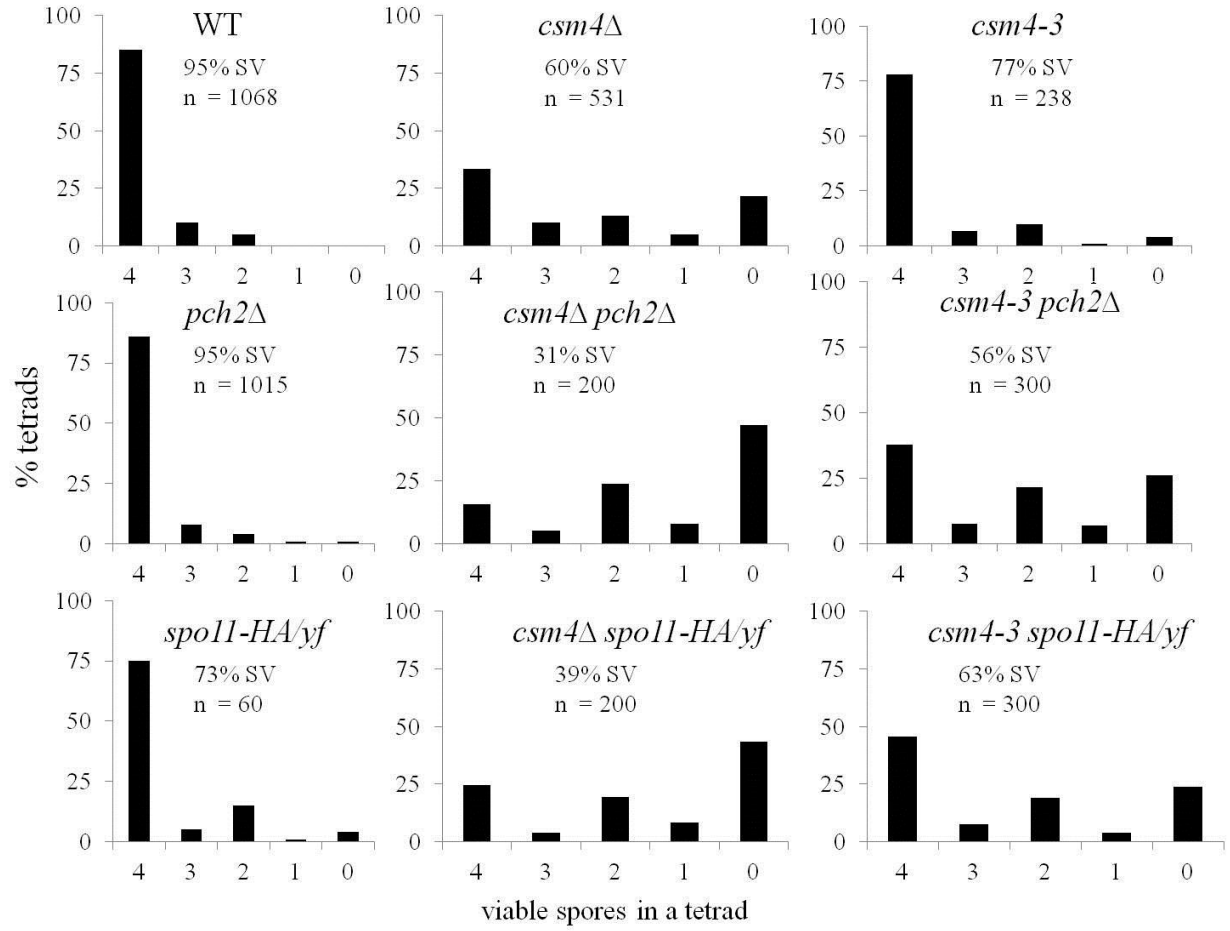

Figure 2.11. Spore viability profile of wild-type and mutant strains. The vertical axis shows the percentage of each tetrad class and the horizontal axis represents the number of viable spores in a tetrad. SV: percentage spore viability; n: total number of tetrad dissected. Data are a graphical representation of Table 2.4.

ALANI, unpublished observations). *pch2*Δ mutants, which maintain WT levels of spore viability, are defective in crossover interference and have very high levels of crossing over (ZANDERS and ALANI 2009). If *csm4-3* is more effective in the repair of recombination intermediates than *csm4Δ* due to higher levels of chromosome motion and pairing, one might expect *csm4-3 pch2*Δ to show higher spore viability relative to *csm4*Δ *pch2*Δ. As shown in Table 2.4 and Figure 2.11, the *pch2Δ* mutation conferred a more severe effect on spore viability in *csm4Δ* strains (31% spore viability in *csm4*Δ *pch2*Δ, a 53% decrease from *csm4Δ*) compared to *csm4-3* strains (56% spore viability in *csm4-3 pch2Δ,* a 36% decrease from *csm4-3*). Both double mutants showed a spore viability pattern indicative of MI nondisjunction (Figure 2.11). Genetic map distances, as measured on chromosome XV, were much higher than WT in tetrads of *csm4-3 pch2Δ* and single spore data of *csm4Δ pch2Δ* (Table 2.4 and data not shown). This is expected because both *csm4-3* and *pch2*Δ single mutants show increased crossing over (Table 2.4). These data suggest that a lack of crossing over is not likely to be the cause of low spore viability in *csm4Δ pch2Δ*. In the DISCUSSION we interpret the *csm4 spo11-HA/yf* and *csm4 pch2Δ* analyses to suggest that chromosome motion is important for facilitating the MI division by controlling the *placement* of crossovers between homologs.

DISCUSSION

In this study we analyzed two mutants, *csm4*Δ and *csm4-3*, that show defects in telomere-led chromosome motions during meiotic prophase in baker's yeast. Using the one-dot/two-dot tetR-GFP pairing assays, we found that both mutants showed delays in homolog pairing, with *csm4Δ* strains displaying more severe delays. Analysis of *csm4-3* mutants in chromosome

motion assays suggests that fast moving chromosomes could play an important role in homolog pairing and that the timing of pairing is likely to be important for meiotic progression.

At least two hypotheses have been proposed to explain the role of chromosome motion in baker's yeast meiosis. In one model, motion is important to directly pull apart nonhomologous interactions between chromosomes, such as nonhomologous pairings or interlocks that occur during SC formation (RASMUSSEN 1986; SCHERTHAN, BAHLER and KOHLI 1994; WANAT *et al.* 2008; STORLAZZI *et al.* 2010). Our data appears inconsistent with motion being necessary to pull apart nonhomologous pairings, since in this view we would have expected either less and/or a delay in nonhomologous "unpairings" in *csm4*Δ, which were not observed (Figure 2.2 D and E; Figure 2.8 D and E). At present, we do not have a suitable assay to monitor whether interlocks form during SC formation in baker' yeast, and if they did, whether they occur more frequently in *csm4Δ* or *csm4-3*. In a second model, fast chromosome movements contribute to pairing. Telomere-led chromosome movements could directly contribute to homolog pairing by bringing homologs together. They could also contribute indirectly by freeing chromosomes from inappropriate interactions, such as interlocks (described above). One observation that argues against the former possibility is that DSBs have been shown at one recombination hotspot, *HIS4::LEU2*, to have already engaged the homolog at the onset of zygotene, when chromosome motion initiates (KOSZUL *et al.* 2008; ZICKLER 2006; HUNTER and KLECKNER 2001). However, it is unclear whether this hotspot is representative of the entire genome. The back and forth motion typically seen in telomere-led chromosome motion is more consistent with the pulling apart of unwanted interactions rather than facilitating pairing (see arguments in WANAT *et al.* 2008, and as reported in KOSZUL *et al.* 2008; CONRAD *et al.* 2008). It is important to note that some studies suggest that chromosome motion takes place

prior to zygotene; for example, PARVINEN and SODERSTROM (1976) observed chromosome movements in rat spermatocytes in leptotene, and, in *S. cerevisiae*, movements were seen in leptotene in cells containing Rap1-GFP tagged chromosomes (TRELLES-STICKEN *et al.* 2005). Regardless of when motion initiates, our data show that chromosome motion is important for homolog pairing, directly and/or indirectly through removing inappropriate interactions.

Genetic analyses of *csm4* mutations analyzed in combination with mutations that affect recombination (*spo11, pch2*) suggest that a lack of crossovers is not the cause of the low spore viability seen in *csm4Δ spo11-HA/yf* and *csm4Δ pch2Δ* (Table 2.4; Figure 2.11). We suggest that chromosome motion regulates the placement of crossovers that facilitate MI. This idea is supported by two previous studies in baker's yeast. ROCKMILL, VOELKEL-MEIMAN and ROEDER (2006) showed that defects in crossover placement in *sgs1* mutants caused a significant increase in chromosome missegregation, primarily through precocious separation of sister chromatids. WANAT *et al.* (2008) found evidence of an altered distribution of crossovers in *csm4*Δ cells that underwent chromosome III MI nondisjunction compared to those with normal disjunction. Based on these observations and our data, we suggest that the increased chromosome motion seen in *csm4-3* is important for crossover placements that promote an accurate MI division. Testing the crossover placement model in greater detail will require either genome-wide molecular methods (e.g. MANCERA *et al*. 2008), or more completely marked chromosomes.

It is important to note that the synthetic defects in spore viability observed in *csm4Δ spo11-HA/yf* and *csm4Δ pch2Δ* could also be explained by fast moving chromosomes being necessary to remove SC interlocks, as discussed above. The *pch2*Δ mutation affects the localization of the SC components Hop1 and Zip1 on meiotic chromosomes (SAN-SEGUNDO

and ROEDER 1999; BORNER, BAROT, and KLECKNER 2008), and *spo11* hypomorphs also show defects in the SC (HENDERSON and KEENEY 2004). If residual interlocks remain in *csm4*Δ cells, challenging these cells with additional SC defects could be detrimental, leading to the decreased spore viabilities seen in *csm4*Δ *pch2*Δ and *csm4*Δ *spo11-HA/yf*.

S. pombe mutants defective in chromosome motion show a much more severe defect in meiosis than analogous mutants in budding yeast (SCHERTHAN, BAHLER and KOHLI 1994; CHIKASHIGE *et al.* 2006; MIKI *et al.* 2004). This difference in phenotype illustrates the different requirements for chromosome motion in the two organisms. In contrast to budding yeast, fission yeast lack both synaptonemal complex (SC) and crossover interference. One possibility is that in organisms that lack SC chromosome motions play a more critical role in promoting homolog interactions. If chromosome motions are important for crossover placement, as suggested above, a more severe defect in meiosis might be expected in organisms that lack crossover interference. In budding yeast, which contains chromosomes as small as 230 KB, crossover interference plays an important role in ensuring widely spaced crossovers on all chromosomes (reviewed in MARTINEZ-PEREZ and COLAIÁCOVO 2009). Chromosome motion may be less critical to regulate crossover placement in this system, because crossover interference could presumably perform this role, though less efficiently when chromosome motion is absent. Chromosome motion in budding yeast could thus serve as a backup to crossover interference, providing another way to promote pairing and disjunction on small chromosomes. Such a model explains the more severe spore viability defect seen in *pch2Δ csm4Δ* mutants that are defective in both crossover interference and motion. Thus the presence of the SC could strengthen/confirm interactions between homologous chromosomes that promote crossover placement and disjunction. In other organisms, such as *pombe*, that lack SC,

chromosome motion would then play a more primary role in chromosome pairing and crossover placement.

ACKNOWLEDGEMENTS

We are grateful to Angelika Amon, Nancy Kleckner and Scott Keeney for yeast strains, Beth Weiner and Nancy Kleckner for microscopy training and providing GFP strains, Paula Cohen for the use of her Zeiss microscope for initial studies, and Damien Garbett for advice on tracking chromosome movement. We also thank Anthony Bretscher, Jen Wanat and members of the Alani laboratory for helpful advice and comments on the manuscript. This work was supported by NIH grant GM53085 to E. A. supplemented with an ARRA award. M. S. B. was supported by a Biochemistry, Cell, and Molecular Biology NIH training grant and S. Z. was supported by a Cornell Presidential Fellowship and a Genetics and Development NIH training grant.

REFERENCES

ALEXANDRU, G., F. UHLMANN, K. MECHTLER, M. A. POUPART and K. NASMYTH, 2001 Phosphorylation of the cohesin subunit Scc1 by Polo/Cdc5 kinase regulates siser chromatid separation in yeast. Cell **105**: 459-472.

ALLERS, T. and M. LICHTEN, 2001 Intermediates of yeast meiotic recombination contain heteroduplex DNA. Mol. Cell **8**: 225-231.

ARGUESO, J. L., A. W. KIJAS, S. SARIN, J. HECK, M. WAASE, *et al*., 2003 Systematic mutagenesis of the *Saccharomyces cerevisiae* MLH1 gene reveals distinct roles for Mlh1p in meiotic crossing over and in vegetative and meiotic mismatch repair. Mol. Cell. Biol. **23**: 873-886.

ARGUESO, J. L., J. WANAT, and Z. GEMICI, 2004 Competing crossover pathways act during meiosis in *Saccharomyces cerevisiae*. Genetics **168**: 1805-1816.

BASS, W. H., 2003 Telomere dynamics unique to meiotic prophase: formation and significance of the bouquet. Cell Mol. Life Sci. **60**: 2319-2324.

BELGAREH, N. and V. DOVE, 1997 Dynamics of nuclear pore distribution in nucleoporin mutant yeast cells. J. Cell Biol. **136**: 747-759.

BÖRNER, G. V., A. BAROT, and N. KLECKNER, 2008 Yeast Pch2 promotes domainal axis organization, timely recombination progression, and arrest of defective recombinosomes during meiosis. Proc. Natl. Acad. Sci. USA **105**: 3327-3332.

BÖRNER, G. V., N. KLECKNER and N. HUNTER, 2004 Crossover/noncrossover differentiation, synaptonemal complex formation, and regulatory surveillance at the leptotene/zygotene transition of meiosis. Cell **117**: 29-45.

BRAR, G. A., A. HOCHWAGEN, L. S. EE, and A. AMON, 2009 The multiple roles of cohesin in meiotic chromosome morphogenesis and pairing. Mol. Biol. Cell **20**: 1030-1047.

BUHLER, C., V. BORDE and M. LICHTEN, 2007 Mapping meiotic single-strand DNA reveals a new landscape of DNA double-strand breaks in *Saccharomyces cerevisiae*. PLoS Biol. **5**: e324.

BURGESS, S. M., N. KLECKNER and B. M. WEINER, 1999 Somatic pairing of homologs in budding yeast: existence and modulation. Genes Dev. **13**: 1627-1641.

CHIKASHIGE, Y., C. TSUTSUMI, M. YAMANE, K. OKAMASA, T. HARAGUCHI, *et al*., 2006 Meiotic proteins Bqt1 and Bqt2 tether telomeres to form the bouquet arrangement of chromosomes. Cell **125**: 59-69.

CHIKASHIGE, Y., T. HARAGUCHI, and Y. HIRAOKA, 2007 Another way to move chromosomes. Chromosoma **116**: 497-505.

CHUA, P. R. and G. S. ROEDER, 1997 Tam1, a telomere-associated meiotic protein, functions in chromosome synapsis and crossover interference. Genes Dev. **11**: 1786-1800.

CHUA, P. R. and G. S. ROEDER, 1998 Zip2, a meiosis-specific protein required for the initiation of chromosome synapsis. Cell **93**: 349-359.

CONRAD, M. N., A. M. DOMINGUEZ, and M. E. DRESSER, 1997 Ndj1p, a meiotic telomere protein required for normal chromosome synapsis and segregation in yeast. Science **276**: 1252-1255.

CONRAD, M. N., C. Y. LEE, J. L. WILKERSON, and M. E. DRESSER, 2007 MPS3 mediates meiotic bouquet formation in *Saccharomyces cerevisiae*. Proc. Natl. Acad. Sci. USA **104**: 8863-8868.

CONRAD, M. N., C. Y. LEE, G. CHAO, M. SHINOHARA, H. KOSAKA, *et al*., 2008 Rapid telomere movement in meiotic prophase is promoted by NDJ1, MPS3, and CSM4 and is modulated by recombination. Cell **133**: 1175-1187.

DAVIS, L., and G. R. SMITH, 2006 The meiotic bouquet promotes homolog interactions and restricts ectopic recombination in *Schizosaccharomyces pombe*. Genetics **174**: 167-177.

DE LOS SANTOS, T., N. HUNTER, C. LEE, B. LARKIN, J. LOIDL, *et al*., 2003 The Mus81/Mms4 endonuclease acts independently of double-Holliday junction resolution to promote distinct subset of crossovers during meiosis in budding yeast. Genetics **164**: 81-94.

DIAZ, R. L., A. D. ALCID, J. M. BERGER, and S. KEENEY, 2002 Identification of residues in yeast Spo11p critical for meiotic DNA double-strand break formation. Mol. Cell. Biol. **22**: 1106-1115.

GALBRAITH, A. M., S. A. BULLARD, K. JIAO, J. J. NAU, and R. E. MALONE, 1997 Recombination and the progression of meiosis in *Saccharomyces cerevisiae*. Genetics **146**: 481-489.

GIETZ, R. D., R. H. SCHIESTL, A. R. WILLEMS, and R. A. WOODS, 1995 Studies on the transformation of intact yeast cells by the LiAc/SS-DNA/PEG procedure. Yeast **11**: 355-360.

GOLDMAN, A. S. and M. LICHTEN, 2000 Restriction of ectopic recombination by interhomolog interactions during *Saccharomyces cerevisiae* meiosis. Proc. Natl. Acad. Sci. USA **97**: 9537-9542.

GOLDSTEIN, A. L. and J. H. MCCUSKER, 1999 Three new dominant drug resistance cassettes for gene disruption in *Saccharomyces cerevisiae*. Yeast **15**: 1541-1553.

GOLUBOVSKAYA, I. N., L. C. HARPER, W. P. PAWLOWSKI, D. SCHICHNES, and W. Z. CANDE, 2002 The *pam1* gene is required for meiotic bouquet formation and efficient homologous synapsis in maize (*Zea mays L.*) Genetics **162**: 1979-1993.

GRUSHCOW, J. M., T. M. HOLZEN, K. J. PARK, T. T. WEINERT, M. LICHTEN, *et al*., 1999 *Saccharomyces cerevisiae* checkpoint genes *MEC1, RAD17,* and *RAD24* are required for normal meiotic recombination partner choice. Genetics **153**: 607-620.

HARPER, L., I. GOLUBOVSKAYA and W. Z. CANDE, 2004 A bouquet of chromosomes. J. Cell Sci. **117**: 4025-4032.

HASSOLD, T. and P. HUNT, 2001 To err (meiotically) is human: the genesis of human aneuploidy. Nat. Rev. Genet. **2**: 280-291.

HENDERSON, K. A. and S. KEENEY, 2004 Tying synaptonemal complex initiation to the formation and programmed repair of DNA double-strand breaks. Proc. Natl. Acad. Sci. USA **101**: 4519-4524.

HUNTER, N. and N. KLECKNER, 2001 The single-end invasion: an asymmetric intermediate at the double-strand break to double-holliday junction transition of meiotic recombination. Cell **106**: 59-70.

JOSEPH, I. and A. J. LUSTIG, 2007 Telomeres in meiotic recombination: the yeast side story. Cell Mol. Life Sci. **64**: 125-130.

JOSHI, N., A. BAROT, C. JAMISON and G. V. BÖRNER, 2009 Pch2 links chromosome axis remodeling at future crossover sites and crossover distribution during yeast meiosis. PLoS Genet. **5**: e1000557.

KEENEY S., 2001 Mechanism and control of meiotic recombination initiation. Curr. Topics Dev. Biol. **52**: 1-53.

KOSAKA, H., M. SHINOHARA, and A. SHINOHARA, 2008 Csm4-dependent telomere movement on nuclear envelope promotes meiotic recombination. PLoS Genet. **4**: e1000196.

KOSZUL, R., S. KAMEOKA and B. M. WEINER, 2009 Real-Time Imaging of Meiotic Chromosomes in *Saccharomyces cerevisiae*. Methods Mol. Biol. **558**: 81-89.

KOSZUL, R., K. KIM, M. PRENTISS, N. KLECKNER, and S. KAMEOKA, 2008 Meiotic chromosomes move by linkage to dynamic actin cables with transduction of force through the nuclear envelope. Cell **133**: 1188-1201.

LACEFIELD, S., and A. W. MURRAY, 2007 The spindle checkpoint rescues the meiotic segregation of chromosomes whose crossovers are far from the centromere. Nat. Genet. **39**: 1273-1277.

LAO, J. P., S. D. OH, M. SHINOHARA, A. SHINOHARA, and N. HUNTER, 2008 Rad52 promotes postinvasion steps of meiotic double-strand-break repair. Mol. Cell **9**: 517-524.

LOIDL, J., F. KLEIN, and H. SCHERTHAN, 1994 Homologous pairing is reduced but not abolished in asynaptic mutants of yeast. J. Cell Biol. **125**: 1191-1200.

LYDALL, D., Y. NIKOLSKY, D. K. BISHOP, and T. A. WEINERT, 1996 A meiotic recombination checkpoint controlled by mitotic checkpoint genes. Nature **383**: 840-843.

MANCERA, E., R. BOURGON, A. BROZZI, W. HUBER, and L. M. STEINMETZ, 2008 High-resolution mapping of meiotic crossovers and non-crossovers in yeast. Nature **454**: 479-485.

MARSTON, A. L., W. H. THAM, H. SHAH, and A. AMON, 2004 A genome-wide screen identifies genes required for centromeric cohesion. Science **303**: 367-370. .

MARTINEZ-PEREZ, E. and M. P. COLAIÁCOVO, 2009 Distribution of meiotic recombination events: talking to your neighbors. Curr. Opin. Genet. Dev. **19**: 105-112.

MARTINI, E., R. L. DIAZ, N. HUNTER and S. KEENEY, 2006 Crossover homeostasis in yeast meiosis. Cell **126**: 285-295.

MIKI, F., A. KURABAYASHI, Y. TANGE, K. OKAZAKI, M. SHIMANUKI, *et al.*, 2004 Two-hybrid search for proteins that interact with Sad1 and Kms1, two membrane-bound components of the spindle pole body in fission yeast. Mol. Genet. Genomics **270**: 449-461.

NIWA, O., M. SHIMANUKI and F. MIKI, 2000 Telomere-led bouquet formation facilitates homologous chromosome pairing and restricts ectopic interaction in fission yeast meiosis. EMBO J. **19**: 3831-3840.

PAGE, S. L. and R. S. HAWLEY, 2004 The genetics and molecular biology of the synaptonemal complex. Annu. Rev. Cell Dev. Biol. **20**: 525-558.

PARVINEN, M. and K. O. SODERSTROM, 1976 Chromosome rotation and formation of synapsis. Nature **260:** 534-535.

PEOPLES, T. L., E. DEAN, O. GONZALEZ, L. LAMBOURNE, and S. M. BURGESS, 2002 Close, stable homolog juxtaposition during meiosis in budding yeast is dependent on meiotic recombination, occurs independently of synapsis, and is distinct from DSB-independent pairing contacts. Genes Dev. **16**: 1682-1695.

RABITSCH, K. P., A. TÓTH, M. GÁLOVÁ, A. SCHLEIFFER, G. SCHAFFNER, *et al.*, 2001 A screen for genes required for meiosis and spore formation based on whole-genome expression. Curr. Biol. **11**: 1001-1009.

RASMUSSEN, S. W., 1986 Chromosome interlocking during synapsis-a transient disorder. Tokai J. Exp. Clin. Med. **11**: 437–451.

ROCKMILL, B., and G. S. ROEDER, 1998 Telomere-mediated chromosome pairing during meiosis in budding yeast. Genes Dev. **12**: 2574-2586.

ROCKMILL, B., K. VOELKEL-MEIMAN, and G. S. ROEDER, 2006 Centromere-proximal crossovers are associated with precocious separation of sister chromatids during meiosis in *Saccharomyces cerevisiae.* Genetics **174**: 1745-1754.

ROEDER, G. S., 1997 Meiotic chromosomes: it takes two to tango. Genes Dev. **11**: 2600-2621.

ROSE, M. D., F. WINSTON and P. HIETER, 1990 Methods in yeast genetics: A laboratory course manual. Cold Spring Harbor, NY: Cold Spring Harbor Laboratory Press.

SAN-SEGUNDO, P. A., and G. S. ROEDER, 1999 Pch2 links chromatin silencing to meiotic checkpoint control. Cell **97**: 313-324.

SATO, A., B. ISAAC, C. M. PHILLIPS, R. RILLO, P. M. CARLTON, *et al*., 2009 Cytoskeletal forces span the nuclear envelope to coordinate meiotic chromosome pairing and synapsis. Cell **139**: 907-919.

SCHERTHAN, H., J. BAHLER and J. KOHLI, 1994 Dynamics of chromosome organization and pairing during meiotic prophase in fission yeast. J. Cell Biol. **127**: 273-285.

SCHERTHAN, H., H. WANG, C. ADELFALK, E. J. WHITE, C. COWAN, *et al.*, 2007 Chromosome mobility during meiotic prophase in *Saccharomyces cerevisiae*. Proc. Natl. Acad. Sci. USA **104**: 16934-16939.

SCHERTHAN, H., S. WEICH, H. SCHWEGLER, C. HEYTING, M. HÄRLE, *et al*., 1996 Centromere and telomere movements during early meiotic prophase of mouse and man are associated with the onset of chromosome pairing. J. Cell Biol. **134**: 1109-1125.

SCHWACHA, A. and N. KLECKNER, 1995 Identification of double Holliday junctions as intermediates in meiotic recombination. Cell **83**: 783-791.

STORLAZZI, A., S. GARGANO, G. RUPRICH-ROBERT, M. FALQUE, M. DAVID, *et al*., 2010 Recombination proteins mediate meiotic spatial organization and pairing. Cell **141**: 94-106.

TÓTH, A., K. P. RABITSCH, M. GÁLOVÁ, A. SCHLEIFFER, S. B. BUONOMO, *et al*., 2000 Functional genomics identifies monopolin: a kinetochore protein required for segregation of homologs during meiosis I. Cell **103**: 1155-1168.

TRELLES-STICKEN, E. J. LOIDL and H. SCHERTHAN, 1999 Bouquet formation in budding yeast: initiation of recombination is not required for meiotic telomere clustering. J. Cell Sci. **112**: 651-658.

TRELLES-STICKEN, E. M. E. DRESSER, and H. SCHERTHAN, 2000 Meiotic telomere protein Ndj1p is required for meiosis-specific telomere distribution, bouquet formation and efficient homologue pairing. J. Cell Biol. **151**: 95-106.

TRELLES-STICKEN, E., C. ADELFALK, J. LOIDL, and H. SCHERTHAN, 2005 Meiotic telomere clustering requires actin for its formation and cohesin for its resolution. J. Cell Biol. **170**: 213-223.

TSUBOUCHI, H. and G. S. ROEDER, 2003 The importance of genetic recombination for fidelity of chromosome pairing in meiosis. Dev. Cell **5**: 915-925.

WACH, A., A. BRACHAT, R. POHLMANN, and P. PHILIPPSEN, 1994 New heterologous modules for classical or PCR-based gene disruptions in *Saccharomyces cerevisiae.* Yeast **10**: 1793-1808.

WANAT, J. J., K. P. KIM, R. KOSZUL, S. ZANDERS, B. WEINER, *et al.*, 2008 Csm4, in collaboration with Ndj1, mediates telomere-led chromosome dynamics and recombination during yeast meiosis. PLoS Genet. **4**: e1000188.

WEINER, B. M. and N. KLECKNER, 1994 Chromosome pairing via multiple interstitial interactions before and during meiosis in yeast. Cell **77**: 977-991.

WU, H. Y., and S. M. BURGESS, 2006 Ndj1, a telomere-associated protein, promotes meiotic recombination in budding yeast. Mol. Cell. Biol. 26: 3683-3694.

WU, H. Y., H. C. HO and S. M. BURGESS, 2010 Mek1 kinase governs outcomes of meiotic recombination and the checkpoint response. Curr. Biol. **20**: 1707-1716.

YAMAMOTO, A., R. R. WEST, J. R. MCINTOSH and Y. HIRAOKA, 1999 A cytoplasmic dynein heavy chain is required for oscillatory nuclear movement of meiotic prophase and efficient meiotic recombination in fission yeast. J. Cell Biol. 1**45**: 1233-1249.

YANG, H.D. and L. A. PON, 2002 Actin cable dynamics in budding yeast. Proc. Natl. Acad. Sci. USA **99**: 751-756.

ZANDERS, S. and E. ALANI, 2009 The *pch2Delta* mutation in baker's yeast alters meiotic crossover levels and confers a defect in crossover interference. PLoS Genet. **5**: e1000571.

ZICKLER, D., 2006 From early homologue recognition to synaptonemal complex formation. Chromosoma **115**: 158-174.

ZICKLER, D. and N. KLECKNER, 1999 Meiotic chromosomes: Integrating structure and function. Ann. Rev. Genet. **33**: 603-754.

Chapter 3

A SEARCH FOR HIGH COPY SUPPRESSORS OF THE *CSM4-3* MUTATION

INTRODUCTION

Chromosome motion during zygotene of meiosis I is highly conserved, and appears to involve the cytoskeleton in all organisms studied (Chikashage *et al.* 2007, Koszul *et al.* 2008; see Chapters 1 and 2). In organisms such as *S. pombe*, these movements appear to be microtubule dependent, because they are inhibited by addition of colchicine. However, addition of colchicine in budding yeast only slightly decreases chromosome motion (Trelles-Sticken *et al*. 2005). In budding yeast, addition of Latrunculin B, which prevents actin polymerization, stops chromosome motion to an even larger extent than the *csm4Δ* mutation (see Chapter 2). Csm4 is a known component of the motion-generating system (Figure 3.1; Scherthan *et al.* 2007, Koszul *et al.* 2008). These data suggest a role for actin, and not microtubules, in chromosome motion in *S. cerevisiae.* Koszul *et al.* (2008) were able to visualize actin cables illuminated with Abp140-GFP in combination with DAPI and Nup49-GFP (a component of the nuclear envelope (NE)). No actin cables were seen within the nucleus, however a few were seen to surround the nucleus. This appears to be a very tight connection, as covisualization of Abp140-GFP and Nup49-GFP only gave one signal along the nuclear periphery, even when dynamic nuclear shape changes occurred due to motion of chromosomes. When Abp140-GFP and DAPI are viewed, a chromosome can be seen "following" an actin cable. This attachment appears to be passive, with the actin cables moving and the chromosomes following, since the speed of chromosome motion and actin cable extension are very similar (~0.3 um/s) (Koszul *et al.* 2008; Yang and Pon, 2002). This suggests that chromosome motion, reliant on Csm4, is also intimately connected with the actin cytoskeleton.

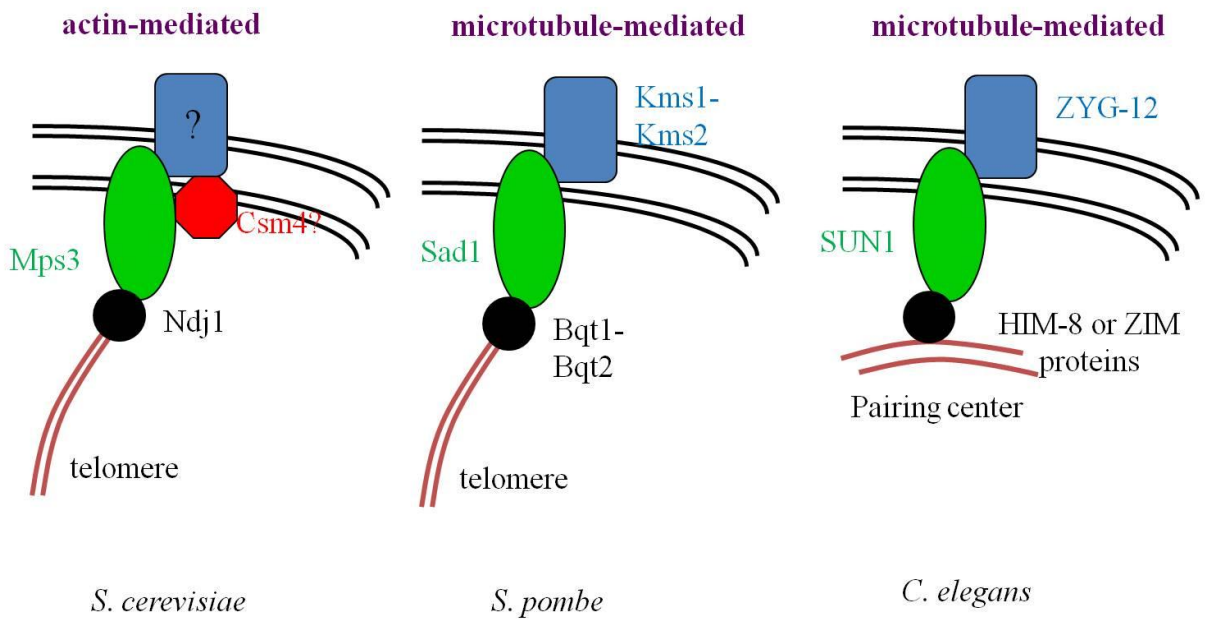

Figure 3.1. Chromosome motion generating system in three organisms. The known components of the chromosome motion generating system in three organisms in shown. In each case, chromosomes in the nucleus are attached to the cytoplasm through a variety of proteins, usually a KASH domain protein in the cytoskeleton and a SUN domain protein in the nucleus (see Introduction). Figure modified from Starr, 2009.

Several components are known to be important for chromosome motion in budding yeast, including Mps3, Ndj1, and Csm4 (Trelles-Stricken *et al.* 2000, Conrad *et al*. 2007, Wanat *et al.* 2008). Mps3 is a SUN domain protein (named for Sad1 in *S. pombe* and Unc84 in *C. elegans),* located on the inner nuclear membrane. SUN domain proteins are thought to provide a bridge between the nucleus and the cytoskeleton (Starr, 2009). The second half of the bridge, found in many organism but not yet in *S. cerevisiae,* are called KASH proteins, named for Klarsicht in *Drosophila*, Anc1 in *C. elegans*, and Syne homology in mammals (Chikashige *et al.* 2007). Mps3 has been found to physically interact with Ndj1, which is a meiosis-specific protein localized to telomeres. Ndj1 and Mps3 are required to attach telomeres to the nuclear envelope, while Csm4 is thought to be needed directly for telomere-led chromosome movements (Conrad *et al.* 2008; Kosaka *et al.* 2008; Koszul *et al.* 2008; Wanat *et al.* 2008). Csm4 physically interacts with both Ndj1 and Mps3 (Conrad *et al*. 2007; Kosaka *et al.* 2008). Csm4 has a transmembrane domain, suggesting that Csm4 might be a KASH domain protein in yeast, despite lacking primary amino acid sequence similarity to other known KASH proteins. The components of the telomere-led chromosome motion system are much better known in other organisms, including *S. pombe* and *C. elegans* (Figure 3.1). The connections between the known components in the nucleus, including Csm4, and the actin network in the cytoskeleton in budding yeast are currently unknown.

Rad17 is a DNA checkpoint protein that recognizes unrepaired breaks in the form of recombination intermediates and gives mutant cells extra time to "catch up" and complete recombination before chromosomes are segregated. A *RAD17* checkpoint can delay meiotic progression in mutant cells unable to complete recombination successfully (Lydall *et al.* 1996). *rad17*Δ is able to rescue the meiotic delay in a variety of meiotic mutants, but almost always at

the cost of lowering spore viability (Lydall *et al.* 1996; Grushcow *et al.* 1999; Wu and Burgess 2006; Wu *et al.* 2010). I used a *rad17*Δ mutation to sensitize my *csm4-3* mutation discussed in Chapter 2, in order to conduct a screen to look for new components of the motion generating system in budding yeast. While I initially found 4 overexpression plasmids that were able to suppress the spore viability defect of *csm4-3 rad17Δ*, I was unable to identify any single gene that was able to suppress the phenotype.

MATERIALS AND METHODS

EAY3368 (*csm4-3, rad17Δ, leu2)*, EAY3367 (*csm4Δ, rad17Δ, leu2)*, EAY3366 (*csm4Δ, pch2Δ, leu2)*, or EAY3370 (*csm4-3, pch2Δ, leu2)* were transformed with the Prelich overexpression library (Jones *et al.* 2008) using methods described in Chapter 2. Strains were sporulated and dissected as described in Chapter 2. Differences in spore viability were analyzed by a Chi-Square test with p-values < 0.05 considered statistically significant.

RESULTS

I utilized a screen previously conducted in the lab in order to find genes that when overexpressed would rescue a spore viability defect in a double mutant (SaraH Zanders, unpublished data). If the interaction region of *csm4-3* is partially compromised, overexpression of genes could permit the formation of enough competent complex through mass action to allow function. Previously, I had discovered that an allele of *CSM4*, *csm4-3*, had a near wild-type spore viability on its own; however, when this allele was combined with a second meiotic mutant, such as *pch2*Δ or *rad17*Δ, the spore viability became significantly lower than either single mutant alone ($P < 0.001$; Chapter 2; Table 3.1). Since this allele confers high functionality on its own, it should be ideal to use to find a component that can still interact with the complex, and Csm4

Table 3.1. Spore viabilities of suppressors in double mutants.

Strain background	Suppressor	Spore Viability (%)
WT	None	90
csm4-3	None	88
*rad17*Δ	None	33
*csm4-3 rad17*Δ	None	3
*csm4-3 rad17*Δ	1	13.1
*csm4-3 rad17*Δ	2	12.0
*csm4-3 rad17*Δ	3	10.6
*csm4-3 rad17*Δ	4	10.4
*csm4*Δ *rad17*Δ	None	1
*csm4*Δ *rad17*Δ	1	1.3
*csm4*Δ *rad17*Δ	2	0.6
*csm4*Δ *rad17*Δ	3	1.3
*csm4*Δ *rad17*Δ	4	0
*csm4-3 pch2*Δ	None	56
*csm4-3 pch2*Δ	1	60.0
*csm4-3 pch2*Δ	2	60.0
*csm4-3 pch2*Δ	3	52.5
*csm4-3 pch2*Δ	4	64.38
*csm4*Δ *pch2*Δ	None	31
*csm4*Δ *pch2*Δ	1	33.75
*csm4*Δ *pch2*Δ	2	38.14
*csm4*Δ *pch2*Δ	3	31.3
*csm4*Δ *pch2*Δ	4	35.89

Spore viabilities of controls and starting strains are shown, along with the spore viability of each suppressor in each background.

specifically.

The Prelich library contains 1,588 2μ *LEU2* plasmids covering 97.2% of the 12-Mbp genome of budding yeast, or 95% coverage of the functional genome (119 genes are completely missing; Jones *et al.* 2008). The library has an average insert size of 8.7 kb, which on average contains about four complete genes. The Prelich library was obtained (Jones *et al.* 2008) and transformed into *E. coli* in order to amplify the DNA. Approximately 5,300 colonies were obtained, and 2 plasmid preps were made of the amplified library, which were called library 1 and library 2. Library 1 and 2 were then separately transformed into the starting strain, *csm4-3 rad17*Δ *leu2*Δ, and 3400 transformant colonies were obtained. Each colony was patched onto an SC-*Leu* plate in order to retain the plasmid. After 2 days, the patches were replica-plated to sporulation plates and kept at 30˚ C for 5 days. The sporulation plates were then replica-plated to YPD plates, and growth on the YPD plates was scored after both 1 and 2 days. As a proof-of-principle, wild-type (SV ~90%), *csm4*Δ (SV~60%), and *csm4-3 rad17*Δ strains were used, and clear differences in spore viability were observed (Figure 3.2).

Approximately 150 strains passed this first round of screening. These 150 strains were patched out again, and taken through the same protocol a second time. 80 strains passed two rounds of screening in this manner, and frozen stocks of these 80 were made. Examples of positive hits, where colony patches show increased growth, are shown in Figure 3.3. The top 28 strains based on increased growth phenotype were picked and further analyzed. After isolating the plasmids and sequencing 25 strains, I found that 17 were unique, with five plasmids found at least twice. Three strains were dissected but were not sequenced because they did not show improved spore viability. If a gene on the plasmid rescued the *csm4-3* defect, a maximum spore viability of ~30% (the spore viability of *rad17*Δ alone) would be observed. If a gene on the

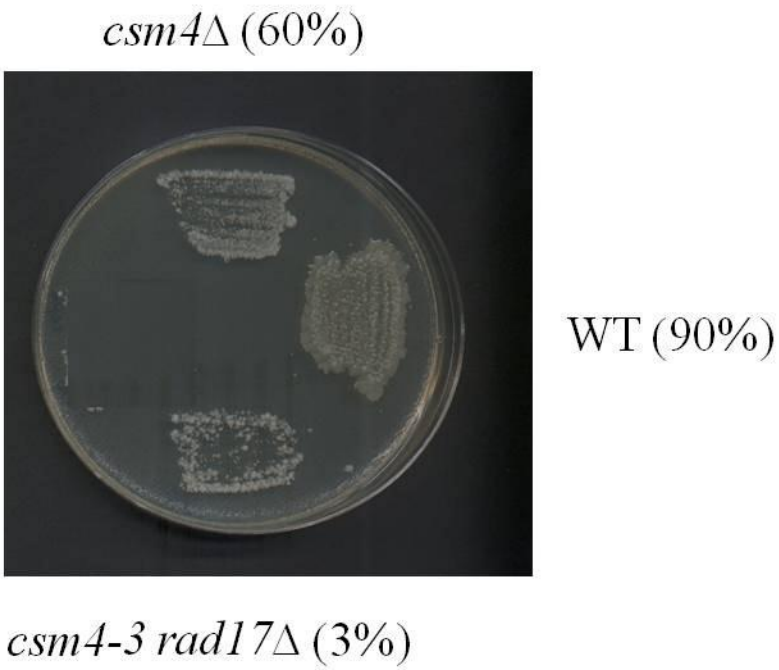

Figure 3.2. Patch assay proof-of-concept. The patch assay was conducted with WT, *csm4Δ*, and *csm4-3 rad17Δ* cells to verify that differences in spore viabilities can be observed. Patches of each diploid genotype are shown after two days on YPD following sporulation. Spore viabilities of each strain are listed in parentheses next to each strain genotype.

Figure 3.3. Examples of positive hits. Each square patch represents a unique transformant. Two examples of positive hits on an initial screen plate (circled) are shown. Positive and negative controls (data not shown) were conducted on the same day, and compared to each patch to identify positive hits.

plasmid rescued the *rad17*Δ defect, the spore viability could reach near WT levels, similar to *csm4-3* alone. Of the 17 unique strains dissected, four showed an increase in spore viability, ranging from 10-13% ($P < 0.1$ for Sup3 and Sup4, $P < 0.05$ for Sup 1 and Sup2; Table 3.1; Figure 3.4A). I named these four suppressors Sup1, Sup2, Sup3, and Sup4.

Since the goal of the screen was to find new components of the chromosome motion-generating system, I was mostly interested in plasmids that carried genes able to rescue the *csm4-3 rad17*Δ strain, but unable to rescue *csm4*Δ *rad17*Δ. This would imply that the rescue of spore viability requires Csm4 protein presence, if not function. If the plasmids also were able to rescue *csm4Δ rad17Δ*, it would suggest that the rescue involved a Csm4-independent mechanism, and would not lead to the identification of a new component in our system. Similarly, I also tested the specificity of the plasmid rescue in a different background, *csm4-3 pch2*Δ and *csm4*Δ *pch2*Δ, to see if the rescue was due to the specific combined defect of Csm4 and Rad17, or whether it was specific to Csm4. Appropriate *Leu-* diploid strains were made in each background, and Sup1-4 were transformed into each strain separately. No plasmid rescued the spore viability of *csm4Δ rad17Δ* (Figure 3.4B). There was also little-to-no rescue of the spore viability of *csm4Δ pch2Δ* of any plasmid, however there was mild to moderate rescue of spore viability of *csm4-3 pch2Δ* (Table 3.1).

In order to determine which of the multiple genes on a plasmid was responsible for the rescue in spore viability, I first made a deletion construct in one of the plasmids, completely eliminating *SAE2* and *YGL176C* in Sup2 by using restriction enzymes and religating the plasmid. This deletion construct did not rescue the spore viability of *csm4-3 rad17*Δ (spore viability 0.6%), suggesting that either *SAE2* or *YGL176C* is responsible for the suppression. Since there were relatively few full length genes on each plasmid (Table 3.2), I decided that the most

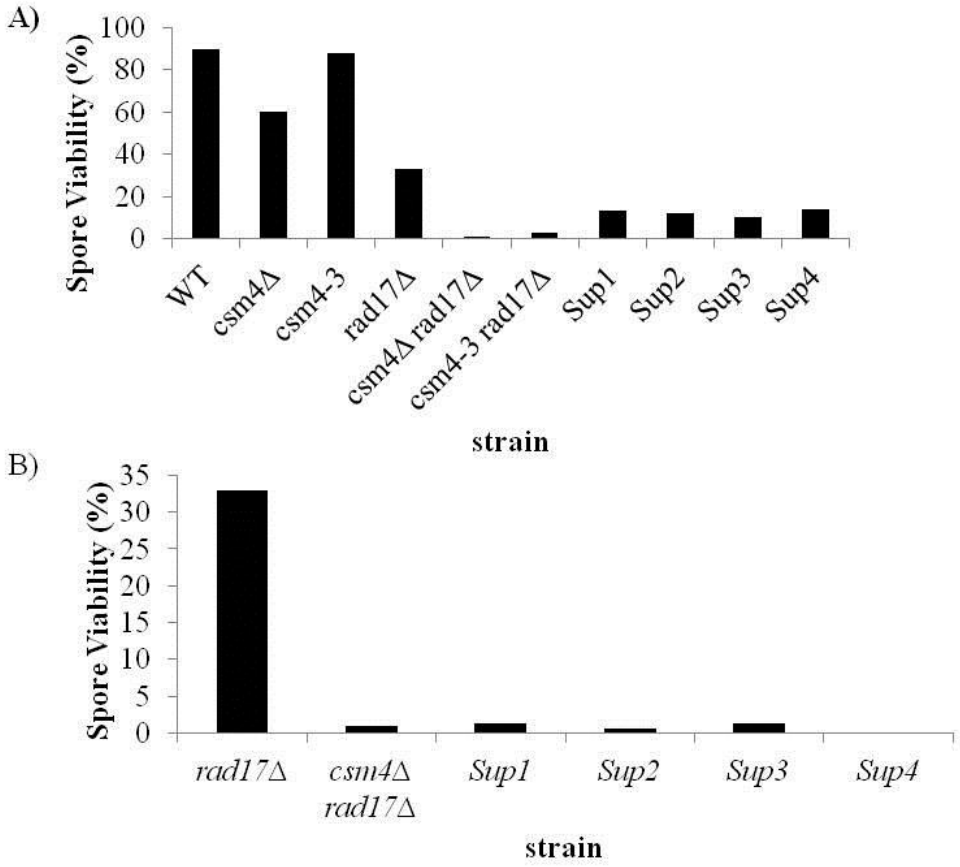

Figure 3.4. Spore viabilities graphs of plasmids in *csm4-3 rad17*Δ and *csm4*Δ *rad17*Δ. A) The spore viabilities of controls and starting strains are shown along with the four suppressors identified. B) Spore viabilities of the suppressors in *csm4Δ rad17Δ* are shown.

Table 3.2. **Genes present on each supressor plasmid.**

Suppressor	Gene	Proposed function
1	*TCO89**	Subunit of Torc1, regulates growth in response to nutrients
1	*PPQ1*	Serine/Threonine phosphatase; translational regulator
1	*tE(UUC)P*	tRNA
1	*CBC2*	RNA cap-binding, splicing
1	*CUP9*	Transcriptional repressor
1	*YPL176C*	Plasma membrane, involved in ubiquitination and vacuole targeting
1	*SPT14**	Regulates glycosylphosphatidylinositol (GPI) biosynthesis
2	*MPT5**	binds to mRNAs encoding chromatin modifiers
2	*YGL177W*	Dubious ORF
2	*YGL176C*	Putative protein, function unknown
2	*SAE2*	Involved in meiotic and mitotic double-strand break repair
2	*BUD13*	nuclear pre-mRNA retention and splicing; involved in bud-site selection
2	*XRN1**	5'-3' exonuclease involved in mRNA decay; plays a role in microtubule-mediated processes, filamentous growth, and telomere maintenance
3	***SRM1****	Macromolecule trafficking;
3	*TOS8*	Transcription factor
3	*tE(UUC)G1*	tRNA
3	*VPS45*	Vacuole protein sorting
3	*PAN2**	Controls poly (A) tail length
4	*ARO1**	Biosynthesis of chorismate
4	*YDR128W*	Telomere capping, associates with vacuole
4	*SAC6*	Maintenance of actin cytoskeleton
4	*FIN1*	Spindle pole body-related intermediate filament protein
4	*YDR131C**	recruits substrates to a core ubiquitination complex

Each gene on Suppressor 1-4 is shown, with a brief description of its known function from yeastgenome.org. *, only part of the gene is present on the suppressor plasmid.

efficient route would be to clone each individual full length gene into the 2μ plasmid backbone and test for spore viability rescue. Primers were designed to be complimentary to a portion at least 500 bp upstream of each gene, or 150 bp downstream of each gene. If there was an endogenous restriction site present near the desired location, primers were designed to overlap with these locations. Otherwise, an overhang was created to introduce a restriction site. Using these primers, a full length copy of the gene was created using PCR. Both the plasmid backbone and the PCR product were then digested with the appropriate restriction enzymes, and the gene was ligated into the backbone. Candidates were then screened using restriction digests to check for the correct insert.

Once a gene was cloned into the 2μ plasmid, it was then introduced into the starting strain, *csm4-3 rad17*Δ *Leu-* and spore viability was determined. Eight of twelve full length genes present on the plasmids, excluding tRNAs, were cloned and dissected. The largest increase in spore viability was for *TOS8,* which rescued spore viability to 6.6%, compared to 10.4% spore viability of the original plasmid, Sup3 (Table 3.3). I determined that this increase in spore viability was not large enough that we would see differences in other less sensitive assays. Furthermore, none of our candidates seemed likely based on known information to play a direct role in the chromosome-motion machinery, thus I did not pursue any construct further.

DISCUSSION

I conducted a screen with the goal of identifying a new component of the motion generating system in budding yeast. By using a patch assay to assess spore viability, I looked for overexpression plasmids that could increase the spore viability of our starting strain, *csm4-3 rad17*Δ. While I found four unique plasmids that were able to rescue the spore viability of this

Table 3.3. Spore viabilities of cloned genes in *rad17*Δ *csm4-3*.

Strain	Spore Viability (%)
*csm4-3 rad17*Δ	3
w/ *SAE2*	2.1 (n = 60)
w/ *SAC6*	0.4 (n = 60)
w/ *FIN1*	1.25 (n = 40)
w/ *BUD13*	1.9 (n = 40)
w/ *YGL176C*	5.4 (n = 60)
w/ *YPL176C*	2.5 (n = 40)
w/ *CUP9*	4.1 (n = 80)
w/ *TOS8*	6.6 (n = 40)

Spore viabilities of the starting strain (*csm4-3 rad17*Δ*)* with each a candidate gene cloned into the plasmid backbone are shown. n, number of tetrads dissected.

strain from ~3% to ~12%, when the individual genes were cloned, no single gene was able to rescue the spore viability to the same degree. This could be for a variety of reasons. First, except for the first two prospects, I did not sequence the cloned genes. While I used a high fidelity polymerase, it is possible, although unlikely, that a mutation was introduced during the PCR, leaving the gene nonfunctional. Thus, when introduced into the background strain, overexpression of this mutated gene would not produce a functional product like that which was present in the original overexpression plasmid, and thus this construct would not rescue the spore viability of our starting strain, *csm4-3 rad17*Δ.

Second, it is possible that the spore viability rescue I observed in the four original overexpression plasmids is dependent on a transcription factor or regulatory element not present in the cloned construct. In order to prevent this, at least 500 bp upstream of the start codon and 200 bp downstream of the stop codon were included in the cloned constructs. While most regulatory elements in budding yeast are located close to the gene, there are exceptions. Very little is known about some of the genes identified in this study (for example, *YGL176C*), and thus not much is known about their regulation, either. Similarly, although unlikely, a combination of genes on each plasmid might be needed for the rescue in spore viability. Operons are rare in yeast, and none of the genes on the plasmids are known to be part of one. Furthermore, the genes found on each plasmid appeared to have diverse function, and it seems unlikely that more than one would be interacting with each other in an overexpression construct to increase spore viability in the starting strain.

Third, expression levels of the constructs were not tested. Both Fin1 and Sac6 are known to be lethal when overexpressed under certain conditions; however, both were recovered in my screen. Sac6 is known to be lethal when overexpressed using a GAL promoter (Sandrock *et al.*

1999; Magdolen *et al.* 1993). It is very likely that Sac6 is not overexpressed to the same extent on the 2μ vector, since a GAL promoter is one of the strongest promoters in budding yeast (Johnston, 1987). Similarily, Fin1 is known to be lethal when overexpressed in haploids. This screen was conducted in diploids, so it is possible that Fin1 overexpression is not lethal under these conditions. Also, since expression levels were not tested either by quantitative PCR or Western blots, it is possible that certain genes on the plasmids, or the entire plasmids were not overexpressed to a large degree, or at all. This could have prevented me from recovering what would have been positive hits, although it is unlikely the reason why the initial positive hits were inconclusive.

There still remain a few untested candidates on the candidate plasmids. Suppressor 2 was thoroughly tested, due to the creation of a deletion construct from the initial plasmid that did not suppress. On Suppressor 1, a lot of untested candidates remain (Table 3.2). The most likely candidates are *PPQ1*, a Serine/Threonine phosphatase, and *SPT14* which regulates glycosylphosphatidylinositol biosynthesis. A lot of phosphorylation events occur during meiosis through the Mec1 pathway (Schindler, 2011; Carballo and Cha, 2007), and altering *PPQ1* expression levels could modify these events. I was unable to clone *PPQ1* into the backbone 2μ vector in order to test whether it would suppress the spore viability defect. I was also unable to clone *SPT14* into our backbone construct. *spt14*Δ is able to rescue a dominant-negative *mps3* allele (Sue Jasperson, personal communication). Since Mps3 is likely in the same complex as Csm4, it is easy to envision that overexpression of Mps3 could suppress the *csm4-3 rad17*Δ spore viability defect. However, I would not envision this protein to be a new component in the motion generating system. Instead, I would propose that if Spt14 overexpression were to suppress the spore viability defect, it would be through misregulation of the

phosphatidylinositols in the nuclear membrane, artificially altering the connections between the telomeres in the nucleus with the actin cytoskeleton in the cytoplasm. I was unable to obtain a PCR product in which to attempt cloning the *CBC2* gene, and did not attempt to clone *tE(UUC)P*, a tRNA, due to it being completely uninteresting if it were to suppress. Also partially present on this plasmid is *TCO89*, a subunit of Torc1, which regulates growth in response to nutrients. Due to the starvation conditions on sporulation plates on which these strains were tested, a protein involved with growth response to nutrients could have been the reason we initially picked out this plasmid for study in the initial screen using the patch assays, however it is unclear how overexpression of this gene would promote spore viability. This gene is also only partially present on the plasmid, missing approximately 2.1 kb of the gene, making it unlikely to be functional.

Only *TOS8* from Suppressor 3 was tested (Table 3.2). This was a prime candidate due to a parallel screen I performed looking for suppression of a spore viability defect in *csm4*Δ *pch2*Δ. This gene was pulled out in initial rounds of this screen, but from a different plasmid, due to the overlapping nature of the library. The spore viability of this second plasmid was not tested in either the *csm4*Δ *pch2*Δ background or the *csm4-3 rad17*Δ background. Tos8 overexpression resulted in the largest increase in spore viability of any single gene tested, however it was still lower than the spore viability observed with the entire Suppressor 3 plasmid. I did not pursue this gene further. Another tRNA, *tE(UUC)G1* is also present on this plasmid, which was not tested for similar reasons as to the tRNA on Suppressor 1. The only other full length gene on this plasmid was *VPS45*, which we were unable to clone. Other partial genes present are *SRM1* and *PAN2*, which due to their proposed functions, seem unlikely to suppress the spore viability (Table 3.2).

Finally, suppressor 4 was my original favorite, containing both *FIN1* and *SAC6* (see results). However, neither of these suppressed the spore viability defects, and the only other full length gene (*YDR128W*) we were unable to get a PCR product to attempt cloning. Similar to Suppressor 3, the 2 partial genes on this plasmid seem unlikely to suppress the spore viability of our starting strain due to their proposed functions. This plasmid contained both of the genes that are known to be lethal when overexpressed under certain conditions. It is possible, therefore, that this particular plasmid had a mutation lowering expression levels to a sub-lethal level and optimal levels for suppression of our spore viability mutant. If this were the case, when I cloned in each gene individually into the backbone, this mutation would no longer be present, and thus suppression would not take place. It would be interesting to look at deletion constructs of the original plasmid to verify this hypothesis.

Another caveat to this screen is that I never recovered *CSM4* or *RAD17* on a candidate plasmid, even though they are both present in full length in the Prelich library. Clearly, since each of the nulls is recessive (see Chapter 2), reintroducing each of these genes should have suppressed the null, thereby increasing the spore viability back up to the level of the respective single mutant. That I did not recover either *CSM4* or *RAD17* suggests that the coverage of the library was not very high, or that the patch assay selection was flawed. In order to get enough plasmid library DNA for the yeast transformation, I first amplified the DNA in *E. coli*. This could have selected for certain plasmids, and I almost certainly lost a number of unique plasmids in this step (5,300 colonies, 1588 unique plasmids in the library). Out of 25 plasmids sequenced after the yeast transformation and selection, five plasmids were identified more than once. This suggests either that certain plasmids were highly overrepresented in the yeast transformation, or that the coverage was actually quite high. Due to only ~3500 yeast colonies analyzed, and 1600

unique plasmids, the maximum coverage was a little over 2-fold. Since I recovered certain plasmids more than twice (35 #32, 23 #14, 80 #21), likely there was some degree of selection in the *E. coli* amplification step.

Finally, it is possible that the basic concept of the patch assay selection was flawed. Out of the top 28 candidates (20 unique), only four showed an increase in spore viability, and only one of these was selected more than once. This suggests that in the patch assay selection, I selected candidates that showed increased growth to reasons other than an increase in spore viability. Some of these reasons could be changes in growth factors, non-spore survival, or contamination. As further evidence that I selected for unrelated plasmids, a former graduate student in the lab, Sarah Zanders conducted a similar screen, looking for the rescue of spore viability of a *pch2*Δ *spo11-df* mutant. Two of my sixteen unique plasmids that did not rescue spore viability were also pulled out in Sarah's initial rounds. These plasmids did not rescue spore viability of her mutant, either, suggesting that they increased the apparent growth in the selection for reasons independent of our screen. Also, sporulation efficiency, which was not analyzed, could have played a major role in our selection process. With reduced sporulation efficiency, even if the spore viability was rescued, I would never have picked it up in my selection process, since the two might offset, leading to a "normal" amount of growth.

The goal of this screen was to find new components of the motion-generating system in budding yeast. While I did find some overexpression plasmids that slightly rescued the spore viability, it does not seem probable that any of these candidates is acting directly in this motion generating pathway. It is possible that the *rad17* deletion is too strong of a phenotype to overcome. Doing a similar screen starting with a different double mutant, such as *mlh1*Δ or *pch2*Δ could be done. However, while it was easy to select strains in the patch assay that

different from very little growth similar to the *csm4-3 rad17*Δ strain, it was much more difficult to differentiate between medium growth levels, such as *csm4*Δ *(65%), csm4-3 pch2*Δ *(56%),* and *csm4*Δ *pch2*Δ *(31%).*

Because Csm4 is a proposed transmembrane protein with the N terminus located in the cytoplasm, a split-ubiquitin two hybrid screen could be used to find interacting partners, instead of a more traditional two hybrid (Beilharz *et al.* 2003). Split ubiquitin screens are specific to membrane proteins, cleverly bypassing the need for the protein to be in the nucleus. They work very similarly to the two hybrid screen, working off the basis that if two proteins interact, they can reconstitute ubiquitin, instead of Gal4. Once ubiquitin is reconstituted, it cleaves a LexA transcription factor from the bait protein, in this case Csm4. The transcription factor then travels into the nucleus, activating *LACZ*, or another reporter protein (Iyer *et al*. 2005). At first, candidate genes would be tested for interactions with Csm4. These include actin binding proteins such as Abp1, Sac6, Abp140, Bnr1, Myo1, Myo2, Myo3, Myo4, and Myo5 (list provide by Tony Bretscher). Failing interactions with these proteins, another, larger candidate screen, including meiosis-related proteins would follow. If this does not show any positive interactions, then a library would be used to screen the entire genome. The library would include a selectable marker such as *LEU2*.

Once positive interactors have been identified, similar assays would be performed on mutants to determine the phenotype of this protein during meiosis. Presumably, similar phenotypes such as low spore viability, a meiotic delay, and decreased chromosome motion would be seen in these mutants if they are a part of the same system as Csm4.

REFERENCES

Beilharz, T., B. Egan, P. A. Silver, K. Hofmann, T. Lithgow, 2003 Bipartite signals mediate subcellular targeting of tail-anchored membran proteins in *Saccharomyces cerevisiae.* Journal of Biological Chemistry, 278: 8219-23.

Carballo, J. A., R. S.Cha, 2007 Meiotic roles of Mec1, a budding yeast homolog of mammalian ATR/ATM. Chromosome Res 15: 539-550.

Chikashige, Y., T. Haraguchi, Y. Hiraoka, 2007. Another way to move chromosomes. Chromosoma, 116: 497-505.

Conrad, M. N., C. Y. Lee, J. L. Wilkerson, M.E. Dresser, 2007 MPS3 mediates meiotic bouquet formation in *Saccharomyces cerevisiae*. PNAS, 104: 8863-8.

Conrad, M. N., C. Y. Lee, G. Chao, M. Shinohara, H. Kosaka, *et al*., 2008 Rapid telomere movement in meiotic prophase is promoted by NDJ1, MPS3, and CSM4 and is modulated by recombination. Cell **133**: 1175-1187.

Grushcow, J. M., T. M. Holzen, K. J. Park, T. Weinert, M. Lichten, *et al.*, 1999 *Saccharomyces cerevisiae* checkpoint genes MEC1, RAD17, and RAD24 are required for normal meiotic recombination partner choice. Genetics 153: 607-620.

Iyer, K., L. Burkle, D. Auerbach, S. Thaminy, M. Dinkel, *et al.*, 2005 Utilizing the split-ubiquitin membrane yeast two-hybrid system to identify protein-protein interactions of integral membrane proteins. Sci STKE 275: 13.

Johnston, M., 1987 A model fungal gene regulatory mechanism: the GAL genes of *Saccharomyces cerevisiae.* Microbiol Rev 51: 458-476.

Kosaka, H., M. Shinohara, A. Shinohara A, 2008 Csm4-dependent telomere movement on nuclear envelope promotes meiotic recombination. PLoS Genet. **4**: e1000196.

Koszul, R., K. Kim, M. Prentiss, N. Kleckner, S. Kameoka, 2008 Meiotic chromosomes move by linkage to dynamic actin cables with transduction of force through the nuclear envelope. Cell **133**: 1188-1201.

Lydall, D., Y. Nikolshy, D. K. Bishop, T. Weinert, 1996 A meiotic checkpoint controlled by mitotic checkpoint genes. Nature 383: 840-843.

Magdolen, V., D. G. Drubin, G. Mages, W. Bandlow, 1993 High levels of profiling suppress the lethality caused by overproduction of actin in yeast cells. FEBS Lett 316: 41-47.

Jones, G. M., J. Stalker, S. Humphray, A. West, T. Cox, *et al.*, 2008 A systematic library for comprehensive overexpression screens in *Saccharomyces cerevisiae.* Nat Methods 5: 239-241.

Sandrock, T. M., J. L. O'Dell, A. E. M. Adams, 1999 Allele-specific suppression by formation of new protein-protein interactions in yeast. Genetics 147: 1635-1642.

Scherthan, H., 2007 Telomere attachment and clustering during meiosis. Cell Mol Life Sci 64: 117-124.

Schindler, K., 2011 Protein kinases and protein phosphotases that regulate meiotic maturation in mouse oocytes. Results Probl Cell Diff 53: 309-341.

Starr, D. A., 2009 A nuclear-envelope bridge positions nuclei and moves chromosomes. J Cell Sci, 122: 577-86.

Trelles-Sticken, E., M. E. Dresser, H. Scherthan, 2000 Meiotic telomere protein Ndj1p is required for meiosis-specific telomere distribution, bouquet formation and efficient homologue pairing. J Cell Biol. 151: 95-106.

Trelles-Sticken, E., C. Adelfalk, J. Loidl, H. Scherthan, 2005 Meiotic telomere clustering requires actin for its formation and cohesin for its resolution. J. Cell Biol. **170**: 213-223.

Wanat, J. J., K. P. Kim, R. Koszul, S. Zanders, B. Weiner, *et al.*, 2008 Csm4, in collaboration with Ndj1, mediates telomere-led chromosome dynamics and recombination during yeast meiosis. PLoS Genet. **4**: e1000188.

Wu, H. Y., S. M. Burgess, 2006 Ndj1, a telomere-associated protein, promotes meiotic recombination in budding yeast. Mol Cell Biol, 26: 3683-3694.

Wu, H. Y., H. C. Ho, S. M. Burgess, 2010 Mek1 kinase governs outcomes of meiotic recombination and the checkpoint response. Curr Biol 20: 1707-1716.

Yang, H. C., L. A. Pon , 2002 Actin cable dynamics in budding yeast. PNAS, 99: 751-6.

Chapter 4

GENETIC ANALYSIS OF *MLH3* HYPOMORPH ALLELES SUPPORTS A LATE AND FLEXIBLE ROLE FOR MLH1-MLH3 IN CROSSOVER RESOLUTION DURING MEIOSIS

Megan Sonntag Brown[1], Elisha Lim[1], Cheng Chen[1], K. T. Nishant[2] and Eric Alani[1]

[1]Department of Molecular Biology and Genetics, Cornell University, Ithaca, New York

[2]School of Biology, Indian Institute of Science Education and Research, Thiruvananthapuram, India

Contributions: E. Lim created most *mlh3* ATPase single mutant strains used in Table 4.2 (top) and 4.7 (top). E. Lim conducted the mismatch repair assays in Table 4.7 (top), and contributed to the tetrad dissection data in Table 4.2 (top). C. Chen created most strains used in Table 4.4, and contributed to the tetrad dissection data in Table 4.4, 4.5, and 4.6. K. T. Nishant supervised E. Lim.

ABSTRACT

Crossover placement during meiosis in baker's yeast is carefully regulated through an interference-dependent pathway involving Msh4-Msh5 and Mlh1-Mlh3. This pathway helps ensure that every pair of homologs receives an obligate crossover that facilitates chromosome segregation during the first meiotic division. Previously the Alani Lab detected a crossover threshold in yeast *msh4/5-t* mutants in which meiotic crossing over on Chr. XV could be decreased by up to two-fold without compromising meiotic viability. Based on these and other observations we proposed that disjunction-promoting crossovers are prioritized in *msh4/5-t* mutants. Curiously, *mlh3Δ* strains display crossover levels at or above the threshold seen in *msh4/5-t* mutants, yet show defects in meiotic viability. To further understand Mlh3 functions in meiosis, I analyzed eight *mlh3* ATP binding domain mutations and found that they showed a roughly linear relationship between spore viability and map distance. These data and *mlh3 msh5* double mutant analyses support the idea that Mlh1-Mlh3 acts downstream of Msh4-Msh5, after crossover decisions that maintain the obligate crossover have been made. To further test a late role for Mlh1-Mlh3, I analyzed crossing over on four chromosomes in *mlh3*Δ *mms4*Δ cells. I found a strong decrease (6 to 17-fold) at all intervals despite relatively high spore viability. Together, these phenotypes are consistent with a terminal decision role for Mlh1-Mlh3 in the interference-dependent crossover pathway

INTRODUCTION

During gametogenesis in most eukaryotes, crossing over between homologous chromosomes occurs during prophase of Meiosis I, and is critical for both chromosome segregation and exchange of genetic information between homologs (reviewed in Zickler, 2006). Meiotic recombination in *S. cerevisiae* is initiated by the induction of about 200 *SPO11*-dependent double strand breaks (DSBs) that occur throughout the genome (Cao *et al.* 1990; Gilbertson and Stahl 1996; Keeney, 1997; Chen *et al.* 2008; Robine *et al.* 2007). Roughly 40% of these DSBs are repaired to form crossovers between homologous chromosomes; the rest are repaired as noncrossovers or by using a sister chromatid as template. In the crossover pathway, DSB resection results in 3'single strand tails whose repair is directed primarily to the complementary sequence in the other homolog (Schwacha and Kleckner 1995). The 3' tails are acted upon by strand exchange enzymes to form single-end invasion intermediates (SEIs). SEIs are subsequently converted into double Holliday junctions (dHJs) that are ultimately resolved into crossovers (Hunter and Kleckner 2001).

Two MutS and MutL homolog (MSH and MLH) complexes, Msh4-Msh5 and Mlh1-Mlh3, respectively, act in meiosis to promote widely spaced crossovers that result from an interference-dependent crossover pathway. In this pathway the presence of one crossover decreases the likelihood of another nearby (Stahl *et al.* 2004; Kleckner *et al.* 2004; Shinohara *et al.* 2008). A second, interference-independent crossover pathway is mediated by the endonuclease complex Mus81-Mms4, and is activated by the polo-like kinase Cdc5 (de los Santos *et al.* 2003; Argueso *et al.* 2004; Clyne *et al.* 2003; Matos *et al.* 2011; Sourirajan and Lichten 2008). Little is known about the intermediates in this pathway; however, the Mus81-Mms4 complex is thought to act directly in Holliday junction resolution or by cleaving D-loops

and half-HJ intermediates (Kaliraman *et al.* 2001; Hollingsworth and Brill 2004; Gaskell *et al.* 2007).

Genetic, biochemical, and physical studies have shown that Msh4-Msh5 acts in meiosis by stabilizing SEI and dHJ intermediates (Borner *et al.* 2004; Snowden *et al.* 2004; Nishant *et al.* 2010). Mlh3 was found to co-immunoprecipitate with Msh4, suggesting that the Mlh1-Mlh3 heterodimer is recruited to the Msh4-Msh5-DNA complex (Santucci-Darmanin *et al.* 2002). This interaction is thought to reinforce the crossover decision by providing a substrate for a dHJ resolvase(s) during early- to mid- pachytene stages in meiosis (Wang *et al.* 1999; Santucci-Darmanin *et al.* 2002; Hoffman and Borts 2004; Whitby 2005; Nishant *et al*. 2008). Consistent with these observations are cytological observations showing that ~140 Msh4-Msh5 foci are present per mouse spermatocyte nucleus in zygotene. The number of Msh4 foci decrease to about two to three foci per chromosome in mid-pachytene. At this stage, Mlh1 foci begin to appear. Initially, there is high (95-100%) co-localization between the two foci; however, as pachytene progresses, this co-localization gradually disappears (Svetlanov and Cohen 2004; Kneitz *et al.* 2000; Santucci-Darmanin *et al.* 2000). The presence of a large number of Msh4-Msh5 foci in zygotene supports early roles for Msh4-Msh5 in meiosis, perhaps during initial interhomolog interactions (Storlazzi *et al.* 2010).

Crossover placement in meiosis is carefully regulated through the Msh4-Msh5 interference pathway and the actions of Sgs1 helicase, which may play a role in promoting crossing over, but mainly serves as an anti-crossover factor by removing aberrant recombination intermediates (Jessop *et al.* 2006; Oh *et al.* 2007; de Muyt *et al.* 2012; Zakharyevich *et al.* 2012). Crossover levels are also regulated by a homeostasis mechanism that ensures that when DSB levels are reduced crossovers are maintained at the expense of noncrossovers. This mechanism

facilitates proper disjunction of homologs (Martini *et al.* 2006; Zanders and Alani 2009). At least one crossover per homolog, called the obligate crossover, appears necessary for proper homolog disjunction. Steps that ensure the obligate crossover in the interference-dependent pathway are thought to occur during the crossover/noncrossover decision step, just before single-end invasion (Allers *et al.* 2001; Hunter and Kleckner 2001).

To explore mechanisms that ensure obligate crossover formation the Alani Lab analyzed a large set of *msh4* and *msh5* yeast mutants for defects in crossing over and spore viability (Nishant *et al.* 2010). We detected the presence of a threshold in which crossover levels could be decreased up to two-fold without compromising spore viability. Based on these and double mutant analyses we proposed that the threshold represents an extension of crossover homeostasis; *msh4/5* threshold mutants can promote the formation of the obligate crossover prior to the formation of additional, non-obligate crossovers (Nishant *et al.* 2010). Interestingly, *mlh3Δ* diploids display spore viability and Meiosis I disjunction defects despite displaying crossover levels that would confer high spore viability in *msh4/5* threshold mutant backgrounds (Nishant *et al*. 2008; 2010).

During DNA mismatch repair (MMR), MSH proteins bind to mismatches that form primarily as the result of DNA replication errors. Repair of base-base and single insertion/deletion mismatches is initiated primarily by Msh2-Msh6, while the repair of small (~2-15 nt) insertion and deletion mutations, often resulting from DNA slippage events that occur during replication, is initiated mainly by Msh2-Msh3 (Kunkel and Erie 2005; Bowers *et al.* 2000; Habraken *et al.* 1996; Habraken *et al.* 1997). In the baker's yeast *S. cerevisiae* both MSH complexes interact primarily with a single MLH complex, Mlh1-Pms1, to reinforce the repair decision and activate downstream excision and resynthesis steps. Mlh1-Mlh3 performs a minor

role in the repair of insertion and deletions, presumably through interactions with Msh2-Msh3 (New *et al.* 1993; Kolodner and Marsischky, 1999; Marti *et al.* 2002; Surtees *et al.* 2004). Mlh3 contains an ATP binding domain that is highly conserved among MLH proteins. It also contains an endonuclease domain that is detected in specific classes of MLH proteins (Figure 4.1; Flores-Rozas and Kolodner 1998; Prolla *et al.* 1994a; Prolla *et al.* 1994b). Previous work from our laboratory indicated that the endonuclease domain present near the C-terminus of Mlh3 is critical for its MMR and crossover functions (Nishant *et al.* 2008).

In this study I investigated the role of Mlh3 in meiosis by analyzing eight *mlh3* ATPase mutants for defects in meiotic recombination. These mutants showed a roughly linear relationship between spore viability and genetic map distance. My observations are consistent with Mlh1-Mlh3 acting downstream of Msh4-Msh5, after crossover homeostasis decisions have been made. Consistent with this idea is recent work from the Lichten and Hunter labs showing that Mlh1-Mlh3 plays a crossover resolution role independent of Mus81-Mms4 (De Muyt *et al.* 2012; Zakharyevich *et al.* 2012). To further test this hypothesis I analyzed crossing over on four chromosomes in *mlh3*Δ *mms4*Δ cells and found a strong decrease in crossing over at all intervals despite relatively high spore viability. Finally, I found that mutations in the ATPase domain of Mlh3 generally confer a stronger defect in MMR, suggesting structural roles for Mlh3 in meiosis.

MATERIALS AND METHODS

Media. *S. cerevisiae* strains were grown at 30˚C in either yeast extract-peptone, 2% dextrose (YPD) media or minimal selective media (SC) containing 2% dextrose, sucrose, or galactose (Rose *et al.* 1990). When required for selection, geneticin (Invitrogen, San Diego) and

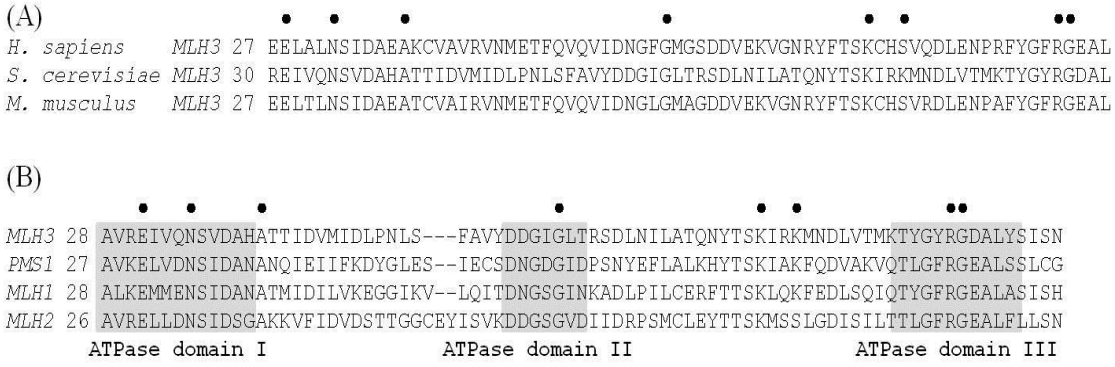

Figure 4.1. The ATPase domain of Mlh3 is highly conserved across eukaryotic species and within the MLH protein family. A) Location of the *mlh3* mutations analyzed in this study with respect to *Homo sapiens, Saccharomyces cerevisiae*, and *Mus musculus* protein sequences. B) Location of the *mlh3* mutations created with respect to the conserved ATPase domains in the *Saccharomyces cerevisiae* MLH family of proteins (Ban and Yang 1998; Tran and Liskay 2000). ATPase domain IV is not shown. ●, locations of *mlh3* alleles analyzed in this study

nourseothricin (Werner BioAgents, Germany) were used at recommended concentrations (Wach *et al.* 1994; Goldstein and McCusker 1999). Sporulation plates and media were prepared as described in Argueso *et al*. (2004).

Plasmids and strains. Plasmids containing each of the *mlh3* alleles were constructed via QuickChange mutagenesis (Stratagene, La Jolla, CA) using the single step integration vector pEA1254 as a template. pEAI254 contains the SK1 *MLH3* gene with a *KANMX4* selectable marker inserted 40 bp downstream of the stop codon (Nishant *et al*. 2008). Mutations created by QuickChange were confirmed by DNA sequencing (Sanger method) of the entire *MLH3* open reading frame. Primers used to create the *mlh3* alleles are available upon request. pEAI254 and mutant derivatives were digested with *BamHI* and *SalI* prior to introduction into yeast by the lithium acetate transformation method (Gietz *et al*. 1995). Plasmids used for the dominant negative assay were constructed by QuickChange mutagenesis (using pEAE220 (S288C, *GAL10-MLH3, 2μ, URA3)* as a template (Nishant *et al*. 2008). The mutated regions created by QuickChange were subcloned into a new pEAE220 backbone to eliminate other possible mutations.

The SK1 *mlh3* alleles described in this study were introduced by gene replacement into SK1 congenic and isogenic strain backgrounds (Table 4.1). The effect of the eight alleles on spore viability and crossing over was measured in EAY1108/1112 (SK1 congenic; Argueso *et al*. 2004). *mlh3 msh5* double mutants were constructed in EAY1108/1112. More specifically, *mlh3* alleles were introduced by gene replacement into the *msh5*Δ *MATα* strain EAY1279, and *msh5* alleles were introduced into the *mlh3*Δ *msh5*Δ *MATa* strain EAY3312. The *mlh3*Δ and *mlh3*Δ *mms4*Δ strains were derived from the SK1 isogenic NHY942/NHY943 background (de los

Table 4.1. Yeast strains used in this study.

Strain	Genotype
EAY1062	*MATa ho::hisG, ura3, leu2::hisG, ade2::LK, his4xB, lys214::insE-A14*
EAY2186	*MATa ho::hisG, ura3, leu2::hisG, ade2::LK, his4xB, lys214::insE-A14, MLH3::KANMX4*
EAY2037	*MATa ho::hisG, ura3, leu2::hisG, ade2::LK, his4xB, lys214::insE-A14, mlh3::KANMX4*
EAY3117	*MATa ho::hisG, ura3, leu2::hisG, ade2::LK, his4xB, lys214::insE-A14, mlh3-E31A::KANMX4*
EAY3119	*MATa ho::hisG, ura3, leu2::hisG, ade2::LK, his4xB, lys214::insE-A14, mlh3-N35A::KANMX4*
EAY3121	*MATa ho::hisG, ura3, leu2::hisG, ade2::LK, his4xB, lys214::insE-A14, mlh3-A41F::KANMX4*
EAY3123	*MATa ho::hisG, ura3, leu2::hisG, ade2::LK, his4xB, lys214::insE-A14, mlh3-G63R::KANMX4*
EAY3125	*MATa ho::hisG, ura3, leu2::hisG, ade2::LK, his4xB, lys214::insE-A14, mlh3-K80E::KANMX4*
EAY3127	*MATa ho::hisG, ura3, leu2::hisG, ade2::LK, his4xB, lys214::insE-A14, mlh3-K83E::KANMX4*
EAY3129	*MATa ho::hisG, ura3, leu2::hisG, ade2::LK, his4xB, lys214::insE-A14, mlh3-R96A::KANMX4*
EAY3131	*MATa ho::hisG, ura3, leu2::hisG, ade2::LK, his4xB, lys214::insE-A14, mlh3-G97A::KANMX4*
EAY1269	*MATa ura3, leu2, trp1, lys2::insE-A14*
EAY1366	*MATa leu2, ura3, trp1, his3, lys2::insE-A14 mlh1Δ::KANMX4*
EAY3308	*MATa ura3, leu2, trp1, lys2::insE-A14 w/ pEAE220 (GAL10-MLH3, 2μ)*
EAY3309	*MATa ura3, leu2, trp1, lys2::insE-A14 w/ pEAE374 (GAL10-mlh3-E31A, 2μ)*
EAY3310	*MATa ura3, leu2, trp1, lys2::insE-A14 w/ pEAE375 (GAL10-mlh3-R96A, 2μ)*
EAY3311	*MATa ura3, leu2, trp1, lys2::insE-A14 w/ pEAE376 (GAL10-mlh3-G97A, 2μ)*
EAY1108	*MATa trp1:hisG leu2::hisG ho::hisG ura3 lys2 URA3insertion@CENXV LEU2insertion@chromXV, LYS2 insertion at position 505193*
EAY2413	Same as EAY1108, but *mlh3Δ::NatMX4*
EAY3007	Same as EAY1108, but *mlh3-E31A*
EAY3009	Same as EAY1108, but *mlh3-N35A*
EAY3011	Same as EAY1108, but *mlh3-A41F*
EAY3013	Same as EAY1108, but *mlh3-G63R*
EAY3015	Same as EAY1108, but *mlh3-K80E*
EAY3017	Same as EAY1108, but *mlh3-K83A*
EAY3019	Same as EAY1108, but *mlh3-R96A*
EAY3021	Same as EAY1108, but *mlh3-G97A*
EAY2423	Same as EAY1108, but *msh5-D76A::KANMX4*
EAY2439	Same as EAY1108, but *msh5- T423A::KANMX4*
EAY2032	Same as EAY1108, but *mlh3Δ::KANMX4, msh5Δ::NATMX4*
EAY1281	Same as EAY1108, but *msh5Δ::NATMX4*
EAY1847	Same as EAY1108, but *mlh3Δ::KANMX4*
EAY1845	Same as EAY1108, but *mms4Δ::NATMX4*
EAY2030	Same as EAY1108, but *mlh3Δ::KANMX4, mms4Δ::NATMX4*
EAY3312	Same as EAY1108, but *mlh3Δ::HPHMX4, msh5Δ::NATMX4*
EAY3313	Same as EAY1108, but *mlh3Δ::HPHMX4, msh5-D76A::KANMX4*
EAY3314	Same as EAY1108, but *mlh3Δ::HPHMX4, msh5-T423A::KANMX4*
EAY1112	*MATα ura3, trp1::hisG, leu2::hisG, lys2, ho::hisG, ade2::hisG, his3Δ::hisG, TRP1insertion@CENXV*
EAY1848	Same as EAY1112, but *mlh3Δ::KANMX4*
EAY1846	Same as EAY1112, but *mms4Δ::NATMX4*
EAY1279	Same as EAY1112, but *msh5Δ::NATMX4*
EAY2031	Same as EAY1112, but *mlh3Δ::KANMX4, mms4Δ::NATMX4*
EAY2033	Same as EAY1112, but *mlh3Δ::KANMX4, msh5Δ::NATMX4*
EAY3315	Same as EAY1112, but *mlh3-R96A::KANMX4, msh5Δ::NATMX4*
EAY3316	Same as EAY1112, but *mlh3-G97A::KANMX4, msh5Δ::NATMX4*
EAY1425/NHY942	*MATα ho::hisG ade2Δ can1 ura3(ΔSma-Pst) met13-B trp5-S CENVIII::URA3 thr1-A cup1s*
EAY2904	Same as EAY1425, but *mlh3Δ::KANMX4*
EAY3290	Same as EAY1425, but *mms4Δ::KANMX4*
EAY3296	Same as EAY1425, but *mlh3Δ::KANMX4 mms4Δ::KANMX4*
EAY1426/NHY943	*MATa ho::hisG ade2Δ ura3(ΔSma-Pst) leu2::hisG CENIII::ADE2 lys5-P his4-B cyh2*
EAY2906	Same as EAY1426, but *mlh3Δ::KANMX4*
EAY3323	Same as EAY1426, but *mms4Δ::NATMX4*
EAY3298	Same as EAY1426, but *mlh3Δ::KANMX4 mms4Δ::NATMX4*

Strains EAY1062, EAY1108, EAY1112, EAY1425, EAY1426 and their derivatives are SK1, while EAY1269 and its derivatives are from the S288c background.

Santos *et al.* 2003).

The isogenic SK1 strain EAY1062 (*lys2::InsE-A$_{14}$)* (Nishant *et al.* 2008) was used to measure the effect of *mlh3* mutations on mutation rate. For the dominant negative assay, pEAE220 (2μ, S288c *GAL10-MLH3*), and mutant derivatives pEAE374 (*GAL10-mlh3-E31A*), pEAE375 (*GAL10-mlh3-R96A*), and pEAE376 (*GAL10-mlh3-G97A*) were transformed into EAY1269 (S288c *lys::InsE-A$_{14}$).*

Genetic Map Distance Analysis. EAY1108/EAY1112 and NHY942/NHY942 background diploids were sporulated using the zero growth mating protocol (Argueso *et al.* 2003) and tetrad dissected. For the EAY1108/EAY1112 background strains, tetrads were dissected and spores were germinated on synthetic complete media. For the NHY942/NHY943 background strains, tetrads were dissected and germinated on YPD media supplemented with complete amino acids. Differences in spore formation and viability were analyzed by a Chi-Square test with p-values < 0.05 considered statistically significant. Spore clones were incubated 3-4 days at 30 C and then replica-plated to various selective media. The replica plates were scored after one day of incubation at 30 C. Spore clones were analyzed using the recombination analysis software RANA (Argueso *et al.* 2004*),* which analyzes map distances. Genetic map distances $\pm$ the standard error were calculated using the Stahl Laboratory Online Tools (http://www.molbio.uoregon.edu/,fstahl/) which utilizes the formula of Perkins (1949).

Lys$^+$ reversion assays. The *mlh3* allele constructs were transformed into EAY2037 (SK1, *mlh3*Δ*::KANMX4, lys2::InsE-A$_{14}$),* and strains were analyzed for reversion to Lys$^+$ (Tran *et al.* 1997). At least 15 independent cultures for each allele were analyzed, and experiments were

conducted with two independent transformants. Mutation rates were determined as previously described (Heck *et al.* 2006; Drake 1991). Each median rate was normalized to the wild-type median rate to calculate the fold-increase in mutation rate. 95% confidence intervals were determined as described (Dixon and Massey, 1969).

For the dominant negative assays, EAY1269 bearing pEAE220 and mutant derivatives were grown for five days on uracil dropout SC agar plates containing 2% sucrose or 2% sucrose and 2% galactose. Individual colonies were picked and grown overnight in liquid (-agar) versions of the respective media for 26 hours. Appropriate dilutions were made, and cells grown in sucrose only were plated on uracil, lysine dropout SC agar plates containing 2% sucrose, and uracil dropout SC agar plates containing 2% glucose. Cells grown in sucrose and galactose were plated on uracil, lysine dropout SC agar plates containing 2% sucrose and 2% galactose and uracil dropout SC agar plates containing 2% glucose. Eleven independent colonies from two independent transformations were analyzed, using *GAL10-MLH3* and *mlh1*Δ as controls.

RESULTS

mlh3 alleles do not show a crossover threshold level similar to *msh4/5* alleles

The Alani Lab identified a pattern in a collection of strains bearing *msh4* and *msh5* alleles in which crossing over could be decreased to about 50% of wild-type levels without an apparent defect in spore viability (Nishant *et al*. 2010; Figure 4.2A). We call this pattern a crossover threshold, where excess crossovers can be eliminated to a point at which spore viability drops concomitantly with crossover levels. Based on these data we proposed that crossover designation functions executed by Msh4-Msh5 are prioritized in yeast to maintain the obligate crossover, ensuring that each homolog pair receives at least one disjunction-promoting crossover (Nishant *et al.* 2010, Kaback *et al.* 1992; Kaback *et al.* 1999).

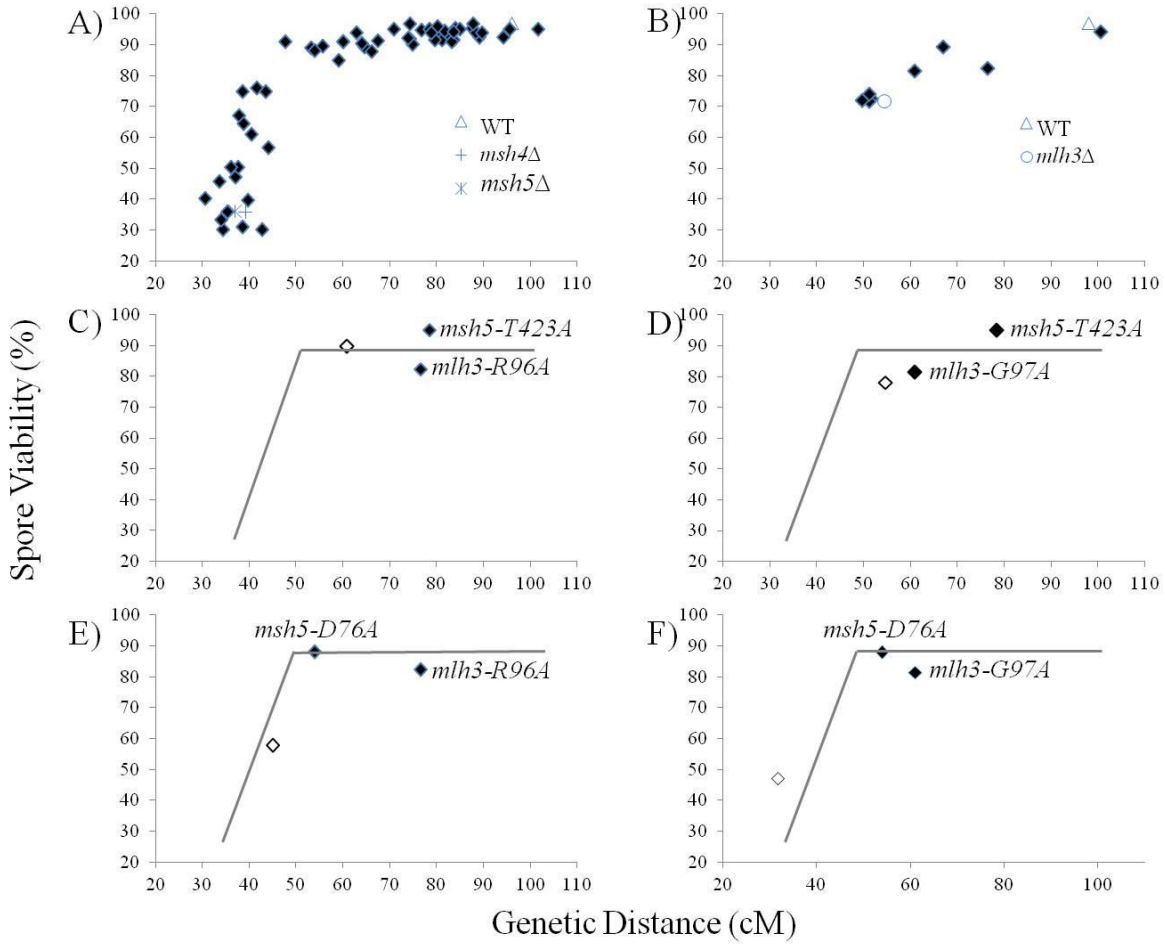

Figure 4.2. A crossover threshold level observed in *msh5* alleles is absent in *mlh3* alleles. A) Spore viabilities are plotted vs. genetic map distance on chromosome XV for 57 *msh4* and *msh5* alleles. Data are from Nishant *et al.* (2010). B) Spore viabilities are plotted vs. genetic map distances on chromosome XV for eight *mlh3* ATP binding domain mutations, wild type, and *mlh3*Δ. C,D,E,F). Spore viabilities and genetic map distances are plotted for the indicated single mutants (filled diamonds) and the double mutants (open diamonds). The line in the background represents the crossover threshold level pattern for *msh4/5* alleles (Nishant *et al*. 2010), as seen in A).

mlh3Δ strains show crossover levels similar to that seen at the *msh4/5* threshold, but show significant defects in spore viability (Nishant et al. 2008; 2010). Because of this phenotype and the finding that Msh4-Msh5 colocalizes with a subset of Mlh1-Mlh3 foci at pachytene in mouse spermatocytes, I was interested in determining the phenotype of *mlh3* hypomorph mutations in meiosis in budding yeast (Hunter and Borts 1997; Wang *et al.* 1999; Santucci-Darmanin *et al.* 2002; Argueso *et al.* 2004; Svetlanov and Cohen 2004; Kneitz *et al.* 2000; Santucci-Darmanin *et al.* 2000). One explanation for the above observations is that rather than responding to Msh4-Msh5 functions that prioritize the obligate crossover, Mlh1-Mlh3 acts downstream of the obligate crossover decision. Consistent with this observation is that while crossover levels on Chr. XV in *mlh3Δ* strains were similar to levels seen in *msh4/5* threshold strains showing high spore viability, crossover levels on other chromosomes (e.g. VII and VIII) were significantly lower (Tables 4.2 to 4.4; Nishant et al. 2010). For example in *msh4-E276A* mutants, which display wild-type spore viability, crossing over at Chr. XV (53.2 cM) was similar to that seen in *mlh3Δ* strains (54.5 cM), but was considerably higher at Chr. VII (39.1 cM) and Chr. VIII (30.8 cM) compared to *mlh3Δ* strains (32.4 cM for Chr. VII, 20.3 cM for Chr. VIII). One interpretation of these data is that *mlh3* mutants are defective in the formation of obligate crossovers due to a late defect that results in the random resolution of only a subset of crossovers. This defect can cause the loss of obligate crossovers and an increase in chromosome non-disjunction.

To further test the above model we analyzed spore viability and crossover levels in four intervals on chromosome XV in EAY1108/1112 SK1 congenic strains that contain mutations in the Mlh3 ATP binding domain (Figure 4.1). Three of the eight mutations were also analyzed by Cotton *et al*. (2010). Their work indicated that ATP binding, but not ATP hydrolysis, by the

Mlh3 subunit is important for crossover formation. Our studies using the predicted ATP binding mutation *mlh3-N35A* confirmed that ATP binding is important for Mlh3's meiotic because *mlh3-N35A* conferred a null phenotype (Cotton *et al.* 2010). However, we found that *mlh3-E31A,* an *mlh3* mutant predicted to be proficient in ATP binding but defective in ATP hydrolysis, is partially defective in crossover formation (67 cM for *mlh1-E31A* vs. 100.9 cM for wild-type and 55 cM for *mlh3Δ*) and spore viability (89% for *mlh1-E31A* vs. 97% for wild-type and 72% for *mlh3Δ*; Table 4.2) assays. Thus both ATP binding and hydrolysis by Mlh3 appear important for crossover formation. Four out of eight of the *mlh3* mutations (*mlh3-N35A, -A41F, G63R, K80E*) conferred null phenotypes, while one mutation, *mlh3-K83A*, conferred a wild-type phenotype. Finally, three mutations, *mlh3-E31A*, *mlh3-R96A,* and *mlh3-G97A,* conferred intermediate phenotypes (Table 4.2). We observed a roughly linear relationship between map distance and spore viability (Figure 4.2B), in contrast to the crossover threshold pattern observed in *msh4/5* mutants (Figure 4.2A).

To further examine the phenotype of *mlh3* hypomorph strains, we made double mutants involving two *mlh3* hypomorph alleles (*mlh3-R96A* and *mlh3-G97A*; Table 4.2; Table 4.3) and *msh5* alleles either right at the *msh4/5* threshold (*msh5-D76A*), or well above the threshold range (*msh5-T423A*). As shown below (Figure 4.2, panels C-F), *mlh3 msh5* mutants showed significant decreases in spore viability only when chromosome XV genetic map distances were below 50 cM, the threshold level seen in *msh4/5* mutants. As described below, this observation, combined with the analysis of *mlh3* null and hypomorph mutations, suggests that *mlh3* mutants are unlikely to display a threshold crossover pattern.

When *mlh3-R96A* was combined with *msh5-T423A,* very little change in spore viability or map distance was observed (Figure 4.2C). However, when the *mlh3-R96A* was combined

Table 4.2. Spore viabilities, map distances, qualitative MMR phenotypes, and known *mlh1* homolog phenotypes for the *mlh3* alleles, *msh5*Δ, and *mlh3 msh5* double mutants.

Strain	Spore Viability (%)	cM	MMR	*mlh1 allele*	MMR
mlh3 mutant analysis					
*MLH3**	97.0	100.9 (1068)	+	*MLH1*	+
*mlh3*Δ**	71.7	54.5 (582)	-	*mlh1*Δ	-
mlh3-E31A	89.2	67.0 (330)	-	*mlh1-E31A*[1,4]	+/-
mlh3-N35A	72.7	51.5 (229)	-	*mlh1-E35A*	ND
mlh3-A41F	71.6	51.2 (214)	-	*mlh1-A41F*	ND
mlh3-G63R	74.1	51.2 (216)	-	*mlh1-G64R*	ND
mlh3-K80E	71.8	49.8 (221)	-	*mlh1-K81E*[3]	-
mlh3-K83A	94.1	100.5 (289)	+	*mlh1-K84A*[4]	+/-
mlh3-R96A	82.4	76.4 (177)	-	*mlh1-R97A*[4]	-
mlh3-G97A	81.5	61.0 (210)	-	*mlh1-G98A*[1,2]	-
msh5 mutant analysis					
*msh5*Δ*	36.0	37.0 (540)			
*msh5*Δ *mlh3*Δ	31.8	38.5 (43)			
msh5-D76A[&]	87.8	53.9 (77)			
msh5-T423A[&]	95.2	78.3 (101)			
msh5-D76A mlh3 R96A	57.8	45.0 (81)			
msh5-D76A mlh3 G97A	47.1	31.7 (82)			
msh5-T423A mlh3 R96A	89.6	60.9 (160)			
msh5-T423A mlh3 G97A	78.3	54.7 (130)			

Spore viabilities (%) and cumulative genetic map distances from four spore-viable tetrads (number dissected in parentheses) on chromosome XV are shown for wild-type, *mlh3* and *msh5* strains in the SK1 congenic EAY1108/1112 background. The qualitative MMR phenotype of each allele (see Table 4.7) is shown for comparison. MMR data are also shown for the homologous *mlh1* alleles, if known. *, ** and [&] indicate data obtained from Argueso *et al*. (2004), Nishant *et al.* (2008), and Nishant *et al*. (2010), respectively. [1] Data from Tran *et al.* (2000). [2] Data from Hoffman *et al.* (2003) [3] data from Wanat *et al.* (2007). [4] Data from Argueso *et al*. (2003).

Table 4.3. Genetic map distances for chromosome XV from single spores and tetrads with distributions of parental and recombinant progeny.

	Single spores				Tetrads				
Genotype	n	Par.	Rec	cM	n	PD	TT	NPD	cM
URA3-LEU2:									
wild type*	4644	3635	1009	21.7	1068	607	456	5	21.8-23.8
*msh5*Δ*	5674	5352	322	5.7	757	643	76	1	5.0-6.4
*mlh3***	3023	2682	341	11.3	582	460	114	8	12.3-15.5
*msh5*Δ *mlh3*Δ	382	352	30	7.9	43	34	8	0	6.5-12.6
msh5-D76A[&]	351	310	41	11.7	77	57	17	0	9.0-13.9
msh5-T423A[&]	457	378	79	17.3	101	62	33	0	14.9-19.8
mlh3- R96A	840	676	164	19.5	177	105	69	0	18.0-21.7
mlh3- G97A	978	841	137	14.0	210	152	55	2	13.6-18.5
msh5-D76A mlh3 R96A	462	409	53	11.5	81	63	16	0	7.9-12.4
msh5-D76A mlh3 G97A	490	455	35	7.1	82	71	11	0	4.8-8.6
msh5-T423A mlh3 R96A	717	583	134	18.7	160	96	64	0	18.1-21.9
msh5-T423A mlh3 G97A	622	552	70	11.3	130	100	28	1	10.3-16.1
LEU2-LYS2:									
wild type*	4644	3388	1256	27.0	1068	496	569	3	26.6-28.4
*msh5*Δ*	5674	5047	627	11.1	757	562	155	3	11.0-13.0
*mlh3*Δ**	3023	2610	413	13.7	582	460	114	8	12.3-15.5
*msh5*Δ *mlh3*Δ	382	338	44	11.5	43	31	10	1	11.5-26.6
msh5-D76A[&]	351	308	43	12.3	77	58	16	0	8.4-13.2
msh5-T423A[&]	457	365	92	20.1	101	57	38	0	17.5-22.5
mlh3- R96A	840	695	145	17.3	177	112	62	0	16.0-19.6
mlh3- G97A	978	825	153	15.6	210	140	68	1	15.6-19.8
msh5-D76A mlh3 R96A	462	422	40	8.7	81	67	12	0	5.6-9.6
msh5-D76A mlh3 G97A	490	457	33	6.7	82	72	10	0	4.3-7.9
msh5-T423A mlh3 R96A	717	606	111	15.5	160	111	49	0	13.5-17.1
msh5-T423A mlh3 G97A	622	535	87	14.0	130	91	37	1	13.7-19.6
LYS2-ADE2:									
wild type*	4644	4052	592	12.7	1068	803	263	2	12.1-13.7
*msh5*Δ*	5674	5409	265	4.7	757	659	61	0	3.7-4.7
*mlh3*Δ**	3023	2822	201	6.6	582	501	81	0	6.2-7.7
*msh5*Δ *mlh3*Δ	382	363	19	5.0	43	39	3	0	1.6-5.6
msh5-D76A[&]	351	320	31	8.8	77	60	14	0	7.2-11.7
msh5-T423A[&]	457	405	52	11.4	101	75	20	0	8.4-12.6
mlh3- R96A	840	775	65	7.7	177	149	25	0	5.9-8.5
mlh3- G97A	978	898	80	8.2	210	173	35	1	7.9-11.7
msh5-D76A mlh3 R96A	462	437	25	5.4	81	68	11	0	5.0-8.9
msh5-D76A mlh3 G97A	490	464	26	5.3	82	75	7	0	2.73-5.8
msh5-T423A mlh3 R96A	717	669	48	6.7	160	141	19	0	4.7-7.2
msh5-T423A mlh3 G97A	622	591	31	5.0	130	116	13	0	3.7-6.4
ADE2-HIS3:									
wild type*	4644	3033	1611	34.7	1068	343	709	16	36.5-38.9
*msh5*Δ*	5674	4797	877	15.5	757	496	215	9	17.2-20.2
*mlh3*Δ**	3023	2485	538	17.8	582	379	201	2	17.1-19.5
*msh5*Δ *mlh3*Δ	382	328	54	14.1	43	30	12	0	10.8-17.8
msh5-D76A[&]	351	277	74	21.1	77	43	31	0	18.1-23.8

msh5-T423A[&]	457	322	135	29.5	101	44	49	2	27.4-36.9
mlh3- R96A	840	600	240	28.6	177	74	98	2	28.7-34.5
mlh3- G97A	978	801	177	18.1	210	136	73	0	15.8-19.1
msh5-D76A mlh3 R96A	462	395	67	14.5	81	57	20	2	14.6-25.9
msh5-D76A mlh3 G97A	490	422	68	13.9	82	58	24	0	12.1-17.1
msh5-T423A mlh3 R96A	717	575	142	19.8	160	97	63	0	17.8-21.6
msh5-T423A mlh3 G97A	622	507	115	18.5	130	83	45	1	16.8-22.8

Strains used are isogenic derivatives of the congenic SK1 EAY1108/1112 background. Single spore data is shown with n, total number of spores, and parental and recombinant data. Map distances (cM) were calculated by recombination frequency (recombinant spores/total spores) x 100. Tetrad data is shown with n, number of complete tetrads. Map distances (cM) were calculated using the Perkins formula (Perkins, 1949). 95% confidence intervals were calculated using the Stahl Laboratory Online Tools website (http://www.molbio.uoregon.edu/~fstahl/). * Data from Argueso *et al.* (2004). ** Data from Nishant *et al.* (2008). [&]Data from Nishant *et al.* (2010).

with *msh5-D76A*, a strong synthetic defect was observed for spore viability with only a slight decrease in crossing over (Figure 4.2E). Similar results were obtained when each of these *msh5* alleles was combined with *mlh3-G97A*, except the results were even more extreme (*mlh3-G97A msh5D76A* vs. *mlh3-R96A msh5D76A* $P < 0.02$; *mlh3-G97A msh5T423A* vs. *mlh3-R96A msh5T423A* $P < 0.01$; Figure 4.2D and F). This analysis confirms that *mlh3-G97A* confers a more severe defect compared to *mlh3-R96A*, as expected if a threshold did not exist for *mlh3* alleles. The *mlh3-G97A msh5-D76A* double mutant was especially interesting because spore viability and genetic map distances approached the level seen in *mlh3*Δ *msh5*Δ strains (Table 4.2). Consistent with these observations, *mlh3-G97A* conferred a mild non-disjunction phenotype, as measured by an excess of 4, 2, 0 viable spore tetrads compared to 3 and 1 viable tetrads (Ross-McDonald and Roeder 1994), but *mlh3-G97A msh5-D76A* conferred a more extreme non-disjunction pattern (Figure 4.3). Together, these studies indicate that *mlh3* alleles do not appear to confer their own threshold crossover pattern (see below and Discussion)

*mlh3*Δ *mms4*Δ show dramatically decreased crossing over across four different chromosomes

Previous studies showed that there are at least two types of crossover pathways in budding yeast: an Msh4-Msh5-Mlh1-Mlh3 pathway, and an interference-independent pathway involving Mus81-Mms4 (see Introduction). In addition, three meiotic joint molecule resolvase complexes have been identified based on structures and *in vitro* studies: Mus81-Mms4, Yen1, and Slx1-Slx4 (Schwartz and Heyer 2011; Boddy *et al.* 2001; Cromie *et al.* 2006; Jessop and Lichten 2008; Oh *et al.* 2008; Fricke and Brill 2003; Muñoz *et al.* 2009; Svendsen *et al.* 2009; Furukawa *et al.* 2003; Ip *et al.* 2008; Ishikawa *et al.* 2004). These resolvases appear to play

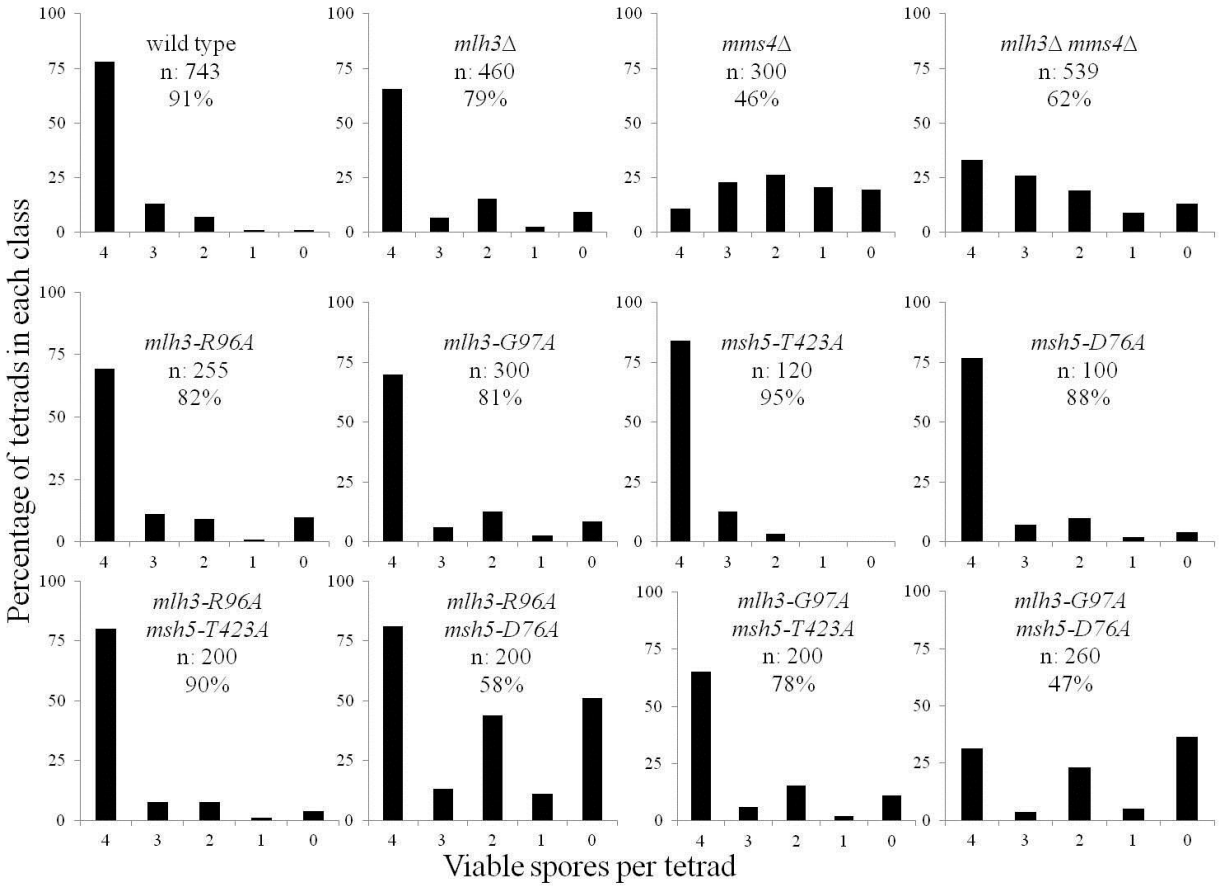

Figure 4.3. Spore viability profile of wild type and select mutants. The horizontal axis shows the number of viable spores per tetrad, and the vertical axis shows the percentage of tetrads in each class. n, the total number of tetrads dissected, and percent spore viability are shown. Data for wild type are from Zanders and Alani (2009).

different roles in different organisms. For example, Mus81-Mms4 plays a major role in fission yeast (Smith *et al.* 2003), but only a minor role in budding yeast, *Arabidopsis*, mouse, and *Drosophila* (Argueso *et al.* 2004; Berchowitz *et al.* 2007; de los Santos *et al.* 2003; Higgins *et al.* 2008; Holloway *et al.* 2008; Jessop and Lichten 2008; Oh *et al.* 2008; Trowbridge *et al.* 2007).

The data presented in the previous section are consistent with Mlh1-Mlh3 acting late in meiosis at crossover resolution (Nishant *et al.* 2010; Argueso *et al.* 2004; Zakharyevich *et al.* 2010; Zakharyevich *et al.* 2012; De Muyt *et al.* 2012). Such models, in conjunction with the identification of two major crossover pathways in budding yeast, predict that a genome wide decrease in crossing over would be observed in *mlh3Δ mms4Δ* mutants. Our lab showed previously that on a large chromosome, *mlh1*Δ *mms4*Δ double mutants have a significant (~13 to 15-fold) decrease in crossing over compared with wild type (Argueso *et al.* 2004). Based on these and other data we suggested that Mus81-Mms4 and Mlh1-Mlh3 were in competing crossover pathways (Arguesto *et al.* 2004), with Mus81-Mms4 dependent crossovers promoting proper chromosome disjunction in the absence of Mlh1-Mlh3. Consistent with this, the Hunter lab and Lichten groups recently provided evidence for Msh4-Msh5-Mlh1-Mlh3-Exo1 and Mus81-Mms4 acting in independent crossover pathways (Zakharyevich *et al.* 2012; De Muyt *et al.* 2012). The Hunter lab previously showed that *mlh3Δ* decreases crossover levels without changing joint molecule levels, also suggesting a late role for Mlh3 (Zakharyevich *et al.* 2010). Using Southern blot analysis at the well-studied *HIS4LEU2* hotspot, they showed that *exo1* alone reduced crossing over 49%, *mms4 yen1* by 39%, and *exo1 mms4 yen1* by 86%. This further suggests that Mus81-Mms4 and Exo1-Mlh1-Mlh3 contribute independently to the formation of crossovers. Furthermore, crossover levels decreased roughly 20-fold in *mlh3 mms4 slx4 yen1 sgs1* cells. The Lichten group (De Muyt *et al*. 2012) showed that in *msh4Δ mms4 yen1Δ* triple

mutants, nuclear divisions do not take place. Furthermore, they found that unresolved joint molecules accumulated to similar levels to *msh4*Δ *ndt80*Δ, where joint molecule resolution cannot take place, suggesting that the Mus81-Mms4 and Yen1 pathways are responsible for resolving crossover intermediates that are not resolved by the Msh4-Msh5-Mlh1-Mlh3 pathway. Because they found that most joint molecules were resolved in *mms4 yen1*Δ *slx1*Δ mutants, their data suggests that Msh4-Msh5-Mlh1-Mlh3 acts in this resolution step. Together these studies provide strong evidence that Exo1-Mlh1-Mlh3 and Mus81-Mms4 are responsible for the majority of crossovers in budding yeast.

While each of the above studies presented convincing data for the presence of two independent crossover pathways in yeast, almost all of the physical data were obtained at a single locus, the *HIS4LEU2* hotspot, and genetic data were obtained in only one chromosome arm (Argueso *et al*. 2004; Nishant *et al.* 2008). To further understand the role of Mlh3 and Mms4 in the crossover pathways on a genome-wide level, we analyzed spore viability and crossovers across four chromosomes in *mlh3*Δ *mms4*Δ double mutants. A total of 250 centimorgans (cM) of map distance were measured, representing ~6.2% of the yeast genome. These double mutants were likely to be the most informative for this purpose because they formed viable spores at a reasonable frequency. As shown in Tables 4.4 and 4.5 and Figure 4.4, we found that for all loci examined crossing over was drastically reduced (6 to 17-fold) in *mlh3*Δ *mms4*Δ strains compared to wild-type. Interestingly, crossing over was decreased by the smallest amount on chromosome III, which was observed previously in other meiotic mutants (Zanders and Alani 2009; see Discussion). While *mlh3*Δ mutants show a characteristic 4:2:0 pattern of viable spores per tetrad indicative of nondisjunction (Ross-Macdonald and Roeder 1994; Hollingsworth *et al.* 1995; Hunter and Borts 1997; Argueso *et al.* 2003; Nishant *et al.* 2008; this study), neither *mms4*Δ nor

Table 4.4. Spore viabilities and genetic map distances for wild type, *mlh3*Δ, *mms4*Δ, and *mlh3*Δ *mms4*Δ for chromosomes III, VII, VIII, and XV.

Genotype	**Spore Viability (%)**	**n**	**Map Distance (cM)**			
Chromosome			III (333kb)	VII (1040kb)	VIII (582kb)	XV (1095kb)
Wild Type*	91.0	572	34.9	68.7	46.2	96.1**
*mlh3*Δ	79.0	306	29.3	32.4	20.3	54.5[&]
*mms4*Δ	46.3	32	32.7	50.0	31.8	83.4**
mms4Δ^	45.4	272	25.2	62.1	35.3	
*mlh3*Δ *mms4*Δ	61.9	170	5.7	9.6	2.8	8.4[&]
Fold decrease in *mlh3*Δ *mms4*Δ vs. wild type:			6.1	7.2	16.5	11.4

Spore viabilities (%), number of tetrads dissected (n), and genetic map distances in cM (number of complete tetrads) on chromosomes III, VII, VIII, and XV are shown for *mlh3*Δ*, msh5*Δ*, mlh3* alleles, *msh5* alleles, and the double mutants. Sizes of each chromosome are shown below each chromosome number, and the fold decrease in crossing over in *mlh3*Δ *mms4*Δ compared with wild type is shown below. Chromosome III, VII, and VIII data are from derivatives of the isogenic SK1 NHY942/943 background. Data for chromosome XV are from derivatives of the congenic SK1 EAY1108/1112 background. *Data from Zanders and Alani (2009). **Data from Argueso *et al.* (2004). [&] Data from Nishant *et al.* (2008). ^ Data from de los Santos *et al.* (2003).

Table 4.5. Genetic map distances for chromosomes III, VII, and VIII from single spores and tetrads with distributions of recombinant and parental progeny.

	Single spores				Tetrads				
Genotype	n	Par.	Rec.	cM	n	PD	TT	NPD	cM
Chromosome III									
HIS4-LEU2:									
Wild Type*	2711	2360	351	12.9	572	413	141	2	12.6-15.0
*mlh3*Δ	1453	1333	120	8.3	306	252	47	1	7.4-10.3
*mms4*Δ**	555	508	47	8.5	32	21	5	0	5.8-13.5
*mlh3*Δ *mms4*Δ	1336	1304	32	2.4	170	158	2	0	0.2-1.1
LEU2-CEN3:									
Wild Type*	2711	2527	184	6.8	572	488	68	0	5.4-6.8
*mlh3*Δ	1453	1314	139	9.6	306	261	39	1	6.1-8.9
*mms4*Δ**	555	482	73	13.2	32	22	3	1	5.8-28.8
*mlh3*Δ *mms4*Δ	1336	1302	34	2.5	170	156	4	0	0.6-1.9
CEN3-MAT:									
Wild Type*	2711	2309	402	14.8	572	395	160	1	13.9-15.9
*mlh3*Δ	1453	1246	207	14.2	306	223	78	0	11.7-14.2
*mms4*Δ**	555	464	91	16.4	32	23	3	0	2.6-8.9
*mlh3*Δ *mms4*Δ	1336	1288	48	8.5	170	153	6	1	1.8-5.8
Chromosome VII									
TRP5-CYH2:									
Wild Type*	2711	1803	908	33.5	572	197	337	9	34.2-37.8
*mlh3*Δ	1453	1215	238	16.4	306	198	100	0	15.4-18.2
*mms4*Δ**	555	391	164	29.5	32	11	11	0	19.7-30.3
*mlh3*Δ *mms4*Δ	1336	1289	47	3.5	170	151	11	0	2.4-4.4
CYH2-MET13:									
Wild Type*	2711	2451	260	9.6	572	442	101	0	8.5-10.1
*mlh3*Δ	1453	1350	103	7.1	306	266	32	0	4.5-6.3
*mms4*Δ**	555	500	55	9.9	32	18	4	0	5.0-13.2
*mlh3*Δ *mms4*Δ	1336	1302	34	2.5	170	156	6	0	1.1-3.0
MET13-LYS5:									
Wild Type*	2711	2152	559	20.6	572	334	205	4	19.6-22.6
*mlh3*Δ	1453	1307	146	10.0	306	242	55	1	8.7-11.7
*mms4*Δ**	555	461	94	16.9	32	15	7	0	10.9-20.9
*mlh3*Δ *mms4*Δ	1336	1271	65	4.9	170	148	14	0	3.2-5.4
Chromosome VIII									
CEN8-THR1:									
Wild Type*	2711	2105	606	22.4	572	317	219	2	20.2-22.8
*mlh3*Δ	1453	1305	148	10.2	306	251	45	0	6.6-8.6
*mms4*Δ**	555	463	92	16.6	32	16	6	0	8.9-18.4
*mlh3*Δ *mms4*Δ	1336	1288	48	3.6	170	157	3	0	0.4-1.5
THR1-CUP1:									
Wild Type*	2711	2043	668	24.6	572	277	260	1	23.5-25.9
*mlh3*Δ	1453	1258	195	13.4	306	226	69	1	11.1-14.2
*mms4*Δ**	555	427	128	23.1	32	14	8	0	13.1-23.3
*mlh3*Δ *mms4*Δ	1336	1292	44	3.3	170	154	6	0	1.1-2.6

Strains analyzed are isogenic derivatives of the SK1 NHY942/943 background. Single spore data are shown with n, total number of spores, and parental and recombinant data. Map

distances (cM) were calculated by recombination frequency (recombinant spores/total spores) x 100. Tetrad data are shown with n, number of complete tetrads. Map distances (cM) were calculated using the Perkins formula (Perkins, 1949). 95% confidence intervals were calculated using the Stahl Laboratory Online Tools website (http://www.molbio.uoregon.edu/~fstahl/).
*Data from Zanders and Alani (2009).

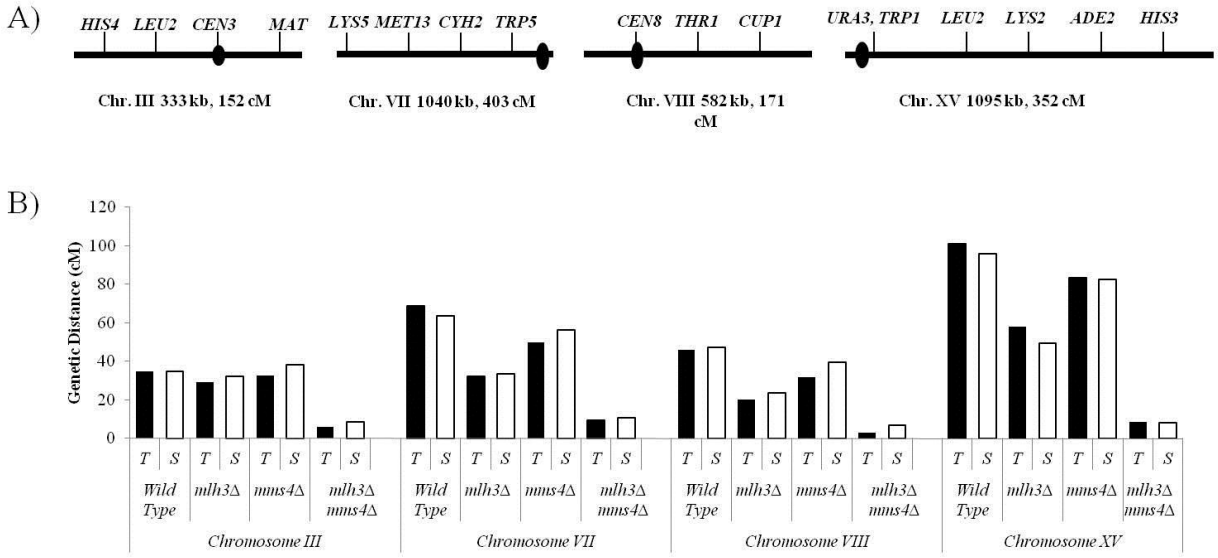

Figure 4.4. Cumulative Genetic Distances for wild type, *mlh3*Δ, *mms4*Δ, and *mlh3*Δ *mms4*Δ on four chromosomes. A) Location of genetic markers used to determine map distances in the NHY942/NHY943 background for chromosomes III, VII, VIII, and the EAY1108/EAY1112 background for chromosome XV. B) The cumulative genetic distance for each chromosome is shown for both complete tetrad data (black) and single spore data (white). Raw data are shown in Table 4.5. Data for wild type for chromosomes III, VII, and VIII are from Zanders and Alani (2009). Data for wild type and *mms4*Δ for chromosome XV are from Argueso *et al. (*2004). Data for *mlh3*Δ and *mlh3*Δ *mms4*Δ on chromosome XV are from Nishant *et al.* (2008).

*mlh3*Δ *mms4*Δ showed this pattern (Figure 4.3). Thus our analysis provides further support to the hypothesis that Mlh1-Mlh3 and Mus81-Mms4 independently contribute late roles for meiotic crossover formation.

mlh3Δ partially suppresses *mms4Δ* spore formation and viability defects

Previous work showed that *mms4Δ* strains display both low spore efficiency (~10%) and viability (~40%), as well as high levels of aberrant recombination events (de los Santos *et al.* 2001; 2003). We found that the *mlh3Δ* mutation can partially suppress the spore viability, sporulation defects, and high frequency of aberrant events observed in *mms4Δ* strains. In the SKI isogenic background NHY942/943, *mms4Δ* strains displayed low sporulation efficiency (16%) and viability (54%) whereas *mlh3Δ* displayed higher levels (73% spore formation vs. 88% for wild-type, 79% spore viability). *mlh3Δ mms4Δ* displayed significantly higher sporulation (43%, $P < 0.001$) and viability (62%, $P < 0.001$) compared to *mms4Δ.* Additionally, *mlh3Δ mms4Δ* mutants showed gene conversion levels that were similar to wild-type, but lower than *mms4Δ* alone (Table 4.6, aberrant levels for our small *mms4Δ* data set are similar to those seen in de los Santos *et al.* (2003), who analyzed 272 tetrads). As described in the Discussion our data are consistent with a dissolution pathway for joint molecules that cannot be resolved as crossovers (Jessop *et al.* 2006; Oh *et al.* 2007; De Muyt *et al.* 2012). Such a role would alleviate aberrant recombination events proposed to exist in *mms4Δ* (Roeder and Bailis 2000), thus allowing for increased chromosome segregation and spore viability (see Discussion).

The ATPase domain of *MLH3* has distinct roles in MMR and meiotic crossing over

Table 4.6. Aberrant marker segregation in wild type, *mlh3*Δ, *mms4*Δ, and *mlh3*Δ *mms4*Δ on chromosomes III, VII, and VIII.

Chromosome III	**Four-spore viable tetrads**	***HIS4***	***LEU2***	***ADE2***	***MATa***	**Total**
Wild type	572	2.1	0.3	0.2	0.2	2.8
*mlh3*Δ	306	0.7	0.7	0.3	0.0	1.7
*mms4*Δ	32	9.4	6.3	3.1	3.1	21.9
*mlh3*Δ *mms4*Δ	170	4.1	0.6	0	1.2	5.9
Chromosome VII		***LYS5***	***MET13***	***CYH2***	***TRP5***	
Wild type	572	1.6	2.4	0.3	0.7	5.0
*mlh3*Δ	306	0.7	2.0	0.0	0.0	2.7
*mms4*Δ	32	9.4	0.0	6.3	0.0	15.7
*mlh3*Δ *mms4*Δ	170	1.2	2.4	0.0	1.2	4.8
Chromosome VIII		***URA3***	***THR1***	***CUP1***		
Wild type	572	0.2	5.1	0.7		6.0
*mlh3*Δ	306	0.0	3.3	0.0		3.3
*mms4*Δ	32	0.0	6.3	9.4		15.7
*mlh3*Δ *mms4*Δ	170	0.6	4.7	0.6		5.9

Aberrant segregation (1:3 or 3:1) of markers due to gene conversion is shown. Data are from four-spore viable tetrads and analyzed by RANA software (Argueso *et al.* 2004).

As described in the Introduction, Mlh3 is important in MMR and meiotic crossover formation. Previous structure-function studies have shown that the two subunits in yeast Mlh1-Pms1 are functionally asymmetric. For example, mutations in *MLH1* have a greater impact on frameshift mutation rates than equivalent mutations in *PMS1* (Tran *et al.* 2000; Hall *et al.* 2002). The ATP binding domains located near the N-termini of MLH proteins are thought to regulate asymmetric conformational changes in MLH dimers through cycles of ATP binding and hydrolysis (Tran, 2000; Ban 1998; Ban, 1999; Sacho *et al.* 2008). In addition, in baker's yeast the Mlh1 subunit has been shown to interact with the downstream MMR factor Exo1 in an ATP-dependent manner. Thus ATP-dependent conformational changes in MLH proteins are likely to be important to modulate interactions with downstream MMR effector molecules (Tran *et al.* 2001; Pedrazzi *et al.* 2001).

We analyzed our *mlh3* ATP binding mutations in MMR assays, using the *lys2::InsE-A*$_{14}$ frameshift reporter to measure the frameshift mutation rate (Tran *et al.* 1997). In this assay *mlh3*Δ strains display a roughly six-fold increase in frameshift mutation rate compared to wild-type (Harfe *et al.* 2000; Nishant *et al.* 2008; this study). We observed that all but one of the eight *mlh3* alleles showed MMR defects similar to the null, ranging from 3.2 to 6.7-fold higher than wild-type levels. *mlh3-K83A* strains showed a wild-type phenotype (Table 4.7). Comparing our data to Cotton *et al. (2010*) we found similar results for *mlh3-N35A* and *mlh3-G97A.* However, we observed a much higher mutation rate for *mlh3-E31A*, again suggesting that both ATP binding and hydrolysis are important for Mlh1-Mlh3-mediated MMR.

As mentioned above, mismatch repair rates have been examined in strains bearing *mlh1* mutations in equivalent positions to those made in *MLH3*. *mlh1-K81E, mlh1-R97A,* and *mlh1-G98A* were all shown to confer a null phenotype for MMR, similar to the equivalent mutations in

Table 4.7. *lys2:InsE-A$_{14}$* frameshift mutation rates for *mlh3* alleles

Genotype	n	Mutation Rate(x 10^{-7})	Relative to WT	Phenotype
MLH3	110	4.71 (3.87 – 5.11)	1.0	+
mlh3Δ	110	26.5 (23.5 – 30.4)	5.7	-
mlh3-E31A	15	30.5 (16.7 – 51.6)	6.5	-
mlh3-N35A	15	31.2 (25.6 – 44.4)	6.7	-
mlh3-A41F	15	27.9 (17.1 – 34.3)	6.0	-
mlh3-G63R	15	23.8 (18.2 – 37.1)	5.1	-
mlh3-K80E	15	16.0 (15.1 – 27.7)	3.4	-
mlh3-K83A	15	5.24 (3.49 – 6.34)	1.1	+
mlh3-R96A	15	14.8 (6.42 – 40.6)	3.2	-
mlh3-G97A	15	16.6 (11.8-26.0)	3.6	-
MLH3 + empty vector	11	4.42 (1.02-6.05)	1	+
MLH3 + *pGAL10-MLH3*	11	39,100 (15,700-79,900)	8,850	-
MLH3 + *pGAL10-mlh3E31A*	11	47,800 (28,700-85,900)	10,800	-
MLH3 + *pGAL10-mlh3R96A*	11	23,500 (5,910-38,400)	5,320	-
MLH3 + *pGAL10-mlh3G97A*	11	96,000 (45,800-156,000)	21,700	-
*mlh1*Δ + empty vector	11	218,000 (121,000-283,000)	49,300	-

Top: a *lys2:InsE-A$_{14}$* SK1 strain (EAY1062 and *mlh3* derivatives, Table 4.1) was used to test the frameshift mutation rate as measured by reversion to Lys^+. Bottom: EAY1269 (*lys2:InsE-A$_{14}$*, S288c strain) derivatives with the indicated genotypes (Table 4.1) were tested for reversion to Lys^+. n, the number of independent cultures tested from at least two independent strains. Median mutation rates are presented with 95% confidence intervals, and relative mutation rates compared to the wild type strain are shown.

MLH3. *mlh1-E31A* and *mlh1-K84A*, however, confer different phenotypes compared to the equivalent *mlh3* mutations, with *mlh1-E31A* strains being more proficient in MMR and *mlh1-K84A* strains being less proficient (Table 4.2; Tran *et al.* 2000; Hoffman *et al.* 2003; Wanat *et al.* 2007; Argueso *et al.* 2003). Thus our data, combined with work from Cotton *et al*. (2010), reinforces the hypothesis that the different subunits of Mlh1-Mlh3 provide differential contributions to MMR.

It is important to note that five *mlh3* alleles displayed consistent phenotypes for MMR and meiotic functions (either wild-type or null in both). However, three *mlh3* hypomorph alleles, *mlh3-E31A, -R96A, -G97A,* displayed null phenotypes in MMR, but intermediate meiotic phenotypes as measured in meiotic spore viability and crossover assays (Table 4.2). This observation suggests that, like Mlh1 (Argueso *et al.* 2003), Mlh3 functions are more easily disrupted for MMR.

A simple explanation for many of the *mlh3* phenotypes is that the mutant proteins are unstable. Because single copy levels of Mlh3 could not be detected in vegetative cells (M. Rogacheva and E. Alani, unpublished observations), we tested Mlh3 protein stability using a dominant negative assay. We showed previously that overexpressing Mlh3 using the *GAL10* promoter confers a high mutator phenotype in the *lys2::InsE-A*$_{14}$, reversion assay with rates over 1000-times the wild-type levels. This phenotype was similar to that seen in wild-type strains overexpressing Mlh1 (Shcherbakova and Kunkel 1999; Nishant *et al.* 2008). Overexpressing *mlh3-E529K,* which does not interact with Mlh1, did not confer a dominant negative phenotype (Nishant *et al.* 2008). Based on these observations we hypothesized that increased levels of Mlh3 interfered with mismatch repair by out-competing Pms1 for Mlh1complex, because Mlh1

interacts with both Mlh3 and Pms1 and Mlh1-Pms1 plays the major MLH role in MMR (Wang *et al.* 1999; Kondo *et al.* 2001).

We overexpressed mlh3-E31A, mlh3-R96A, and mlh3-G97A in wild-type cells and assessed mutagenesis using the *lys2::InsE-A14* frameshift reporter. Each allele conferred a strong dominant negative phenotype similar to Mlh3 overexpression, with mutation rates 5,000-20,000-fold higher than wild-type (Table 4.7). This suggests that an intact and stable Mlh1-*mlh3* complex is formed in each of these mutants.

DISCUSSION

Meiotic crossover decisions are made prior to the action of Mlh3

Several groups have suggested a temporal model for crossover distribution in baker's yeast meiosis. In such models obligate crossovers are initially placed on every homolog pair, followed by excess crossovers distributed in an interference-dependent manner (Nishant *et al.* 2010, Kaback *et al.* 1992; 1999; Kleckner *et al.* 2004, Bishop and Zickler 2004). These models are consistent with our analysis of *msh4/5* mutants, where we found that crossover levels could be decreased by almost two-fold before decreases in spore viabilities were observed. When crossing over decreased below the two-fold threshold level, spore viability and crossing over decreased proportionately (Figure 4.2A; Nishant *et al.* 2010).

*mlh3*Δ strains showed a cumulative map distance on chromosome XV of 54.5 cM, which is higher than the threshold limit of crossovers seen in *msh4/5-t* mutants, yet displayed reduced spore viability (~70-80%) and lower crossing over for other chromosomes compared to *msh4/5-t* mutants. We also showed that a set of *mlh3* hypomorphs conferred roughly proportional decreases in spore viability and crossing over (Figure 4.2B). Together, these phenotypes are

consistent with a terminal crossover resolution role for Mlh1-Mlh3 in the interference-dependent crossover pathway. In this model, a decrease in Mlh3 function results in the random resolution of only a subset of crossovers. The result of such a defect is the loss of obligate crossovers and an increase in chromosome non-disjunction.

Chromosome disjunction is mostly functional in *mlh3Δ mms4Δ* despite dramatic genome-wide decreases in crossing over.

Spore viability in *mlh3*Δ *mms4*Δ is high (62%), despite dramatic reductions (6-17 fold) in crossing over. The reduced levels should yield crossover levels below the obligate number (16) required to segregate all yeast homologs. Interestingly, the *mlh3Δ mms4Δ* spore viability is considerably higher than in *msh4/5* null mutants (36%), which show significantly higher crossing over (two to three-fold reduced compared to wild-type; e.g. Argueso *et al*. 2004). One explanation for the high levels of spore viability is that the residual crossovers in *mlh3*Δ *mms4*Δ are exclusively obligate. However, an argument against this idea is that in *mlh3Δ mms4Δ* strains crossing over was reduced the least on the smallest chromosome studied, chromosome III, which due to its size should be one of the first to lose an obligate crossover without interference. Previous studies showed that crossover interference is weaker on smaller chromosomes (Kaback *et al.* 1992; 1999). This and other work (Nishant *et al*. 2010) suggests that the crossovers occurring in *mlh3*Δ *mms4*Δ cells are not regulated by an interference-dependent mechanism. This information, coupled with the fact that a crossover threshold is not seen in *mlh3* mutants, makes an obligate crossover maintenance model unlikely. However, it is possible that an independent obligate crossover mechanism is activated in the absence of both Mlh3 and Mms4.

A second explanation is that additional mechanisms ensure proper disjunction of chromosomes in the absence of the obligate crossover. If we assume that crossover levels decrease to similar extents across the entire length of the chromosomes analyzed, only chromosome VII appears to have crossover rates that could allow at least one crossover in *mlh3Δ mms4Δ*; expected crossovers based on map distances and high resolution genotyping of meiotic spore progeny in wild type are three, eight, four, and seven for chromosomes III, VII, VIII, and XV, respectively (Mancera *et al.* 2008). Thus, due to the six to 17-fold decrease in crossing over observed in *mlh3Δ mms4Δ*, certain chromosomes are not likely to receive a crossover during meiosis but will properly disjoin. Distributive disjunction is a mechanism used to accurately segregate chromosomes in male *Drosophila* meiosis and the fourth chromosome in female *Drosophila* meiosis (Grell 1962; 1976). It also plays a role in budding yeast (Guacci and Kaback 1991; Loidl *et al.* 1994). In this system, achiasmate chromosomes are still thought to physically interact, either through microtubule bridges or protein complexes (Carpenter 1991; Rieder and Salmon 1994). These connections could play analogous roles to chiasmata, ensuring proper tension on the spindles, thought to be necessary to promote proper chromosome disjunction (Nicklas, 1967; 1974).

An alternative mechanism to pair achiasmate chromosomes is achieved through centromere pairing. During early meiosis, centromeres pair in a homology-independent manner that is dependent on the synaptonemal complex protein Zip1 (Tsubouchi and Roeder 2005). Zip1-dependent centromere pairing is important for bipolar spindle attachments and proper chromosome disjunction (Gladstone *et al.* 2009; Newnham *et al.* 2010). This mechanism, in conjunction with distributive disjunction, could ensure that chromosomes are properly disjoined in the absence of chiasmata. Finally, another possibility is that early Msh4-Msh5 dependent

homolog pairing functions, recently described in *Sordaria* (Storlazzi *et al*. 2010), facilitates crossover-independent disjunction mechanisms by establishing stable connections between homologs. Such a scenario could thus explain why *mms4Δ mlh3Δ* mutants display higher spore viability compared to *msh4/5* null mutants, despite having significantly decreased crossover levels.

Based on gene conversion and physical assays performed in various crossover resolution mutants (Zakharyevich *et al*. 2012; Argueso *et al*. 2004; Nishant *et al*. 2010; Table 4.6), meiotically induced DSBs are likely to form at wild-type levels in *mlh3*Δ *mms4*Δ cells. Thus we are left with the question of how the DSBs that are not resolved into crossovers in *mlh3Δ mms4Δ* are ultimately repaired. Based on our observations and extensive genetic studies performed by Zakharyevich *et al.* (2012) and De Muyt *et al*. (2012), we hypothesize that Sgs1 plays a critical role in unwinding joint molecule intermediates in *mlh3Δ mms4Δ* to form non-crossovers (Figure 4.5). Sgs1 is a member of the RecQ family of helicases, and is known to have roles in regulating recombination outcomes during meiosis. First, Sgs1 can dissolve D loop structures and dHJs *in vitro* to create non-crossovers at the expense of crossovers (Adams *et al.* 2003; Bachrati *et al.* 2006; McVey *et al.* 2004; van Brabant *et al.* 2000; Cejka *et al.* 2010; Wu and Hickson 2003). Second, *sgs1* mutants show increased levels of joint molecules, in particular aberrant joint molecules involving sister chromatids and/or containing three or more chromosomes (Jessop *et al.* 2006; Oh *et al.* 2007). Third, *sgs1* mutants are able to suppress meiotic recombination defects in a variety of meiotic mutants, probably due to its ability to resolve aberrant joint molecule structures (Jessop *et al.* 2006; Oh *et al.* 2007; Rockmill *et al.* 2003).

Finally, Sgs1 is known to interact with factors in both the Mus81-Mms4 and the Mlh1-Mlh3 crossover pathways. In the absence of Sgs1, the Mus81-Mms4 pathway is essential to

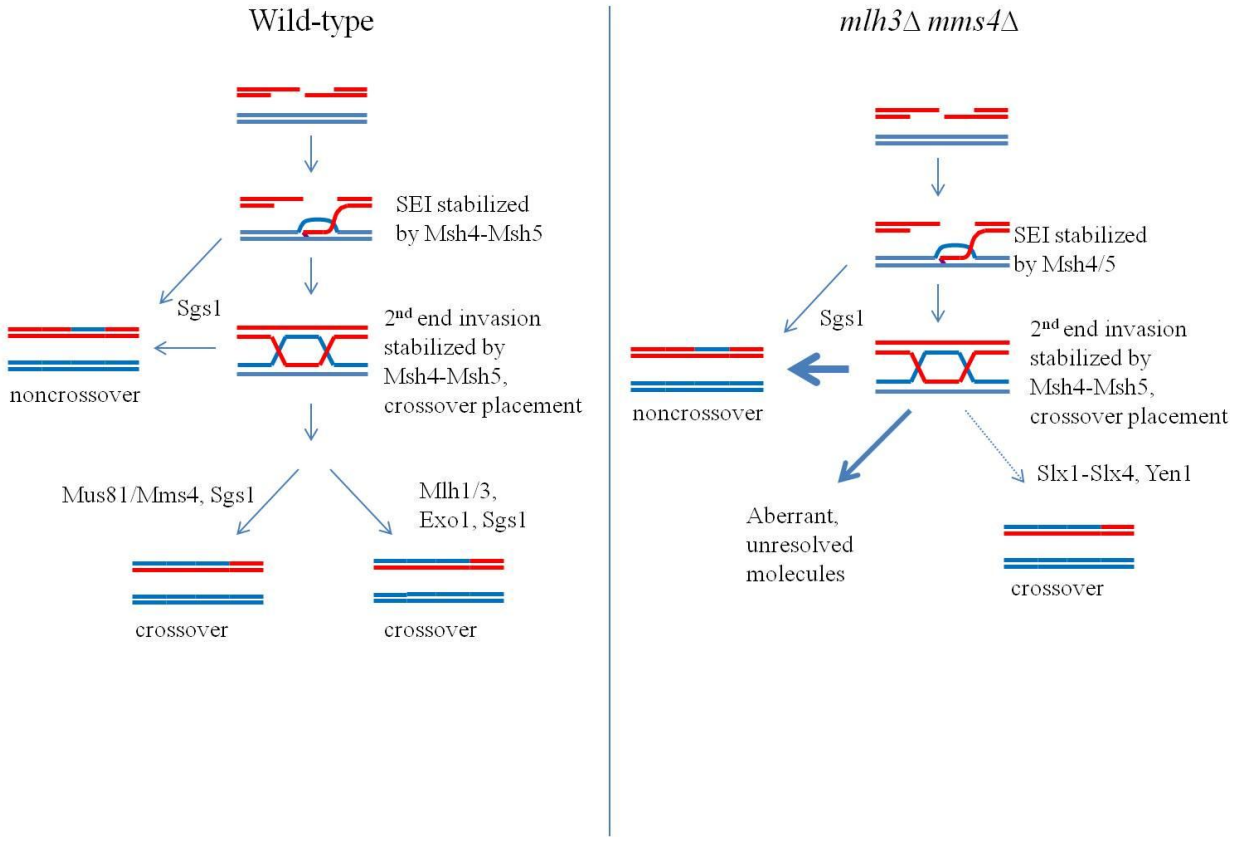

Figure 4.5. Model of crossover pathways during meiosis. A summary of the crossover pathways are shown. In wild type cells (left), DSBs are made and resected, and initial single-end invasion intermediates can be dissolved by Sgs1-dependent mechanisms, leading to noncrossovers. Single-end invasion intermediates that are not resolved as noncrossovers can proceed through the Mus81-Mms4 interference-independent pathway, leading to crossovers, or Msh4-Msh5 can stabilize the SEI in an interference-dependent mechanism. These stabilized joint molecules undergo crossover placement decisions, and are subsequently resolved in an Mlh1-Mlh3-dependent manner. In the absence of Mlh3 and Mms4 (right), initial recombination events occur as in wild type. However, due to the lack of the major Mlh1-Mlh3 and Mus81-Mms4 resolvase functions, other pathways are activated, including Sgs1-dependent resolution to form non-crossovers and other resolution activities (e.g. Slx-Slx4, Yen1), resulting in a larger number of events being resolved into noncrossovers.

resolve accumulated joint molecule structures (Jessop and Lichten 2008; Oh *et al.* 2008). While Sgs1 is traditionally thought to act as an anti-crossover factor, recent evidence has suggested a pro-crossover role for Sgs1 in the Mlh1-Mlh3 pathway. The Hunter and Lichten labs have shown that Sgs1 is important for crossover formation in the Exo1-Mlh1-Mlh3 pathway. They saw reduced levels of crossing over in *mms4 slx4 yen1 sgs1* cells compared to *mms4 slx4 yen1* cells, where Exo1-Mlh1-Mlh3 is hypothesized to be the only acting resolvase. Thus, without Sgs1, Mlh1-Mlh3 is compromised in its ability to form crossovers (Zakharyevich *et al.* 2012; De Muyt *et al.* 2012).

Due to the intricate role of Sgs1 in the Mus81-Mms4 and Mlh1-Mlh3 pathways and its ability to resolve aberrant joint molecule structures, it is a prime candidate for playing a major role in resolving joint molecules into noncrossovers in *mlh3*Δ *mms4*Δ cells (Figure 4.5). We propose that in the absence of these two factors, Sgs1 plays a dominant role in resolving joint molecules. This would explain the rescue in sporulation observed in *mlh3Δ mms4Δ* cells. When Mlh3 is present, normal joint molecules can be cleaved, leading to crossovers. However, any aberrant joint molecules that occur cannot be resolved, resulting in unsegregated DNA and low sporulation (Oh *et al.* 2008). In *mlh3*Δ *mms4*Δ cells, Sgs1 activity plays a larger role in resolution of aberrant joint molecules, so that increased joint molecule resolution occurs, resulting in higher sporulation and spore viability.

Residual crossover levels are still detected in *mlh3*Δ *mms4*Δ mutants. These crossovers are most likely resolved by either Slx1-Slx4, or Yen1. Slx1 has been shown to resolve HJs in vitro (Fricke and Brill 2003; Munoz *et al.* 2009; Svendsen *et al.* 2009), and Yen1 is a member of the Rad2/XPG family of endonucleases that has also been shown to resolve HJs (Furukawa *et al.* 2003; Ip *et al.* 2003; Ishikawa *et al.* 2004; Zakharyevich *et al.* 2012). Analogous to our proposal

for the increased role of Sgs1 in the absence of Mlh3, the Hunter lab proposed that in the absence of Mlh1-Mlh3, other endonucleases such as Yen1 and Slx1-Slx4 could exhibit efficient joint molecule resolution (Zakharyevich *et al.* 2012). They found that joint molecule levels are lower in *sgs1 mms4 mlh3* cells, suggesting that another endonuclease is resolving these intermediates. Specifically, they found that Yen1 does not play a major role in JM resolution in wild type cells, but it plays a major role in *sgs1 mms4* cells (Zakharyevich *et al.* 2012). Thus this information supports the hypothesis that minor recombination resolution factors can substitute to different degrees for the functions of major ones.

Mlh3 has a differential role in meiosis and mismatch repair

A second goal of this study was to analyze the role of the Mlh3 ATP binding domain in meiosis and mismatch repair. To do this, we created a set of eight ATPase domain mutants of *mlh3* and looked at their phenotypes in both mismatch repair and meiotic crossing over. While most of the eight ATP binding domain mutations conferred complete defects in both functions, several mutations conferred more severe defects in MMR. These observations suggest that like Mlh1, Mlh3 structural features are likely to play a more important role in crossover resolution (Argueso *et al*. 2004; Hoffman *et al.* 2003; Cotton *et al*. 2010).

Consistent with its lesser role in MMR, *mlh3* alleles show a lower mutation rate as measured in the *lys::InsE-A*$_{14}$ reversion assay compared to equivalent *mlh1* alleles; however, they appear to be just as sensitive to mutagenesis. Of the five mutations that have been analyzed in both *MLH1* and *MLH3*, three conferred null phenotypes for MMR, one conferred a slightly better MMR phenotype when present in Mlh1 (E31A), and one conferred a slightly better MMR phenotype when present in Mlh3 (K83A) (Tran *et al.* 2000; Argueso *et al.* 2003). Similar

distinctions in MMR function have been found when comparing equivalent alleles in Mlh1 and Pms1. While null mutations in *MLH1* and *PMS1* confer similar mutation rates when deleted, mutations in equivalent positions (e.g. *mlh1-E31A* and *pms1-E61A, mlh1-G98A* and *pms1-G128A)* can confer large differences in mutation rates (Tran *et al.* 2000). Thus our work, in conjunction with previous studies support specialized roles of Mlh1 partner proteins (Pms1, Mlh3) in MMR (Tran *et al.* 2000; Hall *et al.* 2002; Hoffman *et al.* 2003; Argueso *et al.* 2003; Wanat *et al.* 2007; Nishant *et al.* 2008; Cotton *et al.* 2010).

ACKNOWLEDGEMENTS

We thank members of the Alani lab and Sarah Zanders for helpful comments, and Rhona Borts for providing information prior to publication of Cotton et al. (2010). M.S.B. was supported by an NIH Training Grant in Molecular and Cellular Biology. E. L. was supported by a Howard Hughes Medical Institute undergraduate summer research fellowship awarded to Cornell University, and C.C. and E. A. were supported by NIH GM53085. The content is solely the responsibility of the authors and does not necessarily represent the official views of the National Institute Of General Medical Sciences or the National Institutes of Health.

REFERENCES

Allers, T., M. Lichten, 2001 Intermediates of yeast meiotic recombination contain heteroduplex DNA. Mol. Cell 8: 225-231.

Adams, M. D., M. McVey, J. J. Sekelsky, 2003 *Drosophila* BLM in double-strand break repair by synthesis-dependent strand annealing. Science 299: 265-267.

Argueso, J. L., A. W. Kijas, S. Sarin, J. Heck, M. Waase, *et al*., 2003 Systematic mutagenesis of the *Saccharomyces cerevisiae* MLH1 gene reveals distinct roles for Mlh1p in meiotic crossing over and in vegetative and meiotic mismatch repair. Mol. Cell. Biol. 23: 873-886.

Argueso, J. L., J. Wanat, Z. Gemici, E. Alani, 2004 Competing crossover pathways act during meiosis in *Saccharomyces cerevisiae*. Genetics 168: 1805-1816.

Bachrati, C. Z., R. H. Borts, I. D. Hickson, 2006 Mobile D-loops are a preferred substrate for the Bloom's syndrome helicase. Nucl. Acids Res. 34: 2269-2279.

Ban, C., W. Yang, 1998 Crystal structure and ATPase activity of MutL: implications for DNA repair and mutagenesis. Cell 95: 541-552.

Ban, C., M. Junop, W. Yang, 1999 Transformation of MutL by ATP binding and hydrolysis: a switch in DNA mismatch repair. Cell 97: 85-97.

Berchowitz, L. E., K. E. Francis, A. L. Bey, G. P. Copenhaver, 2007 The role of AtMUS81 in interference-insensitive crossovers in A. thaliana. PLoS Genet. 3: e132

Boddy, M. N., P. H. Gaillard, W .H. McDonald, P. Shanahan, J.R. Yates, *et al.*, 2001 Mus81-Eme1 are essential components of a Holliday junction resolvase. Cell 107: 537-548.

Börner, G. V., N. Kleckner, N. Hunter, 2004 Crossover/noncrossover differentiation, synaptonemal complex formation, and regulatory surveillance at the leptotene/zygotene transition of meiosis. Cell 117: 29-45.

Bowers, J., P. T. Tran, R. M. Liskay, E. Alani, 2000 Analysis of yeast MSH2-MSH6 suggests that the initiation of mismatch repair can be separated into discrete steps. J. Mol. Biol. 302: 327-338.

Cao, L., E. Alani, N. Kleckner, 1990 A pathway for generation and processing of double strand breaks during meiotic recombination in *S. cerevisiae*. Genetics 185: 459-467.

Carpenter, A. T., 1991 Distributive Segregation: Motors in the Polar Wind? Cell 64: 885-890

Cejka, P., S. C. Kowalczykowski, 2010 The full-length *Saccharomyces cerevisiae* Sgs1 protein is a vigorous DNA helicase that preferentially unwinds holliday junctions. J. Biol. Chem. 285, 8290-8301.

Chen, S. Y., T. Tsubouchi, B. Rockmill, J.S. Sandler, D.R. Richards, *et al.*, 2008 Global analysis of the meiotic crossover landscape. Dev Cell 15: 401-415.

Clyne, R. K., V. L. Katis, L. Jessop, K. R. Benjamin, I. Herskowitz, *et al.*, 2003 Polo-like kinase Cdc5 promotes chiasmate formation and cosegregation of sister centromeres at meiosis I. Nat. Cell Biol. 5: 480-485.

Cotton, V. E., E. R. Hoffman, R. H. Borts, 2010 Distinct Regulation of Mlh1p Heterodimers in meiosis and mitosis in *Saccharomyces cerevisiae.* Genetics 185: 459-467.

Cromie G. A., R. W. Hyppa, A. F. Taylor, K. Zakharyevich, N. Hunter, *et al.*, 2006 Single Holliday junctions are intermediates of meiotic recombination. Cell 127: 1167-1178.

De Los Santos, T., N. Hunter, C. Lee, B. Larkin, J. Loidl, *et al*., 2003 The Mus81/Mms4 endonuclease acts independently of double-Holliday junction resolution to promote distinct subset of crossovers during meiosis in budding yeast. Genetics 164: 81-94.

De los Santos, T., J. Loidl, B. Larkin, N. M. Hollingsworth, 2001 A role for MMS4 in the processing of recombination intermediates during meiosis in *Saccharomyces cerevisiae.* Genetics 159: 1511-1525.

De Muyt, A., L. Jessop, E. Kolar, A. Sourirajan, J. Chen, *et al.*, 2012 BLM helicase ortholog Sgs1 is a central regulator of meiotic recombination intermediate metabolism. Mol. Cell 46: 42-53

Dixon, F. J., W. J. Massey, 1969 Introduction to statistical analysis. McGraw-Hill 3rd edition.

Drake, J. W., 1991 A constant rate of spontaneous mutation in DNA-based microbes. PNAS 88: 7160-7164.

Flores-Rozas, H., R. D. Kolodner, 1998 The *Saccharomyces cerevisiae MLH3* gene functions in *MSH3*-dependent suppression of frameshift mutations. Proc. Natl. Acad. Sci. USA 95: 12404-12409.

Fricke, W. M., S. J. Brill, 2003 Slx1-Slx4 is a second structure-specific endonuclease functionally redundant with Sgs1-Top3. Genes Dev. 17: 1768-1778.

Furukawa, T., S. Kimura, T. Ishibashi, Y. Mori, J. Hashimoto, *et al.*, 2003 OsSEND-1: a new RAD2 nuclease family member in higher plants. Plant Mol. Biol. 51: 59-70.

Gaskell, L. J., F. Osman, R. J. Gilbert, M. C. Whitby, 2007 Mus81 cleavage of Holliday junctions: A failsafe for processing meiotic recombination intermediates? EMBO J. 26: 1891-1901.

Gietz, R. D., R. H. Schiestl, A. R. Willems, R. A. Woods, 1995 Studies on the transformation of intact yeast cells by the LiAc/SS-DNA/PEG procedure. Yeast 11: 355-360.

Gilbertson, L. A., F. W. Stahl, 1996 A test of the double-strand break repair model for meiotic recombination in *Saccharomyces cerevisiae*. Genetics 144: 27-41

Gladstone, M. N., D. Obeso, H. Chuong, D. S. Dawson, 2009 The synaptonemal complex protein Zip1 promotes bi-orientation of centromeres at meiosis I. PLoS Genet. 5: e1000771.

Goldstein, A. L., J. H. Mccusker, 1999 Three new dominant drug resistance cassettes for gene disruption in *Saccharomyces cerevisiae*. Yeast 15: 1541-1553.

Grell, R. F., 1962 A new hypothesis on the nature and sequence of meiotic events in the female of *Drosophila melanogaster.* Proc. Natl. Acad. Sci. USA 48: 165-172.

Grell, R. F., 1976 Distributive pairing. Genetics and Biology of *Drosophila* 1: 425-486.

Guacci, V., D. B. Kaback, 1991 Distributive Disjunction of Authentic Chromosomes in *Saccharomyces cerevisiae.* Genetics 127: 475-488.

Habraken, Y., P. Sung, L. Prakash, S. Prakash, 1996 Binding of insertion/deletion DNA mismatches by the heterodimer of yeast mismatch repair proteins MSH2 and MSH3. Curr. Biol. 6: 1185-87.

Habraken, Y., P. Sung, L. Prakash, S. Prakash, 1997 Enhancement of MSH2-MSH3-mediated mismatch recognition by the yeast MLH1-PMS1 complex. Curr. Biol. 7: 790-93.

Hall, M. C., P. V. Shcherbakova, T. A. Kunkel, 2002 Differential ATP binding and intrinsic ATP hydrolysis by amino-terminal domains of the yeast Mlh1 and Pms1 proteins. J. Biol. Chem. 277: 3673-3679.

Harfe, B. D., B. K. Minesinger, S. Jinks-Robertson, 2000 Discrete in vivo roles for the MutL homologs Mlh2p and Mlh3p in the removal of frameshift intermediates in budding yeast. Curr. Biol. 10: 145-148.

Heck, J. A., J. L. Argueso, Z. Gemici, R. G. Reeves, A. Bernard, *et al.*, 2006 Negative epistasis between natural variants of the *Saccharomyces cerevisiae* MLH1 and PMS1 genes results in a defect in mismatch repair. Proc. Natl. Acad. Sci. USA 103: 3256-3261.

Higgens, J. D., E. F. Buckling, F. C. Franklin, G. H. Jones, 2008 Expression and functional analysis of *ATMUS81* in Arabidopsis meiosis revelas a role in the second pathway of crossing-over. Plant J. 54: 152-162.

Hoffman, E. R., R. H. Borts, 2004 Meiotic recombination intermediates and mismatch repair proteins. Cytogenet. Genome Res. 197: 232-248.

Hoffman, E. R., P. V. Shcherbakova, T. A. Kunkel, R. H. Borts, 2003 *MLH1* mutations diferentially affect meiotic functions in *Saccharomyces cerevisiae.* Genetics 163: 515-526.

Hollingsworth, N. M., S. J. Brill, 2004 The Mus81 solution to resolution: generating meiotic crossovers without Holliday junctions. Genes Dev. 18: 117-125.

Hollingsworth, N. M., L. Ponte, C. Halsey, 1995 *MSH5*, a novel MutS homolog, facilitates meiotic reciprocal recombination between homologs in *Saccharomyces cerevisiae* but not mismatch repair. Genes Dev. 9: 1728-1739.

Holloway, J. K., J. Booth, W. Edelmann, C. H. McGowan, P.E. Cohen , 2008 MUS81 generates a subset of MLH1-MLH3-independent crossovers in mammalian meiosis. PLoS Genet. 4: e1000186.

Hunter N., R. H. Borts, 1997 Mlh1 is unique among mismatch repair proteins in its ability to promote crossing-over during meiosis. Genes Dev. 11: 1573-1582.

Hunter, N., N. Kleckner, 2001 The single-end invasion: an asymmetric intermediate at the double-strand break to double-holliday junction transition of meiotic recombination. Cell 106: 59-70.

Ip, S. C., M. Bregu, F. X. Barre, D. J. Sherratt, 2003 Decatenation of DNA circles by FtsK-dependent Xer site-specific recombination. EMBO J. 22: 6399-6407.

Ip, S. C., U. Rass, M. G. Blanco, H. R. Flynn, J. M. Skehel, *et al.*, 2008 Identification of Holliday junction resolvases from humans and yeast. Nature 456: 357-361.

Ishikawa, G., Y. Kanai, K. Takata, R. Takeuchi, K. Shimanouchi, et al, 2004 DmGEN, a novel RAD2 family endo-exonuclease from *Drosophila melanogaster*. Nucl. Acids Res. 32: 6251-6259.

Jessop, L., M. Lichten, 2008 Mus81/Mms4 endonuclease and Sgs1 helicase collaborate to ensure proper recombination intermediate metabolism during meiosis. Mol. Cell 31: 313-323.

Jessop, L., B. Rockmill, G. S. Roeder, M. Lichten, 2006 Meiotic chromosome synapsis-promoting proteins antagonize the anti-crossover activity of Sgs1. PLoS Genet. 2: e155

Kaback, D. B., V. Guacci, D. Barber, J. W. Mahon, 1992 Chromosome size-dependent control of meiotic recombination. Science 256: 228-232.

Kaback, D. B., D. Barber, J. Mahon, J. Lamb, J. You, 1999 Chromosome size-dependent control of meiotic reciprocal recombination in *Saccharomyces cerevisiae*: the role of crossover interference. Genetics 152: 1475-1486.

Kaliraman, V., J. R. Mullen, W. M. Fricke, S. A. Bastin-Shanower, S. J. Brill, 2001 Functional overlap between Sgs1-Top3 and the Mms4-Mus81 endonuclease. Genes Dev. 15: 2730-2740.

Keeney, S., C. N. Giroux, N. Kleckner, 1997 Meiosis-specific DNA double-strand breaks are catalyzed by Spo11, a member of a widely conserved protein family. Cell 88: 357-384.

Kleckner, N., D. Zickler, G. H. Jones, J. Dekker, R. Padmore, *et al.*, 2004 A mechanical basis for chromosome function. Proc. Natl. Acad. Sci. USA 101: 12592-12597.

Kneitz B., P. E. Cohen, E. Avdievich , L. Zhu, M. F. Kane, *et al*., 2000 Mut S homolog 4 localization to meiotic chromosomes is required for chromosome pairing during meiosis in male and female mice. Genes Dev. 14: 1085-1097.

Kolodner, R. D., G. T. Marsischky, 1999. Eukaryotic DNA mismatch repair. Curr. Opin. Genet. Dev. 9: 89-96.

Kondo, E., A. Horii, S. Fukushige, 2001 The interacting domains of three MutL heterodimers in man: hMLH1 interacts with 36 homologous amio acid residues within hMLH3, hPMS1 and hPMS2. Nucleic Acids Res. 29: 1695-1702.

Kunkel, T. A., D. A. Erie, 2005. DNA mismatch repair. Annu Rev Biochem 74: 681-710.

Loidl, J., F. Klein, H. Scherthan, 1994 Homologous pairing is reduced but not abolished in asynaptic mutants of yeast. J. Cell Biol. 125: 1191-1200.

Marti, T. M., C. Kunz, O. Fleck, 2002 DNA mismatch repair and mutation avoidance pathways. J. Cell. Physiol. 191: 28-41.

Martini, E., R. L. Diaz, N. Hunter, S. Keeney, 2006 Crossover homeostasis in yeast meiosis. Cell 126: 285-295.

Matos, J., M. G. Blanco, S. Maslen, J. M. Skehel, S. C. West, 2011 Regulatory control of the resolution of DNA recombination intermediates during meiosis and mitosis. Cell 147: 158-172.

McVey, M., J. R. Larocque, M. D. Adams, J. J. Sekelsky, 2004 Formation of deletions during double-strand break repair in *Drosophila* DmBlm mutants occurs after strand invasion. Proc Natl Acad Sci USA 101: 15694-15699.

Munoz, I. M., K. Hain, A. C. Declais, M. Gardiner, G. W. Toh, *et al.*, 2009 Coordination of structure-specific nucleases by human SLX4/BTBD12 is required for DNA repair. Mol. Cell 35: 116-127.

New, L., K. Liu, G. F. Crouse, 1993 The yeast gene MSH3 defines a new class of eukaryotic MutS homologs. Mol. Gen. Genet. 239: 97-108.

Newnham, L., P. Jordan, B. Rockmill, G. S. Roeder, E. Hoffmann, 2010 The synaptonemal complex protein, Zip1, promotes the segregation of nonexchange chromosomes at meiosis I. Proc Natl Acad Sci USA 107: 781-785.

Nicklas, R. B., 1967 Chromosome micromanipulation II. Induced reorientation and the experimental control of segregation in meiosis. Chromosoma 21: 17-50.

Nicklas, R. B., 1974 Chromosome segregation mechanisms. Genetics 78: 205-213.

Nishant, K. T., C. Chen, M. Shinohara, A. Shinohara, E. Alani, 2010 Genetic analysis of baker's yeast Msh4-Msh5 reveals a threshold crossover level for meiotic viability. PLoS Genet. 6: e1001083.

Nishant, K. T., A. J. Plys, E. Alani, 2008 A mutation in the putative MLH3 endonuclease domain confers a defect in both mismatch repair and meiosis in *Saccharomyces cerevisiae*. Genetics 179: 747-755.

Oh, S. D., J. P. Lao, P. Y. Hwang, A. F. Taylor, G. R. Smith, *et al.*, 2007 BLM ortholog, Sgs1, prevents aberrant crossing-over by suppressing formation of multichromatid joint molecules. Cell 130: 259-272.

Oh, S. D., J. P. Lao, A. F. Taylor, G. R. Smith, N. Hunter, 2008 RecQ helicase, Sgs1, and XPF family endonuclease, Mus81-Mms4, resolve aberrant joint molecules during meiotic recombination. Mol Cell 31: 324-336.

Pedrazzi, G., C. Perrera, H. Blaser, P. Kuster, G. Marra, 2001 Direct association of Bloom's syndrome gene product with the human mismatch repair protein MLH1. Nucleic Acids Res. 29: 4378-86.

Perkins, D. D., 1949 Biochemical mutants in the smut fungus *Ustilago maydis.* Genetics 34: 607-626.

Prolla, T. A., D. M. Christie, R. M. Liskay, 1994a Dual requirement in yeast DNA mismatch repair for MLH1 and PMS1, two homologs of the bacterial mutL gene. Mol. Cell. Biol. 14: 407-415.

Prolla, T. A., Q. Pang, E. Alani, R. D. Koldoner, R. M. Liskay, 1994b MLH1, PMS1, and MSH2 interactions during the initiation of DNA mismatch repair in yeast. Science 265: 1091-1093

Rieder, C. L., E. D. Salmon, 1994 Motile kinetochore and polar ejection forces dictate chromosome position on the vertebrate mitotic spindle. J Cell Biol. 124: 223-233.

Robine, N., N. Uematsu, F. Amiot, X. Gidrol, E. Barillot, *et al.*, 2007 Genome-wide redistribution of meiotic double-strand breaks in *Saccharomyces cerevisiae*. Mol Cell Biol. 275: 1868-1880.

Rockmill, B., J. C. Fung, S. S. Branda, G. S. Roeder, 2003 The Sgs1 helicase regulates chromosome synapsis and meiotic crossing over. Curr. Biol. 13: 1954-1962.

Roeder, G. S., J. M. Bailis, 2000 The pachytene checkpoint. Trends Genet. 16: 395-403.

Ross-Macdonald, P., G. S. Roeder, 1994 Mutation of a meiosis-specific MutS homolog decreases crossing over but not mismatch correction. Cell 79: 1069-1706.

Sacho, E .J., F. A. Kadyrov, P. Modrich, T. A. Kunkel, D. A. Erie, 2008 Direct visualization of asymmetric adenine-nucleotide-induced conformational changes in MutL alpha. Mol. Cell. 29: 112-121.

Santucci-Darmanin, S., D. Walpita, F. Lespinasse, C. Desnuelle, T. Ashley, *et al.*, 2000 MSH4 acts in conjunction with MLH1 during mammalian meiosis. FASEB J. 14: 1539-1547.

Santucci-Darmanin, S., S. Neyton, F. Lespinasse, A. Saunieres, P. Gaudray, *et al.*, 2002 The DNA mismatch-repair MLH3 protein interacts with MSh4 in meiotic cells, supporting a role for this MutL homolog in mammalian meiotic recombination. Hum. Mol. Genet. 11: 1697-1706.

Schwacha, A., N. Kleckner, 1995 Identification of double Holliday junctions as intermediates in meiotic recombination. Cell 83: 783-791.

Schwartz, E. K., W. D. Heyer, 2011 Processing of joint molecule intermediates by structure-selective endonucleases during homologous recombination in eukaryotes. Chromosoma 120: 109-127.

Shcherbakova, P. V., T. A. Kunkel, 1999 Mutator phenotypes conferred by MLH1 overexpression and by heterozygosity for mlh1 mutations. Mol. Cell. Biol. 19: 3177-3183.

Shinohara, M., S. D. Oh, N. Hunter, A. Shinohara, 2008 Crossover assurance and crossover interference are distinctly regulated by the ZMM proteins during yeast meiosis. Nat Genet. 40: 299-309

Smith, G. R., M. N. Boddy, P. Shanahan, P. Russell, 2003 Fission yeast Mus81-Eme1 Holliday junction resolvase is required for meiotic crossing over but not for gene conversion. Genetics 165: 2289-2293.

Snowden, T., S. Acharya, C. Butz , M. Berardini, R. Fishel, 2004 hMSH4-hMSH5 recognizes Holliday Junctions and forms a meiosis-specific sliding clamp that embraces homologous chromosomes. Mol Cell 15: 437-451.

Sourirajan, A., M. Lichten, 2008 Polo-like kinase Cdc5 drives exit from pachytene during budding yeast meiosis. Genes Dev. 22: 2627-2632.

Stahl, F. W., H. M. Foss, L. S. Young, R. H. Borts, M. F. Abdullah, *et al.*, 2004 Does crossover interference count in *Saccharomyces cerevisiae*? Genetics 168: 35-48.

Storlazzi, A., S. Gargano, G. Ruprich-Robert, M. Falque, M. David, *et al*., 2010 Recombination proteins mediate meiotic spatial organization and pairing. Cell 141: 94-106.

Surtees, J., J. L. Argueso, E. Alani, 2004 Mismatch repair proteins: key regulators of genetic recombination. Cytogenet. Genome Res. 107: 146-59.

Svendsen, J. M., A. Smorgorzewska, M. E. Sowa, B. C. O'Connell, S. P. Gygi, et al., 2009 Mammalian BTBD12/SLX4 assembles a Holliday junction resolvase and is required for DNA repair. Cell 138: 63-77.

Svetlanov, A., P. E. Cohen, 2004 Mismatch repair proteins, meiosis, and mice: understanding the complexities of mammalian meiosis. Exp Cell Res. 296: 71-79.

Tran, H. T., J. D. Keen, M. Kricker, M. A. Resnick, D. A. Gordenin, 1997 Hypermutability of homonucleotide runs in mismatch repair and DNA polymerase proofreading yeast mutants. Mol. Cell. Biol. 17: 2859-2865.

Tran, P. T., R. M. Liskay, 2000 Functional studies on the candidate ATPase domains of *Saccharomyces cerevisiae* MutLalpha. Mol. Cell. Biol. 20: 6390-6398.

Tran, P. T., J. A. Simon, R. M. Liskay, 2001 Interactions of Exo1p with components of MutLα in *Saccharomyces cerevisiae.* Proc. Natl. Acad. Sci. USA 98: 9760-9765.

Trowbridge, K., K. McKim, S .J. Brill, J. Sekelsky, 2007 Synthetic lethality of *Drosophila* in the absence of the MUS81 endonuclease and the DmBlm helicase is associated with elevated apoptosis. Genetics 176: 1993-2001.

Tsubouchi, T., G. S. Roeder, 2005 A synaptonemal complex protein promotes homology-independent centromere coupling. Science 308: 870-873.

Van Brabant, A .J., T. Ye, M. Sanz, J. L. German, N. A. Ellis, *et al.*, 2000 Binding and melting of D-loops by the Bloom syndrome helicase. Biochemistry 39: 14617-14625.

Wach, A., A. Brachat, R. Pohlmann, P. Philippsen, 1994 New heterologous modules for classical or PCR-based gene disruptions in *Saccharomyces cerevisiae.* Yeast 10: 1793-1808.

Wanat, J.J., N. Singh, E. Alani, 2007 The effect of genetic background on the function of *Saccharomyces cerevisiae mlh1* alleles that correspond to HNPCC missense mutations. Human Mol. Genet. 16: 445-452.

Wang T. F., N. Kleckner, N. Hunter, 1999 Functional specificity of MutL homologs in yeast: evidence for three Mlh1-based heterocomplexes ith distinct roles during meiosis in recombination and mismatch correction. Proc. Natl. Acad. Sci. USA 96: 13914-13919.

Whitby, M. C., 2005 Making crossovers during meiosis. Biochem. Soc. Trans. 33:1451-1455.

Wu, L., I. D. Hickson, 2003 The Bloom's syndrome helicase suppresses crossing over during homologous recombination. Nature 426: 870-874.

Zakharyevich, K., Y. Ma, S. Tang, P. Y. Hwang, S. Boiteux, *et al.*, 2010 Temporally and biochemically distinct activities of Exo1 during meiosis: double-strand break resection and resolution of double Holliday Junctions. Mol. Cell 40: 1001-1015.

Zakharyevich, K., S. Tang, Y. Ma, N. Hunter, 2012 Delineation of joint molecule resolution pathways in meiosis identifies a crossover-specific resolvase. Cell 149: 1-14.

Zanders, S. E. Alani, 2009 The *pch2Delta* mutation in baker's yeast alters meiotic crossover levels and confers a defect in crossover interference. PLoS Genet. 5: e1000571.

Zickler, D., 2006 From early homologue recognition to synaptonemal complex formation. Chromosoma 115: 158-174.

Chapter 5

FUTURE DIRECTIONS

Some remaining questions involving telomere-led chromosome motion

In Chapters 2 and 3, I discuss work investigating the role of Csm4 in telomere-led chromosome motion. In Chapter 2, I found that defects in chromosome motion correlate with defects in homolog pairing (Sonntag Brown *et al.* 2011). It is still unclear whether chromosome motion may directly promote pairing by bringing chromosomes together, or whether pairing is indirect, brought about by removal of inappropriate interactions between chromosomes. Removal of inappropriate interactions would then allow homologous chromosomes to pair.

In order to test whether chromosome motion directly promotes homolog pairing, live cell imaging should be used to track chromosome motion and homolog pairing simultaneously. I initially thought to do this using Nup49-GFP and the one-dot/two-dot assay, both of which I utilized individually in Chapter 2. Using these two fluorescent markers, I thought I could track chromosome motion through distortions of the nuclear envelope and homolog pairing in real time to see if rapid chromosome movements would bring a cell from the "two-dot" (unpaired) stage to the "one-dot" (paired) stage (Figure 5.1). However, I found while performing my pairing assays that I was unable to see motion of the dots in the one-dot/two-dot assay, although extensive experiments were not conducted. Furthermore, often the two dots, if present, were in slightly different focal points. A better tactic may be to use FISH to track a chromosome pair. This way, a larger portion of the chromosome would be visible and there would be a greater chance that at least part of each homolog would be in the same field of view.

Chromosome motion may also play a role in removing inappropriate interactions between

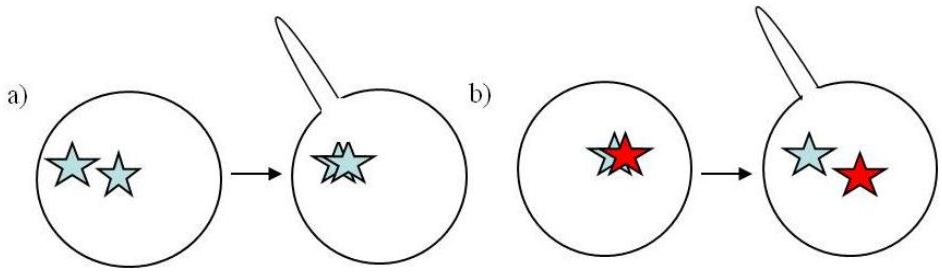

Figure 5.1. Chromosome motion may directly promote homolog pairing. a) NE distortion leading to homologous chromosomes pairing. b) NE distortion breaking apart two nonhomologous chromosomes. Stars represent fluorescent dots seen in the pairing assay.

homologs, such as ectopic pairing or synaptonemal complex interlocks. To see whether chromosome motion may help remove ectopic pairing events, I would use a set of strains created by the Boeke Lab (Scheifele *et al.* 2009). This strain set has increased numbers of the Ty1 element, ranging from five to ten-fold more than wild-type strains. This increase in repetitive elements provides more loci where ectopic pairing can occur. Ectopic pairing can lead to chromosome rearrangements and cell death (Figure 5.2). If chromosome motion is important for removing ectopic pairing interactions, then cells defective in chromosome motion (like *csm4Δ*, see Chapter 2), would show lower spore viability in each strain background compared to wild-type controls. Furthermore, the more repetitive elements, the lower the spore viability should be.

In order to see if chromosome motion removes interlocks, I would employ a chromosome conformation capture method (Dekker *et al.* 2002). Chromosome interlocks occur when two nonhomologous chromosomes form a knot, either through the DNA itself or through the synaptonemal complex (Figure 5.3). Briefly, this method involves crosslinking chromosomes in 3-dimensional space, cutting the DNA into fragments, and then amplifying and sequencing the regions that were crosslinked. Cells that are defective in chromosome motion should have an increased number of interchromosome crosslinks. However, this method would not say that these chromosomes that were close in 3-dimensional space were part of an interlock, per se. Furthermore, averaging over a population of cells may prevent any meaningful data from being collected. Unfortunately, microscopy techniques and chromosome size in budding yeast are limiting in visualizing such synaptonemal complex interlocks directly.

While some proteins involved in chromosome motion in budding yeast have been identified, the mechanism is not as well known as in some other organisms (see Chapter 3). In

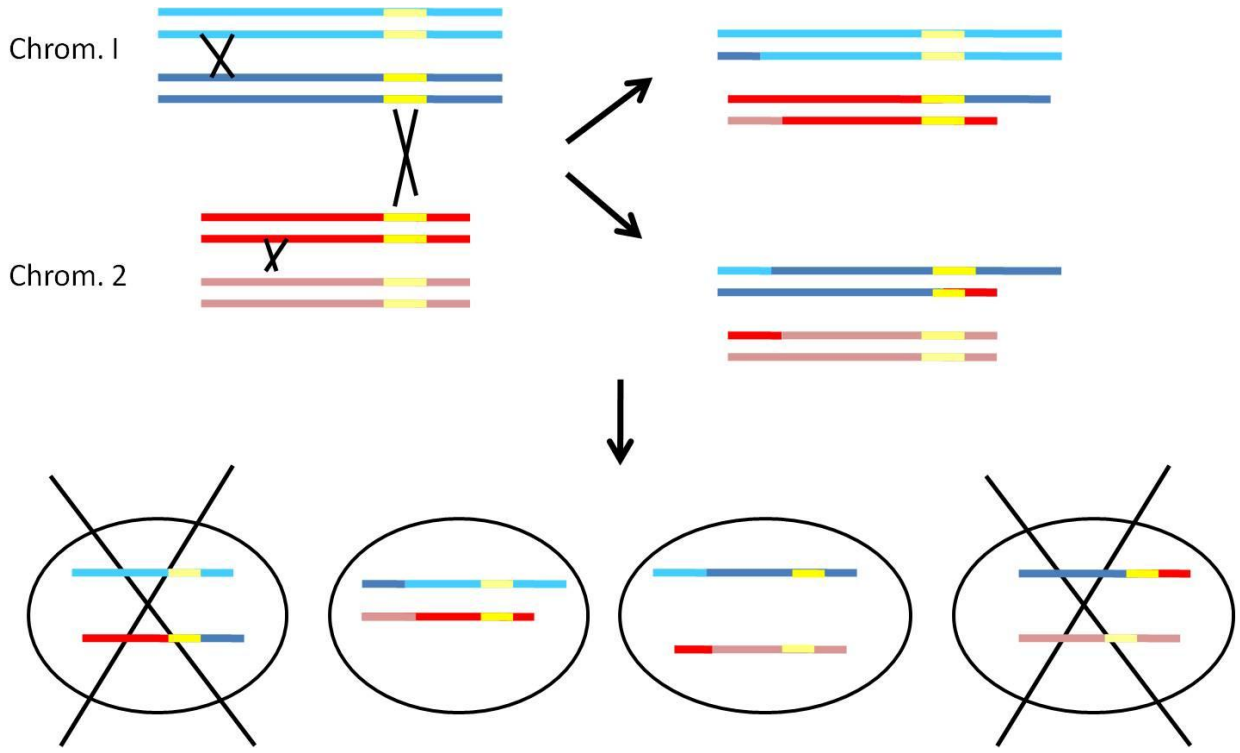

Figure 5.2. Ectopic chromosome pairing can lead to cell death. Two chromosome pairs (one in red, one in blue) are shown that share a region of homology (yellow). After recombination occurs between the sites of ectopic homology, two of the four spores are missing part of a chromosome, resulting in cell death.

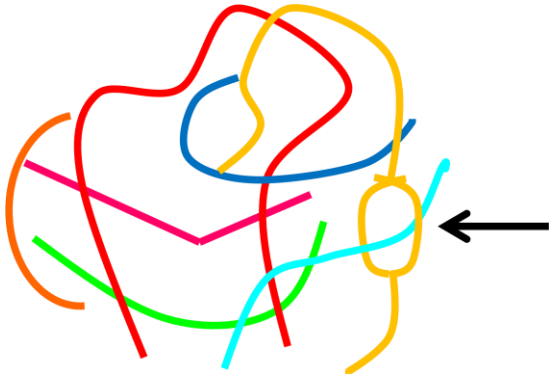

Figure 5.3. A synaptonemal complex chromosomal interlock. A cartoon of an interlock is shown. Each chromosome is colored in a different color, and the arrow points to the interlock. Figure modified from Storlazzi *et al.* 2010.

Chapter 3, I outline my initial attempts at finding a new component of the motion-generating system in budding yeast and I mention a split-ubiquitin 2-hybrid screen that could be utilized to find proteins that interact with Csm4.

*csm4*Δ has some interesting phenotypes when combined with other meiotic mutants. First, *csm4Δ pch2Δ* cells have a lower spore viability than either single mutant (see Chapter 2). This is especially surprising given that *pch2Δ* has a wild-type spore viability on its own (Zanders and Alani, 2009). It is thought that Pch2 plays a role in recombination partner choice during meiosis (Appendix; Zanders *et al.* 2011). It would be interesting to see how both chromosome motion and DSB repair partner choice are affected in the double mutant. Methods used in Chapter 2 to study chromosome motion and homolog pairing and methods in the Appendix to study repair partner choice would be used to see if there is a more severe phenotype in any assay in the double mutant.

Second, the spore viability of *csm4*Δ *ndj1*Δ is higher than either single mutant. Ndj1 is another component of the motion-generating system in budding yeast (see Chapter 3). It is thought that Ndj1 plays a role in connecting telomeres to the nuclear envelope (Trelles-Sticken *et al.* 2000; Conrad *et al.* 2008). It has been proposed that this increase in spore viability may be due to the release of chromosomes from the nuclear envelope, allowing chromosomes more freedom to move in the nucleus. However, while *csm4Δ ndj1Δ* cells do show slightly more motion that *csm4Δ* alone, it is very similar to the level of motion seen in *ndj1Δ* (Wanat *et al.* 2008). Why this double mutant has such high spore viability remains a mystery, but it would be interesting to see if *ndj1Δ* could also rescue the homolog pairing defect observed in *csm4Δ*.

<u>Potential projects involving the role of Mlh3 in crossover regulation</u>

While the lack of a crossover threshold pattern we saw in Chapter 4 is convincing, it would be ideal to look at more alleles of *mlh3* in order to fill in holes to the linear pattern. The Alani Lab is currently working on a larger-scale screen of Mlh3 using charged-to-alanine scanning mutagenesis. Analysis of these additional alleles for spore viability and crossing over will be conducted by other members of the lab. Since tetrad dissecting 50+ strains is tedious work, a method developed by the Keeney Lab will be used. This system has different strains marked with different fluorescent markers at multiple loci in the genome. By combining different strains, crossover frequency and nondisjunction phenotypes can be scored (Thacker *et al.* 2011). This will expedite the process and be more fun, however a small amount of tetrad dissections will need to be conducted in order to determine spore viability.

While methods are available to visualize Msh5 foci in budding yeast, no methods currently exist to visualize the downstream factor Mlh3. I have begun two methods in order to do this. First, an HA tag was inserted in the linker arm of Mlh3. This tag was able to complement an *mlh3Δ* strain, suggesting Mlh3-HA is functional. However, initial attempts to visualize foci by immunofluorescence were unsuccessful. This could be due to either low expression levels of Mlh3 during meiosis or to my inexpertise at immunofluorescence. Strains are being made to express Mlh3-HA at a higher level. We could send these strains to our expert collaborators at immunofluorescence (Shinohara Lab), or spend more time ourselves to work out the details.

Second, an Mlh3-$(GFP)_3$ tag was constructed to try to visualize Mlh3 foci directly. Initial results suggest that the GFP tag is being expressed, although the construct may not complement an *mlh3Δ* strain. Experiments to see whether GFP foci observed are meiosis dependent and Msh4/5 dependent are underway.

REFERENCES

Conrad, M. N., C. Y. Lee, G. Chao, M. Shinohara, H. Kosaka, *et al*., 2008 Rapid telomere movement in meiotic prophase is promoted by NDJ1, MPS3, and CSM4 and is modulated by recombination. Cell 133: 1175-1187.

Dekker, J., K. Rippe, M. Dekker, N. Kleckner, 2002 Capturing chromosome conformation. Science 295: 1306-11.

Thacker, D., I. Lam, M. Knop, S. Keeney, 2011 Exploiting spore-autonomous fluorescent protein expression to quantify meiotic chromosome behaviors in *Saccharomyces cerevisiae.* Genetics 189: 423-439.

Scheifele, L. Z., G. J. Cost, M. L. Zupancic, E. M. Caputo, J. D. Boeke, 2009 Retrotransposon overdose and genome integrity. PNAS 106: 13927-13932.

Sonntag Brown, M., S. Zanders, E. Alani, 2011 Sustained and rapid chromosome movements are critical for chromosome pairing and meiotic progression in budding yeast. Genetics 188:21-32.

Storlazzi, A., S. Gargano, G. Ruprich-Robert, M. Falque, M. David, *et al.,* 2010 Recombination proteins mediate meiotic spatial chromosome organization and pairing. Cell 141: 94-106.

Trelles-Sticken, E. M. E. Dresser, and H. Scherthan, 2000 Meiotic telomere protein Ndj1p is required for meiosis-specific telomere distribution, bouquet formation and efficient homologue pairing. J. Cell Biol. 151: 95-106.

Zanders, S. and E. Alani, 2009 The *pch2Delta* mutation in baker's yeast alters meiotic crossover levels and confers a defect in crossover interference. PLoS Genet. 5: e1000571.

Zanders, S., M. Sonntag Brown, C. Cheng, E. Alani, 2011 Pch2 modulates chromatid partner choice during meiotic double-strand break repair in *Saccharomyces cerevisiae.* Genetics 188: 511-21.

Wanat, J. J., K. P. Kim, R. Koszul, S. Zanders, B. Weiner, *et al.*, 2008 Csm4, in collaboration with Ndj1, mediates telomere-led chromosome dynamics and recombination during yeast meiosis. PLoS Genet. 4: e1000188.

APPENDIX

Pch2 modulates chromatid partner choice during meiotic double-strand break repair in *S. cerevisiae*

Sarah Zanders*, Megan Sonntag Brown, Cheng Chen, and Eric Alani

Department of Molecular Biology and Genetics

Cornell University, Ithaca, NY 14853-2073

*Present address: Division of Basic Sciences, Fred Hutchinson Cancer Research Center, Mail Stop A2-025, P.O. Box 19024, Seattle, WA 98109-1024

This chapter was originally published in the July 2011 issue of Genetics:

Zanders, S., M. Sonntag Brown, C. Cheng, E. Alani, 2011 Pch2 modulates chromatid partner choice during meiotic double-strand break repair in *S. cerevisiae*. Genetics 188: 511-521.

Contributions: M. Sonntag Brown created the strains, conducted the experiments and analyzed the data in Tables A1.4 and A1.5

ABSTRACT

In most organisms, the segregation of chromosomes during the first meiotic division is dependent upon at least one CO between each pair of homologous chromosomes. COs can result from chromosome double strand breaks (DSBs) that are induced and preferentially repaired using the homologous chromosome as a template. The *PCH2* gene of budding yeast is required to establish proper meiotic chromosome axis structure and to regulate meiotic interhomolog DSB repair outcomes. These roles appear conserved in the mouse ortholog of *PCH2*, *Trip13*, which is also involved in meiotic chromosome axis organization and the regulation of DSB repair. Using a combination of genetic and physical assays to monitor meiotic DSB repair, we present data consistent with *pch2*Δ mutants showing defects in suppressing intersister DSB repair. These defects appear most pronounced in *dmc1Δ* mutants, which are defective for interhomolog repair, and explain the previously reported observation that *pch2Δ dmc1Δ* cells can complete meiosis. Results from genetic epistasis analyses involving *spo13Δ*, *rad54Δ*, and *mek1/MEK1* alleles and an intersister recombination reporter assay are also consistent with Pch2 acting to limit intersister repair. We propose a model in which Pch2 is required to promote full Mek1 activity and thereby promotes intersister repair and regulates interhomolog repair outcomes.

INTRODUCTION

DNA double-strand breaks (DSBs) that occur during vegetative growth are preferentially repaired via homologous recombination in which the Rad51 recombinase and its partner Rad54 mediate strand exchange with the sister-chromatid. This intersister repair occurs even in diploids cells where a homologous chromosome template is available and is thought to help prevent chromosome rearrangements (KADYK and HARTWELL 1992; ARBEL, ZENVIRTH and SIMCHEN 1999; SHINOHARA *et al*. 1997b; KROGH and SYMINGTON 2004). In meiosis, formation of programmed DSBs and their repair using the homologous chromosome as a template is essential for the production of viable gametes (ROEDER 1997). Although Rad51 and Rad54 are still present, meiotic interhomolog strand exchange is accomplished by their respective orthologs, Dmc1 and Rdh54 (ARBEL, ZENVIRTH and SIMCHEN 1999; SHINOHARA *et al*. 1997a, 1997b; DRESSER *et al.* 1997; KLEIN 1997; HOLLINGSWORTH 2010). Interhomolog DSB repair creates linkages provided by genetic exchanges, or crossovers (CO), between homologous chromosomes. In many organisms these COs are required for reductional chromosome segregation at the meiosis I (MI) division, which lowers cell ploidy by one-half, allowing for the generation of haploid gametes (ROEDER 1997). If any pair of homologous chromosomes fails to receive a CO, MI nondisjunction can occur and produce aneuploid gametes, which cause conditions such as Down syndrome or infertility in humans (HASSOLD, HALL and HUNT 2007).

During meiotic prophase I in budding yeast, ~140-170 DNA DSBs are introduced into the genome by a group of ten proteins, of which Spo11 is the catalytic component (BUHLER *et al.* 2007; MANCERA *et al*. 2008; BLITZBLAU *et al*. 2007). Although COs are the only repair products known to promote MI disjunction, only ~50% of DSBs in yeast meiosis are repaired as

interhomolog COs. Some DSBs are repaired using the homologous chromosome without producing a CO; this is known as a noncrossover (NCO). Obligate CO formation, CO interference, and CO homeostasis are manifestations of interhomolog DSB repair regulation acting to ensure each pair of homologous chromosomes disjoins at MI (BUHLER, BORDE and LICHTEN 2007; BLITZBLAU *et al*. 2007; MANCERA *et al*. 2008; CHEN *et al.* 2008; BISHOP and ZICKLER 2004; BORNER, KLECKNER and HUNTER 2004, MARTINI *et al*. 2006; BERCHOWITZ and COPENHAVER 2010). The obligate CO refers to the observation that all homologous chromosome pairs receive at least one CO. CO interference describes the nonrandom, evenly spaced distribution of CO events and CO homeostasis describes the finding that CO levels are maintained as DSB frequencies are decreased (reviewed in BERCHOWITZ and COPENHAVER 2010; JONES and FRANKLIN 2006). Little is known about the mechanisms or relatedness of the different aspects of CO control, although one mutant, *pch2*Δ, has decreased CO interference and may also be defective for CO homeostasis (ZANDERS and ALANI 2009; JOSHI *et al*. 2009).

The ~10-33% of meiotic DSBs estimated to not be repaired using a homologous chromosome are repaired by homologous recombination using the sister chromatid as a template (e.g. GOLDFARB and LICHTEN 2010). The shift in DSB repair template preference from the sister chromatid in the mitotic cell cycle, to the homologous chromosome in meiosis, is referred to as "interhomolog bias" (JACKSON and FINK 1985; SCHWACHA and KLECKNER 1994; 1997; GOLDFARB and LICHTEN 2010; WAN *et al*. 2004; WEBBER, HOWARD and BICKEL 2004; NIU *et al*. 2005; 2007; 2009). Interhomolog bias is established shortly after DSB formation and requires components of the axial elements, which are linear structures that form along each pair of sister chromatids early in meiotic prophase (HOLLINGSWORTH 2010).

An early step in instituting interhomolog bias is phosphorylation of Hop1 of the Hop1/Red1 axial element duo by the Mec1 and Tel1 kinases (HOLLINGSWORTH and BYERS 1989; HOLLINGSWORTH, GOETSCH and BYERS 1990; ROCKMILL and ROEDER 1990; CARBALLO *et al*. 2008). Red1 and phosphorylated Hop1 are required for the activation of the effector kinase Mek1 (NIU *et al.* 2005; 2007; CARBALLO *et al*. 2008). Mek1 appears to directly promote interhomolog repair (TERENTYEV *et al*. 2010). In addition, Mek1 phosphorylates Rad54, which inhibits the interaction between Rad51 and Rad54 (NIU *et al*. 2009). Phosphorylation of Rad54 contributes to, but is not sufficient for complete interhomolog bias (NIU *et al*. 2009). The meiosis-specific protein Hed1 also acts to prevent Rad51-Rad54 complex formation by competing with Rad54 for Rad51 binding, although the role of Hed1 in interhomolog bias is yet to be determined (TSUBOUCHI and ROEDER 2006; BUSYGINA *et al.* 2008). Interhomolog bias is maintained in haploid meiosis and inhibits DSB repair, suggesting that interhomolog interactions are not required (CALLENDER and HOLLINGSWORTH 2010; DEMASSY, BAUDAT and NICOLAS 1994). At hemizygous DSB sites in diploid meiosis, intersister repair is constrained by a Mek1-dependent delay, although efficient intersister DSB repair does occur (GOLDFARB and LICHTEN 2010).

The mechanisms promoting interhomolog bias are often studied in *dmc1* null mutant backgrounds in which unrepaired DSBs trigger the meiotic recombination checkpoint to arrest cells at pachytene, the last stage of meiotic prophase before cells are committed to undergoing the MI division (HOLLINGSWORTH 2010). There are two ways recombination checkpoint arrest can be overcome in a *dmc1* mutant background. The first is to eliminate any of the essential recombination checkpoint genes such as *MEC1*, *RAD17*, or *RAD24*. In such cases, meiosis proceeds with unrepaired breaks to form inviable gametes (LYDALL *et al.* 1996). The

second is to eliminate (or reduce; see below) the checkpoint-eliciting DNA lesions by either preventing DSB formation or by allowing inappropriate Dmc1-independent DSB repair (SCHWACHA and KLECKNER 1994; 1997; BISHOP *et al.* 1992; XU, WEINER and KLECKNER 1997; BISHOP *et al*. 1999; THOMPSON and STAHL 1999). The latter can be accomplished by several mechanisms. Overexpressing *RAD51* or *RAD54* and/or mutating *HED1* in a *dmc1* background allows for meiotic progression and the production of moderate to wild-type levels of interhomolog COs and thus viable spores (TSUBOUCHI and ROEDER 2003; 2006; BUSYGINA *et al*. 2008; BISHOP *et al.* 1999). Alternatively, when *RED1*, *HOP1*, or *MEK1* are mutated, interhomolog bias is lost and DSBs are rapidly repaired via Rad51-Rad54-dependent strand exchange using the sister chromatid as a template, and meiosis progresses to produce inviable spores (WAN *et al.* 2004; NIU *et al*. 2005; 2007; BISHOP *et al.* 1999).

Pch2 (Pachytene checkpoint) is a putative AAA ATPase that promotes the checkpoint arrest/delays observed in *zip1*, *rad17*, *mms4*, and *sae2* recombination mutants. The *pch2*Δ mutation also suppressed the *dmc1*Δ checkpoint arrest in some but not all studies (ZANDERS and ALANI 2009; SAN-SEGUNDO and ROEDER 1999; WU and BURGESS 2006; MITRA and ROEDER 2007; ZIERHUT *et al*. 2004; HOCHWAGEN *et al*. 2005). In budding yeast, Pch2 is also required for wild-type kinetics of meiotic progression, CO interference, and establishing proper organization of Hop1 and Zip1 on meiotic chromosomes (ZANDERS and ALANI 2009; JOSHI *et al*. 2009; SYM and ROEDER 1995; BORNER, BAROT and KLECKNER 2008). Several of these roles appear conserved in the mouse *PCH2* ortholog *Trip13*, which is required for wild-type levels of DSB repair, CO interference, wild-type CO distribution, and proper organization of HORMADs (which share homology with Hop1) and the

synaptonemal complex central element protein SYCP1 on meiotic axes (LI and SCHIMENTI 2007; WOJTASZ *et al*. 2009; ROIG *et al*. 2010).

Here we investigated the mechanisms by which the *pch2*Δ mutation suppresses the meiotic arrest/delay phenotypes of *dmc1*Δ mutations. First, we found that lowering DSB levels in *dmc1Δ* mutants reduced the fraction of cells that arrest, indicating that the recombination checkpoint is sensitive to DSB levels. Second, we found that Pch2 inhibited some DSB repair in *dmc1Δ* cells that likely includes, but may not be limited to, intersister recombination. Third, we identified genetic interactions between *PCH2* and *RAD54* and *PCH2* and *MEK1* that support a role for Pch2 in limiting intersister repair. Finally, we present a genetic assay that demonstrates an increase in intersister repair at one locus in *pch2Δ* mutants. We synthesize our data with published results to propose a model in which Pch2 is required for full Mek1 activity.

MATERIALS AND METHODS

Media and yeast strains: All yeast strains (Table A1.1) were grown at 30°C on YPD (yeast peptone dextrose) supplemented with complete amino acid mix, synthetic complete, or synthetic complete –histidine (ARGUESO *et al*. 2004). All strains were sporulated at 30°C. The sporulation media and sporulation conditions used to generate the data in Tables A1.2-A1.4 were described previously (ZANDERS and ALANI 2009). Differences in spore formation and viability were analyzed by a Chi-Square test with p-values < 0.05 considered statistically significant. Geneticin (Invitrogen), nourseothricin (Hans-Knoll Institute fur Naturstoff-Forschung), and hygromycin B (Calbiochem) were added in standard concentrations to YPD media when required (WACH *et al*. 1994; GOLDSTEIN and MCCUSKER 1999).

Table A1.1. Yeast strains used in this study

Strain Names	Genotype
NH943/EAY2580	*MATa/α,* homozygous for: *ho::hisG ade2Δ, ura3(ΔSma-Pst), leu2::hisG, CEN3::ADE2, lys5-P, cyh2^r, his4-B*
EAY2581/EAY2210	as NH943/EAY2580 except *pch2Δ::NATMX4*
EAY2582/SKY635	as NH943/EAY2580 except *spo11-HA3His6::KANMX4*
EAY2787/EAY2263	as NH943/EAY2580 except *pch2Δ::NATMX4, spo11-HA3His6::KANMX4*
EAY2637/EAY2638	as NH943/EAY2580 except *dmc1Δ::KANMX4*
EAY2639/EAY2640	as NH943/EAY2580 except *pch2Δ::NATMX4, dmc1Δ::KANMX4*
EAY2619/EAY2630	as NH943/EAY2580 except *spo11-HA3His6::KANMX4*, *dmc1Δ::KANMX4*
EAY2631/EAY2632	as NH943/EAY2580 except *pch2Δ::NATMX4, spo11-HA3His6::KANMX4, dmc1Δ::KANMX4*
EAY2582/SKY665	as NH943/EAY2580 except *spo11-HA3His6::KANMX4*/*spo11(Y135F)-HA3His6::KANMX4*
EAY2787/EAY2265	as NH943/EAY2580 except *pch2Δ::NATMX4*, *spo11-HA3His6::KANMX4*/*spo11(Y135F)-HA3His6::KANMX4*
EAY2620/EAY2800	as NH943/EAY2580 except *spo11-HA3His6::KANMX4*/*spo11(Y135F)-HA3His6::KANMX4, dmc1Δ::KANMX4*
EAY2622/EAY2802	as NH943/EAY2580 except *pch2Δ::NATMX4*, *spo11-HA3His6::KANMX4*/*spo11(Y135F)-HA3His6::KANMX5, dmc1Δ::KANMX4*
EAY2589/EAY2590	as NH943/EAY2580 except *spo13::URA3*
EAY2591/EAY2592	as NH943/EAY2580 except *pch2Δ::NATMX4, spo13::URA3*
EAY2595/EAY2596	as NH943/EAY2580 except *spo11-HA3His6::KANMX4*, *spo13::URA3*
EAY2593/EAY2594	as NH943/EAY2580 except *pch2Δ::NATMX4*, *spo11-HA3His6::KANMX4*, *spo13::URA3*
EAY2643/EAY2644	as NH943/EAY2580 except *dmc1Δ::KANMX4, spo13::URA3*
EAY2641/EAY2642	as NH943/EAY2580 except *pch2Δ::NATMX4, dmc1Δ::KANMX4, spo13::URA3*
EAY2633/EAY2634	as NH943/EAY2580 except *spo11-HA3His6::KANMX4*, *dmc1Δ::KANMX4, spo13::URA3*
EAY2635/EAY2636	as NH943/EAY2580 except *pch2Δ::NATMX4, spo11-HA3His6::KANMX4, dmc1Δ::KANMX4, spo13::URA3*
EAY2578/EAY2579	as NH943/EAY2580 except *rad50S::URA3*
EAY2585/EAY2586	as NH943/EAY2580 except *pch2Δ::NATMX4*, *rad50S::URA3*
EAY2587/EAY2588	as NH943/EAY2580 except *spo11-HA3His6::KANMX4*, *rad50S::URA3*
EAY2583/EAY2584	as NH943/EAY2580 except *pch2Δ::NATMX4*, *spo11-HA3His6::KANMX4*, *rad50S::URA3*
EAY2722/EAY2723	as NH943/EAY2580 except *rad54Δ::HPHMX4*
EAY2681/EAY2746	as NH943/EAY2580 except *pch2Δ::NATMX4, rad54Δ::HPHMX4*
EAY2740/EAY2741	as NH943/EAY2580 except *spo11-HA3His6::KANMX4*, *rad54Δ::HPHMX4*

EAY2726/EAY2727	as NH943/EAY2580 except *pch2Δ::NATMX4, spo11-HA3His6::KANMX4, rad54Δ::HPHMX4*
EAY2742/EAY2743	as NH943/EAY2580 except *rad54Δ::HPHMX4, dmc1Δ::KANMX4*
EAY2728/EAY2729	as NH943/EAY2580 except *pch2Δ::NATMX4, rad54Δ::HPHMX4, dmc1Δ::KANMX4*
EAY2738/EAY2739	as NH943/EAY2580 except *spo11-HA3His6::KANMX4, rad54Δ::HPHMX4, dmc1Δ::KANMX4*
EAY2724/EAY2725	as NH943/EAY2580 except *pch2Δ::NATMX4, spo11-HA3His6::KANMX4, rad54Δ::HPHMX4, dmc1Δ::KANMX4*
NH942	*MATα, ho::hisG, ade2Δ, can1, ura3(ΔSma-Pst), met13-B, trp5-S, CEN8::URA3, thr1-A, cup1^{S}*
EAY2209/EAY2210	as NH942/NH943 except *pch2Δ::NATMX4*
EAY2681/EAY2685	as NH942/NH943 except *pch2Δ::NATMX4, rad54Δ::HPHMX4*
EAY2951/EAY2952	*MATa/α* homozygous for *ho::hisG*, *ura3*, and *his3Δ::KANMX4* hemizygous for *his3-Δ5′ his3-Δ3′::URA3*
EAY2955/EAY2956	as EAY2951/2952 except *pch2Δ::NATMX4*
EAY3077	*MATa, ho::hisG, leu2*
EAY3078	*MATα, ho::hisG, leu2*
EAY3079	*MATa, ho::hisG, HIS4, lys5-P, mek1Δ::LEU2::mek1Q241G::URA3*
EAY3080	*MATα, ho::hisG, HIS4, mek1Δ::LEU2::mek1Q241G::URA3*
EAY3081	*MATa, ho::hisG, HIS4, lys5-P, mek1Δ::LEU2::mek1Q241G::URA3, pch2Δ::NATMX4*
EAY3082	*MATα, ho::hisG, HIS4, mek1Δ::LEU2::mek1Q241G::URA3, pch2Δ::NATMX4*
EAY3083	*MATa, ho::hisG, HIS4, mek1Δ::LEU2::mek1Q241G::URA3, spo11-HA::KANMX4*
EAY3084	*MATα, ho::hisG, HIS4, mek1Δ::LEU2::mek1Q241G::URA3, spo11-HA::KANMX4*
EAY3085	*MATa, ho::hisG, HIS4, mek1Δ::LEU2::mek1Q241G::URA3, pch2Δ::NATMX4, spo11-HA::KANMX4*
EAY3086	*MATα, ho::hisG, his4, mek1Δ::LEU2::mek1Q241G::URA3, pch2Δ::NATMX4, spo11-HA::KANMX4*
EAY3087	*MATa, ho::hisG, his4*
EAY3088	*MATα, ho::hisG, his4, ade2Δ*
EAY3089	*MATa, ho::hisG, HIS4, ura3, MEK1-GST-KANMX4*
EAY3090	*MATα, ho::hisG, his4, MEK1-GST-KANMX4*
EAY3091	*MATa, ho::hisG, his4, MEK1-GST-KANMX4, pch2Δ::NATMX4*
EAY3092	*MATα, ho::hisG, his4, MEK1-GST-KANMX4, pch2Δ::NATMX4*
EAY3093	*MATa, ho::hisG, his4, ura3, MEK1-GST-KANMX4, spo11-HA::KANMX4*
EAY3094	*MATα, ho::hisG, his4, ura3, MEK1-GST-KANMX4, spo11-HA::KANMX4*
EAY3095	*MATa, ho::hisG, his4, ura3, ade2Δ, leu2::hisG, MEK1-GST-KANMX4, pch2Δ::NATMX4, spo11-HA::KANMX4*
EAY3096	*MATα, ho::hisG, HIS4, ura3, MEK1-GST-KANMX4, pch2Δ::NATMX4, spo11-HA::KANMX4*

The diploid strain names are composites of the haploid strains used to create them.

Strains described in Tables A1.2 and A1.3 are isogenic to the NHY943 or NHY942 SK1 strains described in DE LOS SANTOS *et al*. (2003). The *spo11* hypomorphic mutants and the NHY943 strains containing these alleles are described in MARTINI *et al*. (2006). As in MARTINI *et al*. (2006), we refer to *spo11-HA3His6* as *spo11-HA*. The *dmc1*Δ, and *rad54*Δ alleles used in this work were all complete open reading frame (ORF) deletions. The *pch2*Δ allele contains a deletion of amino acids 17-587 (ZANDERS and ALANI 2009). All deletion cassettes were made via PCR and the deleted regions were replaced with *HPHMX4*, *KANMX4*, or *NATMX4* as shown in Table A1.1. A *Bam*HI fragment of pNKY58 was integrated into the genome to create the *spo13::hisG-URA3-hisG* mutation and a *Bgl*II to *Eco*RI fragment of pNKY349 was used to replace *RAD50* with *rad50S::URA3* (ALANI, PADMORE and KLECKNER 1990). All mutations were initially integrated into the genome using standard transformation techniques (GIETZ *et al*. 1995). Standard genetic crosses were used to generate the various mutant combinations. Details on strain construction and primer sequences are available upon request.

The *pch2Δ spo11-HA mek1-as* and *pch2Δ spo11-HA MEK1-GST* strains presented in Table 4 were constructed as follows. The *mek1-as* strain was constructed by digesting the plasmid pJR2 with *Rsr*II and then transforming the *mek1-Q241G::URA3* segment into the *ura3 mek1Δ* SK1 diploid YTS1 (plasmid and strain provided by Nancy Hollingworth). The diploid was then tetrad dissected, selecting for Ura^+ haploid segregants. The homozygous *MEK1-GST* diploid SK1 strain SBY2901 (provided by Sean Burgess) was also tetrad dissected to obtain haploid segregants. The *mek1-as* and *MEK1-GST* segregants described above were mated to EAY2581 (*pch2Δ);* EAY2263 (*pch2Δ spo11-HA);* and SKY635 (*spo11-HA).* The resulting

diploids were sporulated and tetrad dissected to obtain the haploids in Table A1.1 that were then mated to create diploids that were tetrad dissected.

To create the strains used in the sister chromatid exchange assays, the *HIS3* gene was deleted from a haploid segregant of the SK1 diploid EAY28 to create EAY2908. A cross of EAY2908 by EAY2209 (*pch2*Δ in NHY943; ZANDERS and ALANI 2009) generated EAY2910 and EAY2913. The *HIS3* sister chromatid recombination reporter assay contained on plasmid pNN287 (provided by Mike Fasullo) was integrated into the genome near *TRP1* in EAY2913 as described by FASULLO and DAVIS (1987) to create EAY2918. Correct integration of the sister-chromatid recombination assay in EAY2918 was confirmed using Southern blot analysis. EAY2918 was then crossed to EAY2910 to generate strains EAY2951-EAY2952 (wild-type) and EAY2955-EAY2956 (*pch2*Δ*)* used in the sister chromatid recombination experiments.

To measure sister chromatid recombination, saturated YPD overnight cultures were diluted into 22 ml YPA and grown for 17 hours. A sample of each YPA culture (0.4 to 2 ml) was plated on synthetic complete –HIS plates to detect early mitotic sister-chromatid recombination events that would skew meiotic analyses. No such His^+ jackpots were observed in cells plated from YPA cultures (generally, fewer than 1 His^+ cell/ml plated was observed for all strains). After 17 hours, the YPA cultures were spun down, washed once in 1% potassium acetate, resuspended in 10 ml 1% potassium acetate and then allowed to sporulate 24 hours. Undiluted sporulated cells were then plated on synthetic complete –HIS and cell dilutions were plated on synthetic complete media. The frequency of His^+ colony forming units (cfu; His^+ prototrophy in sporulated cells in which spores in asci were not separated) was found by dividing the number of His^+ cfu/ml by the total number of cfu/ml. Experimental replicates in which fewer than 90% of cells sporulated were not included in the data presented.

Meiotic time courses and DSB Southern blotting: For the time courses to analyze meiotic DSB levels, 0.3 ml (for *RAD54* strains) or 0.6 ml (for *rad54*Δ strains) of a saturated YPD overnight culture from each strain to be analyzed was diluted into 200 ml YPA (2% potassium acetate) plus complete amino acid mix and grown for 17 hours. The YPA culture was then spun down, washed once in 1% potassium acetate, and resuspended in 100 ml 1% potassium acetate (ZANDERS and ALANI 2009). All strains were grown in the same batches of media and treated identically. DNA was isolated from meiotic cultures as in BUHLER *et al*. (2007) for *dmc1*Δ strains and as in GOYON and LICHTEN (1993) for *rad50S* strains. The percent DSBs was calculated using Image Quant software. In this analysis a lane profile was generated and used to calculate the total lane signal. Lane background was determined from the blot regions below DSB signals. Only the peaks above lane background were quantified as DSB-specific signals.

Meiotic intrachromatid/intersister and interhomolog recombination assays: his4X::ADE2-his4B/his4XB and his4X/his4B strains were used to measure intrachromatid/intersister (SHINOHARA *et al.,* 1997) and interhomolog (ALANI *et al.,* 1990) recombination events, respectively (Table A1.5). Saturated YPD overnight cultures of wild-type and pch2Δ derivatives of these strains were diluted into YPA and sporulated as described in the meiotic sister-chromatid recombination assay above. To measure vegetative recombination frequencies YPD cultures were diluted and plated onto synthetic complete –HIS and synthetic complete media. To measure meiotic recombination frequencies SPM cultures were treated with zymolyase prior to dilution onto synthetic complete –HIS and synthetic complete media. The frequency of His+ cells was determined by dividing the number of His+ cells/ml by the total number of cells/ml.

RESULTS

***pch2*Δ suppresses *dmc1*Δ arrest by allowing DSB repair:** We initiated this study in SK1 budding yeast to examine a role for Pch2 in ensuring a meiotic arrest/delay in the absence of Dmc1 (ZANDERS and ALANI 2009; SAN-SEGUNDO and ROEDER 1999; WU and BURGESS 2006; MITRA and ROEDER 2007; ZIERHUT *et al*. 2004; HOCHWAGEN *et al*. 2005). Based on recent work showing a role for Pch2 in regulating crossing over in meiosis, we and others hypothesized that Pch2 acts directly in DSB repair (ZANDERS and ALANI 2009; JOSHI *et al.* 2009; WU and BURGESS 2006; HOCHWAGEN *et al*. 2005; BORNER, BAROT and KLECKNER 2008). In such a model *pch2*Δ relieves the *dmc1*Δ arrest by allowing Dmc1-independent DSB repair. Below are physical and genetic studies that are consistent with Pch2 inhibiting DSB repair in *dmc1Δ* cells.

We analyzed visible meiotic DSBs at the *YCR048W* (Chr. III) and *HIS2* (Chr. VI) hot spots in *pch2Δ*, *dmc1Δ*, *spo11-HA*, *rad50S*, and *rad54Δ* strain backgrounds. Six hours after meiotic induction, *dmc1*Δ mutants averaged 11.7±3.0% (standard deviation; n=4 independent cultures) DSBs at *YCRO48W*. *pch2*Δ *dmc1*Δ (9.2±1.0%, n=2) and *spo11-HA dmc1*Δ (7.3±3.0%, n=2) mutants displayed slightly fewer DSBs at this hotspot. Consistent with previous results, the *pch2*Δ *spo11-HA dmc1*Δ triple mutant showed lower DSB levels (2.7±0.7%, n=4; Figure A1.1A; ZANDERS and ALANI 2009). A similar pattern of DSBs was observed at the *HIS2* DSB hotspot on chromosome VI (Figure A1.1B; BULLARD *et al*. 1996).

One explanation for the reduced level of breaks observed in *pch2*Δ *spo11-HA dmc1*Δ mutants is that fewer DSBs are formed in *pch2*Δ mutants. Previous genetic analyses, however, suggest that *pch2Δ* mutants do not form fewer DSBs; *pch2Δ* mutants have increased COs on

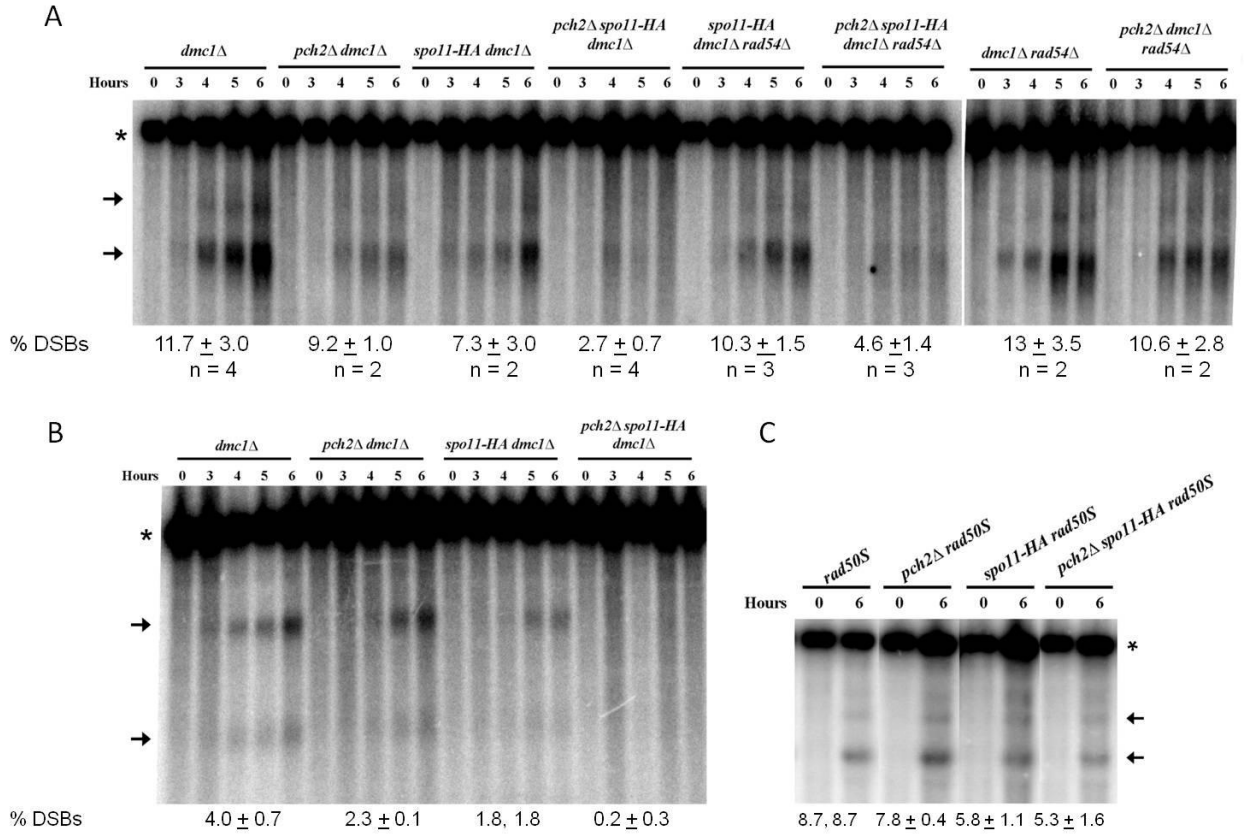

Figure A1.1) DSB levels observed at the *YCRO48W* and *HIS2* hotspots. A. Southern blots were performed on genomic DNA obtained from 0, 3, 4, 5 and 6 hrs post meiotic induction of the indicated strains to measure DSBs at the *YCR048W* hotspot on chromosome III (ZANDERS and ALANI 2009). DNA was digested with *BglII* and probed with a Chr III fragment (SGD coordinates 215,422-216,703). Representative blots of independent replicates (n = 2 to 4) are shown. Asterisk denotes the 11 kb parental band and the arrows designate the DSB bands quantified. The percent DSBs (% of total lane signal) at 6 hrs +/- standard deviation (SD) is shown for each strain. B. Methods used in A were performed to measure DSBs at the *HIS2* hotspot on chromosome VI. The DNA was digested with *BglII* and probed as in BULLARD *et al*. (1996). The asterisk denotes the 5 kb parental band and the arrows designate the DSB bands quantified. The percent DSBs (% of total lane signal) at 6 hrs +/- SD (n =2) is shown for each strain. S.D. is not shown for *spo11-HA pch2*□ because the same percent DSB value was obtained in two independent experiments. C. Southern blots were performed on genomic DNA as shown in A at the *YCR048W* hotspot in *rad50S* strains. A representative blot (n =2) is shown with the percent DSBs (% of total lane signal) at 6 hrs (+/- SD) shown. An SD is not shown for *rad50S* because the same percent DSB value was obtained in two independent experiments. The asterisk denotes the 11 kb parental band and the arrows designate the DSB bands quantified. For panels A-C, similar results were obtained in independent time courses extended to T = 7 hrs.

large chromosomes and increased gene conversion frequencies on chromosomes of all sizes. The opposite effect would be expected from a mutant with reduced DSB frequencies (ZANDERS and ALANI 2009). To formally test if *pch2Δ spo11-HA dmc1Δ* mutants affect DSB formation, we measured DSBs in the *rad50S* mutant background in which they persist (ALANI, PADMORE and KLECKNER 1990). At the *YCR048w* hotspot, *rad50S* and *pch2*Δ *rad50S* mutants showed similar average DSB levels, 8.7% (same value in two independent experiments), and 7.8±0.4%, respectively (n=2; Figure A1.1C). The *spo11-HA rad50S* (5.8±1.1%) and *pch2*Δ *spo11-HA rad50S* (5.3±1.6%) also showed similar levels of DSBs, although the levels were lower than *rad50S* alone, as expected because of the presence of *spo11-HA* (n=2; Figure A1.1C). These results suggest that the decrease in DSBs observed in *pch2*Δ *spo11-HA dmc1*Δ was not due to a decrease in DSB formation.

Low levels of DSBs were observed in *pch2*Δ *spo11-HA dmc1*Δ. Interestingly, these strains showed a dramatic increase in meiotic completion, 39% spore formation, compared to 0% in *dmc1*Δ strains, which showed high levels of DSBs (BISHOP *et al*. 1999; Table A1.2; p <0.005; Figure A1.1). The *pch2*Δ and *spo11-HA* mutations contribute synergistically to the triple mutant phenotype because only a small percentage of *pch2*Δ *dmc1*Δ (4.6%) and *spo11-HA dmc1*Δ (0.4%) cells formed spores. One explanation for phenotype is that the recombination checkpoint is sensitive to the level of unrepaired breaks (see DISCUSSION), such that fewer breaks elicit a less robust checkpoint arrest. Consistent with this interpretation, the *spo11yf-HA* (~30% of wild-type) alleles increase meiotic progression in *dmc1*Δ mutants (*dmc1*Δ, 0% spore formation; *spo11-HA*/*spo11yf-HA dmc1*Δ/*dmc1*Δ, 5% (Table A1.2; p <0.005)).

Table A1.2. Spore formation efficiency and viability in *pch2Δ* mutants

Genotype	% sporulation	number analyzed	% spore viability	spores analyzed
wild-type	79.1	436	93.5	400
pch2Δ	80.9	429	95.3	400
spo11-HA	81.1	434	92.5	400
pch2Δ spo11-HA	74.9	453	56.8	400
dmc1Δ	0.0	406	NA	NA
pch2Δ dmc1Δ	4.6	431	2.9	148
spo11-HA dmc1Δ	0.4	239	NA	NA
pch2Δ spo11-HA dmc1Δ	39.0	439	1.3	160
spo11-HA/spo11yf-HA	79.6	421	ND	ND
pch2Δ/pch2Δ; spo11-HA/spo11yf-HA	67.7	440	ND	ND
spo11-HA/spo11yf-HA; dmc1Δ/dmc1Δ	4.6	415	ND	ND
pch2Δ/pch2Δ; spo11-HA/spo11yf-HA; dmc1Δ/dmc1Δ	42.8	523	ND	ND
rad54Δ	58.3	439	59.5	400
pch2Δ rad54Δ	46.0	443	47.0	400
spo11-HA rad54Δ	63.5	425	62.8	400
pch2Δ spo11-HA rad54Δ	30.7	440	38.0	400
dmc1Δ rad54Δ	0.2	422	NA	NA
pch2Δ dmc1Δ rad54Δ	0.0	444	NA	NA
spo11-HA dmc1Δ rad54Δ	0.0	409	NA	NA
pch2Δ spo11-HA dmc1Δ rad54Δ	0.0	403	NA	NA
spo13	63.3	441	47.3	400
pch2Δ spo13	49.2	417	44.8	400
spo11-HA spo13	51.8	454	44.8	400
pch2Δ spo11-HA spo13	56.9	457	44.3	400
dmc1Δ spo13	9.6	428	7.3	400
pch2Δ dmc1Δ spo13	43.4	422	15.5	400
spo11-HA dmc1Δ spo13	16.6	441	16.0	400
pch2Δ spo11-HA dmc1Δ spo13	57.9	480	25.5	396
pch2Δ spo11-HA dmc1Δ rad54Δ spo13	14.0	222	0.0	120

Sporulation efficiencies for the above strains were counted after five days on sporulation media at 30° C. Tetrads (for *SPO13* strains) or dyads (from *spo13* strains) were dissected on YPD and scored for spore viability after three days. NA indicates that % spore viability is not applicable for strains that do not sporulate. ND indicates that spore viability was not assayed.

Spores produced by *pch2*Δ *dmc1*Δ and *spo11-HA pch2*Δ *dmc1*Δ were mostly inviable (<3% spore viability for each), suggesting that interhomolog recombination was not restored in these mutants (Table A1.2). We tested whether other types of repair occurred in the *spo13* mutant background in which a mixed chromosome division occurs: some chromosomes undergo an equational division whereas others segregate reductionally (KLAPHOLZ and ESPOSITO 1980; HUGERAT and SIMCHEN 1993). *spo13* mutants can produce viable meiotic progeny in the absence of meiotic DSBs, or if DSB repair does not yield COs (e.g. MALONE and ESPOSITO 1981). Because of this, spore viability analyses in the *spo13* mutant background can detect DSB repair that does not facilitate proper MI chromosome segregation (BISHOP *et al*. 1999).

Similar to previous work in SK1 strains, *spo13 dmc1*Δ showed low levels of sporulation (10%) and spore viability (7%), compared to *spo13* (63% sporulation, 47% viability; Table A1.2; $p < 0.005$ for both sporulation and spore viability; BISHOP *et al*. 1999). Introducing the *spo11-HA* allele to *dmc1*Δ *spo13* increased spore formation in the resulting triple mutant to 17% and spore viability to 16% (Table A1.2; $p < 0.005$ for both sporulation and spore viability). This result is expected because fewer DSBs are produced in *spo11-HA* strains (MARTINI *et al*. 2006; JOHNSON *et al*. 2007). Deleting *PCH2* in *dmc1*Δ *spo13* had a strong effect; sporulation in this triple mutant increased to 43% and spore viability increased to 16% (Table A1.2; $p < 0.005$ for both sporulation and spore viability). The s*po11-HA pch2*Δ *spo13 dmc1*Δ quadruple mutant showed even greater sporulation (58%) and spore viability (26%; Table A1.2; $p < 0.005$ for both sporulation and spore viability). These results are consistent with some Dmc1-independent repair occurring in *pch2Δ dmc1Δ* mutants.

pch2*Δ mutants have an increased dependence on Rad54 mediated repair*: Sporulation of *pch2*Δ *spo11-HA dmc1*Δ mutants and spore viability of the *pch2*Δ *spo11-HA dmc1*Δ *spo13* mutants were Rad54-dependent, suggesting that Rad54 is repairing breaks in these mutants (Table A1.2). During vegetative growth, DSBs are preferentially repaired by homologous recombination involving sister chromatids in steps that are mediated by the Rad51 recombinase and its partner Rad54 (KADYK and HARTWELL 1992; ARBEL, ZENVIRTH and SIMCHEN 1999; SHINOHARA *et al*. 1997b; KROGH and SYMINGTON 2004). Consistent with Rad54-dependent recombination in *pch2*Δ mutants, we observed a reduction in sporulation (46%) and spore viability (47%) in the *pch2*Δ *rad54*Δ double mutant compared to *pch2*Δ (81% sporulation and 95% spore viability) and *rad54*Δ single mutants (58% sporulation and 60% spore viability; Table A1.2; $p < 0.005$ for all comparisons). Interestingly, CO levels were not reduced in *pch2*Δ *rad54*Δ compared to *pch2*Δ, suggesting the Rad54-dependent recombination in *pch2*Δ mutants is intersister (Table A1.3).

An important prediction of the above genetic analyses is that the *rad54*Δ mutation should result in a restoration of observed DSBs in the *pch2*Δ *spo11-HA dmc1*Δ mutant. This prediction was not met; 4.6±1.4% DSBs (n=3) were observed at *YCRO48W* in *pch2*Δ *spo11-HA dmc1*Δ *rad54*Δ, compared to 2.7±0.7% (n=4) in *pch2*Δ *spo11-HA dmc1*Δ and 10.3±1.5% (n=3) in *spo11-HA dmc1*Δ *rad54*Δ six hours after meiotic induction (Figure A1.1). It is possible that both Dmc1 and Rad54-independent repair can occur in the absence of these factors in a *pch2*Δ background. Another possibility is that hyper-resected DSBs form in *pch2*Δ *spo11-HA dmc1*Δ *rad54*Δ that cannot be detected by Southern blot. More experimentation is needed to understand this phenotype.

***pch2 spo11-HA* phenotype is modulated by Mek1 activity.** Previously we showed

Table A1.3. *pch2Δ* and *pch2Δ rad54Δ* display similar meiotic crossover levels

	Total Spores	Recombinant	Parental	% Recombinant
Chromosome III				
HIS3-LEU2				
wild-type	2711	351	2360	12.9
*pch2*Δ	2691	389	2302	14.5
*pch2*Δ *rad54*Δ	458	62	396	13.5
LEU2-CEN3				
wild-type	2711	184	2527	6.8
*pch2*Δ	2691	241	2450	9.0
*pch2*Δ *rad54*Δ	458	41	417	9.0
CEN3-MAT				
wild-type	2711	402	2309	14.8
*pch2*Δ	2691	374	2317	13.9
*pch2*Δ *rad54*Δ	458	65	393	14.2
Chromosome VII				
TRP5-CYH2				
wild-type	2711	908	1803	33.5
*pch2*Δ	2691	1149	1542	42.7
*pch2*Δ *rad54*Δ	458	199	259	43.4
CYH2-MET13				
wild-type	2711	260	2451	9.6
*pch2*Δ	2691	469	2222	17.4
*pch2*Δ *rad54*Δ	458	81	377	17.7
MET13-LYS5				
wild-type	2711	559	2152	20.6
*pch2*Δ	2691	747	1944	27.8
*pch2*Δ *rad54*Δ	458	139	319	30.3
Chromosome VIII				
CEN8-THR1				
wild-type	2711	606	2105	22.4
*pch2*Δ	2691	649	2042	24.1
*pch2*Δ *rad54*Δ	458	116	342	25.3
THR1-CUP1				
wild-type	2711	668	2043	24.6
*pch2*Δ	2691	948	1743	35.2
*pch2*Δ *rad54*Δ	458	123	335	26.9

wild-type (NH942/NH943*), pch2Δ* (EAY2209/EAY2210) *and pch2Δ rad54Δ* strains (EAY2681/EAY2685) were sporulated and analyzed for segregation of genetic markers in the NH942/NH943 strain background. Crossover frequencies in this strain were calculated from recombination frequencies in spores as described previously (ZANDERS and ALANI 2009). Data for wild-type and *pch2Δ* are from ZANDERS and ALANI (2009). Spore viability was 91% for wild-type (n =743 tetrads dissected), 97% for *pch2Δ* (n =707 tetrads) and 45% for *pch2Δ rad54Δ* (n = 256 tetrads).

(ZANDERS and ALANI 2009) that *pch2*Δ *spo11-HA* strains have a spore viability defect, and hypothesized that the decreased spore viability was due to defects in CO interference and partner choice. If a compromised interhomolog bias contributes to the *pch2Δ spo11-HA* phenotype, then further undermining interhomolog bias should enhance the phenotype. Alternatively, reinforcing interhomolog bias should suppress the *pch2Δ spo11-HA* phenotype. To test this hypothesis we utilized two *MEK1* alleles: *mek1-as* (*mek1-Q241G* hypomorph; CALLENDER and HOLLINGSWORTH, 2010) and *MEK1-GST* (hypermorph; WU, HO, and BURGESS 2010). *mek1-as* strains complete meiosis efficiently in the absence of 1-Na-PP1 inhibitor and display nearly wild-type spore viability; however, Mek1-as has reduced affinity for ATP *in vitro*, and in one *dmc1Δ* strain background the *mek1-as* mutation conferred phenotypes consistent with defects in interhomolog bias (CALLENDER and HOLLINGSWORTH 2010; WAN *et al.* 2004; NIU *et al.* 2009). WU, HO and BURGESS (2010) recently showed that *MEK1-GST* is a semi-dominant allele that shows increased interhomolog recombination events, primarily noncrossovers, and fewer intersister events, with no change in DSB levels.

As shown in Table A1.4, we constructed *mek1-as pch2*Δ *spo11-HA* and *MEK1-GST pch2*Δ *spo11-HA* strains and examined their spore formation efficiency and viability (*mek1-as* strains were analyzed in the absence of 1-Na-PP1 inhibitor). We found that the *mek1-as* mutation reduced the spore viability of *pch2*Δ *spo11-HA* strains from 57% to 41% ($p < 0.005$). The *mek1-as* mutation did not significantly affect the spore viability of either single mutant alone (Table A1.4). The *MEK1-GST* allele increased spore viability in *pch2*Δ *spo11-HA* strains from 57% to 89% ($p < 0.005$); however, as described previously (WU, HO and BURGESS 2010), there was a general defect in spore formation due to *MEK1-GST*. *MEK1-GST* did not increase

Table A1.4. Spore formation efficiency and viability in *mek1-as and MEK1-GST* mutants

Genotype	% sporulation	number analyzed	% spore viability	spores analyzed
wild-type	79.1	436	93.5	400
*pch2*Δ	80.9	429	95.3	400
spo11-HA	81.1	434	92.5	400
mek1-as	84.7	163	98.8	80
MEK1-GST	66.9	178	87.5	160
*pch2*Δ *spo11-HA*	74.9	453	56.8	400
mek1-as spo11-HA	87.8	164	92.3	400
mek1-as pch2Δ	88.5	191	92.0	400
MEK1-GST spo11-HA	69.8	162	85.4	546
MEK1-GST pch2Δ	67.5	155	86.5	408
pch2Δ spo11-HA mek1-as	85.8	183	40.8	400
pch2Δ spo11-HA MEK1-GST	63.5	143	89.0	552

Sporulation efficiencies for the above strains were counted after five days on sporulation media at 30° C. Tetrads were dissected on YPD and scored for spore viability after three days.

the spore viability in either single mutant (Table A1.4). These data are consistent with our hypothesis that excess intersister repair contributes to spore inviablity of *pch2Δ spo11-HA*.

Evidence that Pch2 promotes interhomolog DSB repair: We assayed DSB repair outcomes using the his4X::ADE2-his4B/his4XB recombination reporter assay in which His+ colonies can arise via intrachromatid or intersister recombination and the his4X/his4B assay in which interhomolog repair can yield His+ colonies (Table A1.5; (ALANI *et al.*, 1990, SHINOHARA *et al.*, 1997). Reminiscent of previous work showing that the pch2Δ mutation did not alter chromosome III genetic map distances (ZANDERS and ALANI, 2009), the pch2Δ mutation did not significantly alter His+ frequency in either assay (see Discussion). To more directly test if there is an increase in intersister repair in *pch2Δ* we adapted an assay developed by FASULLO and DAVIS (1987) to measure sister chromatid exchange in meiosis. This assay utilizes a *HIS3* reporter gene in which cells become His^+ if a sister-chromatid recombination event (either a CO or gene conversion) occurs between two *his3* truncations to produce full length *HIS3*. The mean frequency of His^+ colonies was 1.6×10^{-6} (n=22 independent cultures) in wild-type and 5.3×10^{-6} in cells lacking Pch2 (n=24). *pch2*Δ values were significantly higher than wild-type (p=0.008, Mann-Whitney U test).

DISCUSSION

We provide several independent lines of evidence consistent with a role for Pch2 in inhibiting Dmc1-independent intersister DSB repair in meiosis. First, *pch2Δ* contributes to a reduction of unrepaired DSBs visible on Southern blots in *spo11-HA dmc1Δ* mutants (Figure A1.1). This reduction in detectable DSBs appears to be due to DSB repair because the levels of DSBs formed, as measured in a *rad50S* background, are not affected by *pch2Δ* and the spore

Table A1.5 Recombination frequency in vegetative growth and meiosis as measured in intrachromatid/intersister and interhomolog recombination assays.

Strain, independent replicates	Vegetative Frequency ($x10^{-3}$)		Meiotic Frequency ($x10^{-3}$)	
	His^+ Ade^+	His^+ Ade^-	His^+ Ade^+	His^+ Ade^-
His4X::ADE2-his4B/hisXB				
1	0.10	0.038	8.2	6.3
2	0.011	0.040	18.1	9.7
3	0.0078	0.0072	0.70	1.2
4	0.0056	0.0044	8.5	8.7
5	0.00094	0.0015	1.1	3.0
6	0.18	0.12	1.9	2.8
7	0.02	0.02	11.3	21.5
8	0.24	0.17	17.7	45.2
9			4.0	6.0
10			7.5	13.3
Mean	0.071	0.05	7.9	11.8
Median	0.016	0.029	7.9	7.5
pch2Δ/pch2Δ, his4X::ADE2-his4B/his4XB				
1	0.01	0.04	6.0	4.0
2	0.015	0.011	5.9	3.2
3	0.015	0.0075	3.9	3.3
4	0.0035	0.0019	18.8	43.8
5	0.64	0.27	1.9	4.9
6	0.081	0.049	5.4	11.6
7	0.026	0.01	12.8	31.2
8			9.2	26.5
9			2.2	4.9
10			14.6	19.9
Mean	0.11	0.056	8.1	15.3
Median	0.015	0.011	6.0	8.3

Strain ***His4X/his4B***	Vegetative His^+ Freq. ($x10^{-3}$)	Meiotic His^+ Freq. ($x10^{-3}$)
1	1.6	10.7
2	0.031	8.4
3	0.024	18.9
4	0.0013	13.0

5	0.78	17.6
6	0.0031	24.0
7	0.0031	15.4
8		1.2
9		49.0
Mean	0.35	17.6
Median	0.02	15.4
pch2Δ/pch2Δ,his4X/his4B		
1	0.0041	4.1
2	0.025	3.9
3	0.00083	6.8
4	0.00034	62.5
5	0.47	92.6
6	0.0019	14.0
7	0.087	24.5
8		43.5
9		1.0
10		1.5
Mean	0.084	25.4
Median	0.0041	10.4

Plating of vegetative and meiotic cultures was performed as described in the Materials and Methods. The vegetative and meiotic frequencies are matched-the same vegetative (YPD) culture used to measure vegetative frequency was sporulated. Sporulation efficiencies, 85 to 97%, were similar in wild-type and pch2Δ strains. Strains used for the his4X::ADE2-his4B assays were the parental DKB763/DKB765 (wild-type) and pch2Δ::KANMX/pch2Δ::KANMX (EAY3028/EAY3029) derivative. Strains used for the his4X/his4B assays were the parental NKY859/860 (wild-type), and the pch2Δ::KANMX/pch2Δ::KANMX (EAY3024/EAY3025) derivative.

A one-sided Mann-Whitney test was used to assess the significance of the data:

		p-value, *his4X::ADE2-his4B/his4XB* assay	p-value, *his4X/his4B* assay
vegetative	WT vs. *pch2*Δ	0.43 (Ade^+), 0.45 (Ade^-)	0.22
meiotic	WT vs. *pch2*Δ	0.41 (Ade^+), 0.31 (Ade^-)	0.42

inviability seen in *pch2Δ dmc1Δ* and *pch2Δ spo11-HA dmc1Δ* mutants is suppressed by *spo13Δ* (Table A1.2). We hypothesize that the DSB repair occurring in *pch2Δ spo11-HA dmc1Δ* is intersister because it does not facilitate proper MI chromosome segregation. Our epistasis analysis of *pch2Δ rad54Δ* suggests that *pch2Δ* mutants are more dependent on Rad54-dependent repair, but that Rad54 does not appear to contribute to interhomolog CO repair in *pch2Δ.* These data further support the idea that *pch2Δ* mutants have increased intersister repair. In addition, we demonstrated that a *mek1* hypomorph enhanced the spore death phenotype of *pch2Δ spo11-HA* whereas a *MEK1* gain of function allele suppressed the phenotype. These experiments are consistent with excess intersister DSB repair contributing to spore inviability of *pch2Δ spo11-HA.* Finally, our genetic reporter assay demonstrated an increase in intersister DSB repair at one locus.

We did not observe significant changes in recombination using the his4X::ADE2-his4B/his4XB or the his4X/his4B assays (Table A1.5; ALANI *et al.,* 1990, SHINOHARA *et al.,* 1997). Additionally, our physical assays of break formation showed less Rad54-dependence in pch2Δ mutants than our genetic experiments. These results may stem from the fact that the physical assays involve loci located on chromosome III. Previously, we reported a dramatic increase in interhomolog crossover frequencies in pch2Δ on chromosomes VIII, VII, and XV (ZANDERS and ALANI, 2009), but no such change was seen on chromosome III. It is unclear why the phenotype of the pch2Δ mutant appears different on chromosome III, but we suspect the small size of this chromosome could play a role; smaller chromosomes have higher map distances per physical distance and weaker interference relative to larger chromosomes (e.g. CHEN *et al.,* 2008). These results, combined with those of HYPPA and SMITH (2010) demonstrating different DSB repair preferences at different sites in Schizosaccharomyces pombe

genome, illustrate the challenge of interpreting data obtained from a limited number of chromosomal sites. This may be especially true for chromosome III in S. cerevisiae, which is arguably the most studied site for meiotic recombination.

Our data and those of other groups are consistent with recombination checkpoint signaling being sensitive to unrepaired DSB levels, such that more DSBs trigger checkpoint arrest in a greater proportion of the cell population (GOLDFARB and LICHTEN 2010; CALLENDER AND HOLLINGSWORTH 2010; JOHNSON *et al.* 2007; BHALLA AND DERNBURG 2005; MALKOVA *et al*. 1996; MACQUEEN *et al.* 2005). In wild-type cells, DSBs are quickly repaired and the Mek1-mediated checkpoint delay is transient. In *dmc1Δ*, DSBs are not repaired and Mek1 elicits checkpoint arrest. When DSBs are reduced in *dmc1Δ* strains containing *spo11* hypomorph alleles, the checkpoint response is less robust and fewer cells arrest. We hypothesize that the *spo11-HA* and *pch2*Δ mutations independently contribute to reducing the level of unrepaired DSBs available to trigger the recombination checkpoint in *dmc1Δ* mutants: *spo11-HA* forms fewer DSBs and *pch2Δ* acts by allowing Dmc1-independent repair. In this model, the combination of *spo11-HA* and *pch2Δ* in a *dmc1Δ* background synergistically contribute to DSB repair due to a positive feedback loop wherein fewer DSBs elicit less checkpoint activation, which allows even more DSB repair and meiotic progression. At present we do not have a good sense for the number of DSBs that would be needed to elicit checkpoint activation; however, work from MALKOVA *et al*. (1996) showed that a single unrepaired DSB does not arrest meiosis.

Pch2 acts in meiotic CO control to limit CO formation on large chromosomes and promote CO interference (ZANDERS and ALANI 2009; JOSHI *et al*. 2009). This work

suggests a broader role for Pch2 in DSB repair that includes inhibiting intersister DSB repair. Although the mechanism of Pch2 function in DSB repair is unknown, there are several avenues worthy of investigation. RTEL-1, the *C. elegans* homolog of the yeast Srs2 helicase has been shown to be defective in CO interference and CO homeostasis (YOUDS *et al*. 2010). Thus one possibility is that Pch2 facilitates access of a helicase to remove inappropriate strand invasion events. BORNER, BAROT and KLECKNER (2008) first posited another attractive (and not mutually exclusive) hypothesis that Pch2 somehow promotes Mec1 regulatory action. Indeed, at least one Mek1 effector (a Mec1 target) that promotes interhomolog bias is still unknown (HOLLINGSWORTH 2010; NIU *et al*. 2009). This effector could be Pch2 acting to augment or promote Mek1 activity. Under this model Mek1 signaling is attenuated in *pch2Δ* mutants, allowing excess intersister repair. Such an idea is consistent with work from WU, HO and BURGESS (2010) who showed that an activated *MEK1* allele (*MEK1-GST*) promoted an increase in interhomolog events that were primarily repaired as NCOs, and fewer intersister events, with no change in DSB levels (WU, HO and BURGESS 2010), and previous data showing that *pch2Δ* mutants display increased CO events at the expense of NCOs (ZANDERS and ALANI 2009). Experiments to test these hypotheses are underway.

ACKNOWLEDGMENTS

We are grateful to Valentin Boerner, Andreas Hochwagen, Michael Lichten and Scott Keeney for providing unpublished data, and Chip Aquadro, Joshua Filter, Heather Flores, Tamara Goldfarb, Nancy Hollingsworth, and Michael Lichten for critical comments and technical advice. We thank Mike Fasullo for providing the *HIS3* sister chromatid exchange plasmid, and Nancy Hollingsworth and Sean Burgess for providing the *mek1-as* and *MEK1-GST* alleles, respectively. Lastly, we are grateful to Nancy Hollingsworth for helpful discussions.

This work was supported by NIH grant GM53085 supplemented with an ARRA award to E.A. S.Z. and M.S.B. were supported by NIH training grants awarded to Cornell University.

REFERENCES

ALANI, E., R. PADMORE, and N. KLECKNER, 1990 Analysis of wild-type and *rad50* mutants of yeast suggests an intimate relationship between meiotic chromosome synapsis and recombination. Cell **61**: 419-436.

ARBEL, A., D. ZENVIRTH and G. SIMCHEN, 1999 Sister chromatid-based DNA repair is mediated by *RAD54*, not by *DMC1* or *TID1*. EMBO J. **18**: 2648-2658.

ARGUESO, J. L., J. WANAT, Z. GEMICI, and E. ALANI, 2004 Competing crossover pathways act during meiosis in *Saccharomyces cerevisiae*. Genetics **16**8: 1805-1816.

BERCHOWITZ, L. E. and G. P. COPENHAVER, 2010 Genetic Interference: Don't stand so close to me. Current Genomics **11**: 91-102.

BHALLA, N. and A. F. DERNBURG, 2005 A conserved checkpoint monitors meiotic chromosome synapsis in *Caenorhabditis elegans*. Science **310**: 1683-1686.

BISHOP, D. K., Y. NIKOLSKI, J. OSHIRO, J. CHON, M. SHINOHARA, *et al*., 1999 High copy number suppression of the meiotic arrest caused by a *dmc1* mutation: *REC114* imposes an early recombination block and *RAD54* promotes a *DMC1*-independent DSB repair pathway. Genes Cells **4**: 425-444.

BISHOP, D. K., D. PARK, L. XU and N. KLECKNER, 1992 *DMC1*: a meiosis-specific yeast homolog of *E. coli recA* required for recombination, synaptonemal complex formation, and cell cycle progression. Cell **69:** 439-456.

BISHOP, D. K. and D. ZICKLER, 2004 Early decision; meiotic crossover interference prior to stable strand exchange and synapsis. Cell **117**: 9-15.

BLITZBLAU, H. G., G. W. BELL, J. RODRIGUEZ, S. P. BELL and A. HOCHWAGEN, 2007 Mapping of meiotic single-stranded DNA reveals double-stranded-break hotspots near centromeres and telomeres. Curr. Biol. **17**: 2003-2012.

BORNER, G. V., A. BAROT and N. KLECKNER, 2008 Yeast Pch2 promotes domainal axis organization, timely recombination progression, and arrest of defective recombinosomes during meiosis. Proc. Natl. Acad. Sci. USA **105**: 3327-3332.

BORNER, G. V., N. KLECKNER, and N. HUNTER, 2004 Crossover/noncrossover differentiation, synaptonemal complex formation, and regulatory surveillance at the leptotene/zygotene transition of meiosis. Cell **117**: 29-45.

BUHLER, C., V. BORDE, and M. LICHTEN, 2007 Mapping meiotic single-strand DNA reveals a new landscape of DNA double-strand breaks in *Saccharomyces cerevisiae*. PLoS Biol. **5**: e324.

BULLARD, S. A., S. KIM, A. M. GALBRAITH, and R. E. MALONE, 1996 Double strand breaks at the *HIS2* recombination hot spot in *Saccharomyces cerevisiae*. Proc. Natl. Acad. Sci. USA **93**: 13054-13059.

BUSYGINA, V., M. G. SEHORN, I. Y. SHI, H. TSUBOUCHI, G. S. ROEDER, *et al*., 2008 Hed1 regulates Rad51-mediated recombination via a novel mechanism. Genes Dev. **22**: 786-795.

CALLENDER, T. and N. M. HOLLINGSWORTH, 2010 Mek1 suppression of meiotic double strand break repair is specific to sister chromatids, chromosome autonomous and independent of Rec8 cohesin complexes. Genetics **185**: 771-782.

CARBALLO, J. A., A. L. JOHNSON, S. G. SEDGWICK and R. S. CHA, 2008 Phosphorylation of the axial element protein Hop1 by Mec1/Tel1 ensures meiotic interhomolog recombination. Cell **132**: 758-770.

CHEN, S. Y., T. TSUBOUCHI, B. ROCKMILL, J. S. SANDLER, D. R. RICHARDS, *et al*., 2008 Global analysis of the meiotic crossover landscape. Dev. Cell **15**: 401-415.

DE LOS SANTOS, T., N. HUNTER, D. LEE, B. LARKIN, J. LOIDL, *et al.*, 2003 The Mus81/Mms4 endonuclease acts independently of double-Holliday junction resolution to promote a distinct subset of crossovers during meiosis in budding yeast. Genetics **164**: 81-94.

DE MASSY, B., F. BAUDAT, and A. NICOLAS, 1994 Initiation of recombination in *Saccharomyces cerevisiae* haploid meiosis. Proc. Natl. Acad. Sci. USA **91**: 11929-11933.

DRESSER, M. E., D. J. EWING, M. N. CONRAD, A. M. DOMINGUEZ, R. BARSTEAD, *et al*., 1997 *DMC1* functions in a *Saccharomyces cerevi*siae meiotic pathway that is largely independent of the *RAD51* pathway. Genetics **147**: 533-544.

FASULLO, M. T. and R. W. DAVIS, 1987 Recombinational substrates designed to study recombination between unique and repetitive sequences *in vivo*. Proc. Natl. Acad. Sci. USA **84**: 6215-6219.

GIETZ, R. D., R. H. SCHIESTL, A. R. WILLEMS, and R. A. WOODS, 1995 Studies on the transformation of intact yeast cells by the LiAc/SS-DNA/PEG procedure. Yeast **11**: 355-360.

GOLDFARB, T., and M. LICHTEN, 2010 The sister chromatid is frequently and efficiently used for DNA double-strand break repair during budding yeast meiosis. PLoS Biol. **8**: e1000520.

GOLDSTEIN, A. L. and J. H. MCCUSKER, 1999 Three new dominant drug resistance cassettes for gene disruption in *Saccharomyces cerevisiae*. Yeast **15**: 1541-1553.

GOYON, C., and M. LICHTEN, 1993 Timing of molecular events in meiosis in *Saccharomyces cerevisiae*: stable heteroduplex DNA is formed late in meiotic prophase. Mol. Cell. Biol. **13**: 373-382.

HASSOLD, T., H. HALL, and P. HUNT, 2007 The origin of human aneuploidy: where we have been, where we are going. Hum. Mol. Genet. 16: R203-R208.

HOCHWAGEN, A., W. H. THAM, G. A. BRAR, and A. AMON, 2005 The FK506 binding protein Fpr3 counteracts protein phosphatase 1 to maintain meiotic recombination checkpoint activity. Cell **122**: 861-873.

HOLLINGSWORTH, N. M., 2010 Phosphorylation and the creation of interhomolog bias during meiosis in yeast. Cell Cycle **9**: 436-437.

HOLLINGSWORTH, N. M. and B. BYERS, 1989 *HOP1*: a yeast meiotic pairing gene. Genetics **121**: 445-462.

HOLLINGSWORTH, N. M., L. GOETSCH, and B. BYERS, 1990 The *HOP1* gene encodes a meiosis-specific component of yeast chromosomes. Cell **61**: 73-84.

HUGERAT, Y., and G. SIMCHEN, 1993 Mixed segregation and recombination of chromosomes and YACs during single-division meiosis in *spo13* strains of *Saccharomyces cerevisiae*. Genetics **135**: 297-308.

HYPPA, R. W., G. R. SMITH, 2010 Crossover invariance determined by partner choice for meiotic DNA break repair. Cell **142**: 243-255.

JACKSON, J. A. and G. R. FINK, 1985 Meiotic recombination between duplicated genetic elements in *Saccharomyces cerevisiae*. Genetics **109**: 303-332.

JOHNSON, R., V. BORDE, M. J. NEALE, A. BISHOP-BAILEY, M. NORTH, *et al.*, 2007 Excess single-stranded DNA inhibits meiotic double-strand break repair. PLoS Genet. **3**: e223.

JONES, G. H. and F. C. FRANKLIN, 2006 Meiotic crossing-over: obligation and interference. Cell **126**: 246-248.

JOSHI, N., A. BAROT, C. JAMISON, and G. V. BORNER, 2009 Pch2 links chromosome axis remodeling at future crossover sites and crossover distribution during yeast meiosis. PLoS Genet. **5**: e1000557.

KADYK, L. C. and L. H. HARTWELL, 1992 Sister chromatids are preferred over homologs as substrates for recombinational repair in *Saccharomyces cerevisiae*. Genetics **132**: 387-402.

KLAPHOLZ, S., and R. E. ESPOSITO, 1980 Isolation of *SPO12*-1 and *SPO13*-1 from a natural variant of yeast that undergoes a single meiotic division. Genetics **96**: 567-588.

KLEIN, H. L, 1997 *RDH54*, a *RAD54* homologue in *Saccharomyces cerevisiae*, is required for mitotic diploid-specific recombination and repair and for meiosis. Genetics **147**: 1533-1543.

KROGH, B. O., and L. S. SYMINGTON, 2004 Recombination proteins in yeast. Annu. Rev. Genet. **38**: 233-271.

LI, X. C., and J. SCHIMENTI, 2007 Mouse pachytene checkpoint 2 (*trip13*) is required for completing meiotic recombination but not synapsis. PLoS Genet. **3**: e130.

LYDALL, D., Y. NIKOLSKY, D. K. BISHOP and T. A. WEINERT, 1996 A meiotic recombination checkpoint controlled by mitotic checkpoint genes. Nature **383**: 840-843.

MACQUEEN, A. J., C. M. PHILLIPS, A. BHALLA, P. WEISER, A. M. VILLENEUVE, *et al.*,

2005 Chromosome sites play dual roles to establish homologous synapsis during meiosis in *C. elegans*. Cell **123**: 1037-1050.

MALKOVA, A., L. ROSS, D. DAWSON, M. F. HOEKSTRA, and J. E. HABER, 1996 Meiotic recombination initiated by a double-strand break in *rad50* delta yeast cells otherwise unable to initiate meiotic recombination. Genetics **143**: 741-754.

MALONE, R. E., and R. E. ESPOSITO, 1981 Recombinationless meiosis in *Saccharomyces cerevisiae*. Mol. Cell. Biol. **1**: 891-901.

MANCERA, E., R. BOURGON, R. BROZZI, W. HUBER, and L .M. STEINMETZ, 2008 High-resolution mapping of meiotic crossovers and non-crossovers in yeast. Nature **454**: 479-485.

MARTINI, E., R. L. DIAZ, N. HUNTER and S. KEENEY, 2006 Crossover homeostasis in yeast meiosis. Cell **126**: 285-295.

MITRA, N. and G. S. ROEDER, 2007 A novel nonnull *ZIP1* allele triggers meiotic arrest with synapsed chromosomes in *Saccharomyces cerevisiae*. Genetics **176**: 773-787.

NIU, H., X. LI, E. JOB, C. PARK, D. MOAZED, *et al*., 2007 Mek1 kinase is regulated to suppress double-strand break repair between sister chromatids during budding yeast meiosis. Mol. Cell. Biol. **27**: 5456-5467.

NIU, H., L. WAN, B. BAUMGARTNER, D. SCHAEFER, J. LOIDL, *et al.*, 2005 Partner choice during meiosis is regulated by Hop1-promoted dimerization of Mek1. Mol. Biol. Cell **16**: 5804- 5818.

NIU, H., L. WAN, V. BUSYGINA, Y. KWON, J. A. ALLEN, *et al*., 2009 Regulation of meiotic recombination via Mek1-mediated Rad54 phosphorylation. Mol. Cell **36**: 393-404.

ROCKMILL, B., and G. S. ROEDER, 1990 Meiosis in asynaptic yeast. Genetics 126: 563-574.

ROEDER, G. S., 1997 Meiotic chromosomes: it takes two to tango. Genes Dev. **11**: 2600-2621.

ROIG, I., J. A. DOWDLE, A. TOTH, D. G. DE ROOJ, M. JASIN, *et al.*, 2010 Mouse

TRIP13/PCH2 is required for recombination and normal higher order chromosome structure during meiosis. PLoS Genet. **6**: e1001062.

SAN-SEGUNDO, P. A. and G. S. ROEDER, 1999 Pch2 links chromatin silencing to meiotic checkpoint control. Cell **97**: 313-324.

SCHWACHA, A., and N. KLECKNER, 1994 Identification of joint molecules that form frequently between homologs but rarely between sister chromatids during yeast meiosis. Cell **76**: 51-63.

SCHWACHA, A. and N. KLECKNER, 1997 Interhomolog bias during meiotic recombination: meiotic functions promote a highly differentiated interhomolog-only pathway. Cell **90**: 1123-1135.

SHINOHARA, A., S. GASIOR, T. OGAWA, N. KLECKNER, and D. K. BISHOP, 1997a *Saccharomyces cerevisiae* recA homologs RAD51 and DMC1 have both distinct and overlapping roles in meiotic recombination. Genes Cells **2**: 615-629.

SHINOHARA, M., E. SHITA-YAMAGUCHI, J. M. BUERSTEDDE, H. SHINAGAWA, H. OGAWA, *et al*., 1997b Characterization of the roles of the *Saccharomyces cerevisiae RAD54* gene and a homologue of *RAD54*, *RDH54*/*TID1*, in mitosis and meiosis. Genetics **147**: 1545-1556.

SYM, M. and G. S. ROEDER, 1995 Zip1-induced changes in synaptonemal complex structure and polycomplex assembly. J. Cell Biol. **128**: 455-466.

TERENTYEV, Y., R. JOHNSON, M. J. NEALE, M. KHISROON, A. BISHOP-BAILEY, and A. S. GOLDMAN, 2010 Evidence that MEK1 positively promotes interhomologue double-strand break repair. Nucl. Acids Res. **38**: 4349-4360.

THOMPSON, D. A. and F. W. STAHL, 1999 Genetic control of recombination partner preference in yeast meiosis. Isolation and characterization of mutants elevated for meiotic unequal sister-chromatid recombination. Genetics **153**: 621-641.

TSUBOUCHI, H., and G. S. ROEDER, 2003 The importance of genetic recombination for fidelity of chromosome pairing in meiosis. Dev. Cell **5**: 915-925

TSUBOUCHI, H., and G. S. ROEDER, 2006 Budding yeast Hed1 down-regulates the mitotic recombination machinery when meiotic recombination is impaired. Genes Dev. **20**: 1766-

1775.

WACH, A., A. BRACHAT, R. POHLMANN, and P. PHILIPPSEN, 1994 New heterologous modules for classical or PCR-based gene disruptions in *Saccharomyces cerevisiae*. Yeast **10**: 1793-1808.

WAN, L., T. DE LOS SANTOS, C. ZHANG, K. SHOKAT, and HOLLINGSWORTH, 2004 Mek1 kinase activity functions downstream of *RED1* in the regulation of meiotic double strand break repair in budding yeast. Mol. Biol. Cell. **15**: 11-23.

WEBBER, H. A., L. HOWARD, and S. E. BICKEL, 2004 The cohesion protein ORD is required for homologue bias during meiotic recombination. J. Cell. Biol. **164**: 819-829.

WOJTASZ, L. K. DANIEL, I. ROIG, E. BOLCUN-FILAS, H. XU, *et al*., 2009 Mouse HORMAD1 and HORMAD2, two conserved meiotic chromosomal proteins, are depleted from synapsed chromosome axes with the help of TRIP13 AAA-ATPase. PLoS Genet. **5**: e1000702.

WU, H. Y., and S. M. BURGESS, 2006 Two distinct surveillance mechanisms monitor meiotic chromosome metabolism in budding yeast. Curr. Biol. **16**: 2473-2479.

WU, H. Y., H. C. HO and S. M. BURGESS, 2010 Mek1 kinase governs outcomes of meiotic recombination and the checkpoint response. Curr. Biol. **20**: 1707-1716.

XU, L., B. M. WEINER and N. KLECKNER, 1997 Meiotic cells monitor the status of the interhomolog recombination complex. Genes Dev. **11**: 106-118.

YOUDS, J. L., D. G. METS, M. J. MCILWRAITH, J. S. MARTIN, J. D. WARD, *et al*., 2010 RTEL-1 enforces meiotic crossover interference and homeostasis. Science **327**: 1254-1258.

ZANDERS, S. and E. ALANI, 2009 The *pch2Delta* mutation in baker's yeast alters meiotic crossover levels and confers a defect in crossover interference. PLoS Genet. **5**: e1000571.

ZIERHUT, C., M. BERLINGER, C. RUPP, A. SHINOHARA and F. KLEIN, 2004 Mnd1 is required for meiotic interhomolog repair. Curr. Biol. **14**: 752-762.